

Sheffield Hallam University

Design of optimal control systems and industrial applications.

FOTAKIS, Ioannis E.

Available from the Sheffield Hallam University Research Archive (SHURA) at:

<http://shura.shu.ac.uk/19659/>

A Sheffield Hallam University thesis

This thesis is protected by copyright which belongs to the author.

The content must not be changed in any way or sold commercially in any format or medium without the formal permission of the author.

When referring to this work, full bibliographic details including the author, title, awarding institution and date of the thesis must be given.

Please visit <http://shura.shu.ac.uk/19659/> and <http://shura.shu.ac.uk/information.html> for further details about copyright and re-use permissions.

POND STREET
SHEFFIELD S1 1WB

6794

7925306017



Sheffield City Polytechnic Library

REFERENCE ONLY

ProQuest Number: 10694540

All rights reserved

INFORMATION TO ALL USERS

The quality of this reproduction is dependent upon the quality of the copy submitted.

In the unlikely event that the author did not send a complete manuscript and there are missing pages, these will be noted. Also, if material had to be removed, a note will indicate the deletion.



ProQuest 10694540

Published by ProQuest LLC (2017). Copyright of the Dissertation is held by the Author.

All rights reserved.

This work is protected against unauthorized copying under Title 17, United States Code
Microform Edition © ProQuest LLC.

ProQuest LLC.
789 East Eisenhower Parkway
P.O. Box 1346
Ann Arbor, MI 48106 – 1346

Design of Optimal Control Systems and Industrial Applications

Ioannis Emmanuel Fotakis

Collaborating Establishment :

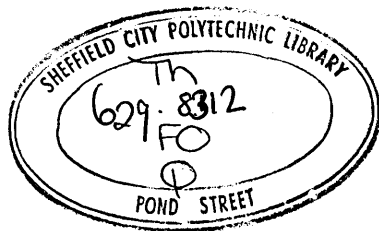
Swinden Laboratories
British Steel Corporation

A thesis presented for the CNAAGree
degree of Doctor of Philosophy.

Department of Electrical and Electronic
Engineering

Sheffield City Polytechnic

June 1981



7925306 —○1

Design of Optimal Control Systems and Industrial Applications

I E Fotakis

Abstract

This thesis describes work on the selection of the optimal control criterion weighting matrices, based on multivariable root loci and frequency domain properties. The case with a crossproduct weighting term in the cost function is examined and a design algorithm is proposed. The frequency domain solution to the finite time optimal control problem for discrete time systems is described and controller expressions in closed loop form are obtained for the regulation and tracking problems. The design of a strip shape control system for a Sendzimir cold rolling steel mill is described and problems of implementation are discussed. Finally, a detailed comparison between an optimal and a multivariable frequency domain design for a dynamic ship positioning system is presented. The effects of using Kalman filters for state estimate feedback in non-optimal systems is discussed.

Summary of Contributions

1. The first solution of the finite time LQP optimal control problem for discrete time systems in the z-domain including a closed loop form output feedback solution for the regulator and tracking problems. [1, 2]
2. The combination of a Kalman filter with the MacFarlane-Kouvaritakis design technique [3].
3. The design of a control scheme for a Sendzimir steel mill to be implemented by the British Steel Corporation in their Shepcote Lane mills [4, 5].

Papers published or to be published

1. J Fotakis and M J Grimble: "Solution of Finite Time Optimal Control Problems for Discrete Time Systems", presented on Conference on Systems Engineering, Coventry 1980.
2. M J Grimble and J Fotakis: "Solution of Finite Time LQP Optimal Control Problems for Discrete-Time Systems", submitted for publication to Trans ASME.
3. J Fotakis, M J Grimble and B Kouvaritakis: "A Comparison of Characteristic Locus and Optimal Designs for Dynamic Ship Positioning Systems", to be published IEEE Transactions on Automatic Control, 1981.
4. M J Grimble and J Fotakis: "Strip Shape Control Systems Design for Sendzimir Mills", invited presentation at IEE Decision and Control Conference, Albuquerque, 1980.
5. M J Grimble and J Fotakis: "The Design of Strip Shape Control Systems for Sendzimir Mills", to be published in IEEE Trans Automatic Control, 1981.

ACKNOWLEDGEMENTS

A PhD thesis, being the result of three years of research work, naturally involves the co-operation, consultation and discussion with many people. I should like to thank everybody concerned.

I would like to express my appreciation to my supervisor, Dr M J Grimble, for his guidance and encouragement all through the period of this research work. Also to the staff of the Department of Electrical and Electronic Engineering, particularly to Dr W A Barraclough.

I am grateful to all the friends whose discussions cleared up points and brought new ideas; I would especially like to thank Dr B Kouvaritakis of Oxford University.

Thanks are also due to our industrial collaborators at British Steel Corporation, Swinden Laboratories, Rotherham, specifically Dr M Foster and Mr K Dutton of the Systems Division. Finally, I should like to thank Mrs L Walker and Mrs S Whittingham for their help in typing this thesis.

CONTENTSPage No

Abstract	i
Summary of Contributions	ii
Acknowledgements	iii
CHAPTER 1	
Introduction to Optimal Control Problems	1
CHAPTER 2	
Optimal Control Systems with Cross-Product Weighting; Weighting Matrices Selection	12
CHAPTER 3	
Finite Time Optimal Control for Discrete-Time Systems	48
CHAPTER 4	
The Design of Strip Shape Control Systems for a Sendzimir Mill	75
CHAPTER 5	
A Comparison of Characteristic Locus and Optimal Control Designs in a Dynamic Ship Positioning Application	118
CHAPTER 6	
Concluding Remarks	169
References	172
Appendices	183

An Introduction to Optimal Control Problems and Methods1.1 Introduction

There have been continuous advances in theoretical control engineering over the last twenty years, particularly in the field of Linear Systems. The work of Kalman is notable in this respect. During the last decade, frequency domain techniques for multivariable systems have been developed by Rosenbrock, Mayne and MacFarlane and their co-workers [18,19,20]. The implementation of new control techniques has led to systems with tighter specifications and better performance. As control engineers take into account the overall needs of the process to be controlled, changes in the priorities of the objectives to be fulfilled lead to the development of appropriate control schemes.

A trend in the design of industrial systems is to consider energy losses in the process and the trade off between system performance and minimization of energy losses. To quantify this improvement, a cost criterion has to be defined. The controller which minimizes this cost function may be found using Optimal Control theory. The use of optimal control theory comes very naturally in the area of aero-space vehicle trajectory control and the design of aircraft control systems. In the following, optimal control will also be shown to provide a framework for the design of certain industrial systems.

As with the main body of control engineering results, the main work on optimal control theory is involved with Linear Systems and in

particular considering quadratic terms in the cost function. The main advantages of Linear Quadratic Optimal Control feedback systems stem from (i) the ease of obtaining the solution to a particular problem once the weighting matrices of the performance criterion are defined; (ii) the guaranteed asymptotic stability of the closed loop system and (iii) its direct and easy applicability to systems with many inputs and outputs. The main disadvantage of optimal control when applied to industrial problems where criteria like step response, overshoot, rise time, etc. , are of prime importance, is that there are few results relating those specifications to the weighting matrices of the performance criterion. In recent years a number of authors have presented papers trying to overcome this difficulty and have described methods of designing such optimal systems.

In the present thesis some contribution is made towards the problem of weighting matrices selection as described in chapter two. The solution to the finite discrete time optimal control problem is described in chapter three. The following chapter deals with the design of the shape control scheme for a Sendzimir cold rolling mill. Chapter five gives a detailed comparison between an optimal controller (obtained using the design methods of chapter two) and one designed with multivariable frequency domain techniques. An overview of the research effort follows in the concluding chapter.

1.2 Complex Frequency Domain Approach to Systems Analysis and Design

The s-domain approach to control systems analysis and design was developed by Wiener during the Second World War years. His famous dissertation on these methods was often referred to as the 'yellow peril'. This stemmed from the yellow cover of the then classified report [1]. In this fundamental treatise on the subject he introduced several ideas which have been incorporated in later work. These may be classified as follows:

(i) Formulation of the filtering and control problems using optimal cost functions and solutions of these problems using s-domain or Parseval theorem approaches.

(ii) Use of the spectral factorisation in the optimal control solution.

(iii) The requirement that the optimal control or filtering solution has to be realised by causal components and the means to achieve this condition.

Wiener's work was classified during the war years but soon after was further developed by other researcher's such as Newton et al [2]. Although the s-domain approach created some interest it was never applied in multichannel filtering or multivariable control problems and the number of real applications were very few. The later work by Kalman [3,4] in the time domain (since 1960) found immediate application in the aerospace industry and in many other fields. In some ways the problem formulation and solution were very similar, the only differences lying in the form that the solution was achieved. The state feedback solution to the control problem was found to be particularly appropriate. Similarly the recursive solution to the

estimation problem enabled filtering algorithms to be implemented easily on digital computers. The calculation of either the optimal control feedback gain matrix or the Kalman filter gain matrix reduced to the solution of a matrix Riccati equation. This difference between the Wiener and Kalman approaches is crucial. The solution of most of the linear quadratic optimal control and estimation problems was reduced to the solution of only one sort of matrix equation which enabled computer solutions to be obtained for general system descriptions. The Wiener approach however cannot be systematised in this way. Each problem and system description must be treated individually and the solution procedure cannot be implemented via a standard algorithm.

The s-domain approach taken here does not overcome this later problem, however the class of problems considered is wider than that considered up to now in the literature. Although not treated in this thesis there is a method recently developed which may offer a solution to the problem of achieving standard algorithms. Peterka [6] and Kucera [5] have developed a polynomial equation approach to systems theory which goes some way towards providing standard solutions. Kucera has proposed algorithms for most of the calculations involved in the polynomial matrix solutions. However there are no applications in this area and computer packages are not yet available nor likely to be, within the next two or three years.

Other authors have made contributions in the area of s-domain analysis and design. Yula et al[7] in a relatively recent paper on Wiener-Hopf methods introduced one new important component into the problem solution. They recognised that the solution to optimal control

problems do not necessarily lead to stable closed loop configurations. They were considering the output feedback situation where a cascade controller is used. For example if a plant is non-minimum phase and a straight-forward minimum variance controller is designed [8] the closed loop system can be unstable. To avoid this situation the problem can be reformulated and in this case the minimum variance controller by Peterka [6] is obtained which leads to a stable closed loop system. In the former case the optimal controller tries to cancel the right half plane zeros of the plant and thus creates unstable and uncontrollable poles. Hidden unstable modes always result in closed loop unstable systems and must therefore be avoided.

To circumvent the above difficulties Yula et al proposed that the control problem specification should be altered to include stability as well as optimality. This extra restriction is manifested in the control solution by additional constraint equations which must be satisfied. These authors were considering infinite time optimal control problems and they did not develop algorithms which could be implemented on computers.

Few authors have considered the solution of finite time optimal control problems. There are two main reasons, first that finite time optimal controllers and filters are more complicated than their infinite time counterparts and second that most filtering and estimation problems fall more naturally into the infinite time problem structure. However Grimble [9] and Fotakis and Grimble [10] have developed a frequency domain approach to the solution of these problems. In chapter three the z-domain solution of the deterministic finite time optimal control problem is described. This procedure has the disadvantages mentioned above; that is, it is difficult to derive

a general algorithm for the multivariable case and finite time problems are not so often found in industrial situations. However, one important role for this approach has been found where these limitations are not so important. This is in the design of optimal controllers for self tuning applications, where the disturbances are of a deterministic rather than a stochastic nature. For example these disturbances may be represented by sudden steps into the plant (instead of white noise). The applications of these controllers in self tuning systems is not considered in the present thesis but the theoretical ground work is presented which will enable such controllers to be designed. It is of interest to note that self tuning controllers based upon optimal control criteria using k-step ahead cost functions are directly related to the deterministic controllers proposed here (for the infinite time situation). The solution of the finite time optimal control problem has not been obtained previously in the z-domain by other authors.

1.3 Frequency Domain Multivariable Design

Many authors have considered the design of systems in the frequency domain, notably Bode, Nyquist and Evans for single input single output systems and Rosenbrock and MacFarlane for multivariable systems. The design of optimal systems in the frequency domain has attracted little attention. Grimble [11] and Fotakis [12] have recently developed a method of specifying the Q, R and G weighting matrices of the performance criterion using frequency domain criteria. The hope is that gain and phase margin type of information may be specified and from this the performance criterion can be developed. One of the difficulties of this approach is that the criteria so specified do not completely define the Q and R matrices. The positive aspect of this is that this freedom in the selection of the matrix elements may be employed fruitfully by the designer. In the same time this causes difficulties in the attempt to program the method as a standard algorithm for the design of systems. However it is hoped that an interactive computer aided design facility (CAD) may be used to overcome this problem. The designer would use the constraints imposed by the frequency domain requirements to partly specify the weighting matrices and then, as at present, use his engineering judgement to fix the remaining elements of the matrices.

Although other authors (eg MacFarlane [13]) have considered the frequency domain properties of optimal systems, few have considered the design of such systems in the frequency domain. The work described here must be extended to incorporate other design criteria, but the simple examples given, show that the performance indices used have produced systems with reasonable response characteristics.

1.4 Review of the basic Optimal Control results

A brief review of the optimal control problem approaches both in s-domain and in state space formulation follows. Considering the linear time invariant plant described by the equations:

$$\dot{\underline{x}}(t) = A\underline{x}(t) + B\underline{u}(t) \quad (1.1)$$

$$\underline{y}(t) = C\underline{x}(t) \quad (1.2)$$

and the criterion:

$$J(\underline{u}) = \langle \underline{y}(T), P_1 \underline{y}(T) \rangle_{E_n} + \int_0^T (\langle \underline{y}(t), Q\underline{y}(t) \rangle_{E_m} + \langle \underline{u}(t), R\underline{u}(t) \rangle_{E_r}) dt \quad (1.3)$$

the problem of determining the control $\hat{\underline{u}}(t)$ for $0 < t < T$ which minimises the criterion $J(\underline{u})$ is known as the deterministic linear optimal control regulator problem [15]. Because of the equation 1.2 the criterion $J(\underline{u})$ may be rewritten as:

$$J(\underline{u}) = \langle \underline{x}(T), C^t P_1 C \underline{x}(T) \rangle_{E_n} + \int_0^T (\langle \underline{x}(t), C^t Q C \underline{x}(t) \rangle_{E_m} + \langle \underline{u}(t), R \underline{u}(t) \rangle_{E_r}) dt$$

As has been proven [14,15] the solution to this problem can be obtained from the matrix Riccati equation:

$$\dot{\underline{P}}(t) = -R^{-1} B^t P(t) \underline{x}(t) \quad (1.4)$$

$$-\dot{P}(t) = C^t Q C - P(t) B R^{-1} B^t P(t) + P(t) A + A^t P(t) \quad (1.5)$$

with terminal condition $P(T) = C^t P_1 C$ (1.6)

This solution is given in a block diagram representation in figure 1. A second way of obtaining the control $\hat{\underline{u}}(t)$ is through augmentation of the state space equations, by considering the cosystem (or adjoint) of system (A,B,C). The optimal trajectories are given by the equations [16]:

$$\begin{bmatrix} \dot{\underline{x}}(t) \\ \dot{\underline{x}}^*(t) \end{bmatrix} = \begin{bmatrix} A & B R^{-1} B^t \\ C^t Q C & -A^t \end{bmatrix} \begin{bmatrix} \underline{x}(t) \\ \underline{x}^*(t) \end{bmatrix} \quad (1.7)$$

$$\underline{x}^*(T) = C^t P_1 C \underline{x}(T) \quad (1.8)$$

this solution is depicted in figure 1b and is equivalent to the

matrices C^tQC and R should be both positive definite. It is interesting that the nature of the problem leads to a state feedback closed loop system and this is asymptotically stable if and only if the pair (A,B) is stabilizable [37].

Next consider the criterion

$$J(\underline{u}) = \langle \underline{e}(T), P_1 \underline{e}(T) \rangle_{E_m} + \int_0^T (\langle \underline{e}(t), Q \underline{e}(t) \rangle_{E_m} + \langle \underline{u}(t), R \underline{u}(t) \rangle_{E_r}) dt \quad (1.9)$$

with $\underline{e}(t) = \underline{y}(t) - \underline{r}(t)$ (1.10)

where $\underline{r}(t)$ is the desired output and $\underline{e}(t)$ is the error between actual and desired output. This problem is known as the deterministic linear optimal control servomechanism. The solution may be obtained either using the Riccati equation or by considering the cosystem equations:

$$\begin{aligned} \dot{\underline{x}}(t) &= A \underline{x}(t) + B R^{-1} B^t \underline{x}^*(t) \\ \dot{\underline{x}}^*(t) &= C^t Q C \underline{x}(t) - A^t \underline{x}^*(t) + C^t Q \underline{r}(t) \end{aligned} \quad (1.11)$$

This solution is shown in figure 2a. The Riccati equation solution is

$$\begin{aligned} \hat{\underline{u}}(t) &= -R^{-1} B^t P(t) \underline{x}(t) + R^{-1} B^t \underline{g}(t) \\ -\dot{P}(t) &= C^t Q C - P(t) B R^{-1} P(t) A + A^t P(t) \\ \dot{\underline{g}}(t) &= (A^t P(t) B R^{-1} B^t) \underline{g}(t) + C^t Q \underline{r}(t) \end{aligned} \quad (1.12)$$

with $P(T) = C^t P_1 C$ and $\underline{g}(T) = -C^t P_1 \underline{r}(T)$

and this is depicted in figure 2b. It is clear that both problems have the same solution structure and the same closed loop properties.

The frequency domain solution is reviewed next: first the system operator W relating input and output is defined through the well known convolution integral of the impulse response matrix $w(t)$ with the system input:

$$\underline{y}(t) = (W \underline{u})(t) = \int_0^t w(t-\tau) \underline{u}(\tau) d\tau \quad (1.13)$$

the criterion $J(\underline{u})$ (of equation 1.9) can be expressed as follows by

$$J(\underline{u}) = \langle \underline{e}, Q\underline{e} \rangle_{H_m} + \langle \underline{u}, R\underline{u} \rangle_{H_r} = \langle (\underline{r} - W\underline{u}), Q(\underline{r} - W\underline{u}) \rangle_{H_m} + \langle \underline{u}, R\underline{u} \rangle_{H_r} \quad (1.14)$$

From this relationship a gradient function $g(\underline{u})$ may be defined and the necessary condition for optimality is that $g(\hat{\underline{u}}) = 0$ [17]. Transforming this into the s-domain and using spectral factorisation [73] the solution is found as [17]:

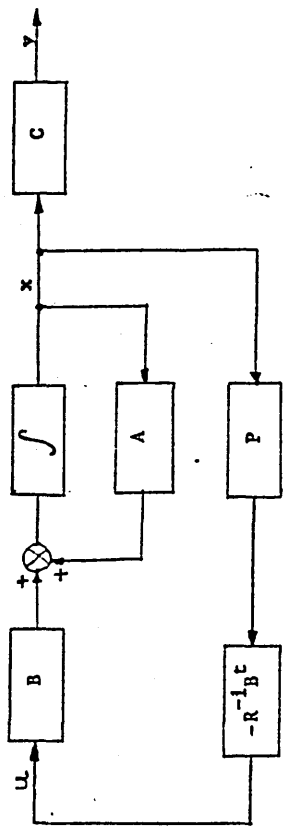
$$\begin{aligned} \hat{\underline{u}}(s) &= [Y(s)]^{-1} \{ [Y^t(-s)]^{-1} W^t(-s) Q \underline{r}(s) \}_+ \\ &= F(s) \underline{r}(s) \end{aligned} \quad (1.15)$$

and $Y^t(-s)Y(s) = W^t(-s)QW(s) + R$

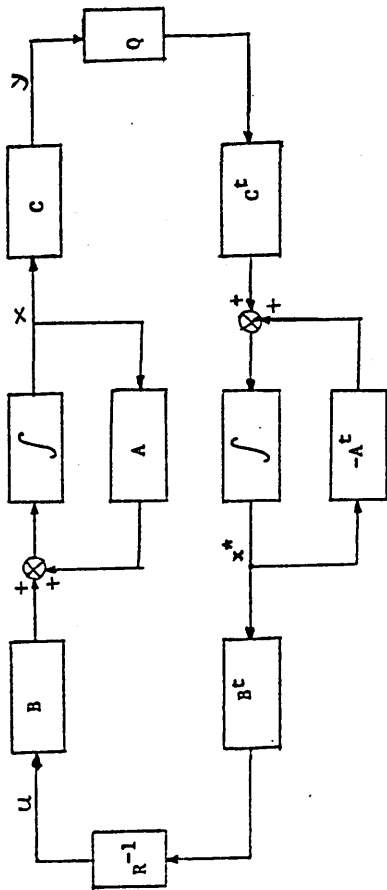
and a feedback closed loop controller can be obtained as:

$$K(s) = F(s) [I - W(s)F(s)]^{-1} \quad (1.16)$$

and this form of solution is shown in figure 2c.

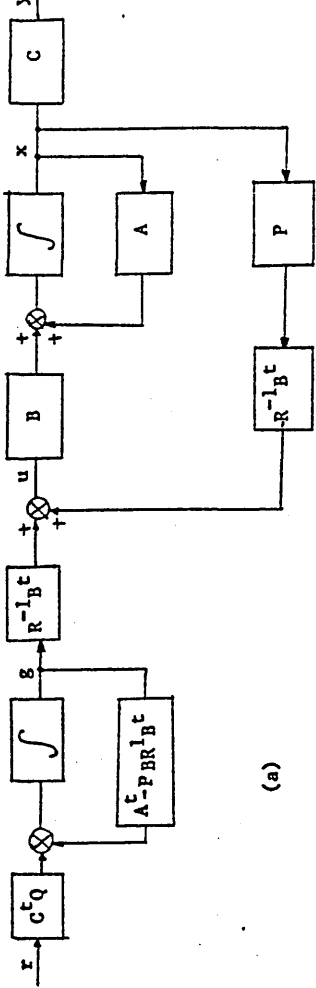


(a)

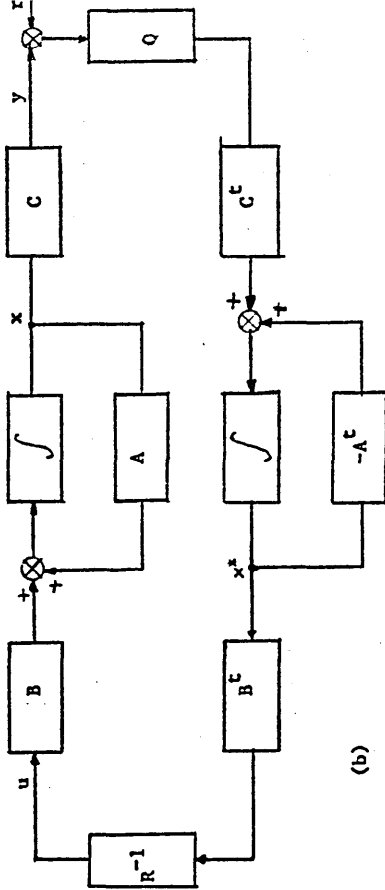


(b)

Figure 1 Optimal Linear Regulator



(a)



(b)



Figure 2 Optimal Linear Servomechanism

CHAPTER 2

Optimal Control Systems with Cross-Product Weighting; Weighting Matrices Selection

2.1 Introduction

In dealing with the design of optimal controllers for industrial applications there has been two main criticisms. The first concerns the selection of the performance criterion weighting matrices and the second is the apparent need for phase advance [21, 22]. This is only a problem when an observer is required for the implementation of the state feedback controllers. The phase advance in LQP systems follows because the determinant of the return difference matrix is greater than unity for all frequencies. [23, 24] This implies that for a single input system the phase margin [25] is greater than 60° . To be able to have a smaller phase margin the locus of $\det F(s)$ must pass within the unit circle, and this can be achieved for an optimal system if a cross product weighting term, between the state and the control, is introduced. In this chapter such a problem is defined, its properties are studied and a design procedure is outlined.

To help with the selection of the weighting matrices, use is made of recent results [33, 34] on the asymptotic root loci properties of optimal systems. The use of root locus to design optimal systems originated by Chang [30] and was extended by Tyler and Tuteur [31]. The relationship between the Q and R matrices and conventional design characteristics has been investigated but there are not any results for the multivariable case [32]. Chen and Shen [33], Solheim [34] produced algorithms for this purpose but their methods have the weakness of considering only the eigenvalues of the system. Harvey and Stein [35] considered the state regulator problem when the system is controllable observable and minimum phase. In this work the output regulator is considered and the plant is assumed to be stabilisable and detectable only.

The initial development of the design technique presented in this Chapter was described in Grimble [22], [36]. The author contributed to the theoretical analysis and was responsible for the computer implementation and the applications of the technique to the industrial problems.

2.2 Optimal Control Problem

We consider the following linear constant plant, controllable and observable represented by the state space equations:

$$\dot{\underline{x}}(t) = A\underline{x}(t) + B\underline{u}(t) \quad (2.1)$$

$$\underline{y}(t) = C\underline{x}(t) \quad (2.2)$$

with A,B,C the plant matrices and define as performance criterion

$$J(\underline{u}) = \frac{1}{2} \int_0^{\infty} \langle \underline{e}(t), Q\underline{e}(t) \rangle_{E_r} + \langle \underline{u}(t), R\underline{u}(t) \rangle_{E_m} \\ + 2 \langle \underline{y}(t), G\underline{u}(t) \rangle_{E_r} + 2 \langle \underline{y}(t), M\underline{r}(t) \rangle_{E_d} \quad (2.3)$$

where the weighting matrices Q and R are positive definite and the error $\underline{e}(t)$ is defined as the difference between the plant output from the desired output $\underline{r}(t)$:

$$\underline{e}(t) = \underline{r}(t) - \underline{y}(t) \quad (2.4)$$

To obtain a unique solution for the above optimal servomechanism problem the two cross product weighting matrices G, M have to be constrained. These constraints are obtained by rearranging equation 2.3 to remove the cross product terms:

$$\langle \underline{u}, R\underline{u} \rangle_{E_m} + 2 \langle \underline{y}, G\underline{u} \rangle_{E_r} = \\ = \langle \underline{u} + R^{-1}G^T\underline{y}, R(\underline{u} + R^{-1}G^T\underline{y}) \rangle_{E_m} - \langle R^{-1}G^T\underline{e}, G^T\underline{e} \rangle_{E_m} \\ - 2 \langle \underline{y}, GR^{-1}G^T\underline{r} \rangle_{E_r} + \langle R^{-1}G^T\underline{r}, G^T\underline{r} \rangle_{E_m} \quad (2.5)$$

by choosing $M = GR^{-1}G^T$ both the cross product matrices depend upon G and if we set:

$$Q_1 = Q - GR^{-1}G^T \quad (2.6)$$

$$\underline{u}_1(t) = \underline{u}(t) + R^{-1}G^T\underline{y}(t) \quad (2.7)$$

the performance criterion may be rewritten as:

$$J(\underline{u}) = \frac{1}{2} \int_0^{\infty} \langle \underline{e}(t), Q_1\underline{e}(t) \rangle_{E_r} + \langle \underline{u}_1(t), R\underline{u}_1(t) \rangle_{E_m} dt \quad (2.8)$$

where the last term in the identity 2.5 is omitted from the criterion since it is constant for any defined $\underline{r}(t)$ and does not affect the minimisation of $J(\underline{u})$. The original plant is equivalent to the following:

$$\dot{\underline{x}}(t) = A_1 \underline{x}(t) + B \underline{u}_1(t) \quad (2.9)$$

$$\underline{y}(t) = C \underline{x}(t) \quad (2.10)$$

where $A_1 = A - BR^{-1}G^T C$ (2.11)

It is clear that a constraint for G comes from equation 2.8

where $Q_1 \geq 0$, that is

$$Q - GR^{-1}G^T \geq 0 \quad (2.12)$$

The optimal control $\hat{\underline{u}}_1(t)$ for the criterion 2.8 and plant 2.9 leads to the desired control $\hat{\underline{u}}(t)$, for the original problem, through equation 2.7. Both, the original system (A,B,C) and the system (A_1,B,C) have the same state trajectories, for the same initial conditions. All the above results apply to the state regulator problem (by setting the matrix C equal to the unity matrix) and to the output regulator by setting the reference $\underline{r} \equiv 0$. It is well known that the state feedback solution for the optimal control problem is obtained by the Riccati differential equation and for the infinite-time problem, from the algebraic Riccati equation.

2.3 Return difference, Optimality condition

The frequency domain solution to the above problem is obtained as follows. Define the optimal state feedback matrix K_1 :

$$K_1 = R^{-1}B^T P_1 \quad (2.13)$$

which leads to the control law (see also section 1.4):

$$\underline{u}_1(t) = -K_1 \underline{x}(t) + R^{-1}B^T \underline{g} \quad (2.14)$$

or for the original plant

$$\begin{aligned} \underline{u}(t) &= -(K_1 + R^{-1}G^T C) \underline{x}(t) + R^{-1}B^T \underline{g} \\ &= -K \underline{x}(t) + R^{-1}B^T \underline{g} \end{aligned} \quad (2.15)$$

where

$$K \triangleq K_1 + R^{-1}G^T C \quad (2.16)$$

Now for the infinite time case the matrix P_1 is the positive semi-definite constant matrix obtained from the algebraic Riccati equation:

$$-P_1 A_1 - A_1^T P_1 + P_1 B R^{-1} B^T P_1 = C^T Q_1 C \quad (2.17)$$

We consider the matrix return difference of the examined system:

$$F(s) \triangleq I + K \phi(s) B \quad (2.18)$$

where

$$\phi(s) \triangleq (sI - A)^{-1} \quad (2.19)$$

$$\text{and the plant transfer function is } W(s) = C \cdot \phi(s) B \quad (2.20)$$

The optimal return difference equation follows after substituting into equation 2.17, equation 2.11 and 2.13:

$$-P_1 A - A^T P_1 + K_1^T G^T C + C^T G K_1 + K_1^T R K_1 = C^T Q_1 C \quad (2.21)$$

so we have

$$P_1 \phi(s)^{-1} + \phi^T(s)^{-1} P_1 = C^T Q_1 C - P_1^T G^T C - C^T G K_1 - K_1^T R K_1$$

premultiplying by $B^T \phi^T(-s)$ and post multiplying by $\phi(s) B$ and using 2.16 leads to

$$\begin{aligned} W^T(-s) Q_1 W(s) + R + W^T(-s) G + G^T W(s) + W^T(-s) G R^{-1} G^T W(s) \\ = F^T(-s) R F(s) \end{aligned} \quad (2.22)$$

This equation can be rewritten by use of equation 2.6 as

$$\boxed{W^T(-s)QW(s) + R + W^T(-s)G + G^TW(s) = F^T(-s)RF(s)} \quad (2.23)$$

or

$$\begin{aligned} W^T(s)Q_1W(s) + (I + W^T(-s)GR^{-1})R(I + R^{-1}G^TW(s)) &= \\ = F^T(-s)RF(s) & \end{aligned} \quad (2.24)$$

Equation 2.23 becomes identical to the one discussed by MacFarlane [23,24] in the case where the crossproduct term G vanishes. The above equation applies direct to the original optimal control problem; the equivalent transformed one is useful only for supplying the constraints on matrix G (equation 2.12).

MacFarlane [23] has shown for the case with no crossproduct term the necessary condition for optimality is

$$|\det F(j\omega)| \geq 1 \quad \forall \omega \in \mathbb{R} \quad (2.25)$$

This implies that the Nyquist locus plot of $\det F(j\omega)$ lies outside the unit circle with centre (0,0) and for a single input plant this means that the phase margin will be greater than 60° [25]. This is out of the range of the usual design criteria and is a drawback if state feedback can't be applied because it requires a significant amount of phase advance to be introduced by a dynamic compensator which can cause noise problems.

By the use of the crossproduct term (matrix G) we can prove that the above equation (2.25) need not be satisfied.

Let $\underline{v}(s)$ be an eigenvector of $F(s)$ corresponding to the eigenvalue $p(s)$:

$$F(s) \underline{v}(s) = p(s) \cdot \underline{v}(s)$$

premultiplying equation (22) by $\underline{v}^T(-s)$ and postmultiplying by $\underline{v}(s)$ we obtain:

$$\begin{aligned} & \underline{v}^T(-s)W^T(-s)QW(s)\underline{v}(s) + \underline{v}^T(-s)[R + W^T(-s)G + G^TW(s)]\underline{v}(s) = \\ & = p(-s)p(s)\underline{v}^T(-s)R\underline{v}(s) \end{aligned}$$

because the term in Q is positive semidefinite on the $j\omega$ axis of the s-plane the above equation leads to the following necessary condition for optimality:

$$|p(j\omega)|^2 \geq \frac{\underline{v}^T(-j\omega)[R + W^T(-j\omega)G + G^TW(j\omega)]\underline{v}(j\omega)}{\underline{v}^T(-j\omega)R\underline{v}(j\omega)} \quad (2.26)$$

in this equation $W^T(-j\omega)G + G^TW(j\omega)$ is Hermitian but not positive definite and thus only when $G = 0$ the above gives $|p(j\omega)|^2 \geq 1$ for all ω . By use of the relation:

$$\det F(j\omega) = \prod_{i=1}^n p_i(j\omega)$$

we see that the condition 2.25 does not necessarily apply when a cross-product term exists. Similarly the criteria developed by Porter [26] do not hold in this case. From the above we can conclude that the necessary condition for optimality becomes

$$|\det F(j\omega)| \geq r_f \quad (2.27)$$

where r_f is the radius of a circle which can be less than unity.

If Q and R are predetermined it may not be possible to choose G so that the $\det F(j\omega)$ locus can enter the unit circle because G must also satisfy the condition of equation 2.12 $Q_1 = Q - GR^{-1}G^T \geq 0$.

So we will assume that Q, R, G can be chosen freely to satisfy equation 2.12 and equation 2.27 for a desired value of $r_f < 1$ so we are not going to evaluate r_f using equation 2.26 which would be a quite difficult task.

From equation 2.23:

$$\begin{aligned} & |\det F(j\omega)|^2 \cdot \det R = \\ & = \det[W^T(-j\omega)QW(j\omega) + R + W^T(-j\omega)G + G^TW(j\omega)] \end{aligned} \quad (2.28)$$

Figure 1 depicts a plot of $\det F(j\omega)$ for a system with cross-product weighting. The point of origin is the critical point for stability so for an open loop stable plant the feedback system will be stable if the origin is not enclosed. Hsu and Chen have shown [27]:

$$\det F(s) = \frac{\prod_{j=1}^n (s - \gamma_j)}{\prod_{i=1}^n (s - \lambda_i)} \quad (2.29)$$

where γ_j are the closed-loop system eigenvalues and λ_i are the open loop system eigenvalues (eigenvalues of the plant matrix A).

The minimum distance from the origin to the plot of $\det F(j\omega)$ is a measure of the degree of stability of the system. And in this method of design this distance is specified in the beginning together with the frequency ω_m at which $\det F(j\omega)$ touches the circle of radius r_f . It is found that this point is often very close to the phase margin point which is the point the $\det F(j\omega)$ plot is cut by a unit circle with centre (1,0). This result is useful as it defines the frequency range up to which the optimal feedback system gives an improvement in sensitivity over the open loop system [25,28]

Rosenbrock and McMorran [21] have also shown that as the frequency tends to infinity $\det F(j\omega)$ tends to the (1,0) since the system is proper and it approaches that point with an angle of -90° .

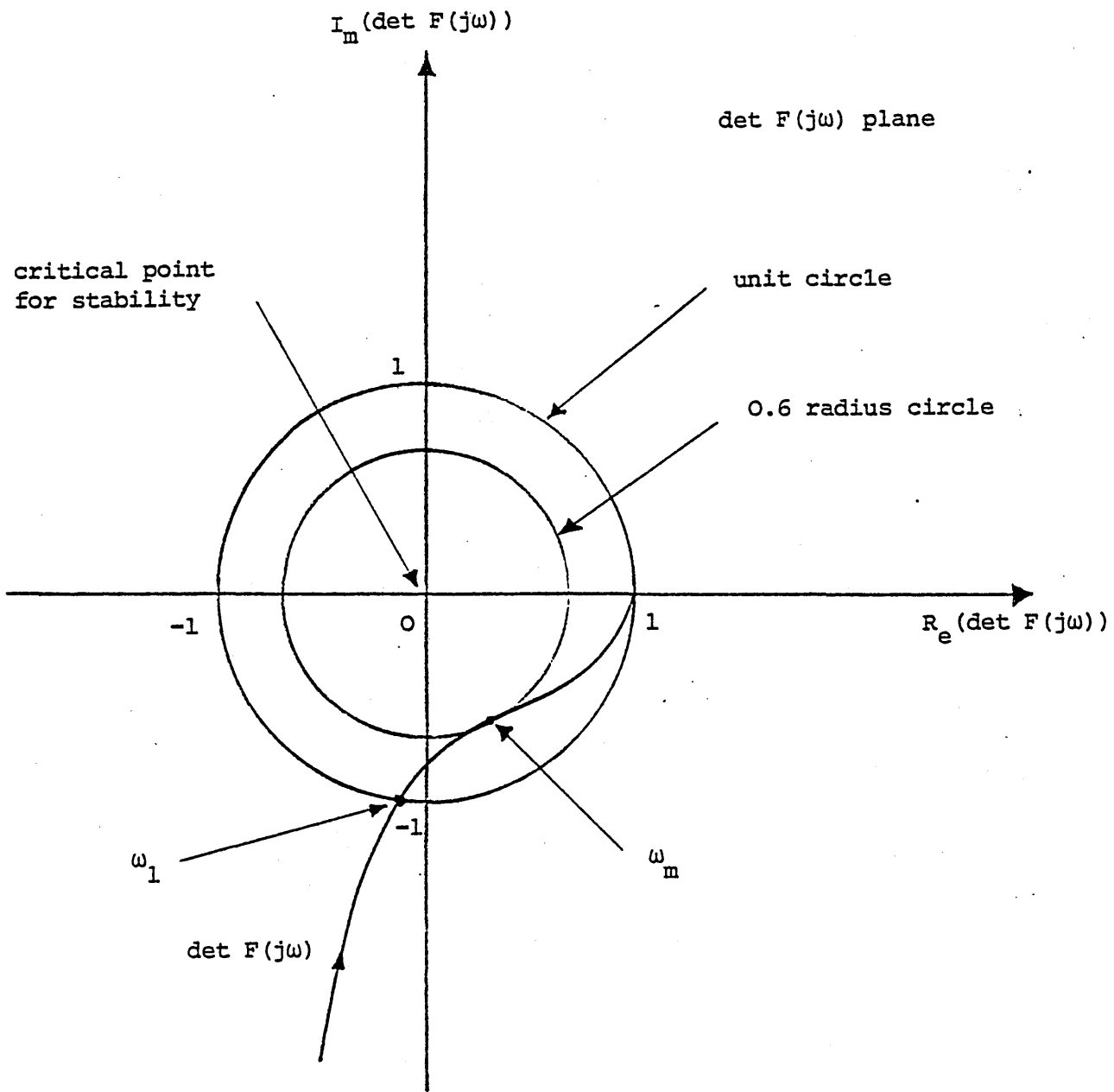


Figure 1 Frequency response plot of $\det F(j\omega)$

With optimal control for a given plant the design reduces to the selection of the weighting matrices Q , R , G . In all the design methods the usual procedure is an iterative process of trial and error until a satisfactory performance of the closed loop system is obtained. The same holds here for this method. In the literature some ways are described of how to choose Q and R to achieve certain conventional system performance characteristics like steady-state error, peak overshoot etc. Those ideas can be applied properly modified to calculate the G matrix.

The design procedure has the following steps:

- 1) Choose the radius r_f and frequency ω_m which is the minimum of $\det F(j\omega)$, ω_m can be chosen very near to the desired system bandwidth or phase margin frequency of the fastest loop in a multiloop system.
- 2) Expand $Q - GR^{-1}G^T \geq 0$ to obtain a set of inequalities which must be satisfied by the elements of Q , R and G .

- 3) Evaluate $\frac{d}{d\omega}(|\det F(j\omega)|^2) = 0$ and set $\omega = \omega_m$ (2.30)

Obtain also the equality

$$\frac{\det[W^T(-j\omega)QW(j\omega) + R + W^T(-j\omega)G + G^TW(j\omega)]}{\det R} = r_f^2 \quad (2.31)$$

This is the necessary condition that $|\det F(j\omega)|$ has minimum r_f at ω_m .

- 4) Collect all equalities and inequalities the elements of Q , R , G must satisfy from steps 2, 3.
- 5) Choose Q , R , G such that the above relationships and any other conventional criteria are satisfied.

Example 1

We consider the following single input three output plant originally considered by Fallside and Seraji [29] for the case with $G = 0$.

$$\dot{\underline{x}} = \begin{bmatrix} -1 & 0 & 0 \\ -1 & 0 & -2 \\ 0 & 1 & -1 \end{bmatrix} \underline{x} + \begin{bmatrix} 1 \\ 0 \\ 0 \end{bmatrix} u \quad (2.32)$$

$$\underline{y} = I_3 \underline{x}$$

The performance criterion is $j(u) = \int_0^{\infty} \langle \underline{x}, Q\underline{x} \rangle + \langle u, Ru \rangle + 2 \langle \underline{x}, Gu \rangle dt$

where $Q \triangleq \text{diag}(q_1 q_2 q_3)$ $R = 1$ $G \triangleq (g_1 g_2 g_3)^T$

The open loop transfer function matrix is

$$W(s) = \frac{1}{p_o(s)} \begin{bmatrix} s^2 + s + 2 \\ -(s + 1) \\ -1 \end{bmatrix} \quad (2.33)$$

$$p_o(s) \triangleq (s+1)(s^2+s+2) = s^3 + 2s^2 + 3s + 2$$

In general restricting Q to be diagonal matrix can result in no feasible solution but in this case with diagonal Q there exists a solution; we choose $g_1 = g_3 = 0$.

$$A(s) = W^T(-s)QW(s) + R + W^T(-s)G + G^T W(s) =$$

$$= \frac{1}{p_o(s)p_o(-s)} [q_1(s^2-s+2), q_2(s-1), -q_3] \begin{bmatrix} s+s+2 \\ -(s+1) \\ -1 \end{bmatrix} \\ + 1 + \frac{1}{p_o(s)} g_2(s-1) + \frac{1}{p_o(s)} (-g_2(s+1))$$

$$\text{or } A(\omega) = \frac{\omega^6 - a\omega^4 - \beta\omega^2 + \gamma}{\omega^6 - 2\omega^4 + \omega^2 + 4} \quad \text{where } \alpha \triangleq 2 - q_1 - 2g_2 \quad (2.34) \\ \beta \triangleq 3q_1 - q_2 + 2g_2 - 1 \\ \gamma \triangleq 4q_1 + q_2 + q_3 + 4 - 4g_2$$

for the local minimum $\frac{dA}{d\omega} = 0$

$$(\alpha-2)\omega_m^2 + (2+2\beta)\omega_m^6 + (12-d-2\beta-3\gamma)\omega_m^4 + (4\gamma-8d)\omega_m^2 - (\gamma+4\beta) = 0$$

and $|A(\omega_m)|^2 = r_f^2$

the restriction on G: $Q_1 = Q - GR^{-1}G^T \geq 0$

$$\begin{aligned} q_1 &\geq 0 \\ q_2 - g_2^2 &\geq 0 \\ q_3 &\geq 0 \end{aligned} \quad (2.35)$$

For $\omega_m = 8$ rad/sec $r_f = 0.7$

we have:

$$\frac{dA}{d\omega} = 0 \therefore 16777216(\alpha-2) + 524288(1+\beta) + 4096(12-\alpha-2\beta-3\gamma) + 256(\gamma-2\alpha) - (\gamma+4\beta) = 0$$

$$\implies 16772608\alpha + 5160928 - 12033\gamma = 32980992$$

$$|A|^2 = r_f^2 : 4096\alpha + 64\beta - \gamma = 13764.$$

since there is no other requirement any solution of 2.34 which satisfies the inequality 2.35 is acceptable. By letting $A(o) = 10^4$ so the d.c. gain $F(o) = 10^2$ gives:

$$\begin{aligned} \gamma &= 410^4 \\ \alpha &= 56.56 \\ \beta &= -843.8 \end{aligned}$$

and from 2.34:

$$\begin{aligned} q_1 &= 1 & g_2 &= -27.28 \\ q_2 &= 790.24 \\ q_3 &= 39091 \end{aligned}$$

The optimal gain matrix becomes:

$$K = [6.634 \quad -55.92 \quad -128.81]$$

and the initial condition responses are shown in the figure 2 these are similar to the responses that Fallside and Seraji obtained but also

the system has a more realistic phase margin.

For the same system but for $\omega_m = 5.5$ rad/sec $r_f = 0.7$ we get the solution

$$q_1 = 2 \quad g_2 = -10$$

$$q_2 = 102$$

$$q_3 = 2$$

which gives $K = [.6637 \quad -9.884 \quad .7214]$

and the responses for this case are shown in figure 3.

An attempt was made to computerise the above design algorithm but the effort was abandoned as the estimated programming time was far more than was available and there was inadequate library routines to obtain solution for the non linear system of equalities and inequalities.

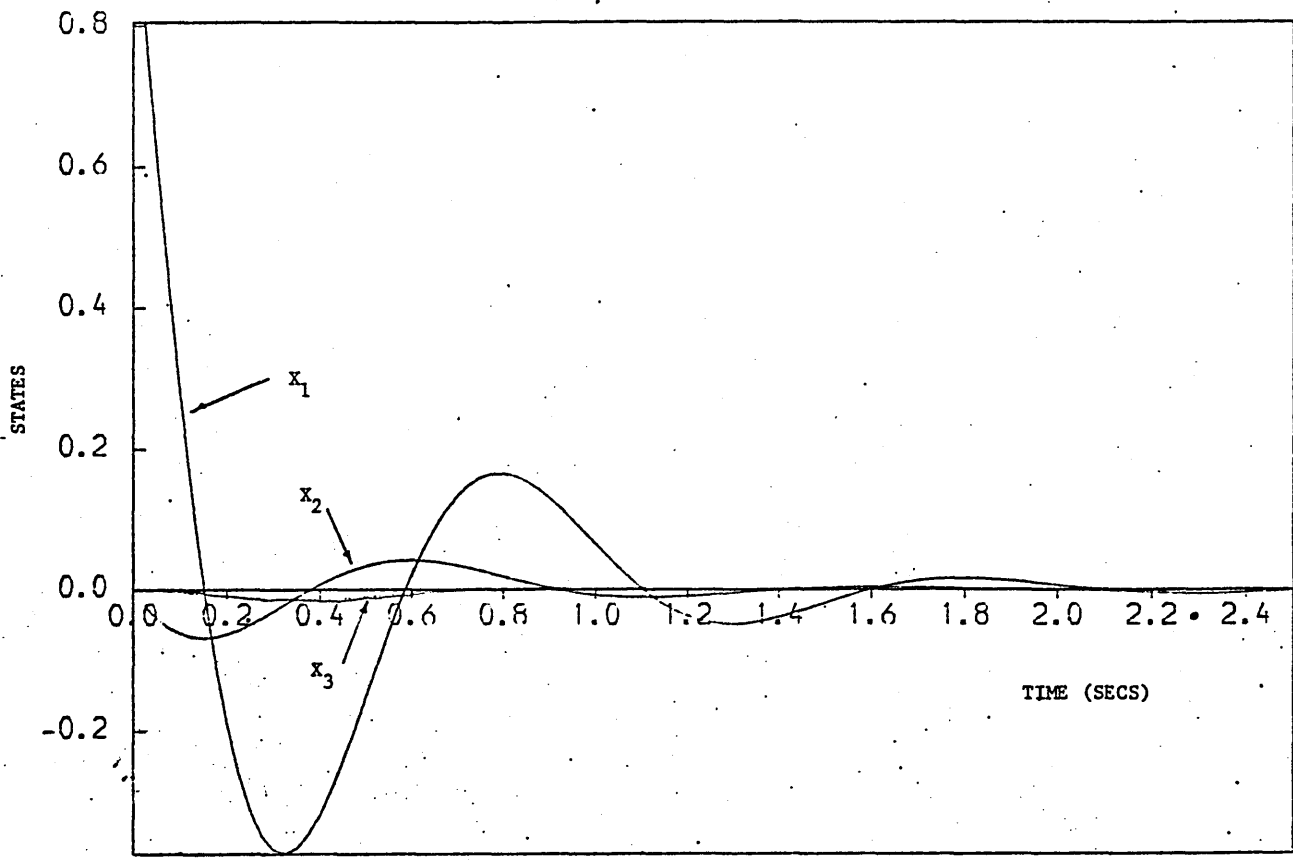


Figure 2 Initial Condition Responses $Q = \text{diag} \{1 \ 790.24 \ 39091\}$
 $G = \begin{bmatrix} 0 & -27.78 & 0 \end{bmatrix}^T$

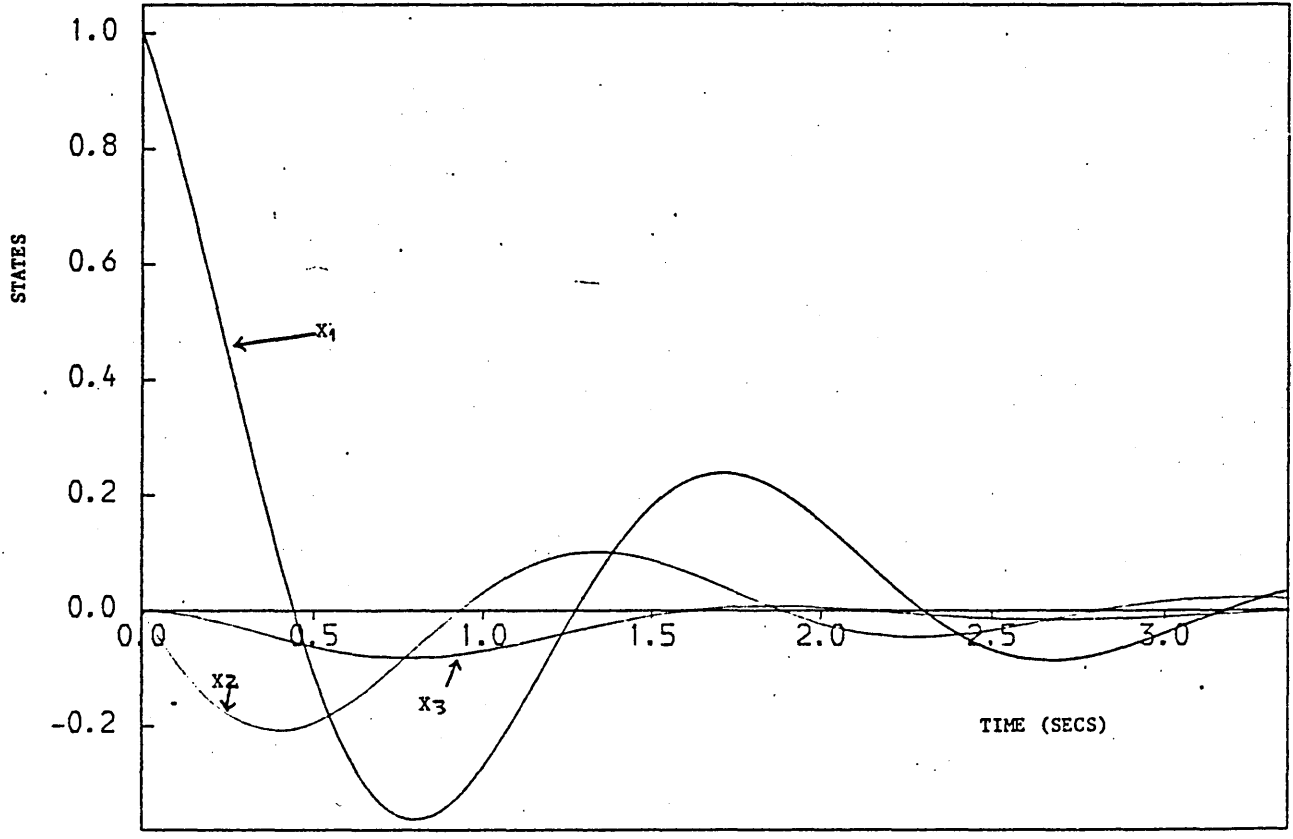


Figure 3 Initial Condition Responses $Q = \text{diag} \{2 \ 102 \ 2\}$
 $G = \begin{bmatrix} 0 & -10 & 0 \end{bmatrix}^T$

2.5 Selection of the Performance-Criterion Weighting Matrices

Let us consider the same plant (A,B,C) as defined in equation 2.1, 2.2, with the further assumption that the system is square. This assumption can be justified [37] since the outputs defined through equation 2.2 need not to coincide with the actual plant outputs; for example, additional outputs may be defined to square up the system. Also CB is assumed full rank; the more general case when CB is not full rank is discussed later. The performance criterion to be minimized has the following form:

$$J(\underline{u}) = \int_0^{\infty} \langle \underline{y}(t), Q\underline{y}(t) \rangle_{E_m} + \mu^2 \langle \underline{u}(t), R\underline{u}(t) \rangle_{E_m} + \mu \langle \underline{y}(t), G\underline{u}(t) \rangle_{E_m} dt \quad (2.36)$$

where Q, R are constant symmetric positive definite matrices and G is constant and $Q_1 \triangleq Q - GR^{-1}G^T$ is positive definite as shown previously. Let us denote by S the mxm full rank square root of Q_1 : $Q_1 = S^T S$ and the pair (A,S) is assumed to be detectable. The control weighting depends on the real positive scalar μ . The solution of the above problem is the same as before (equations 2.14 to 2.23) except for the inclusion of μ :

$$\underline{u}(t) = -K\underline{x}(t) \quad (2.37)$$

$$K = (R^{-1}/\mu^2)(B^T P_1 + \mu G^T C) = R^{-1} B^T P_1 / \mu^2 + R^{-1} G^T C / \mu = K_1 + R^{-1} G^T C \quad (2.38)$$

$$-P_1 A - A^T P_1 + \mu K_1^T G^T C + \mu C^T G K_1 + \mu^2 K_1^T R K_1 = C^T Q_1 C \quad (2.39)$$

this final steady state matrix Riccati equation gives rise to the equivalent frequency domain equation:

$$\mu^2 F^T(-s) R F(s) = W^T(-s) Q W(s) + \mu^2 R + \mu W^T(-s) G + \mu G^T W(s) \quad (2.40)$$

The expressions for calculating the weighting matrices Q and R are obtained from the following theorem. The crossproduct matrix G is not

determined by these results but as already described it can be chosen to shape the system time response and has to satisfy the conditions set above; furthermore $G^T C B$ has to be symmetric or G is null .

Theorem 2.1 Selection of Q and R

For the LQP problem defined above assume that m pairs $(\lambda_i^\infty, \underline{v}_i^\infty)$ are specified. The optimal control weighting matrices can be selected to provide the given asymptotic behaviour, for $\mu \rightarrow 0$:

$$Q = [(CBN)^T]^{-1} (CBN)^{-1} \quad (2.41)$$

and

$$R = (N^T)^{-1} \Lambda^\infty N^{-1} \quad (2.42)$$

where $N = \{\underline{v}_1^\infty, \underline{v}_2^\infty, \dots, \underline{v}_m^\infty\}$ and $\Lambda^\infty = \text{diag}\{(1/\lambda_1^\infty)^2, (1/\lambda_2^\infty)^2, \dots, (1/\lambda_m^\infty)^2\}$.

As $\mu \rightarrow 0$ there are m infinite closed loop eigenvalues of the form

$$\lambda_i = \lambda_i^\infty / \mu \quad (2.43)$$

where $|\lambda_i^\infty| < \infty$ with m corresponding closed loop eigenvectors:

$$\underline{x}_i^\infty = B \underline{v}_i^\infty \quad (2.44)$$

Proof of Theorem 2.1

The proof relies on results from optimal root loci theory and the closed loop eigenvector relationships summarised in Appendix 1. It is shown that the return difference matrix $F(s)$ determines the vectors \underline{v}_i through the relation

$$F(\lambda_i) \underline{v}_i = 0 \quad (2.45)$$

for each $\lambda_i \notin \sigma(A)$. Thus the frequencies $\{\lambda_i\}$ are a set of closed-loop eigenvalues and the vectors $\{\underline{v}_i\}$ relate to the closed loop eigenvectors.

The asymptotic behaviour of the closed loop system poles, is as follows:

As shown in Appendix 2.1 ($n-m$) closed loop eigenvalues remain finite as $\mu \rightarrow 0$. The rest of the m closed loop eigenvalues $\{\lambda_i^\infty / \mu\}$ approach

infinity in m first order Butterworth patterns [38]. These eigenvalues must necessarily be a subset of the controllable modes, since the uncontrollable modes are invariant under feedback, that is, the asymptotically infinite modes $\lambda_i^\infty / \mu \notin \sigma(A)$. The eigenvectors corresponding to the $(n-m)$ finite modes are discussed later in section 2.7, now the eigenvectors corresponding to the m infinite modes are determined as following. Let $\Phi(s)$ be expanded as a Laurent series [39] then $W(s)$ may be written

$$W(s) = C(s^{-1}I_n + s^{-2}A + s^{-3}A^2 + \dots)B \quad (2.46)$$

From the above equation 2.40 gives:

$$\begin{aligned} \mu^2 F^T(-s)RF(s) &= \mu^2 \left\{ R - \frac{1}{\mu^2 s^2} [(CB)^T QCB + O(1/s)] \right. \\ &\quad \left. - \frac{1}{\mu s} [(CB)^T G - G^T CB + O(1/s)] \right\} \end{aligned} \quad (2.47)$$

Assuming that G satisfies the condition $(CB)^T G - G^T CB = 0$ and denoting $s_1 = \mu s$ equation 2.47 becomes

$$F^T(-s)RF(s) = R - \frac{1}{s_1^2} [(CB)^T QCB + O(1/s)] - \frac{1}{s_1} O(1/s) \quad (2.48)$$

thus for a given finite frequency s_1 , as $\mu \rightarrow 0$ then $|s| \rightarrow \infty$ and

$$F^T(-s)RF(s) \rightarrow R - \frac{1}{s_1^2} (CB)^T QCB \quad (2.49)$$

From equations 2.45 and 2.49 for each finite frequency λ_i^∞ corresponding vector \underline{v}_i^∞ and infinite eigenvalue $\lambda_i = \lambda_i^\infty / \mu$:

$$F^T(-\lambda_i)RF(\lambda_i)\underline{v}_i^\infty = 0 \quad (2.50)$$

$$\left[R - \frac{1}{(\lambda_i^\infty)^2} (CB)^T QCB \right] \underline{v}_i^\infty = 0 \quad (2.51)$$

As Q is symmetric positive definite it may be written $Q = E^T E$ with E full rank, this substituted in the last relation:

$$\left[((ECB)^T)^{-1} R (ECB)^{-1} \right] ECB \underline{v}_i^\infty = \frac{1}{(\lambda_i^\infty)^2} ECB \underline{v}_i^\infty \quad (2.52)$$

The above is an eigenvector equation, the matrix within the square

brackets is positive definite and symmetric, therefore has positive real eigenvalues $(1/\lambda_i^\infty)^2$ and orthogonal eigenvectors $ECB\underline{v}_i^\infty$. Assume the magnitude of these eigenvectors to be unity and define

$$N = \{\underline{v}_1^\infty, \underline{v}_2^\infty, \dots, \underline{v}_m^\infty\} \quad (2.53)$$

then

$$(ECBN)^T(ECBN) = I_m \quad (2.54)$$

If N is supposed to be specified then Q follows from equation 2.54:

$$Q = [(CBN)^T]^{-1}(CBN)^{-1} \quad (2.55)$$

The matrix E may be chosen as $E = (CBN)^{-1}$ which is full rank (m) but is not symmetric. Then equation 2.52:

$$(N^T R N) N^{-1} \underline{v}_i^\infty = \frac{1}{(\lambda_i^\infty)^2} N^{-1} \underline{v}_i^\infty$$

from which if Λ^∞ is defined as $\Lambda^\infty = \text{diag}\{1/(\lambda_1^\infty)^2, 1/(\lambda_2^\infty)^2, \dots, 1/(\lambda_m^\infty)^2\}$:

$$R = (N^T)^{-1} \Lambda^\infty N^{-1}$$

Thus the infinite modes are given by $\lambda_i = \lambda_i^\infty/\mu$ as $\mu \rightarrow 0$ and the associated eigenvectors are $\underline{x}_i = B\underline{v}_i$ as shown in Appendix 1.

In the case where N is chosen as the identity then $R = \Lambda^\infty$ is diagonal, $Q = [(CB)^T]^{-1} (CB)^{-1}$ and as $s \rightarrow \infty$ $EW(s) \rightarrow I_m/s$, furthermore, if CB is diagonal then Q will be diagonal also.

2.6 Calculation of the weighting matrices, Example

As it was shown the weighting matrices Q and R depend on the choice of the frequencies λ_i^∞ and the vectors \underline{V}_i^∞ , but even when the matrix G is null (absent from the performance criterion) the process is not complete. The finite value of μ must be selected and this may lead to a modification of Q and R so that all the specification requirements are fulfilled. The full design process is discussed in later sections.

The m closed-loop asymptotically infinite eigenvalues determined by the m frequencies λ_i^∞ may be selected to achieve given bandwidth requirements on the inputs. As an example, for a two-input system with the actuator corresponding to input 1, ten times as fast as that for input 2, then $\lambda_1^\infty = 10\lambda_2^\infty$. The frequency λ_1^∞ may also be normalized, so $\lambda_1^\infty = -1$ and $\lambda_2^\infty = -0.1$. The vectors \underline{v}_i^∞ may be chosen so that the associated inputs are decoupled at high frequency. That is, the matrix N may be defined to be a diagonal matrix. An alternative method of selecting the m-pairs $(\lambda_i^\infty, \underline{v}_i^\infty)$ is to consider the desired output bandwidth and interaction. Define the asymptotic output directions as:

$$\underline{y}_i^\infty = C\underline{x}_i^\infty = CB\underline{v}_i^\infty \quad (2.56)$$

where $i = \{1, 2, \dots, m\}$. Since CB was assumed full-rank

$$\underline{v}_i^\infty = (CB)^{-1}\underline{y}_i^\infty \quad (2.57)$$

and thus the vectors \underline{y}_i^∞ may be chosen so that there is low interaction in the outputs between the fast and slow mode terms. That is, if

$M \triangleq [\underline{y}_1^\infty, \underline{y}_2^\infty, \dots, \underline{y}_m^\infty]$ then M may be defined to be a diagonal matrix.

Example 2 Output Regulator Problem

Consider the open-loop system discussed by Moore [40]. The system matrices are defined as:

$$A = \begin{bmatrix} -1.25 & 0.75 & -0.75 \\ 1 & -1.5 & -0.75 \\ 1 & -1 & -1.25 \end{bmatrix}$$
$$B = \begin{bmatrix} 1 & 0 \\ 0 & 1 \\ 0 & 1 \end{bmatrix} \quad C = \begin{bmatrix} 1 & 0 & 0 \\ 0 & 0 & 1 \end{bmatrix}$$

Let the weighting matrix $G = G^T$ and note that $CB = I_2$. This plant is stabilizable but not controllable. For a finite-gain non-optimal system Moore chooses the following desired output directions:

$$\underline{y}_1' = Cx_1 = \begin{bmatrix} -0.9 \\ 0.32 \end{bmatrix}$$

$$\underline{y}_2' = Cx_2 = \begin{bmatrix} 1 \\ 0.1 \end{bmatrix}$$

corresponding to desired modes $\lambda_2 = -5$ and $\lambda_3 = -6$, respectively. These are taken below as the required asymptotically-infinite output directions and modes, and the Q and R matrices are determined.

For this problem $CB = I_2$ and $\underline{v}_i^\infty = \underline{y}_i^\infty$ thence

$$N = \begin{bmatrix} -0.9 & 1 \\ 0.32 & 0.1 \end{bmatrix}$$

and from (2.56)

$$Q = (N^T)^- N^- = (NN^T)^- = \begin{bmatrix} 0.6687 & 1.1184 \\ 1.1184 & 10.767 \end{bmatrix} \quad (2.58)$$

$$R = (N^T)^{-1} \Lambda^\infty N^{-1} = \begin{bmatrix} 0.0193 & 0.0238 \\ 0.0238 & 0.3718 \end{bmatrix}$$

Note that

$$C^T Q C = \begin{bmatrix} 0.6687 & 0 & 1.1184 \\ 0 & 0 & 0 \\ 1.1184 & 0 & 10.767 \end{bmatrix}$$

and thus in the equivalent state regulator problem state 2 is not weighted.

The time responses for this system are shown in figures 4 to 4e and these responses are discussed in the next section.

2.7 Asymptotically Finite Modes

The expressions for the matrices Q and R were obtained by considering the behaviour of the m asymptotically infinite modes. The equations which determine these modes and the associated closed-loop eigenvectors were also obtained before. In the following the significance of the remaining (n-m) asymptotically finite eigenvalues and eigenvectors is discussed and the defining equations are obtained. This set of eigenvalues contains any uncontrollable modes. The relationship between the asymptotically finite closed loop poles (also referred to as optimal finite zeros) and the system zeros has been discussed by Kouvaritakis [38] and is summarised below.

Theorem 2.2 Asymptotically Finite Modes

The asymptotically finite closed-loop poles of a square minimum phase system $S(A,B,C)$ are equal to the zeros of $S(A,B,C)$. The asymptotically finite closed-loop poles of a square non-minimum phase system $S(A,B,C)$ are given by the union of the set of left-half plane zeros of $S(A,B,C)$ together with the set of the mirror images of the right-half plane zeros of $S(A,B,C)$ about the imaginary axis.

Proof: The proof given by Kouvaritakis [38] depends upon the augmented system $S(A^*,B^*,C^*)$ defined in appendix 1. The system zeros are defined in appendix 3.

Note that the cross-product weighting matrix does not affect the above results (Appendix 1) even when the assumption made in section 2.5 does not hold.

It will now be shown that if the plant is assumed to be minimum phase the asymptotically finite eigenvectors lie within the kernel of C. Thus uncontrollable modes for example, will not be present in the output responses which is a highly desirable practical objective. The following theorem, developed by Kwakernaak [41], is now required on

the maximum achievable accuracy of regulators.

Theorem 2.3 Maximum Achievable Accuracy

Consider the stabilizable and detectable linear system 2.1, 2.2 (B and C full rank) with criterion 2.36 ($Q, R > 0$ and $G = 0$) then $\lim_{\mu \rightarrow 0} J(\underline{u}) = 0$, if and only if, the transmission zeros of $S(A,B,C)$ lie in the open left-half complex plane [41, 42]

Corollary 1 Asymptotically Finite Eigenvector Directions

The asymptotically-finite eigenvector directions $\{\underline{x}_j^0\}$ for the minimum phase plant $W(s)$ lie within the kernel of C, that is $C\underline{x}_j^0 = 0$, for $j \in \{1, 2, \dots, n-m\}$.

Proof: The output may be expressed [40] in terms of the eigenvalues λ_j (the asymptotically finite eigenvalues are assumed distinct) and eigenvectors \underline{x}_j as follows:

$$\underline{y}(t) = \sum_{j=1}^n C\underline{x}_j (p_j^T \underline{x}_0) e^{\lambda_j t} \quad (2.59)$$

where $[p_1 \ p_2 \ \dots \ p_n]^T = [\underline{x}_1 \ \underline{x}_2 \ \dots \ \underline{x}_n]^{-1}$. Assume now that $C\underline{x}_k \neq 0$ and since \underline{x}_0 is arbitrary, assume that the output contains a non-zero term in $e^{\lambda_k t}$. Each output component is therefore composed of n linearly-independent terms on $C(0, \infty)$ and at least one component must include a term in $e^{-\lambda_k t}$. The cost-function weighting matrix $Q > 0$ and thus $\lim_{\mu \rightarrow 0} J(\underline{u}) \neq 0 \Rightarrow W(s)$ is not minimum phase. It follows from the contradiction that $C\underline{x}_k = 0$.

Corollary 2 First Order Multivariable Structure

The closed-loop transfer function matrix $T(s)$ for the square system $S(A-BK^\infty, B, C)$ is of first-order type [43, 44].

Proof: The closed-loop eigenvalues are assumed distinct and thus the matrix $A-BK^\infty$ has a simple diagonal structure and $T(s)$ may be expressed in the dyadic form:

$$T(s) = \sum_{i=1}^n \frac{C \underline{x}_i z_i^T B}{(s + \lambda_i)} = \sum_{j=1}^m \frac{\alpha_j}{(s + \lambda_j)} \underline{y}_j \beta_j^T \quad (2.60)$$

where the set of dual eigenvectors is denoted by $\{\underline{z}_i\}$ and the asymptotically finite eigenvectors (belonging to the kernel of C) have been omitted in the second summation. A square multivariable system that has the dyadic structure in 2.60 was defined by Owens [43] to be of first-order type.

Theorem 2.4 Asymptotically Finite Eigenvector Directions

Consider the optimal control problem described in theorem 2.3 and assume that the plant $S(A,B,C)$ is minimum phase, and the assumptions given in section 2.5 hold. The $(n-m)$ asymptotically finite eigenvalues and eigenvectors are related to the system zeros and zero directions as follows:

- (a) The $(n-m)$ asymptotically finite eigenvalues $\{\lambda_j^0\}$ are equal to the $(n-m)$ zeros of the system $S(A,B,C)$.
- (b) The asymptotically finite eigenvector \underline{x}_j^0 , corresponding to the eigenvalue λ_j^0 , is identical (except possibly for magnitude) to the state zero direction $\underline{\omega}_j^0$, corresponding to the zero λ_j^0 .
- (c) The asymptotically finite input vector $\underline{v}_j^0 \triangleq -K^\infty \underline{x}_j^0$ is identical (except possibly for magnitude) to the input zero direction $\underline{\sigma}_j^0$, corresponding to the zero λ_j^0 .

Proof: Part (a) follows immediately from theorem 2.1. From corollary 1 of previous section the asymptotically finite eigenvalue λ_j^0 and eigenvector \underline{x}_j^0 satisfy

$$(\lambda_j^0 I - A + BK^\infty) \underline{x}_j^0 = 0 \quad |\lambda_j^0| < \infty \quad (2.61)$$

$$C \underline{x}_j^0 = 0, \quad \text{for } j \in \{1, 2, \dots, n-m\} \quad (2.62)$$

The definitions of zeros and zero directions are given in appendix 3. Note that the above equations are satisfied for a given limiting gain

matrix K^∞ (as $\mu \rightarrow 0$). It follows from theorem A3.2 in appendix 3 that λ_j^0 is a zero of the system $S(A,B,C)$ and \underline{x}_j^0 is the corresponding state zero direction. Conversely, if $(\lambda_j^0, \underline{x}_j^0)$ denotes a zero and state zero direction of the system $S(A,B,C)$ and if this zero is assumed to have unit algebraic and geometric multiplicity [45], then the vector $\underline{\omega}_j^0$ is unique (except for magnitude). Thus, identify $\underline{\omega}_j^0 = \underline{x}_j^0$ and part (b) of the theorem follows. Finally, part (c) of the theorem follows from a similar argument, given the above assumption.

The following theorem holds for a more restrictive set of conditions.

Theorem 2.5 (Harvey and Stein [35], 1978)

Consider the LQP optimal control problem described in section 2 with the additional assumptions that the plant is controllable and observable and minimum-phase. Also assume that the transmission zeros of $W(s)$ do not belong to the spectrum of A and are distinct. As $\mu \rightarrow 0$ the $(n-m)$ finite closed-loop eigenvalues $\{\lambda_j^0\}$ and associated input vectors \underline{v}_j^0 are defined by:

$$W(\lambda_j^0)\underline{v}_j^0 = 0 \quad |\lambda_j^0| < \infty \quad (2.63)$$

and the corresponding closed-loop eigenvectors \underline{x}_j^0 are given by:

$$\underline{x}_j^0 = (\lambda_j^0 I_n - A)^{-1} B \underline{v}_j^0 \quad (2.64)$$

for $j \in \{1, 2, \dots, n-m\}$.

Proof: From equations (2.40) and (2.45) the $(n-m)$ finite eigenvalues satisfy (as $\mu \rightarrow 0$)

$$W^T(-\lambda_j^0) Q W(\lambda_j^0) \underline{v}_j^0 = 0, \quad \text{for } j \in \{1, 2, \dots, n-m\} \quad (2.65)$$

The stable closed-loop eigenvalues must therefore satisfy (2.64).

The closed-loop eigenvector (2.65) follows directly from corollary

A2.1 and theorem A2.2 in appendix 2.

The results of this section for minimum phase plants may be summarised as follows. As $\mu \rightarrow 0$ (n-m) closed-loop eigenvalues remain finite and approach either the transmission zeros of $W(s)$ or invariant zeros of $S(A,B,C)$. The system has the desirable characteristic that all uncontrollable modes (assumed less than n-m) become unobservable. The closed-loop transfer function matrix for the system, as $\mu \rightarrow 0$, has a simple dyadic structure and the system is of first-order type. The asymptotically finite eigenvector directions define (A,B) invariant subspaces [46,47] in the kernel of C.

The situation described above is not the same as that discussed in section 2.5, regarding the asymptotically-infinite modes. These modes and the corresponding eigenvectors are determined by the weighting matrices which are specified by the designer (via the $(\lambda_i, \underline{v}_i)$ pairs). However, the asymptotically finite modes are determined by the plant structure. The zeros and zero directions may only be varied by changing the combinations of inputs and outputs from the plant which may not be possible. The above results are nevertheless useful in design since they allow the (n-m) asymptotically closed-loop eigenvalues and eigenvectors to be calculated before the weighting matrices are chosen.

Example 3 Calculation of the Asymptotically Finite Modes

The finite zeros and zero directions, for the output regulator problem may be determined using the results of Kouvaritakis and MacFarlane [48]. The invariant zeros are found by determining matrices N and M such that $NB = 0$, $CM = 0$ and $NM = I_{n-m}$, and then computing the eigenvalues of the matrix NAM . Thence, $NAM = -0.5$ and the system has the invariant zero $s_1 = -0.5$. [49]. Notice that this zero corresponds with the position of the uncontrollable mode. The transfer-function matrix has the form:

$$W(s) = \frac{1}{\rho_0(s)} \begin{bmatrix} (s + 0.5)(s + 2.25) & 0 \\ (s + 0.5) & (s + 0.5)(s + 1.25) \end{bmatrix}$$

where $\rho_0(s) = (s + 0.5)(s + 1.25)(s + 2.25)$. Clearly the assumption that the zero does not belong to the spectrum of A does not hold in this example. The state and control zero directions can be found from the more general theorem 2.4. These directions may be calculated as follows:

$$\begin{bmatrix} s_1 I - A & B \\ C & 0 \end{bmatrix} \begin{bmatrix} \underline{x}_1 \\ \underline{\sigma}_1 \end{bmatrix} = 0$$

thence

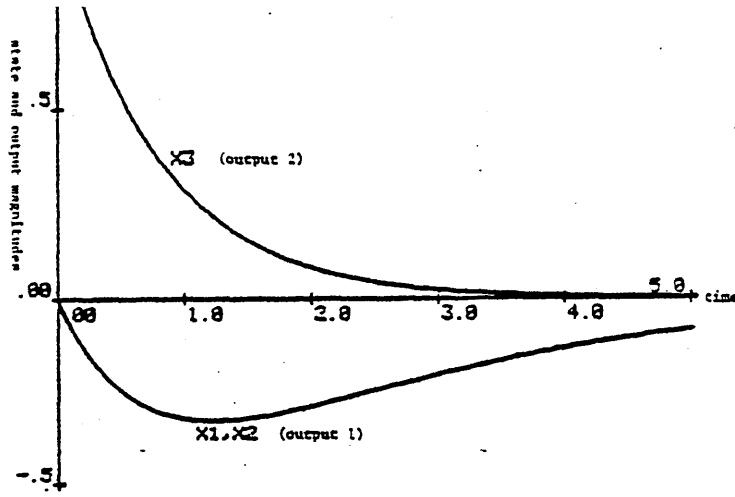
$$\underline{x}_1 = [0 \quad 4 \quad 0]^T$$

$$\underline{\sigma}_1 = [3 \quad -4]^T$$

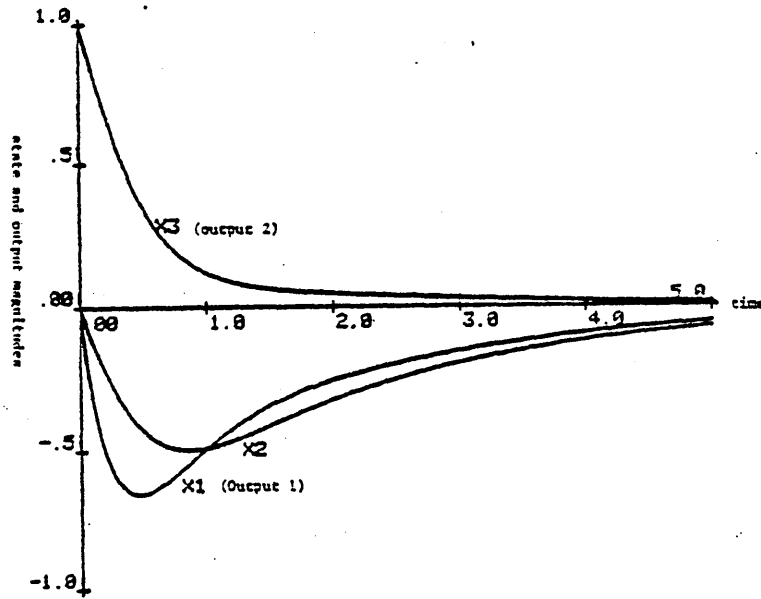
The above invariant zero is also an input decoupling zero for the plant (the number of input decoupling zeros = rank defect of the controllability matrix = 1).

The time responses for various values of μ , are shown in figures 4d to 4e. The initial state is assumed to be $\underline{x}_0 = (0 \quad 0 \quad 1)^T$. As μ tends to zero the two outputs tends to zero almost everywhere. However, the uncontrollable mode has a dominant influence on state 2. This clearly indicates that the eigenvector corresponding to the uncontrollable

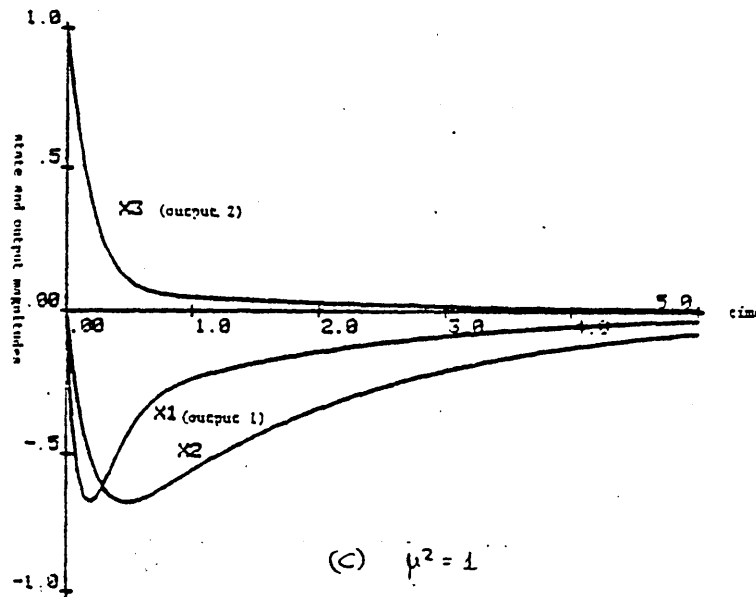
mode belongs to the kernel of C . It is also evident that this eigenvector direction does not change significantly for finite non-zero μ , since the uncontrollable mode does not dominate the outputs for such values of μ . The system responses compare favourably with those obtained by Moore [40]:



(a) $\mu^2 \rightarrow \infty$



(b) $\mu^2 = 10$



(c) $\mu^2 = 1$

Fig. 4: State and Output Responses

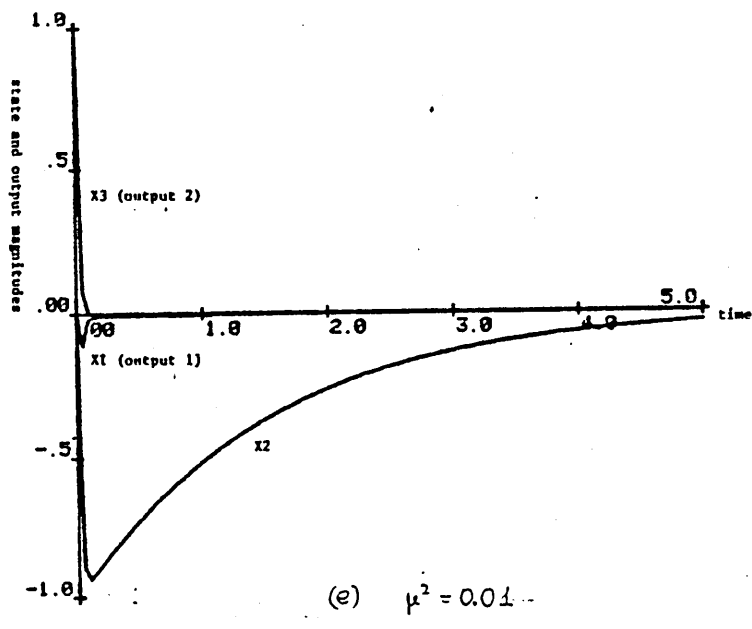
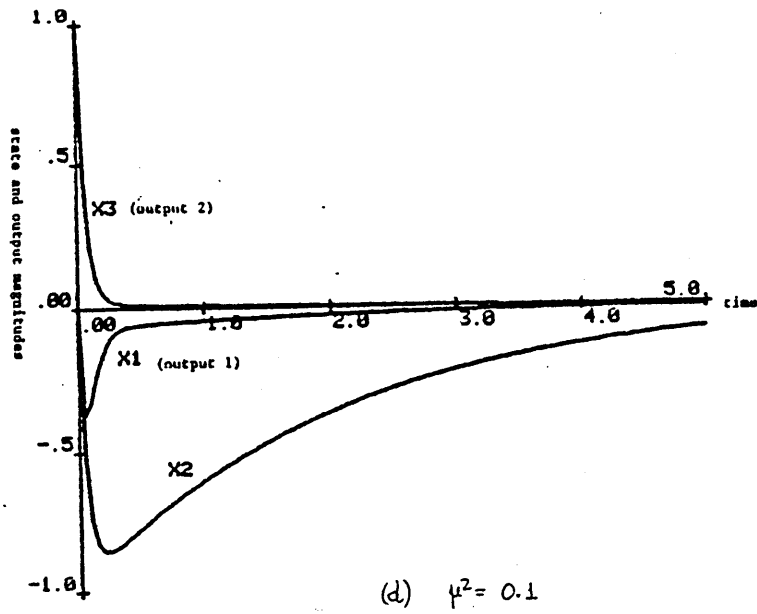


Fig. 4: State and Output Responses

2.8 Locus of the Closed Loop Poles as μ Varies

An initial finite-value for μ may be selected by choosing the distance of the faraway closed-loop poles to the origin and by using the relationship established in Appendix 4. If for example this radius or distance is chosen as r_f , then μ_f becomes:

$$\mu_f = \frac{1}{r_f} (\alpha^2 \det Q / \det R)^{\frac{1}{2}m} \quad (2.66)$$

where α is the coefficient of s^m in the zero polynomial $W(s)$; that is, $\alpha = \det CB$. In example 2 $\det Q = 5.95$, $\det R = 0.00661$, $r_f = 5.5$, $m = 2$ and $\alpha = 1$, thence $\mu_f = 0.996$ (Figure 5).

The values of Q , R and μ_f so defined, are good starting points for a design, however, it is very likely that the value of μ_f will need modification. A suitable value for μ_f may be selected from optimal root-loci plots for the system [53, 55]. The root-loci start at the points for which $\mu \rightarrow \infty$, which correspond to low feedback gains. In this case the closed-loop poles approach either the open-loop stable poles for the plant, or the mirror images of the open-loop unstable poles. These results are summarized in Appendix 2.5. The root-loci tend towards either the plant zeros or the infinite zeros, as $\mu \rightarrow 0$. This case was discussed in previous sections and corresponds to the use of high state-feedback gains [50].

It is clearly desirable to have an efficient root locus plotting program. Such a program may be developed using the primal-dual system discussed in Appendix 1 and a multivariable root locus plotting package (as discussed by Kouvaritakis and Shaked [51]). However, in the present design method the alternative approach of calculating the eigenvalues of the closed loop system matrix $A_c = A - BK$ is more desirable, since eigenvectors may also be easily calculated. Efficient algorithms are readily available for eigenvalue/eigenvector calculations.

The gain calculation poses more of a problem since the gain must be calculated for each value of μ . An approximate expression for the gain matrix is obtained in Appendix 6 and this enables the solution of the steady-state Riccati equation, for each μ_n , to be avoided. The results in this Appendix are particularly useful for hand calculations when μ is small.

For machine computation a more efficient method of calculating the optimal gain matrix $K(\mu)$ is required than repeatedly solving the steady state Riccati equation. Such a technique based upon a parameter imbedding solution of the Riccati equation, due to Jamshidi et al [56 - 58] is summarised in Appendix 7. This approach enables the gain matrix to be calculated for all values of μ within some interval $[\mu_0, \mu_T]$ and involves only the solution of one steady-state Riccati equation and one ordinary differential equation.

2.9 The Case When CB is Not Full Rank

The situation when the first Markov parameter (CB) is not full rank is in general much more complicated than that described previously. The equations which determine the Q and R weighting matrices may still be derived but the Q matrix must be calculated using an iterative algorithm. However, there is an important class of special cases where some of the Markov parameters are not full rank and yet the weighting matrix calculations are again relatively straightforward. For simplicity in the following assume that the weighting matrix $G = 0$.

Consider the situation where the first two Markov parameters are zero (as in the following example), that is $M_0 = CB = 0$ and $M_1 = CAB = 0$. At least m closed loop poles approach infinity as μ tends to zero [37] and these are determined by the higher order terms in equation 2.47:

$$\mu^2 F^T(-s)RF(s) = \mu^2 \left(R - \frac{1}{\mu^2 s^6} ((CA^2B)^T QCA^2B + O(1/s)) \right) \quad (2.67)$$

Assume $s_3 = \mu s^3$ remains finite as $\mu \rightarrow 0$, then

$$F^T(-s)RF(s) \rightarrow \left(R - \frac{1}{s_3^2} ((CA^2B)^T QCA^2B) \right) \quad (2.68)$$

If CA^2B is of full rank then the analysis in section 2.5 may be repeated to obtain:

$$Q = ((CA^2BN)^T)^{-1} (CA^2BN)^{-1} \quad (2.69)$$

$$R = (N^T)^{-1} \Lambda_3^\infty N^{-1} \quad (2.70)$$

where

$$\Lambda_3^\infty \triangleq \text{diag} \{ 1/(\lambda_1^\infty)^6, 1/(\lambda_2^\infty)^6, \dots, 1/(\lambda_m^\infty)^6 \} \quad (2.71)$$

In the more general case where the first k Markov parameters are zero and $M_k = CA^k B$ is full rank, the above expressions become:

$$Q = ((CA^k BN)^T)^{-1} (CA^k BN)^{-1} \quad (2.72)$$

$$R = (N^T)^{-1} \Lambda_{k+1}^\infty N^{-1} \quad (2.73)$$

where

$$\Lambda_{k+1} \triangleq (-1)^k \text{diag} \left\{ (1/\lambda_1^\infty)^{2(k+1)}, \dots, (1/\lambda_m^\infty)^{2(k+1)} \right\}$$

Systems of the above type have more than k cascaded dynamical elements between the inputs and the outputs (recall that $M_k = \lim_{s \rightarrow \infty} s^{k+1} W(s)$).

Example 4 Dynamic Ship Positioning Control System

This example is based upon the dynamic ship positioning control problem described in detail in Chapter 5. From the state space equations we note that $C_\ell B_\ell = 0$, $C_\ell A_\ell B_\ell = 0$ but $C_\ell A_\ell^2 B_\ell$ is full rank reflecting the fact that there are three dynamic cascaded elements between inputs and outputs. Thus,

$$C_\ell A_\ell^2 B_\ell = \begin{bmatrix} 0.84243 & 0.4216 \\ 5.0654 & -2.5327 \end{bmatrix}, \quad \det(C_\ell A_\ell^2 B_\ell) = -4.2692$$

and the weighting matrices may be calculated using the previous results.

Consider the case when the control signal for the first input must be 1.5 times faster than that for the second input. For non-interaction between the two sets of third order modes choose $N = I_2$ and let $\lambda_1^\infty = 1.5$, $\lambda_2^\infty = 1$.

From 2.69 to 2.7

$$\Lambda_3^\infty = \text{diag} \left\{ (1/\lambda_1^\infty)^6, (1/\lambda_2^\infty)^6 \right\} = \text{diag} \{0.08779, 1.0\}$$

$$R = \Lambda_3^\infty = \text{diag} \{0.08779, 1.0\}$$

$$Q = \begin{bmatrix} 1.75974 & -0.175545 \\ -0.175545 & 0.04869 \end{bmatrix}$$

and $\det Q = 0.05487 > 0$. The dominant time constant for the closed-loop system should be approximately 10 seconds. A suitable value of μ^2 is 1.

For inputs responding with the same speed choose $\lambda_1^\infty = \lambda_2^\infty = 1$. Then Q remains as above but $R = \text{diag} \{1.0, 1.0\}$. (For time response plots see Chapter 5.)

.10 Conclusions

A design method has been described for optimal output regulating systems which enables the performance criterion weighting matrices to be specified. The designer chooses a desired set of input directions, corresponding to the fast modes, and a desired set of eigenvalues $\{\lambda_i^\infty/\mu\}$. There are various ways of selecting these quantities. For example, the eigenvalues may be chosen to achieve relative bandwidth requirements and the corresponding input vectors may be chosen to decouple the modes.

After Q and R are specified there remains freedom in the choice of the cross-product weighting matrix G and in the selection of μ . The G matrix may of course be set to zero if desired and μ may be calculated using (2.66). However, it is better to select this latter quantity using an optimal root loci diagram for the system. The most desirable set of closed-loop eigenvalues may then be determined.

A feature of the above design method is its simplicity, however, additional design objectives may be met with some increase in complexity. For example, by modifying the performance criterion appropriately a desired degree of stability may be achieved for all values of μ . Alternatively, after selecting Q, R and μ the closed loop eigenvalues may be shifted to more desirable locations using the technique developed by Solheim

The design method results in a system which has very desirable characteristics under the limiting condition $\mu \rightarrow 0$. The hope must be that the system maintains these characteristics as μ increases and examples have indicated that this is the case. This is a point which clearly deserves more investigation. An important asymptotic property of the optimal system is that uncontrollable modes become unobservable. The remaining closed loop eigenvalues lie on the negative real axis and can

be made fast as desired by letting $\mu \rightarrow 0$. The closed loop transfer function matrix for the system has a simple dyadic structure and is of first order type in this limiting case.

There are several areas for future research. For example, if the plant is non-minimum phase the results given in section 5 regarding the asymptotically finite eigenvector directions and input directions do not apply. Current research is concerned with the situation discussed in section 7 where some of the Markov parameters are rank deficient. The additional freedom offered by the G matrix will be illustrated in a future applications paper on ship positioning.

A further useful property of the system described above is that the system would have a known degree of robustness to parameter variations [101]. As described recently by Postlethwaite et al [99] and Sofonov et al [100] the robustness of a closed loop system can be quantified by the use of the return difference singular values (principal gains). A modification to the design algorithm steps would be to use the above ideas instead of the time response simulation. Thus, to decide upon the weighting matrices selection through an iterative procedure which provides the closed loop system with the desired frequency response characteristics and also good disturbance rejection properties.

3.1 Introduction

A new method of solving finite-time optimal control and filtering problems in the complex frequency domain has been introduced recently by Grimble [61-66]. The approach has enabled new optimal finite-time filters and smoothing filters to be defined having properties somewhere between those of the Kalman and the Wiener filters [64-66]. The solution of the finite-time optimal control problem in the s-domain (for continuous time plants) provided useful s-domain forms for the controllers.

In the following the discrete-time optimal control problem is considered for a finite optimisation interval. This work was prompted by current interest in self-tuning regulators and the discussions in the literature concerning various control strategies [67-68]. The object is to provide a derivation of the z-domain optimal controller and to give an example of the calculation procedure.

It is known that a closed form solution to the infinite-time optimal control problem can be obtained by working in the z-domain [69]. An equivalent result is obtained here for the solution to the finite-time optimal control problem. This is the first general solution, to the finite-time free end point problem, obtained in the z-domain. The results are very similar for the two cases and the solution to the finite-time problem includes the solution to the infinite-time problem. The technique described allows for the presence of an end-state weighting term in the cost function. The method of solution can also be modified to deal with the finite-time problem where either some or all of the states at the final time are specified [63].

The derivation of the expression for the optimal control is obtained as follows. The time-domain gradient of the cost function is calculated

and this is equated to zero to obtain the optimum. This equation is transformed into the Z-domain using the Z-transformation and is solved for the optimal open loop control. If the optimal closed-loop system is required the time varying feedback gain matrix can be obtained from this Z-domain result, using the initial value theorem.

3.2 The Plant Description

The constant linear system to be controlled may be represented in either discrete state equation form or in convolution summation form. It is important to note that a state space description of the plant is not necessary and that a transfer function model is all that is required. However, it will be convenient to introduce the problem using a state equation model. The relationship between the z-domain solution for the optimal control signal and the usual state feedback solution, via the Riccati equation, may then be established.

To ensure the controllers are stable, in the limiting case where $T \rightarrow \infty$, it is assumed that the plant is stabilizable and detectable [14] and may be represented by the system S(A,B,C):

$$\underline{x}(i+1) = A\underline{x}(i) + B\underline{u}(i-k_0), \quad \underline{x}(0) = \underline{x}_0 \quad (3.1)$$

$$\underline{y}(i) = C\underline{x}(i) \quad (3.2)$$

$$\underline{z}(i) = C_0\underline{x}(i), \quad \text{for } i = \{0,1,2,\dots\} \quad (3.3)$$

The time delay $k_0 \Delta$ ($k_0 < N$) is an integer time increment and the vectors $\underline{x}(i) \in R^n$, $\underline{u}(i) \in R^m$ and $\underline{y}(i) \in R^r$. The matrix $C_0 \triangleq C$ in the output regulator problem and $C_0 \triangleq I_n$ in the state regulator problem.

The state trajectory may be calculated, for all $i > 0$, using the convolution summation:

$$\underline{x}(i) = \Phi(i)A\underline{x}_0 + \sum_{j=0}^{i-1} \Phi(i-j)B\underline{u}(j-k_0) \quad (3.4)$$

where

$$\Phi(i) \triangleq A^{i-1}U(i-1) \quad (3.5)$$

where $U(k)$ is the unit step function i.e zero for all $k < 0$ and 1 for $k \geq 0$

and $\Phi(1) = I_n$, $\Phi(i) = 0$ for $i \leq 0$. Equation (3.4) defines $\underline{x}(i)$ for all $i > 0$. For other values of time, outside the optimisation interval, $\underline{x}(i) \underline{\Delta} 0$. The state response is given in operator form as follows:

$$\underline{x}(i) = \underline{d}_0(i) + (D_0 W_0 \underline{u})(i) \quad (3.6)$$

where

$$\underline{d}_0(i) \underline{\Delta} \Phi(i+1) \underline{x}_0 \quad (3.7)$$

$$(W_0 \underline{u})(i) \underline{\Delta} \sum_{j=0}^{i-1} \Phi(i-j) B \underline{u}(j) \quad (3.8)$$

$$(D_0 \underline{u})(i) \underline{\Delta} \underline{u}(i-k_0) \quad (3.9)$$

Similarly the system response to be controlled, is given by:

$$\underline{z}(i) = \underline{d}(i) + (D_0 W \underline{u})(i) \quad (3.10)$$

where $\underline{d}(i) \underline{\Delta} C_0 \underline{d}_0(i)$, $(W \underline{u})(i) \underline{\Delta} (C_0 W_0 \underline{u})(i)$ and the weighting sequence,

$$\begin{aligned} w(i) &\underline{\Delta} C_0 \Phi(i) B \\ &\underline{\Delta} 0 \quad \text{for all } i \leq 0 \end{aligned}$$

An adjoint equivalent of the system operator is calculated in Appendix 9 and has the form:

$$(W^* \underline{e})(i) = \sum_{k=i+1}^{\infty} w^T(k-i) \underline{e}(k) \quad (3.11)$$

The impulse response of the adjoint system is $w^T(-i) = 0$ for all $i \geq 0$, and the adjoint system is non-causal. The adjoint of the delay operator is defined in Appendix 10 as:

$$(D_0^* \underline{u})(i) = \underline{u}(i+k_0) \quad (3.12)$$

3.3 The Performance Criterion and Control Problem

The performance criterion to be minimised is quadratic and is measured over a finite time interval [70]. The criterion includes tracking error and control terms:

$$J(0,N) = \underline{e}^T(N)F\underline{e}(N) + \sum_{i=0}^{N-1} (\underline{e}^T(i+1)Q\underline{e}(i+1) + \underline{u}^T(i)R\underline{u}(i)) \quad (3.13)$$

where the constant, symmetric weighting matrices $F, Q \geq 0$ and $R > 0$. The criterion may be re-written in a more convenient form by ensuring $\underline{e}(0) = 0$.

Then (3.13) becomes:

$$J(0,N) = \sum_{i=0}^N (\underline{e}^T(i)Q_1\underline{e}(i) + \underline{u}^T(i)R\underline{u}(i)) \quad (3.14)$$

where

$$Q_1 \triangleq Q + F\delta(i-N) \quad (3.15)$$

and $\delta(i)$ is the Kronecker delta function $\delta(i) \triangleq 0$ for $i \neq 0$ and $\delta(0) = 1$.

Since the optimal control $\underline{u}(N) = 0$ the criteria (3.13) and (3.14) are equivalent despite the unit time shift. Let the specified response of the system, within the interval $i \in [1, N]$ be denoted by $z_{d_1}(i)$, and let the error signal $\underline{e}(i) \triangleq z_{d_1}(i) - \underline{z}(i)$ for $i \in [1, N]$.

The calculation of the optimal control law has a much simpler form if the optimisation interval is $[0, \infty]$ instead of $[0, N]$. Therefore the finite-time problem is embedded in an artificial infinite-time problem. If the desired response $z_d(i)$ is chosen appropriately both problems have the same solution for the optimal control in the finite interval $[0, N-1]$. Choose $z_d(i)$ as follows:

$$\underline{z}_d(i) = \underline{z}_{d_1}(i)(U(i-1) - U(i-N-1)) + C_0\phi(i-N)U(i-N-1)\underline{x}_{-n+1} \quad (3.16)$$

The last term in (3.16) represents the free response of the system

$C_0\phi(i-N)\underline{x}_{-n+1}$ for $i > N$. The error signal

$$\underline{e}(i) \triangleq \underline{z}_d(i) - \underline{z}(i)$$

is clearly zero for all $i > N$, when $\underline{u}(i) = 0$ for all $i \geq N$. Clearly the

optimal control signal $\underline{u}(i) = 0$ for all $i \geq N$. Also note that the terminal condition \underline{x}_{n+1} is unknown but $\underline{x}_{n+1} = A\underline{x}_n$, and \underline{x}_n may be calculated. The fact that the optimal control signal is zero for $i \geq N$ ensures that the control which minimizes $J(0, \infty)$:

$$J(0, \infty) \triangleq \lim_{n \rightarrow \infty} J(0, n)$$

within the time interval $[0, N-1]$, is the same as that which minimizes $J(0, N)$.

3.4 Necessary and Sufficient Condition for Optimality

The cost function is expressed below using Hilbert space notation.

The gradient of the cost function is then calculated using the usual variational argument [69]. Thus, from equation (3.14):

$$J(0, \infty) = \langle \underline{e}, Q_1 \underline{e} \rangle_{H_r} + \langle \underline{u}, R \underline{u} \rangle_{H_m} \quad (3.17)$$

where the inner product is defined as:

$$\langle \underline{e}, \underline{y} \rangle_{H_r} = \sum_{i=0}^{\infty} \langle \underline{e}(i), \underline{y}(i) \rangle_{E_r}, \quad (\text{for } \underline{e}, \underline{y} \in H_r) \quad (3.18)$$

For practical purposes the space H_r consists of those functions which are z-transformable.

The error function may be expressed in terms of the reference signal $\underline{r}(i) \triangleq \underline{z}_d(i) - \underline{d}(i)$ as:

$$\underline{e}(i) = \underline{r}(i) = (D_o W \underline{u})(i) \quad (3.19)$$

The cost function may now be written as:

$$\begin{aligned} J(0, \infty) &= \langle (\underline{r} - D_o W \underline{u}), Q_1 (\underline{r} - D_o W \underline{u}) \rangle_{H_r} + \langle \underline{u}, R \underline{u} \rangle_{H_m} \\ &= \langle \underline{u}, W^* Q_1 W \underline{u} \rangle_{H_m} - 2 \langle \underline{u}, W^* D_o^* Q_1 \underline{r} \rangle_{H_m} \\ &\quad + \langle \underline{r}, Q_1 \underline{r} \rangle_{H_r} + \langle \underline{u}, R \underline{u} \rangle_{H_m} \end{aligned} \quad (3.20)$$

Note that the following property of the delay operator (Appendix 10)

$$\langle D_o z, Q D_o z \rangle_{H_r} = \langle z, D_o^* Q D_o z \rangle_{H_r} = \langle z, Q z \rangle_{H_r} \text{ was used in simplifying (3.20).}$$

The Gradient of the cost function, with respect to \underline{u} , follows as:

$$\delta J = 2 \langle \underline{g}, \delta \underline{u} \rangle_{H_m} \quad (3.21)$$

giving

$$\underline{g} = (W^* Q_1 W + R) \underline{u} - W^* D_o^* Q_1 \underline{r} \quad (3.22)$$

$$= (W^* Q W + R) \underline{u} - W^* D_o^* Q \underline{r} - W^* D_o^* F \delta(i-N) \underline{e} \quad (3.23)$$

The final term in the gradient may be simplified as follows:

$$\begin{aligned}
(W^*D_0^*F\delta(i-N)\underline{e})(j) &= \sum_{k=j+1}^{\infty} w^T(k-j)F\delta(k+k_0-N)\underline{e}(k+k_0) \\
&= w^T(N-k_0-j)F\underline{e}(N)U(N-k_0-j-1) \\
&= w^T(N-k_0-j)\underline{c}
\end{aligned} \tag{3.24}$$

where the vector $\underline{c} \triangleq F\underline{e}(N)$ can be calculated once $\underline{x}_n = \underline{x}(N)$ has been determined. The gradient follows from (3.23) and (3.24) as:

$$\underline{g}(i) = ((W^*QW + R)\underline{u})(i) - (W^*D_0^*Q\underline{r})(i) - w^T(N-k_0-i)\underline{c} \tag{3.25}$$

It may be shown that a necessary and sufficient condition for optimality is that the gradient must be zero over the optimisation interval [71], that is

$$\underline{g}(i) = 0 \text{ for all } i \geq 0. \tag{3.26}$$

The solution for the optimal control signal is obtained below by transforming the expression for the gradient (3.26) into the z-domain. The transforms of each term are obtained in Appendices 10 to 12.

$$\begin{aligned} \underline{g}(z) = & (W^T(z^{-1})QW(z) + R)\underline{u}(z) - W^T(z^{-1})z^{k_0}Q\underline{r}(z) \\ & - W^T(z^{-1})z^{k_0} - \underline{N}_c \end{aligned} \quad (3.27)$$

The condition for optimality (3.26) is that the gradient should be zero for all positive time. Thus, the transform of the gradient over the positive time interval $\{\underline{g}(z)\}_+ = 0$, where

$$\underline{g}(z) = \{\underline{g}(z)\}_+ + \{\underline{g}(z)\}_- \quad (3.28)$$

and

$$\{\underline{g}(z)\}_+ = Z_2(\underline{g}(i)U(i)) = 0 \quad (3.29)$$

The control signal $\underline{u}(z)$ can also be expressed as the sum of realisable and non-realisable transforms:

$$\underline{u}(z) = \{\underline{u}(z)\}_+ + \{\underline{u}(z)\}_- \quad (3.30)$$

and since the optimal control signal is required to be realisable $\{\underline{u}(z)\}_- = 0$.

The matrix $(W^T(z^{-1})QW(z) + R)$ may be factorised using standard techniques [72, 73, 74]:

$$Y^T(z^{-1})Y(z) = W^T(z^{-1})QW(z) + R \quad (3.31)$$

The matrix $Y(z)$ is chosen to have a stable inverse and to have the same pole polynomial as $W(z)$. This type of spectral factor was defined by Shaked and is called a generalised spectral factor [75]. Define the matrix $M(z)$ as:

$$M(z) = W(z)Y(z)^{-1} \quad (3.32)$$

and note from equation (3.27):

$$Y^T(z^{-1})^{-1}\underline{g}(z) = Y(z)\underline{u}(z) - M^T(z^{-1})z^{k_0}(Q\underline{r}(z) + z^{-N_c}) \quad (3.33)$$

Let the final term in this equation be denoted by:

$$N(z) = M^T(z^{-1})z^{k_0}(Q\underline{r}(z) + z^{-N_c}) \quad (3.34)$$

$$\{Y^T(z^{-1})^{-1}\underline{g}(z)\}_+ = 0 \quad (3.35)$$

$$\{Y(z)\underline{u}(z)\}_+ = Y(z)\underline{u}(z) \quad (3.36)$$

The solution for the optimal control signal $\hat{u}(z)$ may be obtained by equating the transforms of positive time terms in equation (3.27) and by substituting from (3.35) and (3.36):

$$\hat{u}(z) = Y(z)^{-1}\{N(z)\}_+ \quad (3.37)$$

Assume that the reference signal $\underline{r}(z)$ is separated into terms containing z^{-N} and those not containing z^{-N} ,

$$\underline{r}(z) = \underline{r}_0(z) + \underline{r}_n(z)z^{-N} \quad (3.38)$$

Now define the following vectors:

$$\underline{n}_{11}(z) = \{M^T(z^{-1})z^{k_0}Q\underline{r}_0(z)\}_+ \quad (3.39)$$

$$\underline{n}_{12}(z) = \{M^T(z^{-1})z^{k_0-N}Q\underline{r}_n(z)\}_+ \quad (3.40)$$

$$\underline{n}_2(z) = \{M^T(z^{-1})z^{k_0-N}\underline{c}\}_+ \quad (3.41)$$

and note that from (3.37):

$$\hat{u}(z) = Y(z)^{-1}(\underline{n}_{11}(z) + \underline{n}_{12}(z) + \underline{n}_2(z)) \quad (3.42)$$

This is the desired expression for the open-loop optimal control signal. The first term is identical to that normally found for the solution of the infinite-time optimal control problem [76-79]. The remaining terms are introduced by the finite nature of the problem. If the end state weighting matrix is zero then $\underline{c} = 0$ and thence $\underline{n}_2(z) = 0$. The term $\underline{n}_{12}(z)$ has two functions. The first is to ensure the control signal is zero outside the interval $[0, N-1]$. This results from the problem specification which required that the solution of the finite-time problem be obtained from an equivalent infinite time problem. This equivalent problem was constructed so that the control would be zero outside the interval so that both problems would have the same solution. The second function of the $\underline{n}_{12}(z)$ terms is to modify the control within the interval to achieve an improved finite time performance.

3.6 Calculation of the Vector \underline{c} , Optimal System Response

The optimal control signal is completely determined by equation (3.42) given the vector \underline{c} . This vector depends upon the plant state at time $t = N\Delta$ and an expression is obtained below from which this may be calculated. From the transform of equation (3.6):

$$\underline{x}(z) = \underline{d}_0(z) + z^{-k_0} M_0(z) (\underline{n}_{11}(z) + \underline{n}_{12}(z) + \underline{n}_2(z)) \quad (3.43)$$

where $M_0(z) \triangleq W_0(z) Y(z)^{-1}$. From Appendix 3.4

$$\underline{n}_2(i) = m^T(N-k_0-i)\underline{c}, \quad \text{for } i \in [0, N-k_0-1] \quad (3.44)$$

Inverse transforming (3.43) and letting $\underline{n}_1(i) = \underline{n}_{11}(i) + \underline{n}_{12}(i)$ gives:

$$\begin{aligned} \underline{x}(i) = \underline{d}_0(i) + \sum_{j=0}^{i-k_0-1} m_0(i-k_0-j)\underline{n}_1(j) \\ + \sum_{j=0}^{i-k_0-1} m_0(i-k_0-j) m_0^T(N-k_0-j) C_0^T \underline{F} e(N) \end{aligned} \quad (3.45)$$

for $i \in [0, N]$. Now define the following summations:

$$I_1(i-k_0) = \sum_{j=0}^{i-k_0-1} m_0(i-k_0-j)\underline{n}_1(j) \quad (3.46)$$

$$I_2(i-k_0) = \sum_{j=0}^{i-k_0-1} m_0(i-k_0-j) m_0^T(N-k_0-j) \quad (3.47)$$

and

$$S(N - k_0) = I_2(N - k_0) \quad (3.48)$$

The state \underline{x}_n of the system at time $t = N\Delta$ may be calculated using equation (3.45), since

$$[I_n + S(N - k_0) C_0^T F C_0] \underline{x}_n = [\underline{d}_0(N) + I_1(N-k_0) + S(N-k_0) C_0^T F \underline{z}_d(N)] \quad (3.49)$$

Note that this equation may be simplified further by separating $I_1(N-k_0)$ into terms containing \underline{x}_n and those not containing this vector.

It is interesting to look at the modes in the system response to see how they are determined and how they differ in the finite time and infinite time problems. Let $P_0(z)$ be the characteristic polynomial of the plant $W(z)$ and let the polynomial $P_c(z)$ be defined by the equation:

$$P_c(z^{-1})P_c(z) = P_0(-z)P_0(z) |W^T(z^{-1})QW(z) + R| / |R| \quad (3.50)$$

From (3.31):

$$|Y(z)| = \sqrt{|R|} P_c(z)/P_o(z)$$

and from equation (3.32):

$$M(z) = W(z) \cdot \frac{\text{adj}|Y(z)|}{|Y(z)|} = \frac{W(z)P_o(z)}{P_c(z)} \cdot \frac{\text{adj}|Y(z)|}{\sqrt{|R|}} \quad (3.51)$$

The poles of the system $M(z)$ are the zeros of the polynomial $P_c(z)$.

From equation (3.45) the end point weighting term in \underline{c} will introduce both unstable and stable modes into the system response since it involves the system with impulse response $M(i)$ (and characteristic polynomial $P_c(z^{-1})$).

However, for the present consider the finite time problem where the system has zero initial state, the plant is stable and the end point is not

weighted (so that $\underline{c} = \underline{x}(0) = \underline{0}$). From equation (3.45) the response is then given by:

$$\underline{\hat{x}}(i) = \sum_{j=1}^{i-k_0-1} M(1-k_0-j) \underline{n}_{11}(j) + \sum_{j=1}^{i-k_0-j} M(i-k_0-j) \underline{n}_{12}(j) \quad (3.52)$$

In the previous section it was noted that the term $\underline{n}_{11}(j)$ is the same as that obtained in the usual infinite time optimal control problem, the first term in (3.52) must therefore contribute stable modes and the second term must be the source of the unstable modes that are present in finite time problems. Since the system $M(z)$ is necessarily stable it is clear that $\underline{n}_{11}(j)$ must contain only stable modes and the signal $\underline{n}_{12}(j)$ must contain the unstable modes. Equations (3.39) and (3.40) confirms this result:

$$\underline{n}_{11}(j) = Z^{-1} [\{M^T(z^{-1}) Q \underline{r}_0(z) z^{k_0}\}_+] \quad (3.53)$$

$$\underline{n}_{12}(j) = Z^{-1} [\{M^T(z^{-1}) Q \underline{r}_{-N}(z) z^{k_0-N}\}_+] \quad (3.54)$$

As described in the procedure for evaluating these terms in Appendix 12 $\underline{n}_{11}(z)$ contains stable terms corresponding to the poles of $\underline{r}_0(z)$ and $\underline{n}_{12}(z)$ contains unstable terms due to the adjoint system $M^T(z^{-1})$. The difference between the two cases is caused by the presence of the shift operator z^{-N} in equation (3.54) which moves the adjoint system response into the optimisation interval $[0, N]$, so that it contributes to $\underline{n}_{12}(j)$.

3.7 Algorithm for the Solution of the Finite Time Problem

The steps to be taken in the calculation of the optimal open loop control and the optimal trajectory are summarised as:

1. Find $Y(z)$ from $Y^T(z^{-1})Y(z) = W^T(z^{-1})QW(z) + R$
2. Find $M(z)$ $M(z) = W(z)[Y(z)]^{-1}$ and $M(j) = Z^{-1}[M(z)]$
3. Obtain $\underline{n}_{11}(z)$ from the partial expansion of $M^T(z^{-1})Q\underline{r}_0(z)z^{k_0}$ by selecting only those terms due to poles of $\underline{r}_0(z)$
4. Find $\underline{n}_{11}(i)$ from $\underline{n}_{12}(i) = Z^{-1}[\underline{n}_{11}(z)]$
5. Obtain $\underline{n}_{12}(z)$ from the partial expansion of $M^T(z^{-1})Q\underline{r}_N(z)z^{k_0}$ by selecting only those terms due to poles of $M^T(z^{-1})$
6. Calculate $\underline{n}_1(i) = \underline{n}_{11}(i) + \underline{n}_{12}(i)$ and $\underline{n}_1(z) = \underline{n}_{11}(z) + \underline{n}_{12}(z)$.
7. Calculate $I_1(i-k_0) \triangleq \sum_{j=1}^{i-k_0-1} M(i-k_0-j)\underline{n}_1(j)$
8. Calculate $I_2(i-k_0) \triangleq \sum_{j=1}^{i-k_0-j} M(i-k_0-j)M^T(N-k_0-j)$ and $S(N-k_0) = I_2(N-k_0)$
9. Solve for \underline{x}_n from (3.49):

$$[I_n + S(N-k_0)C_o^TFC_o]\underline{x}_n = d_o(N) + I_1(N-k_0) + S(N-k_0)C_o^TFZ_d(N)$$
10. Calculate $\underline{c} = F(\underline{x}_d(N) - \underline{x}_n)$, $\underline{n}_2(i) = m^T(N-1)\underline{c}$, $\underline{n}_2(z) = Z[\underline{n}(i)]$
11. Calculate $\hat{u}(z) = [Y(z)]^{-1}[\underline{n}_1(z) + \underline{n}_2(z)]$ and $\hat{u}(i) = Z^{-1}[\underline{u}(z)]$
12. Calculate $\hat{X}(i) = \underline{d}_o(i) + I_1(i-k_0) + I_2(i-k_0)\underline{c}$

The one sided and not the two sided Z transform is needed to obtain the solution for the optimal control. This results from the fact that the optimal control consists of the transforms of positive time signals and for this class of functions the single sided and two sided transforms coincide. Several steps of the above algorithm can often be omitted, for example if the end condition is not weighted then F , \underline{c} and $\underline{n}_2(z)$ are all zero.

3.8 A Tracking Problem

Consider the following linear time invariant system in discrete state equation form:

$$\underline{x}(i+1) = a\underline{x}(i) + \underline{u}(i) \quad |a| < 1$$

$$y(i) = c_1 \underline{x}(i)$$

The optimal control performance criterion to be minimised is defined as:

$$J(0,N) = e(N)F e(N) + \sum_{i=0}^{N-1} e^T(i+1)Qe(i+1) + u(i)Ru(i)$$

where $Q = q$, $R = 1$ and $F = f$ and the input time delay k_0 is less than N (for a non-trivial case). The reference input (desired output) is assumed to be a step of height H :

$$r(i) = \begin{cases} H & i \in [1, N] \\ 0 & \text{all other } i \end{cases}$$

The open loop control law is calculated first.

$$\phi(i) = a^{i-1}U(i-1) \quad \text{and} \quad \phi(z) = \frac{1}{z-a}$$

$$W_0(z) = C\phi(z)B = c/(z-a)$$

$$Y^T(z^{-1})Y(z) = W_0^T(z^{-1})QW_0(z) + R = \frac{(1 + 2c_1^2 + a^2) - az - az^{-1}}{(z^{-1} - a)(z - a)}$$

The numerator may be factorised into the form:

$$-az^{-1}(z^2 - (1 + qc_1^2 + a^2)z/a + 1) = -az^{-1}(z - \alpha)(z - 1/\alpha)$$

The spectral factor $Y(z)$ follows as:

$$Y(z) = \left(\frac{a}{\alpha}\right)^{\frac{1}{2}} \frac{(z - \alpha)}{(z - a)}$$

thus

$$M_0(z) = W_0(z)Y(z)^{-1} = \left(\frac{a}{\alpha}\right)^{\frac{1}{2}} \frac{c_1}{z - \alpha}$$

From equation (3.33) first calculate $N(z)_+ = \underline{n}_{11}(z) + \underline{n}_{12}(z) + \underline{n}_2(z)$ by substituting for $r_0(z)$, $r_n(z)$ as:

$$r(z) = r_0(z) + r_n(z)z^{-N} = H \frac{1}{z-1} (1 - z^{-N})$$

$$r_0(z) = \frac{1}{z-1} r_n(z) = \frac{-1}{z-1}$$

thence

$$\begin{aligned} n_{11}(z) &= \{M^T(z^{-1})z^k q r_o(z)\}_+ = \left\{ \left(\frac{\alpha}{a}\right)^{\frac{1}{2}} q H \frac{c_1}{z^{-1} - \alpha} z^k \frac{1}{z-1} \right\}_+ \\ &= \left(\frac{\alpha}{a}\right)^{\frac{1}{2}} c_1 q H \frac{-1/\alpha}{1 - 1/\alpha} \frac{1}{z-1} \end{aligned}$$

$$\begin{aligned} n_{12}(z) &= \{M^T(z^{-1})z^{k-N} q r_n(z)\}_+ = \left\{ \left(\frac{\alpha}{a}\right)^{\frac{1}{2}} q H z^{k-N} \frac{c_1}{z^{-1} - \alpha} \frac{-1}{z-1} \right\}_+ \\ &= -\left(\frac{\alpha}{a}\right)^{\frac{1}{2}} c_1 q H \left(\frac{-1/\alpha}{1/\alpha - 1} \frac{z^{-N+k} - z\alpha^{N-k+1}}{1 - \alpha z} + \frac{-1/\alpha}{(1 - 1/\alpha)} z^{k-N} \frac{1}{z-1} \right) \end{aligned}$$

In the case where the end point weighting is zero $\underline{c} = 0$ and $\underline{n}_2(z) = 0$.

Thus

$$\begin{aligned} \hat{u}(z) &= Y^{-1}(z) [\underline{n}_{11}(z) + \underline{n}_{12}(z) + \underline{n}_2(z)] \\ &= \left(\frac{\alpha}{a}\right)^{\frac{1}{2}} \frac{z-a}{z-\alpha} \left[\left(\frac{\alpha}{a}\right)^{\frac{1}{2}} c_1 q H \frac{-1/\alpha}{1 - 1/\alpha} \frac{1}{z-1} - \left(\frac{\alpha}{a}\right)^{\frac{1}{2}} c_1 q H \left(\frac{-1/\alpha^2}{1/\alpha - 1} \right. \right. \\ &\quad \left. \left. \frac{z^{-N+k} - z\alpha^{N-k+1}}{1 - \alpha z} + \frac{-1/\alpha}{1 - 1/\alpha} \frac{z^{k-N}}{z-1} \right) \right] \end{aligned}$$

The above expression for the open loop control may be written as

$$\hat{u}(z) = N_1(z)r_o(z) + N_2(z).H \quad (.55)$$

for which a closed loop expression can be derived, fig.3.1.

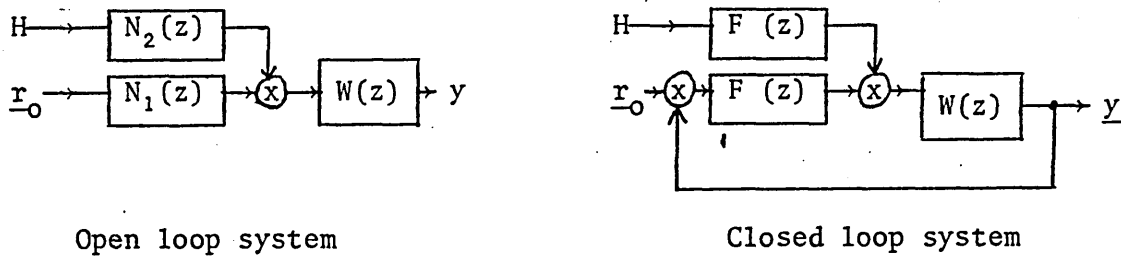


FIGURE 1

$$\hat{u}(z) = F_2(z)H + F_1(z)(r_o(z) - y(z)) = F_2(z)H + F_1(z)(r_o(z) - W(z)\hat{u}(z))$$

or

$$\hat{u}(z) = (I + F_1(z)W(z))^{-1}F_1(z)H + (I + F_1(z)W(z))^{-1}F_1(z)r_o(z) \quad (3.56)$$

by comparison to (3.55) we have

$$N_1(z) = (I + F_1(z)W(z))^{-1}F_1(z) \quad N_2(z) = (I + F_1(z)W(z))^{-1}F_2(z)$$

or

$$F_1(z) = N_1(z)(I - W(z)N_1(z))^{-1} \quad F_2(z) = (I + F_1(z)W(z))N_2(z) \quad (3.57)$$

This shows that a closed loop, output feedback solution is possible for the discrete tracking problem.

The above closed loop solution to the finite time optimal control problem is the first to use output feedback. The advantages of such a scheme in comparison with the more usual state feedback solutions are obvious [82]. Recall that the usual solution to the finite time servomechanism problem involves an optimal state feedback regulator with a time varying gain matrix, fed from a time varying block which represents the adjoint system equations. This latter block has an input from the reference signal. This realisation of the optimal controller is considerably more complicated than that proposed here.

The controllers F_1 , F_2 are time invariant and are therefore simple to implement, whereas the time-domain solution involves time varying feedback gain matrices. The question therefore arises why the solution presented here differs from the usual solution and if there are any disadvantages. The difference in the results is associated with the assumptions made regarding the initial state of the plant. In the above example this was assumed to be zero but it could have been included in the solution and would have resulted in an additional term in the control signal depending upon x_0 . The closed loop solution would have changed this term but would have still resulted in a signal to be added to the output of the controller F_1 depending upon the initial state.

In the event that the output matrix equals the identity matrix the expression for the control signal is the same as that obtained via the time-domain approach. However, the time invariant controller is obtained at the expense of adding the initial condition term. Now in tracking or servomechanism problems the response of the system to external reference inputs is of importance and the initial condition response may be neglected.

This assumption is based upon the observation that if the system has a fast closed loop response initial conditions will also be regulated efficiently (assuming a controllable plant). In these circumstances the z-domain controller has considerable advantages since it is simple, time invariant and is valid for output feedback systems.

3.9 A State Regulator Problem

In this section the state regulator problem is considered and an expression is obtained for the optimal control signal. For the state regulator $C_o = I_n$, $\underline{z}(i) = \underline{x}(i)$ and $\underline{x}_{d_1}(i) = 0$, for $i \in [1, N]$. Thus, from equation (3.16):

$$\underline{x}_d(i) = \Phi(i - N)U(i - N - 1)A\underline{x}_{-n} \quad (3.58)$$

The state reference can be defined as in section 3.4

$$\begin{aligned} \underline{r}(i) &= \underline{x}_d(i) - \underline{d}_o(i) && \text{(for } i > 0) \\ &= \Phi(i - N)U(i - N - 1)A\underline{x}_{-n} - \Phi(i)U(i - 1)A\underline{x}_o \end{aligned} \quad (3.59)$$

Now $\Phi(i) = A^{i-1}U(i - 1)$ and $Z_1(\Phi(i)) = \Phi(z)$, and $Z_1(\Phi(i - N)U(i - N - 1)) = z^{-N}\Phi(z)$. Thence

$$\underline{r}(z) = z^{-N}\Phi(z)A\underline{x}_{-n} - \Phi(z)A\underline{x}_o \quad (3.60)$$

$$\underline{r}_o(z) = -\Phi(z)A\underline{x}_o \quad (3.61)$$

$$\underline{r}_{-n}(z) = \Phi(z)A\underline{x}_{-n} \quad (3.62)$$

From (3.34) and (3.35):

$$\underline{n}_{11}(z) = f_1(z)\underline{x}_o \quad (3.63)$$

$$\underline{n}_{12}(z) = f_2(z, N)\underline{x}_{-n} \quad (3.64)$$

where

$$f_1(z) \triangleq -\{M_o^T(z^{-1})Q\Phi(z)Az^{k_o}\}_+ \quad (3.65)$$

$$f_2(z, N) \triangleq \{M_o^T(z^{-1})Q\Phi(z)Az^{k_o-N}\}_+ \quad (3.66)$$

The following summations may now be defined by substituting into equation (3.41):

$$I_{11}(N - k_o) = \sum_{j=0}^{N-k_o-1} m_o(N - k_o - j)f_1(j) \quad (3.67)$$

$$I_{12}(N - k_o) = \sum_{j=0}^{N-k_o-1} m_o(N - k_o - j)f_2(j, N) \quad (3.68)$$

The optimal control signal depends upon the state \underline{x}_{-n} which may be calculated as follows. From equation (3.44):

$$(I_n + S(N - k_0)F)\underline{x}_n = (\underline{d}_0(N) + I_{11}(N - k_0)\underline{x}_0 + I_{12}(N - k_0)\underline{x}_n$$

or if

$$\Psi(N, k_0) \triangleq (I_n - I_{12}(N - k_0) + S(N - k_0)F)^{-1}(\Phi(n + 1) + I_{11}(N - k_0))$$

then (3.69)

$$\underline{x}_n = \underline{x}(N) = \Psi(N, k_0)\underline{x}_n \quad (3.70)$$

The matrix $\Psi(N, k_0)$ is a transition matrix for the optimally controlled system. For example, assume the delay $k_0 = 0$ and let $\phi(i, 0)$ denote the state transition matrix for a closed-loop optimal system, employing the usual state feedback Kalman gain matrix, then $\phi(i, 0) = \Psi(i, 0)$. Note that $\Psi(0, 0) = I_n$. Also since the optimal system is asymptotically stable, under the assumption in sections 3.2 and 3.3 then $\lim_{N \rightarrow \infty} \Psi(N, 0) = 0$.

It remains only to calculate the term $\underline{n}_2(z)$ in the expression (3.42) for the optimal control. From (3.24) and (3.46):

$$\underline{c} = \underline{F}\underline{e}(N) = -\underline{F}\underline{x}_n \quad (3.71)$$

$$\underline{n}_2(z) = -\{M_0^T(z^{-1})Fz^{k_0-N}\}\underline{x}_n \quad (3.72)$$

$$= -Z_1(M_0^T(N - k_0 - i)F(U(i) - U(i - N + k_0)))\underline{x}_n \quad (3.73)$$

This equation may be written in the form:

$$\underline{n}_2(z) = f_3(z, N - k_0)\underline{x}_n \quad (3.74)$$

The optimal control signal follows from equation (3.37):

$$\hat{u}(z) = Y(z)^{-1}[f_1(z) + (f_2(z, N - k_0) + f_3(z, N - k_0))\Psi(N, k_0)]\underline{x}_0 \quad (3.75)$$

3.10 A State Feedback Solution to the Regulator Problem

An expression is obtained below from which the optimal control gain state feedback gain matrix may be calculated. First define a matrix $K_1(z, N - k_0)$ from equation (3.75):

$$K_1(z, N - k_0) = Y(z)^{-1} [f_1(z) + (f_2(z, N - k_0) + f_3(z, N - k_0))\Psi(N, k_0)]$$

then (3.76)

$$\hat{u}(i) = k_1(i, N - k_0)\underline{x}_0 \quad (3.77)$$

To obtain an expression for the time-varying gain matrix the control action through the optimisation interval must be considered. The control which minimises $J(0, N)$ has an initial value of

$$\hat{u}(0) = k_1(0, N - k_0)\underline{x}(0) \quad (3.78)$$

The system and performance criterion weighting matrices are time-invariant and thus for some other initial time, say time i , the control to minimise $J(i, N)$ is

$$\underline{u}_1(i) = k_1(0, N - k_0 - i)\underline{x}(i) \quad (3.79)$$

This may easily be shown to be the same as the optimal control within the optimisation interval [61] so that

$$\hat{u}(i) = K(i)\underline{x}(i) \quad (3.80)$$

where

$$K(i) \triangleq k_1(0, N - k_0 - i) \quad (3.81)$$

Alternatively, using the z-transform initial value theorem:

$$K(i) \triangleq \lim_{z \rightarrow \infty} K_1(z, N - k_0 - i) \quad (3.82)$$

This expression provides an alternative to the Riccati difference equation by which the state feedback gain matrix may be calculated.

An output feedback solution to the optimal tracking problem may be derived by using the open-loop solution (3.42) (with $\underline{x}_0 = 0$) and the usual relationship between open and closed loop controllers. This type of solution is required in self-tuning control problems.

Consider the following linear time-invariant system in discrete state equation form:

$$x_{i+1} = ax_i + u_i, \quad |a| < 1 \quad (3.83)$$

where $a = 0.5$ and the plant is thus stable and controllable. The optimal control performance criterion to be minimised is defined as:

$$J(0,N) = x_n^T F x_n + \sum_{i=0}^{N-1} x(i+1) + u(i) R u(i) \quad (3.84)$$

where $Q = q$, $R = 1$ and $F = f$. Let the input time delay be of magnitude k_0 seconds (let $\Delta = 1$ second). For a non-trivial problem k_0 is assumed less than N . The open loop and one step control laws are required and the state feedback gain is to be calculated from the former.

$$\phi(i) = a^{i-1} U(i-1) \quad \text{and} \quad \phi(z) = \frac{1}{z-a}$$

$$W_0(z) = \phi(z) B = 1/(z-a)$$

$$\begin{aligned} Y^T(z^{-1}) Y(z) &= W_0^T(z^{-1}) Q W_0(z) + R \\ &= \frac{(1+q+a^2) - az - az^{-1}}{(z^{-1}-a)(z-a)} \end{aligned} \quad (3.85)$$

The numerator polynomial above may be factorised into the form

$-z^{-1}a(z^2 - \frac{(1+q+a^2)}{a}z + 1) = -az^{-1}(z-\alpha)(z-1/\alpha)$ and if $q = 65/28$ then $\alpha = 1/7$. This choice for q ensures the closed loop time response for the infinite time problem includes terms in α^i . Thence, letting $Y(z)$ be defined as a generalised spectral factor:

$$Y^T(z^{-1}) Y(z) = \frac{a}{\alpha} \frac{(z^{-1}-\alpha)(z-\alpha)}{(z^{-1}-a)(z-a)} \quad (3.86)$$

and

$$Y(z) = \left(\frac{a}{\alpha}\right)^{1/2} \frac{(z-\alpha)}{(z-a)} \quad (3.87)$$

thus

$$M_0(z) = W_0(z) Y(z)^{-1} = \left(\frac{\alpha}{a}\right)^{1/2} \frac{1}{(z-\alpha)}$$

$$M_0^T(z^{-1}) Q \phi(z) A = \frac{(\alpha a)^{1/2} q}{(z^{-1}-\alpha)(z-a)}$$

From equation (3.65):

$$\begin{aligned}
 f_1(z) &= - \left\{ \frac{(\alpha a)^{\frac{1}{2}} q z^{k_0}}{(z^{-1} - \alpha)(z - a)} \right\}_+ \\
 &= - (\alpha a)^{\frac{1}{2}} q \left\{ \frac{z^{k_0}}{(1 - \alpha a)} \left(\frac{a}{(z - a)} + \frac{z^{-1}}{(z^{-1} - \alpha)} \right) \right\}_+ \\
 &= - \frac{(\alpha a)^{\frac{1}{2}} q}{(1 - \alpha a)} (a^{k_0} (\gamma + \frac{a}{z - a}) + m) \quad (3.88)
 \end{aligned}$$

where $\gamma = 0$ if $k_0 = 0$ and $\gamma = 1$ if $k_0 > 0$ and $m = 1 - \gamma$. Also define γ_1 as $\gamma_1 = a^{k_0} \gamma + m$. Thence, from equation (3.63):

$$n_{11}(z) = -g_1 \left(\gamma_1 + \frac{a^{k_0+1}}{(z - a)} \right) \underline{x}_0 \quad (3.89)$$

where $g_1 \triangleq (\alpha a)^{\frac{1}{2}} q / (1 - \alpha a) = (a/\alpha)^{\frac{1}{2}} (a - \alpha)$. From equation 3.64:

$$\begin{aligned}
 f_2(z, N) &= \left\{ \frac{(\alpha a)^{\frac{1}{2}} q z^{k_0-N}}{(z^{-1} - \alpha)(z - a)} \right\}_+ \\
 &= (\alpha a)^{\frac{1}{2}} q \left\{ \frac{z^{k_0-N}}{(1 - \alpha a)} \left(\frac{a}{(z - a)} + \frac{z^{-1}}{(z^{-1} - \alpha)} \right) \right\}_+ \\
 &= \frac{(\alpha a)^{\frac{1}{2}} q}{(1 - \alpha a)} \left(\frac{az^{k_0-N}}{(z - a)} + \left\{ \frac{z^{k_0-N}}{(1 - \alpha z)} \right\}_+ \right) \quad (3.90)
 \end{aligned}$$

The final term may be simplified as follows:

$$\begin{aligned}
 \left\{ \frac{z^{k_0-N}}{(1 - \alpha z)} \right\}_+ &= z^{k_0-N} (1 + \alpha z + a^2 z^2 + \dots + \alpha^{N-k_0} z^{N-k_0}) \\
 &= \frac{z^{-N+k_0} - z\alpha^{N-k_0+1}}{(1 - \alpha z)}
 \end{aligned}$$

Thence, from equation (3.64):

$$n_{12}(z) = g_1 \left(\frac{az^{k_0-N-1}}{(1 - az^{-1})} - \frac{\alpha^{-1} z^{-N+k_0-1}}{(1 - z^{-1}/\alpha)} + \frac{\alpha^{N-k_0}}{(1 - z^{-1}/\alpha)} \right) \underline{x}_n \quad (3.91)$$

From equation (3.74):

$$\begin{aligned}
 f_3(z, N - k_0) &= -Z_1 (M^T (n - k_0 - i) f(U(i) - U(i - N + k_0))) \\
 &= -\left(\frac{\alpha}{a}\right) f \left(\frac{z^{-N+k_0}}{(z^{-1} - \alpha)} - \frac{\alpha^{N-k_0}}{(z^{-1} - \alpha)} \right) \quad (3.92)
 \end{aligned}$$

and from equation (3.74):

$$n_2(z) = -g_2 \left(\frac{\alpha^{N-k_0-1}}{(1 - z^{-1}/\alpha)} - \frac{\alpha^{-1} z^{-N+k_0}}{(1 - z^{-1}/\alpha)} \right) \underline{x}_n \quad (3.93)$$

where $g_2 \triangleq (\alpha/a)^{\frac{1}{2}} f$. The time functions corresponding to the above terms may now be defined as:

$$\begin{aligned}
n_{11}(i) &= -g_1(\gamma_1 \delta(i) + a^{k_0+i} U(i-1)) \underline{x}_0 \\
n_{12}(i) &= g_1((a^{k_0+i-N} - \alpha^{N-k_0-i}) U(i-N+k_0) + \alpha^{N-k_0-i} U(i)) \underline{x}_n \\
n_2(i) &= -g_2 \alpha^{N-k_0-1-i} (U(i) - U(i-N+k_0)) \underline{x}_n
\end{aligned}$$

and

$$m_0(i) = \left(\frac{\alpha}{a}\right)^{\frac{1}{2}} \alpha^{i-1} U(i-1)$$

The summation terms in (3.67) may be evaluated using the above results:

$$\begin{aligned}
I_{11}(N - k_0) &= - \sum_{j=0}^{N-k_0-1} \left(\frac{\alpha}{a}\right)^{\frac{1}{2}} g_1 \alpha^{N-k_0-j-1} (\gamma_1 \delta(j) + a^{k_0+j} U(j-1)) \\
&= - \left(\frac{\alpha}{a}\right)^{\frac{1}{2}} g_1 \alpha^{N-k_0-1} \left(\gamma_1 + \left(\frac{a}{\alpha}\right) a^{k_0} \frac{(1 - (a/\alpha)^{N-k_0-1})}{(1 - a/\alpha)} \right)
\end{aligned}$$

and if $k_0 = 0$ this result simplifies to

$$I_{11}(N) = - \left(\frac{\alpha}{a}\right)^{\frac{1}{2}} g_1 \frac{(a^N - \alpha^N)}{(a - \alpha)} = \alpha^N - a^N \quad (3.94)$$

Similarly, from (3.68):

$$\begin{aligned}
I_{12}(N - k_0) &= \sum_{j=0}^{N-k_0-1} \left(\frac{\alpha}{a}\right)^{\frac{1}{2}} g_1 \alpha^{-1} \alpha^{2(N-k_0-j)} \\
&= \left(\frac{\alpha}{a}\right)^{\frac{1}{2}} g_1 \alpha \frac{(1 - \alpha^{2(N-k_0)})}{(1 - \alpha^2)}
\end{aligned} \quad (3.95)$$

and from (3.46):

$$\begin{aligned}
S(N - k_0) &= \sum_{j=0}^{N-k_0-1} \left(\frac{\alpha}{a}\right) \alpha^{2(N-k_0-j-1)} \\
&= \left(\frac{\alpha}{a}\right) \frac{(1 - \alpha^{2(N-k_0)})}{(1 - \alpha^2)}
\end{aligned} \quad (3.96)$$

Thence, from equation (3.69):

$$\Psi(N, k_0) = \frac{(a^N + I_{11}(N - k_0))}{(1 - I_{12}(N - k_0) + S(N - k_0) f)}$$

and

$$\Psi(N, 0) = \alpha^N / (1 - (a - \alpha) \alpha \frac{(1 - \alpha^{2N})}{(1 - \alpha^2)}) + \frac{\alpha}{a} \frac{(1 - \alpha^{2N}) f}{(1 - \alpha^2)} \quad (3.97)$$

Open Loop Control Signal

The optimal control signal follows directly from equation (3.75) and the above results. To simplify the solution consider the case when the delay is zero, then

$$\begin{aligned}\hat{u}(z) &= Y(z)^{-1} [f_1(z) + (f_2(z,N) + f_3(z,N))\Psi(N,0)] \underline{x}_0 \\ \hat{u}(z) &= \left(\frac{-z(a-\alpha)}{(z-\alpha)} + (a-\alpha) \left[\frac{az^{-N}}{(z-\alpha)} - \frac{(z-a)z^{-N}/\alpha}{(z-\alpha)(z-1/\alpha)} \right. \right. \\ &\quad \left. \left. + \frac{(z-a)z\alpha^N}{(z-\alpha)(z-1/\alpha)} \right] \Psi(N,0) \right. \\ &\quad \left. - \frac{\alpha}{a} \frac{f(z-a)}{(z-\alpha)(z-1/\alpha)} (z\alpha^{N-1} - z^{-N+1}\alpha^{-1}) \right) \Psi(N,0) \underline{x}_0\end{aligned}$$

The control sequence, for all $i \geq 0$, is given by:

$$\begin{aligned}\hat{u}(i) &= (-\alpha^i(a-\alpha) + (a-\alpha) [\alpha^{i-N-1} - \alpha^{i-N-1} \frac{(\alpha-a)}{(\alpha^2-1)} \\ &\quad - \frac{(1-\alpha a)}{(1-\alpha^2)} \alpha^{-i+N}] \Psi(N,0) U(i-N-1) \\ &\quad + \alpha^N(a-\alpha) [\alpha \frac{(\alpha-a)}{(\alpha^2-1)} \alpha^i + \frac{(1-\alpha a)}{(1-\alpha^2)} \alpha^{-i}] \Psi(N,0) U(i) \\ &\quad - \frac{\alpha f}{a} (\alpha^{i+N} \frac{(\alpha-a)}{(\alpha^2-1)} + \alpha^{-i} \frac{(1-\alpha a)}{(1-\alpha^2)} \alpha^{N-1}) \Psi(N,0) U(i) \\ &\quad - \frac{\alpha f}{a} (-\alpha^{i-N} \frac{(\alpha-a)}{(\alpha^2-1)} - \alpha^{-i+N} \frac{(1-\alpha a)}{(1-\alpha^2)} \alpha^{-1}) \Psi(N,0) U(i-N)\end{aligned}$$

It is a tedious but simple matter to show that $\hat{u}(i) = 0$ for all $i \geq N$, as required. Clearly terms involving z^{-N} in the expression for the control signal do not contribute to the control within the optimisation interval and may be neglected. Thence, $\hat{u}(z)$ simplifies to the following:

$$\begin{aligned}\hat{u}(z) &= \left(-\frac{z(a-\alpha)}{(z-\alpha)} + \frac{(a-\alpha)(z-a)z\alpha^N}{(z-\alpha)(z-1/\alpha)} \Psi(N,0) \right. \\ &\quad \left. - \frac{\alpha}{a} \frac{f(z-a)z\alpha^{N-1}}{(z-\alpha)(z-1/\alpha)} \Psi(N,0) \right) \underline{x}_0\end{aligned} \quad (3.98)$$

The control sequence, for $i \in [0, N-1]$, becomes:

$$\begin{aligned}\hat{u}(i) &= (-\alpha^i(a-\alpha) + \alpha^N \frac{(a-\alpha)}{(1-\alpha^2)} [(1-\alpha a)\alpha^{-i} - (\alpha^2 - \alpha a)\alpha^i] \Psi(N,0) \\ &\quad - \frac{\alpha^{N+1} f}{a} (\alpha^i \frac{(\alpha-a)}{(\alpha^2-1)} + \alpha^{-i-1} \frac{(1-\alpha a)}{(1-\alpha^2)}) \Psi(N,0) \underline{x}_0\end{aligned} \quad (3.99)$$

The control and state trajectories for this example are illustrated in Figure 2. The above solution and the usual state feedback Riccati equation solution give identical trajectories, as required.

One Step Control Law

Consider the special case when $N = 1$, then the control at time zero becomes:

$$\begin{aligned} \hat{u}(0) = & -(a - \alpha) + \frac{(a - \alpha)}{(1 - \alpha^2)} [(1 - \alpha a)\alpha - (\alpha - a)\alpha]\Psi(1,0) \\ & - \frac{f}{a}(\alpha^2 \frac{(a - \alpha)}{(1 - \alpha^2)} + \alpha \frac{(1 - \alpha a)}{(1 - \alpha^2)})\Psi(1,0) \underline{x}_0 \end{aligned} \quad (3.100)$$

This one step control law may be simplified and written in the form:

$$\begin{aligned} \hat{u}(i) = & \left(\frac{(a - \alpha)}{(1 - \alpha^2)} (-1 + \alpha a + (1 + a)\alpha^2 - (2a + 1)\alpha^3 + \alpha^4) \right. \\ & \left. - f\alpha \right) \underline{x}(i) / \Delta \end{aligned} \quad (3.101)$$

where

$$\Delta \triangleq 1 - \alpha a + \alpha^2 + \alpha f/a$$

This control law is time invariant and minimises, over each sampling interval the criterion:

$$J_i(0,1) = x^2(i+1)(f+q) + u^2(i)$$

State Feedback Control Law

The state feedback control law may now be determined. From (3.76) and (3.98) with $k_0 = 0$, identify $K(z,N)$ and note

$$\lim_{N \rightarrow \infty} K_1(z,N) = -(a - \alpha) + \left((a - \alpha) - \frac{f}{a} \right) \alpha^N \Psi(N,0)$$

Thus, from equation (3.82) the feedback gain matrix becomes:

$$K(t) = -(a - \alpha) + \left((a - \alpha) - \frac{f}{a} \right) \alpha^{N-i} \Psi(N-i,0) \quad (3.102)$$

Note that the one step control law in (3.100) and (3.101) is equivalent to repeated use of $K(0)$, as may be verified easily. Note that $K(N-1)$ given by the above results is the same as that from the Riccati equation:

$$K(N-1) = -(q+f)a/(1+q+f) \quad (3.103)$$

If the controller is to be used in a self-tuning control scheme there exists the possibility of maintaining the closed loop pole, α , fixed or of maintaining the weighting elements fixed. For example, assume that the parameter a is varying then α is chosen so that $(1 + q + a^2)/a = \alpha + 1/\alpha$. Thus, either q may be assumed to vary as α remains fixed, or q may be fixed and α will be a variable. Thus, it is possible to achieve either an optimal control law (fixed q, r), or a suboptimal control law (fixed α) which maintains a fixed closed loop response. This latter controller will be termed an optimal pole assignment regulator. Note that this regulator is not the same as those proposed by Wellstead [79]. At the end of each N second interval an identification algorithm must provide the new parameter estimate a , however, it is not appropriate to consider this problem here.

Note that the above computation of the control law is rather complicated, however, an algorithm has been developed which can be implemented using well-established numerical routines. This has been described for the dual filtering problem by Grimble [81].

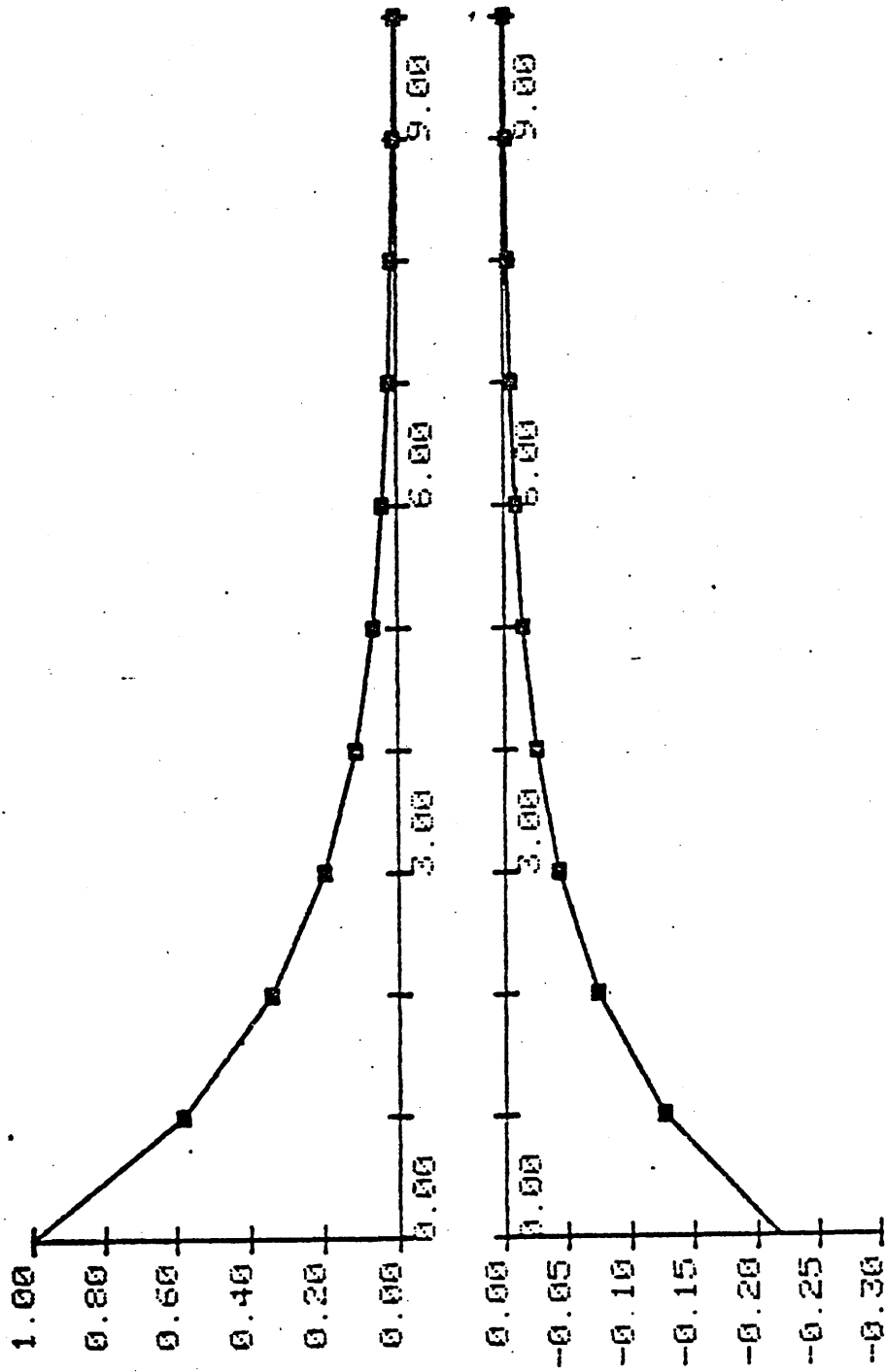


Figure 2: Control and State Trajectories for $\alpha = 0.8$, $q = 0.2$ and $f = 0.5$

3.11 Conclusions

A solution to the discrete finite time optimal control problem was obtained and a z-domain representation for the controller was given. An output feedback transfer function solution was proposed which may be of use in self-tuning control systems. Note that the controller is expressed in terms of the plant parameters and it may therefore be combined with an explicit identification algorithm to obtain a form of self-tuning controller. It may also be possible to use the discrete-time filter previously proposed [65], together with this control law, to obtain a solution to the stochastic optimal control problem. Consider, for example, the situation whereby output measurements are taken every N seconds but the control can be updated every second. The time invariant filter can provide the state estimate $\hat{x}(N|0)$ and the time invariant controller can use this as the initial state for the next time period. The advantage of such a controller is that it is time-invariant and is in transfer function form.

An expression was obtained for the optimal state feedback gain matrix in terms of the z-domain results. This provides a link between the z-domain controller and the usual time-domain state feedback solution. An example was given to illustrate the solution procedure. This illustrated the flexibility of the technique and provided the open loop control signal in both weighting sequence and transfer function forms. The single step and state feedback control laws were also easily calculated. Note that the expression for the controller was obtained in terms of the plant parameters. There is, therefore the possibility of combining the control calculation with an identification algorithm to obtain a form of self-tuning controller. This is an area for future research.

CHAPTER 4

The Design of Strip Shape Control Systems for a
Sendzimir Mill

The Design of Strip Shape Control Systems for Sendzimir Mills4.1 Introduction

It is only recently that the producers of flat rolled steel products have considered the use of closed loop control systems to control the flatness of the product. Shape control refers to control of the internal stress distribution in rolled steel strip so that sections of strip will lie flat on a flat surface. A typical shape defect is for the strip to have "long edge" which will manifest itself in a wavy edge to the rolled strip. Shape control became possible as a result of the appearance of several commercially available instruments for on line "shape" measurement [83]. Shape is the second largest single cause for the rejection of cold-rolled steel strip (gauge being the primary cause). Bad shape may sometimes be corrected by further processing but this is expensive [84]. The customers for rolled products are now in a "buyers market" and they may therefore specify closer shape tolerances. Thus, there are considerable economic pressures for the rapid development of automatic shape control schemes.

The internal stress distribution caused by a transverse variation in the gauge reduction is termed the "shape" of the strip and strip with a uniform stress distribution is said to have perfect shape [85]. The differential elongation causing bad shape is caused by local mismatch between strip and work roll profiles under load. Shapemeters are normally placed from one to two metres from the roll gap and these measure the tension distribution across the lateral stress distribution. The first index of shape measurement was introduced in 1964 by Pearson [86]. He noted that from the users point of view errors in flatness

are generally of more concern than residual stress and he defined shape as being given by $(\Delta l / (l\omega)) 10^4$ mons/unit width where Δl is the length difference between longitudinal elements of mean length l spaced ω across the strip.

Much of the early work on shape control was conducted by Sabatini, Woodcock and Yeomans [87-89] and Wistreich [90] at the British Iron and Steel Research Association. More recently Spooner and Bryant [85,91] have shown how correct scheduling and set up procedures improve the quality of strip shape and they have developed off-line models for shape control and scheduling. The proceedings of the Metals Society 1976 conference on shape control [85] can be taken as a useful guide to the state of the art although many systems have been implemented since that time.

4.2 The Sendzimir Mill

The cluster mill considered in the following study is shown in figure 1. It is 1.6 metres wide and is used for rolling stainless steel. The motor drives the outer second intermediate rolls, I, K, L, N in figure 2. The transmission of the drive to the work rolls is applied through the inter-roll friction. All the inner-rolls (I to T) have thrust bearings and are free to float sideways. The outer-rolls (A to H) are supported by eight saddles per shaft, fixed to the mill housing. The saddles contain eccentric rings which can rotate in the circular saddle bores. These assemblies are used in the screw down and shape control mechanisms. The screwdown racks act upon assemblies B,C and F,G. The top assembly B,C has both screwdown and shape actuator eccentric rings. These actuators are referred to as As-U-Rolls by the manufacturers. A rack position change causes the screw down ring to rotate and thus the roll assembly moves towards or away from the mill housing. The screw down system enables the average load to be varied during rolling, without substantially bending the rolls.

The As-U-Roll eccentric rings on shafts B,C enable roll bending to be achieved, for shape control, during rolling. Each of the eight saddles on those two rolls has an extra eccentric ring which can be moved independently from the screw down eccentric ring. When the screw down system is operated the bearing shafts and screw down eccentrics rotate at all the saddles simultaneously but the As-U-Roll eccentrics do not rotate. Thus the bending profile set up by the As-U-Roll is maintained.

There is also provision for an indirect control of shape with the first intermediate rolls (OPQR). The top rolls, O,P, are tapered at the front of the mill and the bottom rolls QR are tapered at the back

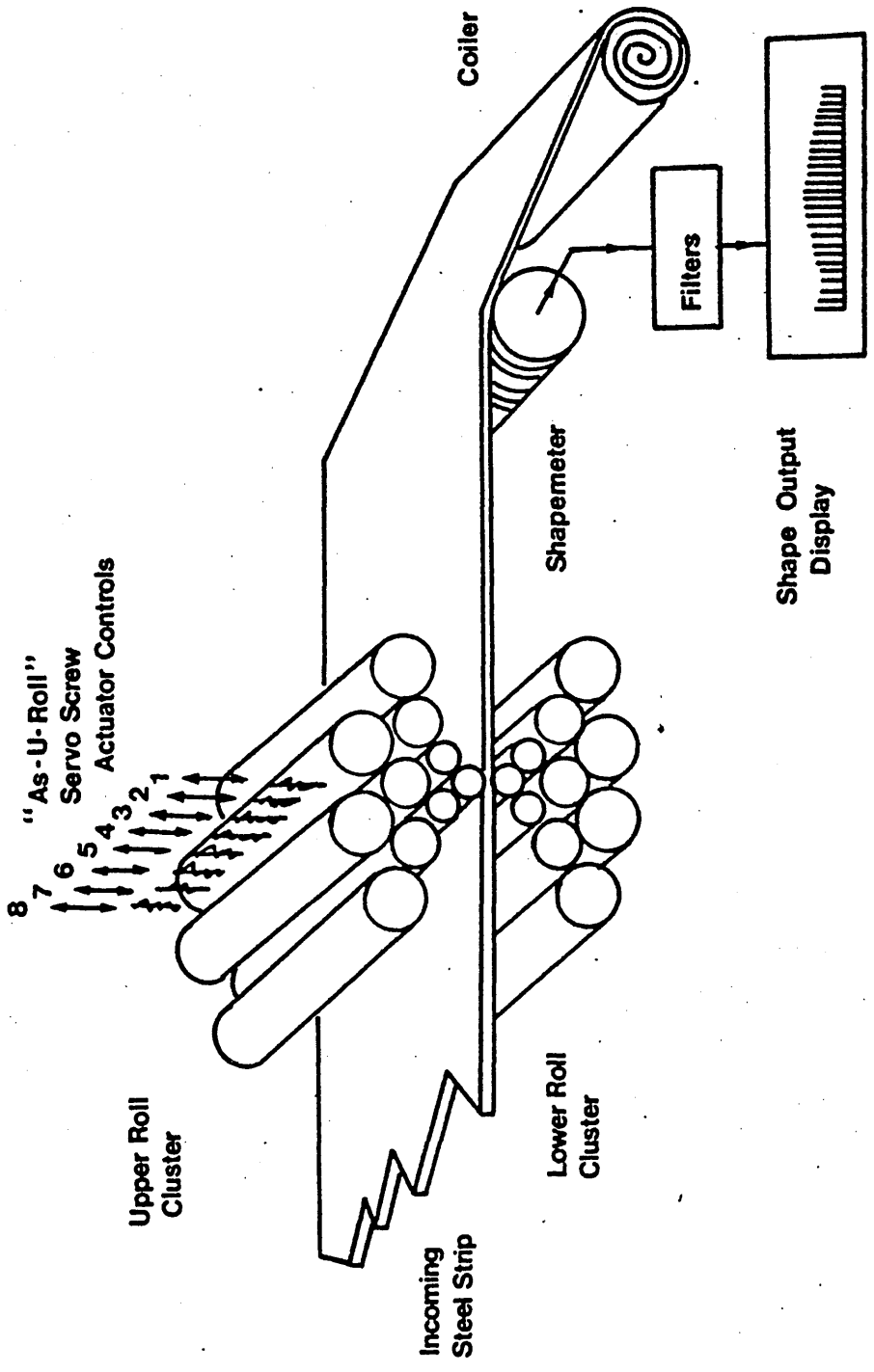


Figure 1: Sendzimir Single Stand Reversing Cold Rolling Mill

Upper Rack
(full open position shown)

Back up assemblies
(A to H)

Arrows show direction
of movement to full
closed position

Eccentric adjustmer
saddle assemblies
(A, D, E, H) (full open
position)

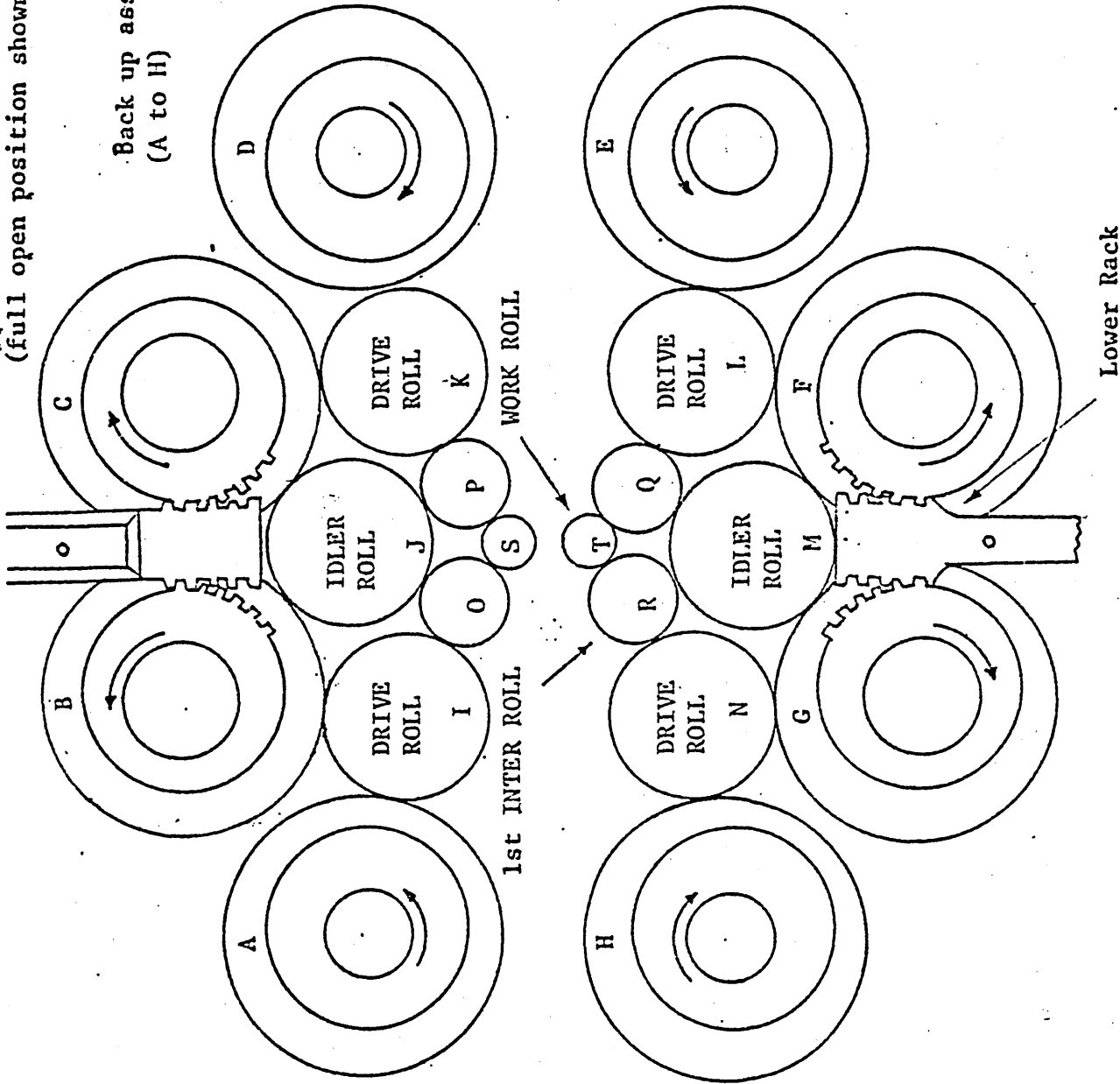
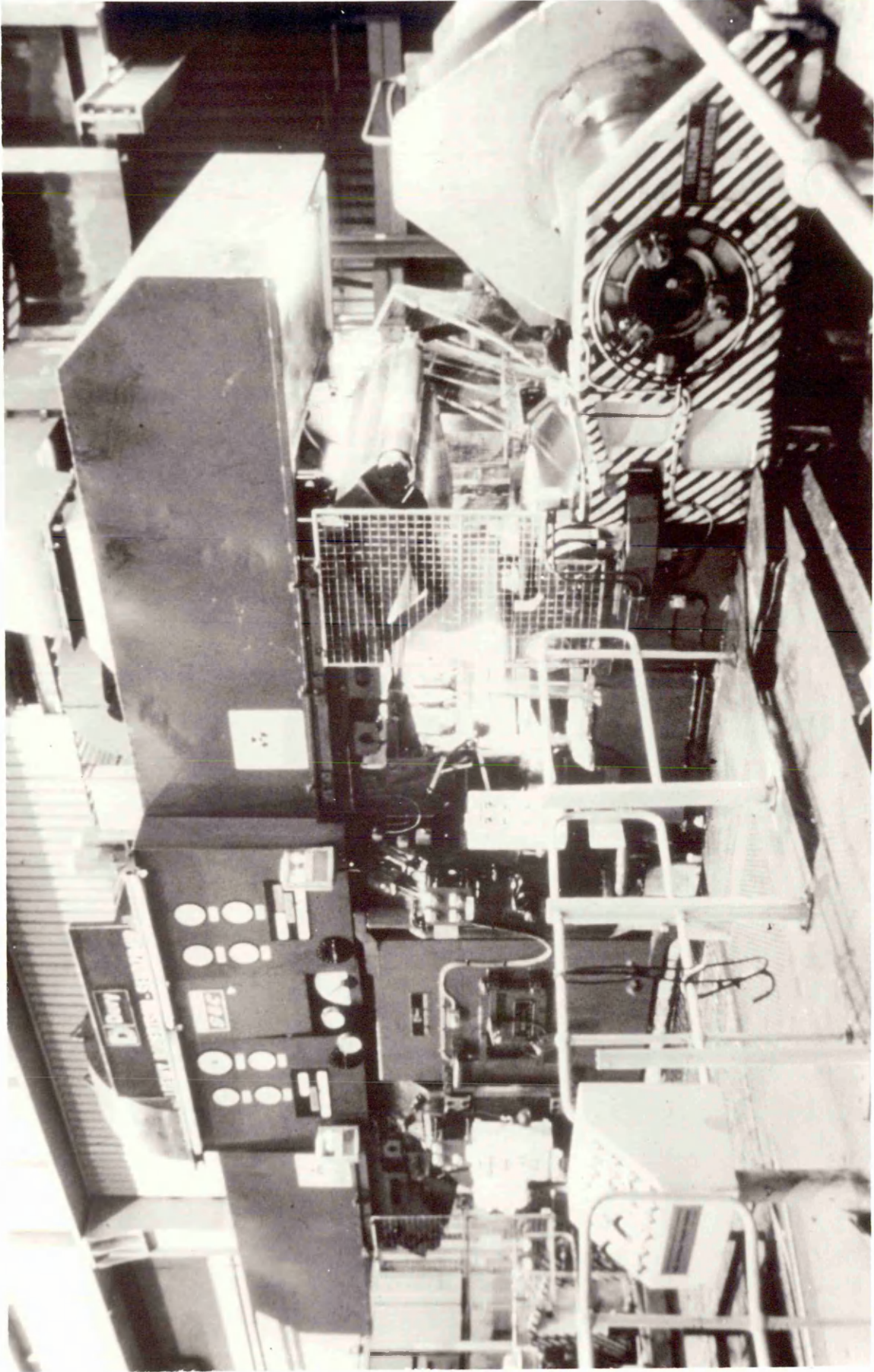


Figure 2 Roll and Back-up Bearing Arrangement and Adjustment

of the mill. Moving these rolls axially in and out of the cluster controls the pressure at the strip edges within certain limits.

As mentioned previously the screw down and As-U-Roll eccentrics (even though they have the same common shaft) are non-interactive. The shape control system proposed involves the continuous use of As-U-Rolls but only intermittent use of the first intermediate rolls. This approach simplifies the design stage.



Sendzimir Cold Rolling Mill

4.3 The Shape Measurement Sub system

Comparing the various types of shape measuring devices [84] the Lowey Robertson Vidimon shapemeter [92] and the ASEA Stressometer shapemeter [93] seem to be the most reliable and successful. The latter is considered here since it is employed on the mills of interest. The stressometer measuring roll, figure 1, is divided into a number of measuring zones across the roll. The stress in each zone is measured independently of that in adjacent zones with magneto-elastic force transducers which are placed in four slots equally spaced in the roll periphery. The periodic signals from each zone are filtered and the stress $\sigma(x)$ in each zone is calculated. The average stress σ is calculated and the difference $\Delta\sigma(x) = \sigma(x) - \sigma_0$ is displayed on a separate indicator for each zone. These signals are also available for feedback purposes.

The shapemeter filter is changed with the line speed and the dominant time-constant may have one of five different values in the range 4.35 to 0.11 seconds. The smoothed signals appear to contain a white noise component. The number of measuring zones which are operating depends upon the width of the strip.

4.4 Static Model of the Mill

To enable us to design a shape control scheme an analysis of the rolling stand is needed. This model has already been developed by Gunawardene, Grimble, Thomson [95]. The static model includes all the mechanical force-deformation relationships. These are both non-linear and schedule dependent.

Considering a small perturbation in an actuator setting the stress profile across the strip is calculated and thus mill gains can be obtained for the given operating point. These gains are used in the dynamic model of the mill, and are valid for small variations around the operating point. If the strip shape deviates significantly from the original point, used to obtain the gains, the non-linear nature of the actual plant would have to be considered.

A set of linearized gains are given below between the 8 actuators and 8 equally spaced points across the strip width. It relates the shape output at the roll gap and the actuator change.

$$G_m = \begin{bmatrix} 3.79 & 3.46 & -0.75 & -1.44 & -1.38 & -1.18 & -1.56 & -0.96 \\ 1.30 & 2.30 & 1.03 & -0.41 & -0.62 & -1.43 & -1.60 & -0.87 \\ -0.44 & 0.86 & 1.88 & 0.67 & 0.23 & -1.04 & -1.33 & -0.80 \\ -1.02 & -0.75 & 1.29 & 1.61 & 1.35 & -0.10 & -1.34 & -0.96 \\ -0.96 & -1.34 & 0.10 & 1.35 & 1.61 & 1.29 & -0.75 & -1.02 \\ -0.80 & -1.33 & -1.04 & 0.23 & 0.67 & 1.88 & 0.86 & -0.44 \\ -0.87 & -1.60 & -1.43 & -0.62 & -0.41 & 1.03 & 2.30 & 1.30 \\ -0.96 & -1.56 & -1.18 & -1.38 & -1.44 & -0.75 & 3.46 & 3.79 \end{bmatrix} \quad (4.1)$$

If the strip is centred across the mill then G_m has the form:

$$G_m = [\underline{g}_1 \quad \underline{g}_2 \quad \underline{g}_3 \quad \underline{g}_4 \quad ; \quad \hat{g}_4 \quad \hat{g}_3 \quad \hat{g}_2 \quad \hat{g}_1] = [g_{ij}]$$

where \underline{g}_i are column vectors and $\hat{\underline{g}}_i$ has the same elements as \underline{g}_i but in reverse order.

By the definition of the shape, as the deviation in the tension stress from the mean, the average value across the strip must be zero ie the column sum must be zero:

$$\sum_{i=1}^8 g_{ij} = 0 \quad \forall j \in \{1, 2, \dots, 8\} \quad (4.2)$$

Also the row elements sum to zero since if each shape actuator is changed by the same amount there will be no effect on the strip shape but only change in the strip thickness.

$$\sum_{j=1}^8 g_{ij} = 0 \quad \forall i \in \{1, 2, 3, 4, \dots, 8\} \quad (4.3)$$

The elements of the matrix G_m vary with the type of the coil being rolled and with the particular pass of the coil as mentioned above. For a different pass G_m becomes:

$$\tilde{G}_m = \begin{bmatrix} 3.9 & 1.8 & -0.5 & -1.3 & -1.3 & -0.7 & -0.6 & -0.3 \\ 1.3 & 3.9 & 0.7 & -0.1 & -1.2 & -1.3 & -1.1 & -0.8 \\ -0.3 & 0.2 & 1.7 & 1.5 & -0.4 & -1.0 & -1.0 & -0.7 \\ -0.9 & -0.8 & 0.9 & 1.6 & 1.0 & -0.5 & -1.0 & -0.7 \\ -0.8 & -1.1 & -0.3 & 0.5 & 1.9 & 0.8 & -0.7 & -0.5 \\ -0.7 & -1.0 & -0.9 & -0.6 & 1.2 & 1.6 & 0.2 & -0.2 \\ -0.8 & -1.1 & -1.2 & -1.3 & -0.5 & 0.9 & 3.4 & 0.9 \\ -0.5 & -0.8 & -0.7 & -1.0 & -1.4 & -0.4 & 1.5 & 2.8 \end{bmatrix} \quad (4.4)$$

These gain matrices obtained from the static model program contain numerical discrepancies, however, using the symmetry properties (eg 4.2, 4.3) these errors can be reduced. That has been done in the case of matrix G_m in 4.1. The control design should be able to cope with this kind of innacuracy in G_m .

4.5 State space description

The basic components of the Sendzimir mill shape control system are depicted in figure 1 and in block diagram form in figure 3 . The description of each subsystem follows.

The back up roll actuators are non interacting and each is represented by a second order system, assumed to be an integrator accompanied by a cascaded time constant. Because there are position feedback loops around each of the actuators their transfer function can be chosen as:

$$T_a(s) = \frac{1}{(1 + 0.2s)^2} I_8 \quad (4.5)$$

The state space equations become:

$$\dot{\underline{x}}_a(t) = A_a \underline{x}_a(t) + B_a \underline{u}_a(t) \quad (4.6)$$

$$\underline{y}_a(t) = C_a \underline{x}_a(t) \quad (4.7)$$

with $\underline{x}_a(t), \underline{u}_a(t) \in \mathbb{R}^8$ and the matrices A_a, B_a, C_a are in block diagonal form. Each block has the form:

$$A_a = \begin{bmatrix} 0 & 1 \\ -25 & -10 \end{bmatrix} \quad B_a = \begin{bmatrix} 0 \\ 25 \end{bmatrix} \quad C_a = \begin{bmatrix} 1 & 0 \end{bmatrix} \quad (4.8)$$

The next subsystem is the mill cluster. Here it is assumed that the dynamics are so fast as to be neglected relative to the rest time constants in the system. Thus any change in the As-U-Roll actuators has an instantaneous effect on the stress distribution at the roll gap. For this linear model the gain matrix G_m , relating the actuators movement to the strip stress, is used. The evolution of G_m was discussed in section 4.4. The mill equation then is:

$$\underline{y}_m(t) = G_m \underline{y}_a(t) \quad (4.9)$$

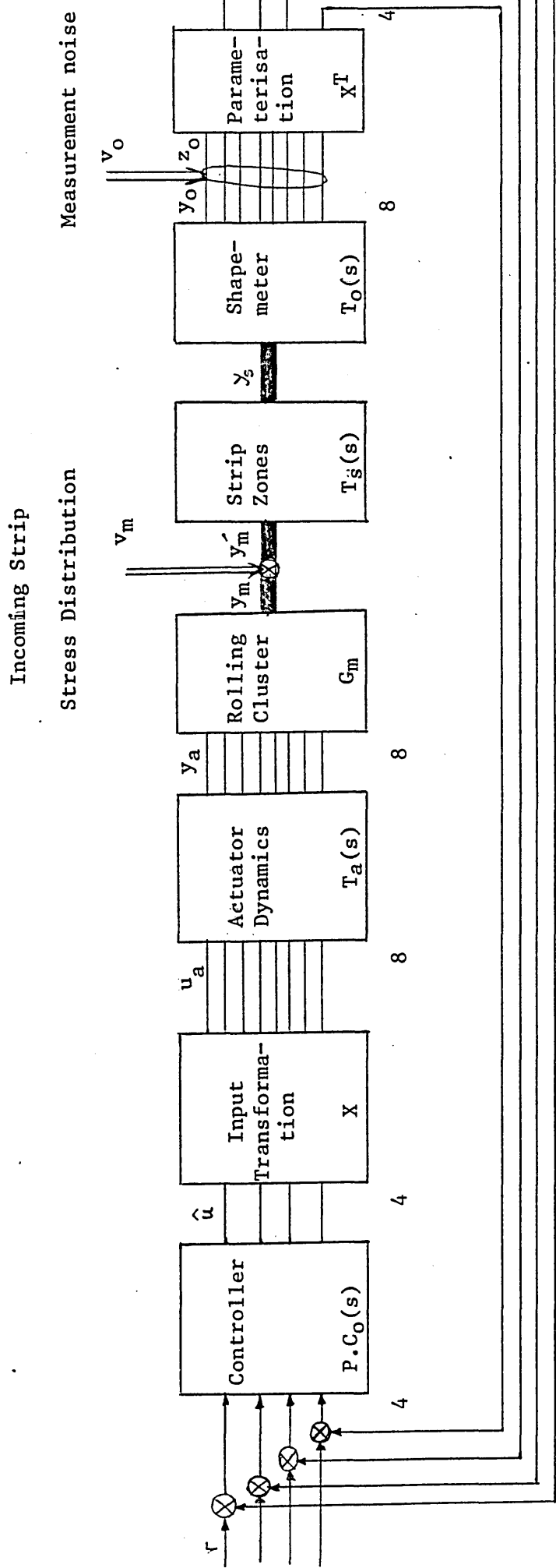


Figure 3: Block Diagram of Shape Control System
 (showing number of signal paths)

$$\underline{y}'_m(t) = \underline{y}_m(t) + \underline{v}_m(t) \quad (4.10)$$

The vector $\underline{v}_m(t)$ represents shape disturbances due to changes of the input shape profile or changes of the strip gauge profile, material hardness or thermal camber. For the present study the number of the outputs $\underline{y}_m(t)$ are taken equal to the number of the actuators (eight,8). This number can be different in the control design because the shape profile is usually parametrized and then a matrix G_{mp} which is a function of the parameters can be used. A further discussion on this matter follows in the parametrisation section which follows.

There is not considerable interaction from the gauge control system of the mill since the screw down system on a Sendzimir mill doesn't involve roll bending, in contrast with four high mills.

The dynamics of the strip exiting from the roll gap to the shape meter is under debate. Previous workers suggest a representation either as a pure delay or as a simple lag [96]. Experience from the plant suggests that both effects are present to a certain degree. In our model the state equations become:

$$\dot{\underline{x}}_s(t) = A_s \underline{x}_s(t) + B_s \underline{y}'_m(t) \quad (4.11)$$

$$\underline{y}_s(t) = C_s \underline{x}_s(t) \quad (4.12)$$

$$\underline{y}'_s(t) = \underline{y}_s(t - T) \quad (4.13)$$

The matrices A_s, B_s, C_s depend upon the strip dimension and the mill speed, ie they are schedule dependent. A convenient representation to model the above dynamics is by a second order transfer function for each zone of the strip. By choosing this TF to be a simple lag and a Pade approximation for the time delay both effects are taken into account [96]. Through simple response tests on the mill the above transfer function may be identified. Thus

$$T_s(s) = \frac{(1 - s\tau/2)}{(1 + s\bar{\tau}/2)(1 + s\tau_1)} I_8 \quad (4.14)$$

with $\tau = D/v$ and $\tau_1 = D_1/v$, v is the strip speed in metres/second, $D = 2.91$ m the distance from the roll bite to the shapemeter and $D_1 = 5.32$ m the distance between the coiler and roll gap.

Finally the last block, the shapemeter, forms the output subsystem and a number of independent second order transfer functions are used as candidate representations. The shape measurement noise consists of a sinusoidal part proportional to the speed of the measuring roll and a wide band component. This noise signal vector $\underline{v}_0(t)$ is assumed to be white noise plus a coloured noise with spectrum $\phi_0/(s^2 + \omega_0^2)$. The state equations are:

$$\dot{\underline{x}}_0(t) = A_0 \underline{x}_0(t) + B_0 \underline{y}'_s(t) \quad (4.15)$$

$$\underline{y}_0(t) = C_0 \underline{x}_0(t) \quad (4.16)$$

$$\underline{z}_0(t) = \underline{y}_0(t) + \underline{v}_0(t) \quad (4.17)$$

The matrices A_0 , B_0 , C_0 are speed dependent and are switched by the shapemeter electronics.

In transfer function form:

$$T_0(s) = \frac{1}{(1 + s\tau_0)(1 + 0.01s)} I_8 \quad (4.18)$$

and the time constant τ_0 is 1.43s for speed up to 2 m/s, $\tau_0 = 0.74$ s for up to 5 m/s and $\tau_0 = 0.3$ s for 15 m/s. These time constants of the filter are switched so that the maximum ripple on the shape measurement signal doesn't exceed 16%.

The combination of the state equations provides the total state space description of the system:

$$\dot{\underline{X}}(t) = A_1 \underline{X}(t) + A_2 \underline{X}(t - \tau) + B \underline{u}(t) + D \underline{V}_m(t) \quad (4.19)$$

$$\underline{Z}_0(t) = C \underline{X}(t) + \underline{V}_0(t) \quad (4.20)$$

$$A_1 = \begin{bmatrix} A_a & 0 & 0 \\ B_s G_m C_a & A_s & 0 \\ 0 & 0 & A_0 \end{bmatrix} \quad A_2 = \begin{bmatrix} 0 & 0 & 0 \\ 0 & 0 & 0 \\ 0 & B_0 C_s & 0 \end{bmatrix}$$

$$B = \begin{bmatrix} B_a \\ 0 \\ 0 \end{bmatrix} \quad C = \begin{bmatrix} 0 & 0 & C_0 \end{bmatrix} \quad D = \begin{bmatrix} 0 \\ B_s \\ 0 \end{bmatrix} \quad \underline{X}(t) = \begin{bmatrix} \underline{X}_a(t) \\ \underline{X}_s(t) \\ \underline{X}_0(t) \end{bmatrix}$$

To use the above differential-difference equation in a model for the mill, will complicate the control design procedure. At the same time it is considered that this approach does not gain greater insight in the system behaviour. It is better to use an ordinary differential equation by use of the already mentioned Pade approximation to the time delay. Thus the equations to be used for control design become:

$$\dot{\underline{x}}(t) = A \underline{x}(t) + B \underline{u}(t) + D \underline{v}_m(t) \quad (4.21)$$

$$\underline{z}_0(t) = C \underline{x}(t) + \underline{v}_0(t) \quad (4.22)$$

$$A = \begin{bmatrix} A_a & 0 & 0 \\ B_s G_m C_a & A_s & 0 \\ 0 & B_0 C_s & A_0 \end{bmatrix}$$

The A matrix being lower triangular allows some computational simplifications. The system Markov parameters are given by

$$M_0 = CB = 0$$

$$M_1 = CAB = 0$$

$$M_2 = CA^2B = C_0B_0C_sB_sG_mCaB_a$$

The matrix M_2 is full rank if the matrix G_m is full rank.

This state space description of the mill forms the basis of the dynamic model simulation. For control design the transfer function form of the plant is more convenient. Also the plant structure is indicated far more clearly than in the time domain equations. As was already noted all the dynamic elements are non-interactive. The As-U-Roll actuators are modelled by eight non-interactive second order transfer functions. As the strip is represented by eight zones the resultant system has eight effective outputs; this has the advantage that the system is square. Combining equations 4.5, 4.9, 4.14 and 4.18 the total plant transfer function matrix is obtained:

$$W(s) = T_0(s) T_s(s) G_m T_a(s) = \frac{n(s)}{d(s)} G_m \quad (4.23)$$

where $n(s)$ and $d(s)$ are the zero and pole polynomials respectively.

The plant is open loop stable, non-minimum phase and speed dependent.

The polynomials $n(s)$ and $d(s)$ take the form:

$$\eta_l(s) = (1 - 0.727 s)$$

$$d_l(s) = [(1 + 0.2 s)^2 (1 + 0.727 s) (1 + 2.66 s) (1 + 43 s) (1 + 0.01 s)]$$

$$\eta_m(s) = (1 - 0.291 s)$$

$$d_m(s) = [(1 + 0.2 s)^2 (1 + 0.291 s) (1 + 0.64 s) (1 + 0.74 s) (1 + 0.01 s)]$$

$$\eta_h(s) = (1 - 0.097 s)$$

$$d_h(s) = [(1 + 0.2 s)^2 (1 + 0.097 s) (1 + 0.355 s) (1 + 0.15 s) (1 + 0.01 s)]$$

for the low, medium and high speed ranges respectively denoted by the subscripts l , m , h . In all cases $n(0) = d(0) = 1$.

4.6 Parameterisation

The use of parameterisation of the shape profile presents several advantages and so is often used. As the shape profile is a smooth curve it can be parameterised by means of a low order polynomial. This gives rise to a system with a small finite number of variables to control. The number of shape measurements varies with the strip width which also makes parameterisation desirable. This results in a system with the same number of effective outputs. For the following discussion it will be assumed that there are eight shape outputs, as in the described dynamic model. Using orthogonal polynomials simplifies the calculations and the effect of increasing the number of parameters (ie increasing the order of the polynomials) is very easy to deduce.

Let $\{P_i(w)\}$ to be a set of orthonormal polynomials and $w \in [-1,1]$ represent the distance across the strip width measured from the mill centre line. The shape profile may be written:

$$S(w,t) = \sum_{i=1}^k P_i(w) y_i(t) \quad (4.24)$$

where k is the number of polynomials used and $y_i(t)$ the i th parameter used to describe the shape at time t . From physical consideration up to fourth order behaviour may be expected thus $k = 4$. Also from the definition of shape, as the deviation from the mean, there is no need to include a constant term or zero order polynomial. Let $z_j(t)$ be the actual shape measurement at the j th zone of the strip at time t . The relation between the vectors $\underline{z}(t)$ and $\underline{y}(t)$ can be expressed as:

$$\underline{z}(t) = X \underline{y}(t) + \epsilon(t) \quad (4.25)$$

or

$$\begin{bmatrix} z_1(t) \\ z_2(t) \\ \vdots \\ z_8(t) \end{bmatrix} = \begin{bmatrix} P_1(w_1) & P_2(w_1) & P_3(w_1) & P_4(w_1) \\ P_1(w_2) & P_2(w_2) & P_3(w_2) & P_4(w_2) \\ \vdots & \vdots & \vdots & \vdots \\ P_1(w_8) & P_2(w_8) & P_3(w_8) & P_4(w_8) \end{bmatrix} \cdot \begin{bmatrix} y_1(t) \\ y_2(t) \\ \vdots \\ y_4(t) \end{bmatrix} + \underline{\varepsilon}(t)$$

so the x_{ij} elements of matrix X is $x_{ij} = P_j(w_i)$ ie the j th order polynomial evaluated at the i th width zone: $w_1 = -1$ $w_2 = -5/7$ $w_3 = -3/7$ $w_8 = 1$. If the polynomials $p_j(w)$ are orthonormal, $X^T X = I$, and the least squares estimates for the parameter $\underline{y}(t)$ are:

$$\hat{\underline{y}}(t) = (X^T X)^{-1} X^T \underline{z}(t) = X^T \underline{z}(t) \quad (4.26)$$

The reference \underline{r} can be defined in relation to the above such that to determine any desired shape profile:

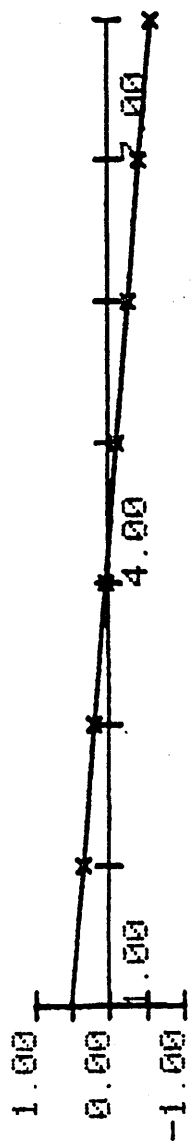
$$S_r(w, t) = \sum_{i=1}^4 P_i(w) r_i(t) \quad (4.27)$$

An input transformation is now required which will relate the 4 controller signals $u(t)$ to the 8 actuator inputs $u_a(t)$. This will produce a new square 4 x 4 system. As all the interaction in the plant comes from the mill matrix G_m , see equation (4.23) the input-output transformation acts on this matrix G_m to produce an effective G_x 4 x 4 matrix. The input transformation may be selected freely so a matrix M which yields a diagonal $G_x = X^T G_m M$ is very attractive. In the case of the mill such a selection is not advisable because of the limited possible range of settings on the As-U-Roll shape actuators ie the difference in the settings of adjacent actuators should not be greater than certain limits. However by choosing the same types of input profile via the actuators as is used for parameterising the shape outputs this property can be achieved (figure 4): $\underline{u}_a(t) = X \underline{u}(t)$ and the transfer function matrix (4.23) becomes:

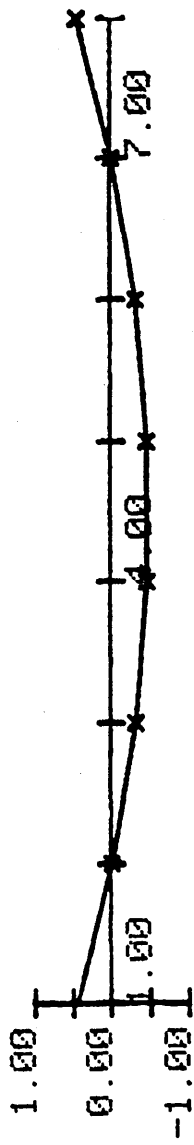
$$W_x(s) = X^T W(s) X$$

$$\text{or } W_x(s) = \frac{\underline{n}(s)}{d(s)} X^T G_m X = \frac{\underline{n}(s)}{d(s)} G_{mx} \quad (4.28)$$

TSEB



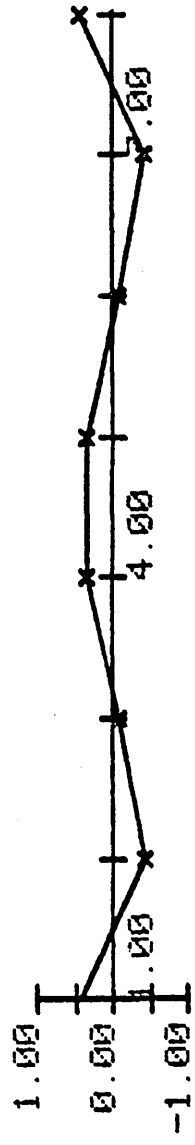
x - T1



x - T2



x - T3



x - T4

Figure 4 Shape Profiles Represented by Tsebychev-Orthogonal Polynomials

4.7 Shape Control Systems Design

To proceed to the control system design the characteristics, requirements and properties of such a system have to be traced and specified. Physical considerations, and the experience of mill operators dictate the following.

An acceptable control scheme will demonstrate:

- (i) Transient response with small overshoot and rise time in the region of 5 seconds
- (ii) Relative insensitivity to errors of calculation and variations of G_m
- (iii) Relative insensitivity to line speed changes
- (iv) High open loop gain at zero frequency for good reference following.

Moreover it may be that certain shape profiles must never be reached, even in transients, for the safe operation of the mill. For the present these aspects are still under discussion with the mill engineers, so it will be neglected in this study.

As described in 4.5 the mill is a multivariable plant with eight inputs and effective outputs. Straight forward application of either of the two modern multivariable design methods ie the Characteristic Locus [20] or the Inverse Nyquist Array [18] will produce compensators highly dependent on G_m^{-1} as all the interaction in the plant stems from G_m . The matrix G_m computed from the static model (4.4), is often full rank but from the aforementioned properties in equations 4.2,4.3 this should not be the case. This is caused by numerical errors. Consequently a control scheme cannot be based on G_m^{-1} as outlined in requirement (ii) above. This disadvantage is not present if output feedback optimal control is used for the controller

design [97]; however these controllers are much more complex to calculate. This is discussed further in section 4.9.

Consider now the use of an input-output transformation of the plant to obtain a system with smaller dimension of input-outputs as described in the previous section 5.6. This yields a four by four multivariable system with significant reduction of sensitivity to the plant matrix G_m ; as demonstrated by the results in Appendix 13. The transformed matrix G_x has some useful properties. Assume that the matrix X is partitioned.

$$X = [X_1 \ X_2]$$

where X_1 represents the low order polynomial terms and X_2 represents the high order terms; for the case under consideration X_1 may contain the first and second order terms and X_2 contains the third and the fourth order terms. The transformed matrix G_x is written as:

$$G_x = X^T G_m X = \begin{bmatrix} X_1^T G_m X_1 & X_1^T G_m X_2 \\ X_2^T G_m X_1 & X_2^T G_m X_2 \end{bmatrix} \quad (4.29)$$

During the calculation of the G_x matrix for different G_m matrices it was observed that the two diagonal blocks $X_i^T G_m X_i$ became almost diagonal, the lower off diagonal term ~~$(X_2^T G_m X_1)$~~ always diminished in size relative to the rest while the upper off diagonal term remained big compared to the diagonal terms. This shows that a high order demand on the mill will produce a significant low order component, in contrast to the case of low order demands which produce negligible high order terms. In addition it was noted that G_x exhibited a different kind of "symmetry". That is, the interaction components were mainly even order if the demand was even and they were odd order for odd order demands. All these properties indicate that the multiroll construction of the mill show up as a smoothing filter in spatial terms.

It was noted that $X_2^T G_m X_1 \rightarrow 0$ but $X_1^T G_m X_2$ cannot be neglected thence G_x can be considered to be essentially block triangular. The interaction between odd and even terms was found to be very small and so the diagonal blocks are almost diagonal. Thus G_x is upper triangular and invertible. A suitable precompensator P for diagonalising the plant can be written as:

$$P = G_x^{-1} = \begin{bmatrix} \Lambda_1^{-1} & -\Lambda_1^{-1} M \Lambda_2^{-1} \\ 0 & \Lambda_2^{-1} \end{bmatrix} \quad (4.30)$$

where $\Lambda_1 = X_1^T G_m X_1$, $\Lambda_2 = X_2^T G_m X_2$ $M = X_1^T G_m X_2$.

The effects of using such a precompensator in the system must be determined because of the uncertainty in the knowledge of G_m , and the inaccuracies during its computation. Now the effect of an additive perturbation δG is examined. Define:

$$\delta \Lambda_1 = X_1^T \delta G_m X_1 \quad \delta \Lambda_2 = X_2^T \delta G_m X_2$$

$$\Sigma = \begin{bmatrix} -1 & M \\ 1 & 2 \end{bmatrix}^{-1} \quad \delta \Sigma = \begin{bmatrix} \Lambda_1^{-1} X_1^T \delta G_m X_2 \Lambda_2^{-1} \\ 1 & 2 \end{bmatrix}$$

then the perturbed plant matrix with the above precompensator

$$\begin{aligned} X^T (G_m + \delta G_m) X \cdot P &= X^T (G_m + \delta G_m) X G_x^{-1} = I + X^T \delta G_m X G_x^{-1} \\ &= I + \begin{bmatrix} \delta \Lambda_1 \Lambda_1^{-1} & -\delta \Lambda_1 \Sigma + \Lambda_1 \delta \Sigma \\ X_2^T \delta G_m X_1 \Lambda_1^{-1} & -X_2^T \delta G_m X_1 \Sigma + \delta \Lambda_2 \Lambda_2^{-1} \end{bmatrix} \end{aligned} \quad (4.31)$$

Under the assumption that the numerical errors in δG_m are due solely to modelling inaccuracies and that the structural properties of the matrix $G_m + \delta G_m$ are correct, since the basic form of the shape changes due to the actuators are well known. It then follows that $\delta \Lambda_1$, $\delta \Lambda_2$ are diagonal matrices and $X_2^T \delta G_m X_1 \rightarrow 0$, thus from equation 4.31

$$X^T (G_m + \delta G_m) X G_X^{-1} = I + \begin{bmatrix} \delta \Lambda_1 \Lambda_1^{-1} & -\delta \Lambda_1 \Sigma + \Lambda_1 \delta \Sigma \\ 0 & \delta \Lambda_2 \Lambda_2^{-1} \end{bmatrix} \quad (4.32)$$

This final relation indicates little effect of the perturbations in the diagonal elements in a high gain system. The off diagonal block in equation 4.32 is not a null matrix and the interaction reappears in the transient response but can be easily overcome in the steady state if sufficiently high gain or integral action is employed.

The selection of the dynamic diagonal compensator is based on good transient response characteristics. This compensator $C_0(s)$ must be such that the interaction introduced by the modelling errors is reduced and limited. It was noted that this interaction is from high-order into low-order loops mainly. From the perturbed transfer function of relation 4.32 the forward path transfer function matrix becomes:

$$\begin{aligned} \tilde{W}_X(s) \cdot P \cdot C_0(s) &= \frac{n(s)}{d(s)} X^T (G_m + \delta G_m) X G_X^{-1} C_0(s) = \\ &= \begin{bmatrix} \tilde{W}_1 & \tilde{W}_3 \\ 0 & \tilde{W}_2 \end{bmatrix} \begin{bmatrix} C_1 & 0 \\ 0 & C_2 \end{bmatrix} \end{aligned} \quad (4.33)$$

The closed loop transfer function matrix becomes:

$$T(s) = \begin{bmatrix} (I + \tilde{W}_1 C_1)^{-1} \tilde{W}_1 C_1 & (I + \tilde{W}_1 C_1)^{-1} \tilde{W}_3 C_2 (I + \tilde{W}_2 C_2)^{-1} \\ 0 & (I + \tilde{W}_2 C_2)^{-1} \tilde{W}_2 C_2 \end{bmatrix} \quad (4.34)$$

In the last expression the diagonal blocks contain diagonal matrices and the interaction is due to the off-diagonal block. To reduce the magnitude of this interaction the gains of the first two loops are chosen to be larger than the gains in the third and fourth loop (block C_2 in (4.33)). Consequently the first and second loops should be faster

than the other two and all loops should be fast relative to the disturbances. This implies that failure of the low order loop has more harmful effects on the plant behaviour than failure in the higher order loops.

A final remark: the use of the above partitioning, as in 4.29, provides a very convenient way to add extra higher order polynomial terms in the transformed system and to study the effect of these on the system. Because of the upper triangular form of the transformed matrix G_x , any higher order terms do not change the compensators for the low order subsystem. All the numerical calculations of the transformation X are described in Appendix 13.

4.8 Performance and Robustness

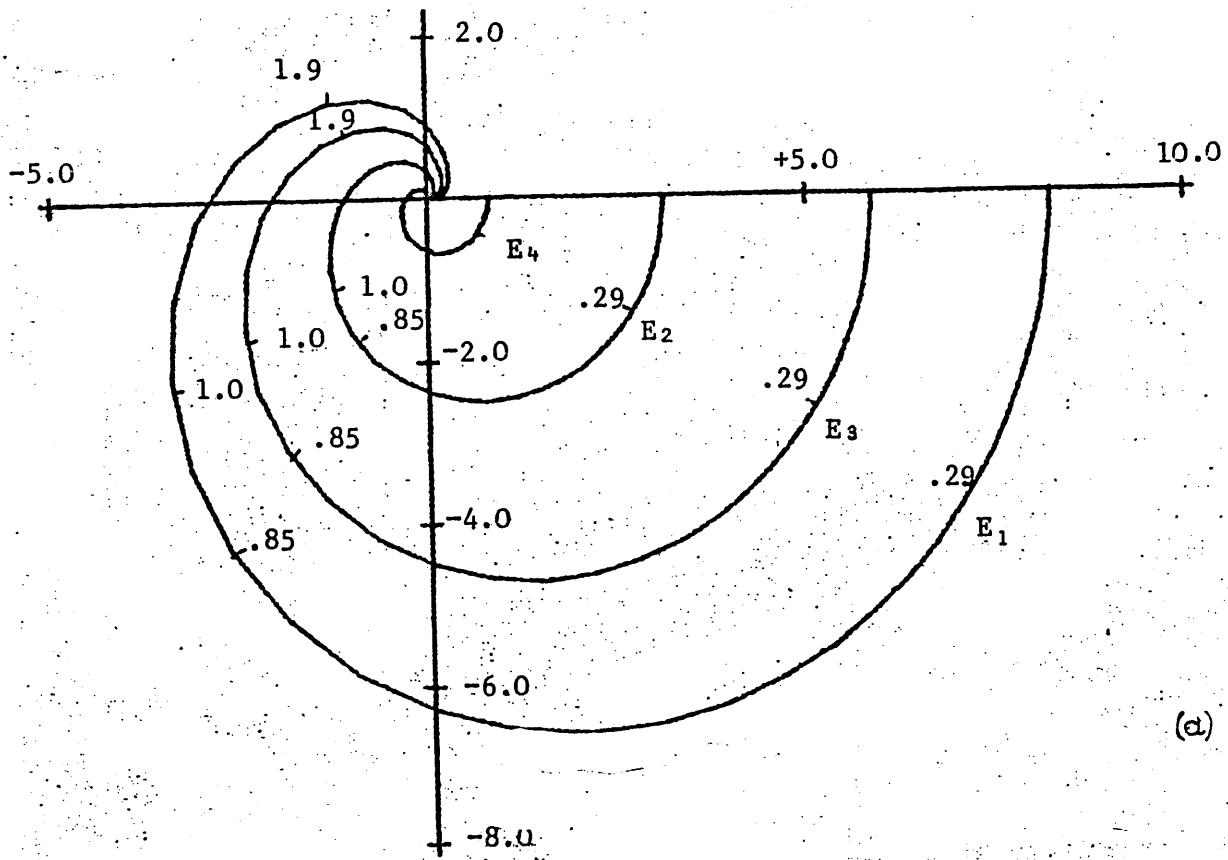
The characteristic loci [20] for the transfer function $W_x(s)$ of the transformed but uncompensated system is shown in figure 5. It is noted that all the loci have the same shape because the dynamics are the same in each signal path. It follows that the loci may be balanced in gain and the interaction can be reduced with the use of a constant precompensator P . The misalignment angles $\{M_i\}$ of the plant characteristic directions from the standard basis vector are independent of frequency (figure 5b) and less than 20° . These angles give a measure of the interaction and may be reduced by choosing P to approximately diagonalise the transfer function $W_x(s)$. As was noted in section 4.7 the transformed mill matrix $G_x = X^T G_m X$ has approximately upper triangular form and then the condition $G_x P \approx I_4$ is very easily solved to give P

$$P = \begin{bmatrix} 0.1 & 0 & 0.05 & 0 \\ 0 & 0.1 & 0 & 0.25 \\ 0 & 0 & 0.3 & 0 \\ 0 & 0 & 0 & 1 \end{bmatrix}$$

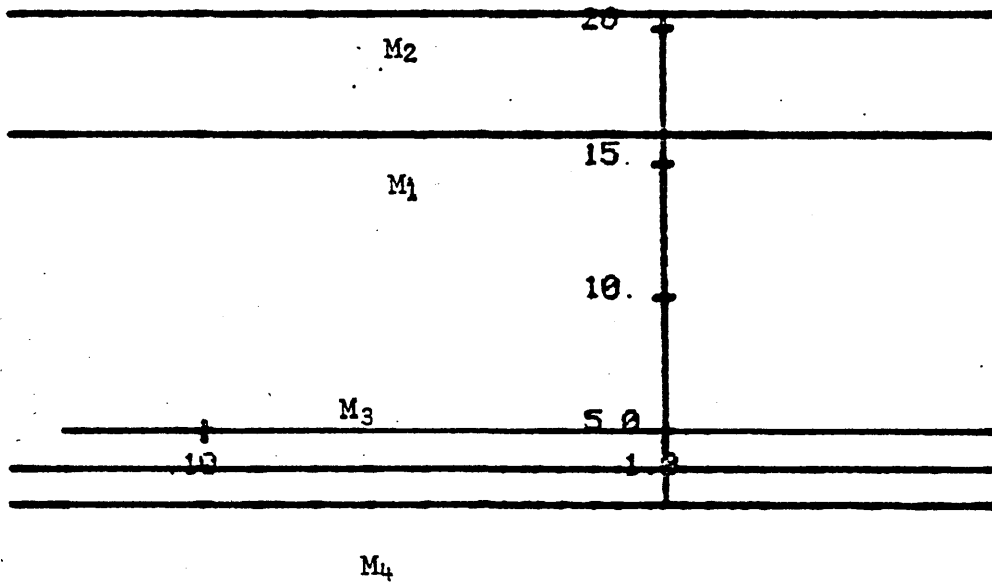
The characteristic loci and misalignment angles of the compensated system are shown in figure 6a,6b. A very similar precompensator is obtained by applying the ALIGN algorithm [20]. It has to be noted that exact diagonalization is not important because of the uncertainty in the G_m values.

To improve the transient and tracking characteristics of the system and to allow the closing of the loop the following dynamic compensator may be introduced:

$$C_0(s) = \frac{0.4(s + 0.7)}{s} I_4$$

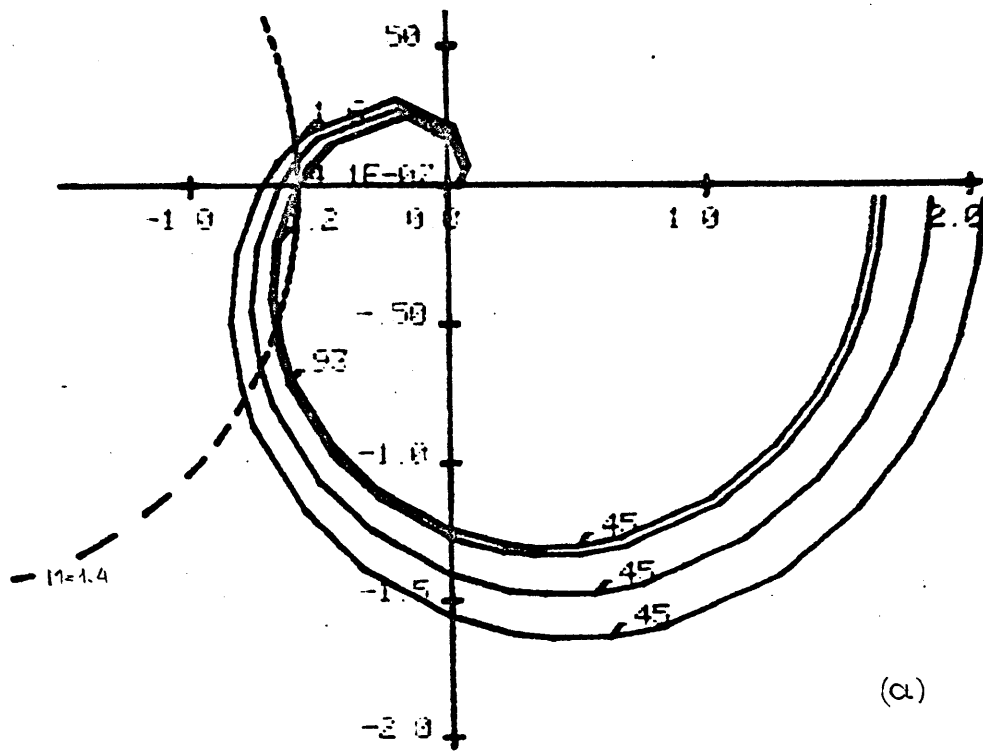


(a)

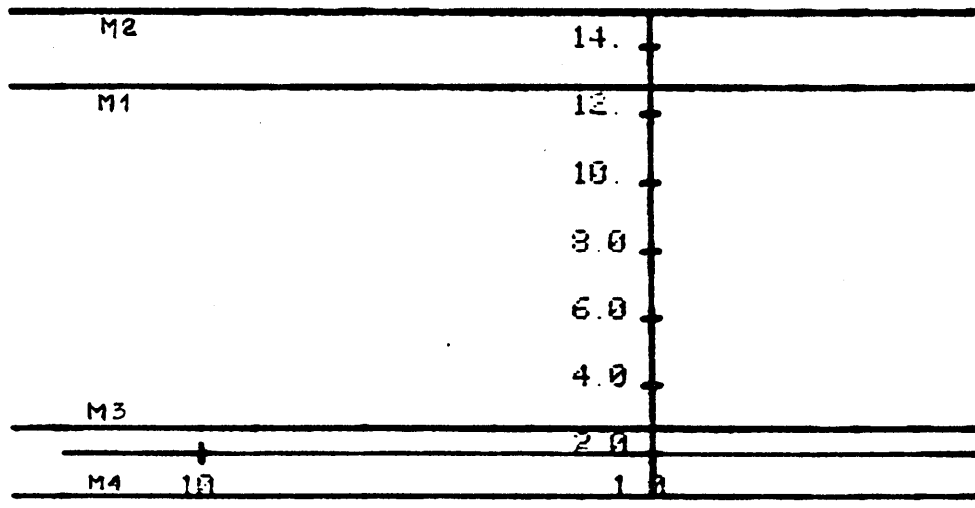


(b)

Figure 5 (a) Characteristic Loci (b) Misalignment Angles for the transformed but uncompensated system



(a)



(b)

Figure 6 (a) Characteristic Loci (b) Misalignment Angles for the system with constant precompensator P

This yields a high low frequency loop gain for good trucking characteristics. The characteristic loci for the dynamically compensated plant $W_x(s) \cdot P \cdot C_0(s)$ are shown in figure 7. These show that the closed loop system has an adequate degree of stability, no overshoot in time responses, and interaction will also be limited.

The responses of the system, using the above controller, were obtained from the dynamic simulation program [98]. The shape profile disturbance is added at the output of the roll gap and has the form shown in Fig 8. The outgoing strip shape is shown in Fig 9 and the control signal to the shape actuators is shown in Fig 10. The closed loop controller was not introduced until after 1 second and this enables the open and closed loop responses to be compared. The variation of the demanded change to the shape actuator does not exceed the maximum of 2 volts (one division) recommended by the manufacturer. The shape actuator racks can move roughly up to ± 80 mm corresponding to the full scale demand signal of ± 10 volts.

The above controller was designed for the medium speed range and is calculated to give good transient performance for that line speed. The effect of line speed changes may now be investigated. Assume that the same precompensators $P, C_0(s)$ are used while the plant operates in either the high or the low speed. The responses for a step into the first reference input are shown in figure 11 for the high, low and medium speed ranges. These responses show that it may be necessary to switch the controller parameters with line speed. However, it is encouraging that the system remains stable over the whole speed range with the same controller.

Because of the structure of $G_x = X^T G_m X$ the major interaction is caused by interaction between high and low order loops, as was already

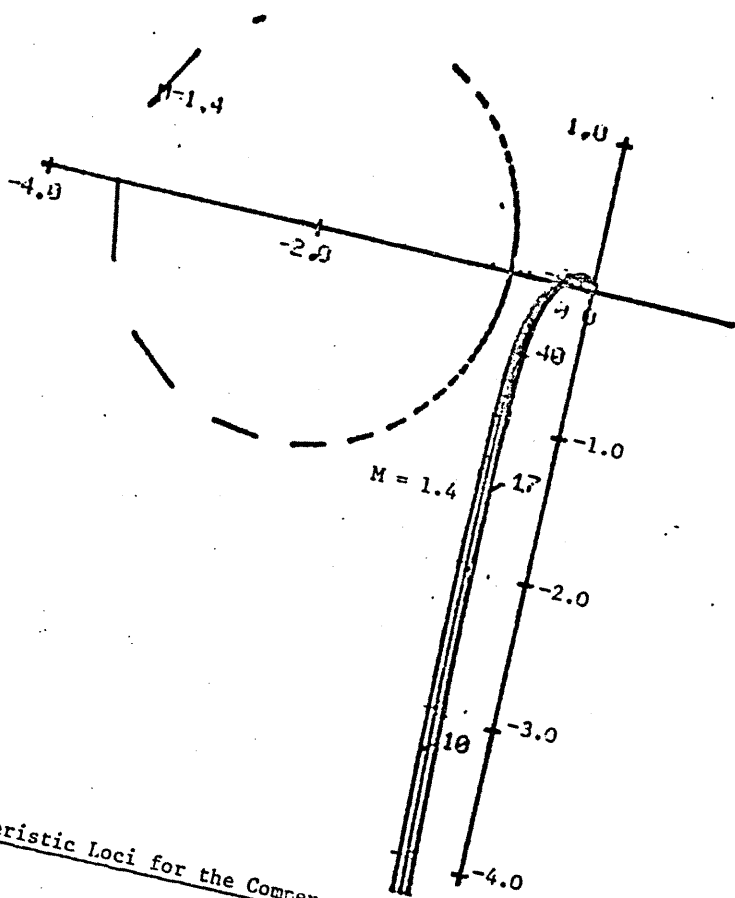


Figure 7: Characteristic Loci for the Compensated System

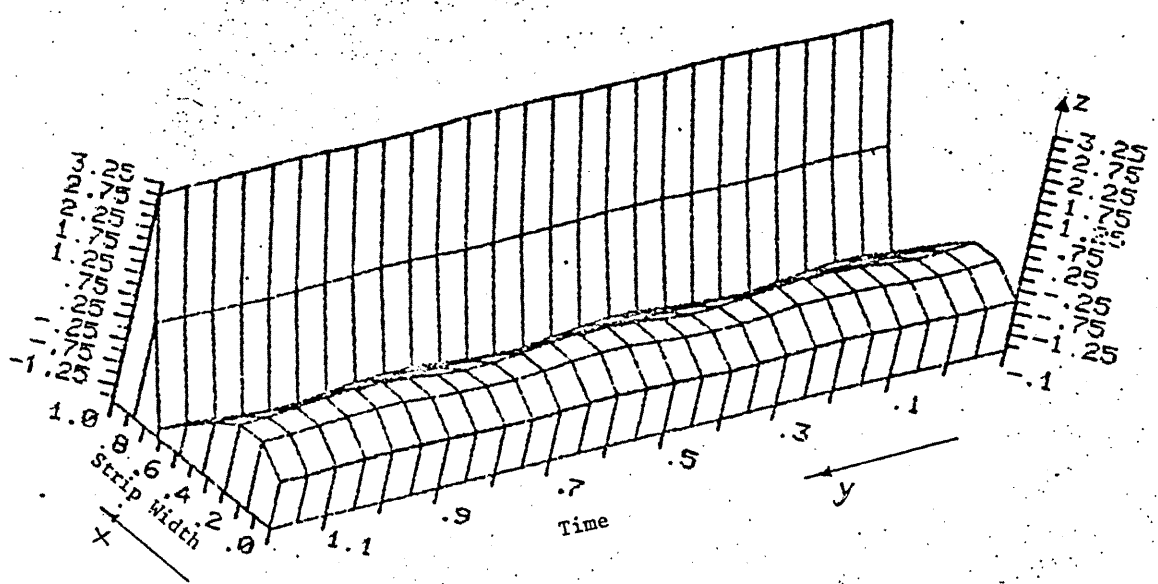


Figure 8: Shape Profile Disturbance

discussed in section 4.7. The precompensator P reduces this interaction when the mill matrix G_m is at its modelled value. The effect of mismatch between the calculated and actual mill gain matrices was investigated using a range of simulation tests. As is noted from the calculations for G_x in Appendix 4.1, although the diagonal terms of G_x decrease with increasing loop order the interaction terms tend to become larger. Thus the worst cases of interaction result from reference changes in the highest order (number 4) loop and the same was demonstrated in the simulation results, figures 12,13,14. The mill gain matrices used in these simulations are G_m and \tilde{G}_m the nominal and perturbed respectively given in (4.1) and (4.4). The situation represented here is similar to that when the controller is used for the wrong coil pass for which it was designed. In the three cases shown in figures 12 to 14 the following controllers are used:

$$(i) C_0(s) = \frac{0.4(s + 0.7)}{s + 0.001} I_4$$

$$(ii) C_0(s) = \frac{0.4(s + 0.7)}{s + 0.001} \text{diag} \{1. , 1. , 0.25 , 0.25\}$$

$$(iii) C_0(s) = \text{diag} \{0.4(s + 0.7), 0.4(s + 0.7), 0.1(s + 2), 0.1(s + 2)\} / (s + 0.01)$$

For the first case the same dynamic compensator is employed in all loops and mismatch produces overshoot and interaction but the system settles down relatively quickly. In the second case the ideas described in section 4.7 are followed and thus the gain in the high order loops is reduced to a quarter of that for the low order loops. This results in slower, but acceptable responses and the interaction is considerably reduced. In the final case, the high order loops are made slower than the low order loops, but the low frequency gain is reduced by a factor of 0.71. There is an obvious trade-off between speed of response and amount of interaction. Thus the actual desired specifications by

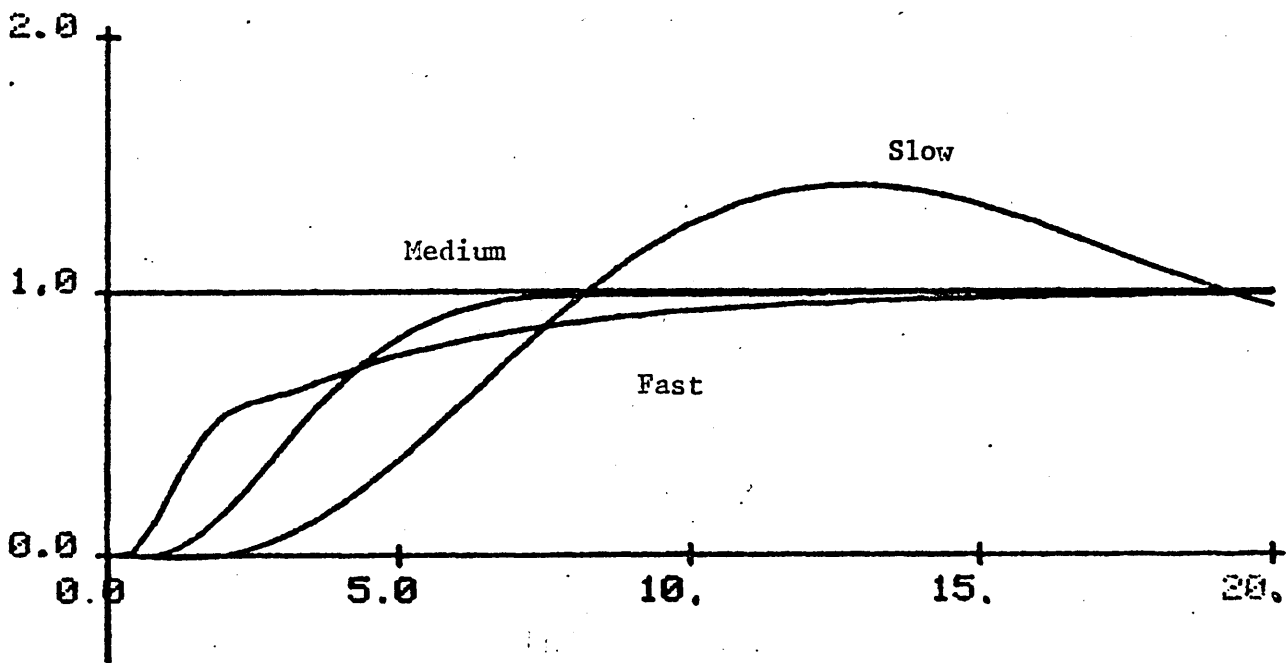


Figure 11: System Responses using the Medium Speed Controller

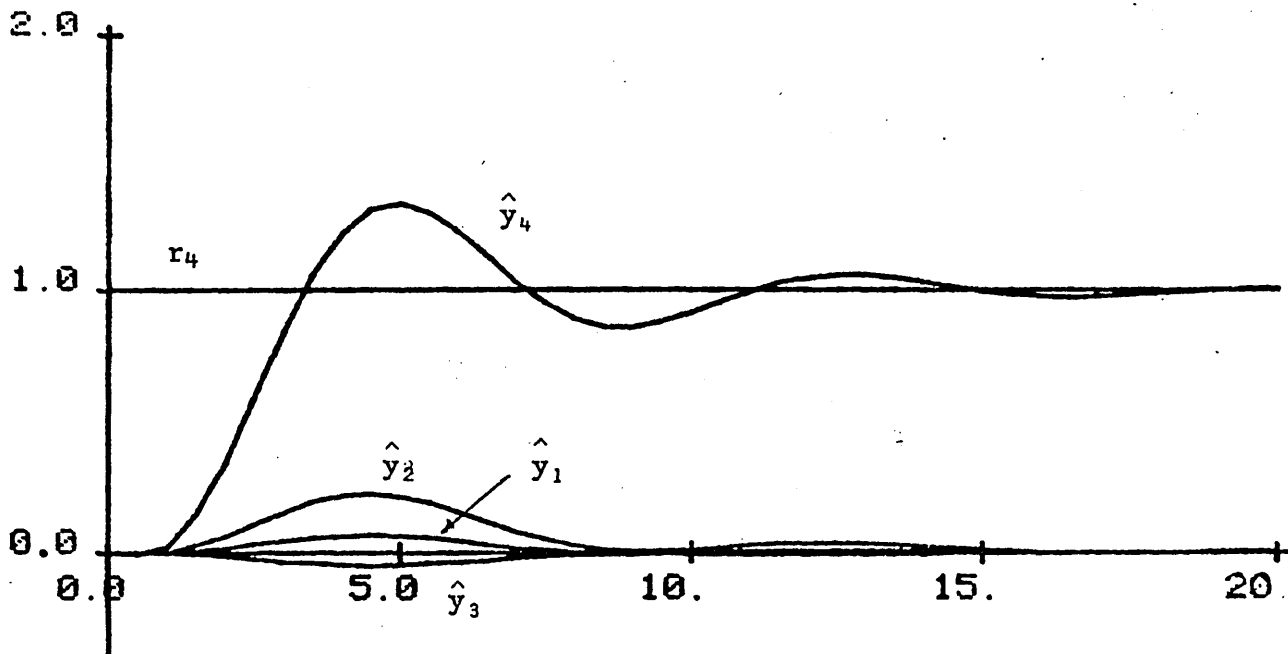


Figure 12: System Outputs when Mismatch is present (case i)

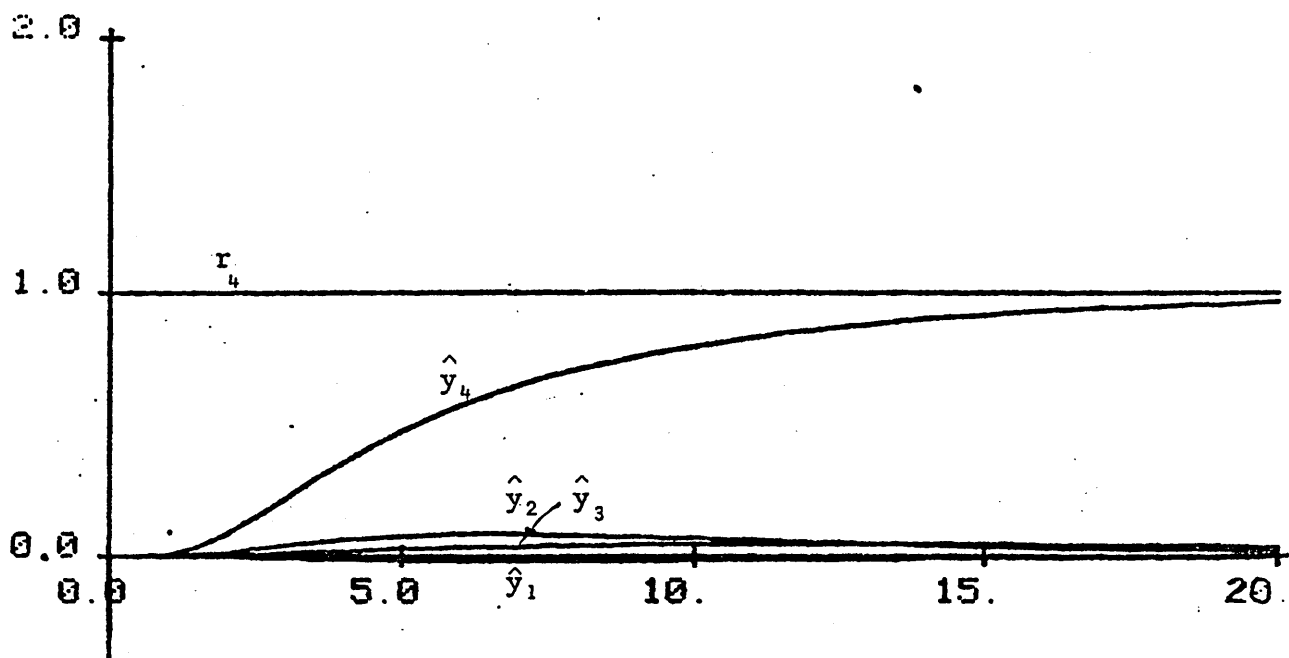


Figure 13: System Outputs when Mismatch is present (case ii)

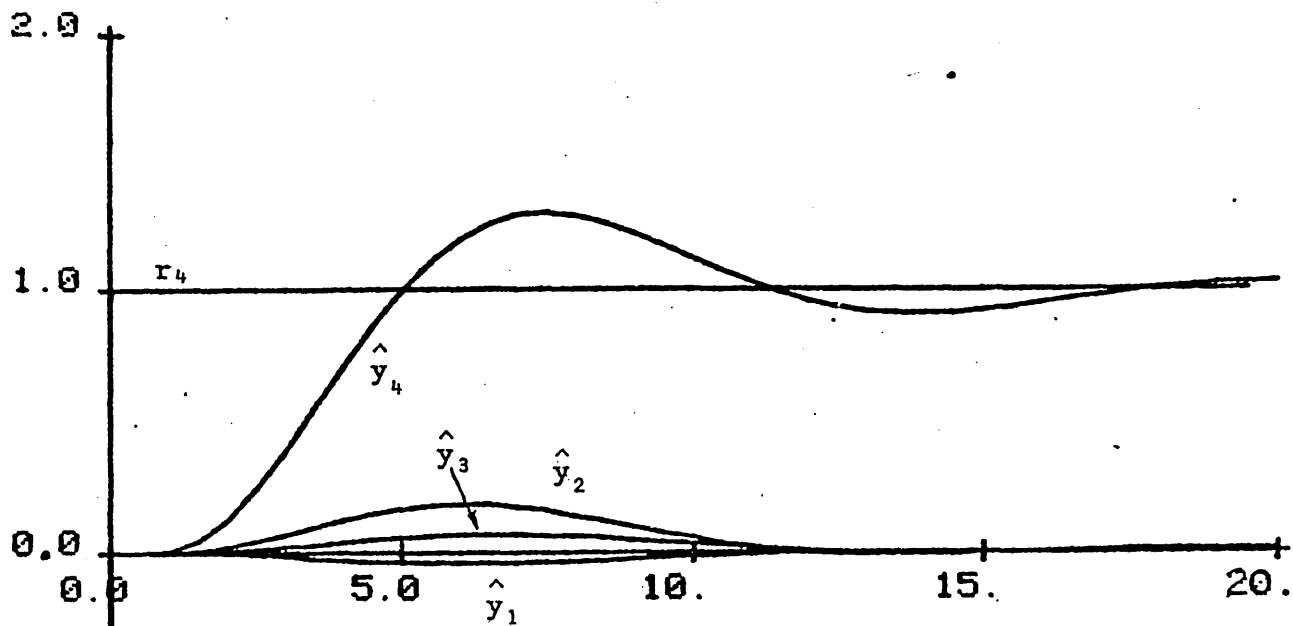


Figure 14: System Outputs when Mismatch is present (case iii)

the plant engineers dictate the controller to be implemented. For the present, the results preferred are those with case (ii).

Due to modelling errors and second order effects the mill matrix G_m may not be singular. Then a possible design would be to use as precompensator the inverse of G_m together with some dynamic compensation. The effect of mismatch was to produce unacceptable interaction and in some cases unstable responses, although the same perturbed G_m as before was used. The explanation lies in the fact that the inverses of the two matrices are quite different; G_m^{-1} has elements in the range $[0.1, 11]$ but \tilde{G}_m^{-1} within $[10, 420]$, and this makes such a design impractical.

The transformed 4-loop system performed much better than the original 8-loop square system. Some of the reasons for this may be considered. The eigenvalue spectra for G_x has a much smaller range than that for G_m and the perturbed \tilde{G}_x has a very similar spectrum to that for G_x , given in Appendix 13. (both in the range 1 to 8). The characteristic direction set is also the same as the eigenvector set for the constant precompensated mill matrix. The low order eigenvectors are already aligned before the use of the compensator P, thus predicting low interaction in low order demands and high order outputs. All this phenomena provide further confirmation for the use of the parameterization approach.

A further useful property of the transformation is that the eigenvalues of G_x (or \tilde{G}_x) are similar to the dominant four eigenvalues of G_m (or \tilde{G}_m). That is, the transformation maintains the larger modes in G_m and also limits the range of the spectrum. These larger modes remain relatively the same for a range of different mill gain matrices ie in the range $[0.7, 9.0]$. The improvement in robustness properties may be attributed to this transformation which rejects the lower and sensitive modes. Similar remarks apply to the singular values of G_x

and G_m (singular values of a real matrix F are the non-negative square roots of the eigenvalues of $F^T F$). Following the work of Postlethwaite et al [99], and Safonov et al [100], robustness may be analysed using principal gains (singular values) and in figure 16a plot of the principal gains for the return difference matrix of the system $F(s) = [I + M(s)]^{-1}$. The forward path transfer function is

$$M(s) = W_x(s) \cdot P C_0(s) = G_x \frac{n(s)}{d(s)} \cdot P C_0(s) = X^T G_m X K(s)$$

and considering an additive perturbation δG_m in G_m ie $\tilde{G}_m = G_m + \delta G_m$ then

$$\tilde{M}(s) = X^T (G_m + \delta G_m) X K(s) = X^T G_m X K(s) + X^T \delta G_m X K(s) = M(s) + \delta M(s)$$

The largest principal gain of $[I + M(s)]^{-1}$ is 1.6 (figure 15) and thus from the small gain theorem [99] the system will remain stable under all perturbations $\delta \Delta(s)$ which are stable and have maximum principal gain $1/1.6 = 0.625$. Unfortunately this result does not translate easily into percentage allowable variations in G_m , as the relations between the elements, the eigenvalues and singular values of a matrix (in this case δM) is very complicated.

The optimal output controller expressions which are obtained in the next section can also be used with the transformed system. Their performance is as good or better than that obtained with the simple controllers considered above; that is with faster and more damped response. Also results on the robustness of optimal controllers exist (Athans [101]). This of course had to be expected as these controllers are much more complex and this reason puts them in reserve for the practical implementation. For the simple controller the quality of responses is considered acceptable for the present.

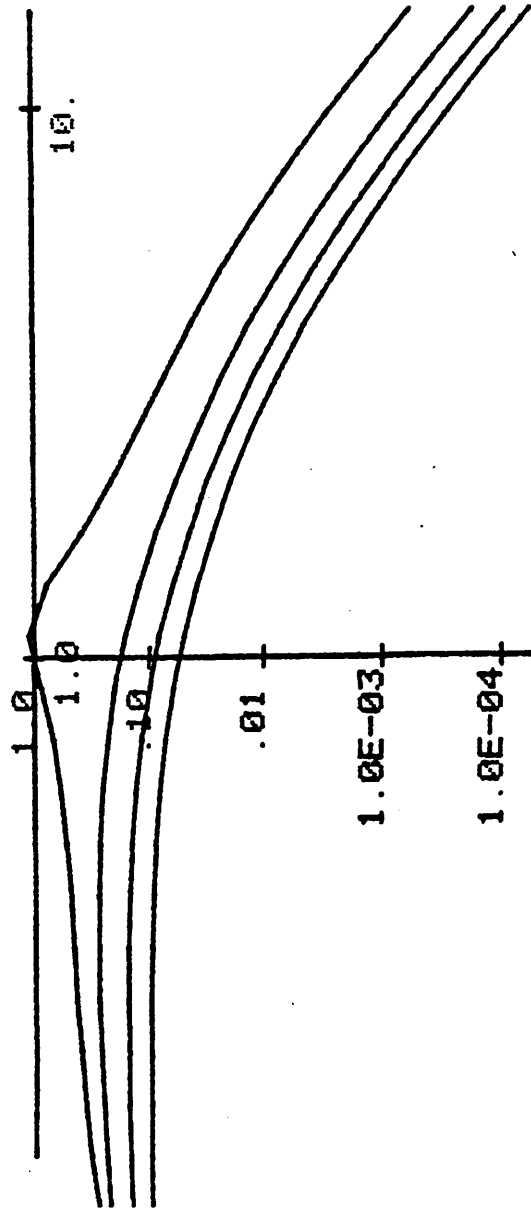


Figure 15: Principal gains loci for the closed loop system

4.9 Output Feedback Optimal Control Solution

An output feedback optimal controller $C_0(s)$ is obtained first for the deterministic case and then the stochastic controller is considered. The state feedback solution for the problem would be quite impractical in view of the number of states of the plant and the fact that all remain inaccessible except the actuator states which are directly available and for which already local feedback is used to obtain the desired actuator dynamics. The step response for the system is important and hence the reference is chosen as $\underline{r}(s) = \underline{k}/s$ with \underline{k} a constant vector. Initial conditions for the plant are assumed to be zero : $\underline{x}_0 = 0$. This is a reasonable assumption since the closed loop system will be made fast so that initial condition response may be neglected.

The performance criterion to be minimized is defined as:

$$J(\underline{u}) = \int_0^{\infty} \left[\langle \underline{L}\underline{e}(t), Q_1 \underline{L}\underline{e}(t) \rangle_{E_r} + \langle \underline{u}(t), R_1 \underline{u}(t) \rangle_{E_m} \right] dt \quad (4.35)$$

where Q_1, R_1 are the weighting matrices and L is a linear dynamic operator. The optimal controller $C_0(s)$ is calculated from the following theorem:

Theorem 4.1

For the asymptotically open loop stable plant $W(s)$ the closed loop controller to minimize the criterion $J(\underline{u})$ is given by:

$$C_0(s) = F_0(s) (I_m - W(s)F_0(s))^{-1} \quad (4.36)$$

where $F_0(s)$ is defined from the equation

$$Y(s)^{-1} \{Y(-s)^{-T} W^T(-s)L^T(-s)Q_1L(s)\underline{r}(s)\}_+ = F_0(s)\underline{r}(s) \quad (4.37)$$

and $Y(s)$ is the generalised spectral factor [75] obtained:

$$Y^T(-s) Y(s) = W^T(-s)L^T(-s)Q_1L(s)W(s) + R_1 \quad (4.38)$$

The proof of this theorem is given in Chapter 1 of this thesis.

The above defined controller may be simplified by substituting $L(s) \underline{\underline{=}} I_m$ and for the plant matrix $W(s)$ from equation (5.25). First the spectral factors are written in terms of the polynomial matrix $N(s)$ (ie $Y(s) = N(s)/d(s)$):

$$Y^T(-s) Y(s) = W^T(-s)Q_1W(s) + R_1 = \frac{n(-s)G_m^T Q_1 G_m n(s)}{d(-s) d(s)} + R_1 = \frac{N^T(-s)N(s)}{d(-s) d(s)} \quad (4.39)$$

Then equation (5.39) becomes:

$$F_0(s)\frac{1}{s} = Y(s)^{-1}\{N(-s)^{-T}G_m^T n(-s)Q_1\frac{1}{s}\}_+ = Y(s)^{-1} N(o)G_m^T Q_1\frac{1}{s} \quad (4.40)$$

The closed-loop feedback controller follows from (4.38):

$$C_0(s) = \left[Q_1^{-1} G_m^{-T} N(o)^T N(s) = n(s)G_m \right]^{-1} d(s) \quad (4.41)$$

and if G_m^{-1} exists (or G_x^{-1})

$$C_0(s) = \left[G_m^{-1} Q_1 G_m^{-T} N_0(o)^T N(s) - n(s)I_m \right]^{-1} G_m^{-1} d(s) \quad (4.42)$$

It has to be noted that the polynomial matrix inside the square brackets in the last equation is not diagonal except when the frequency is zero and when the control weighting matrix R_1 is zero, which is physically unrealistic. Thus in general this controller does not attempt to make the system diagonal. Another choice for the error weighting matrix Q_1 which leads to a diagonalized closed loop system is as follows.

Let

$$Q_1 = G_m^{-T} Q_0 G_m^{-1}$$

and choose Q_0 and R_1 diagonal then $N(o) = (Q_0 + R_1)^{\frac{1}{2}}$ and from (4.41)

$$C_0(s) = \left[Q_0^{-1} (Q_0 + R_1)^{\frac{1}{2}} N(s) - n(s)d_m \right]^{-1} G_m^{-1} d(s) \quad (4.43)$$

where the matrix in the square brackets is diagonal. This choice for Q_1 corresponds to the case where a transformed shape error

profile is weighted. This transformed shape error represents the error profile which the outputs of the shape actuators must correct and thus it is important to limit these errors because of the mechanical construction of the mill.

An alternative way to obtain a diagonalised closed loop system is the control weighting matrix chosen so that the spectral factors are diagonalised. Let $R_1 = G_m^T R_0 G_m$ and for Q_1, R_0 chosen diagonal equation (4.40) becomes:

$$\begin{aligned} Y^T(-s)Y(s) &= \frac{n(-s)G_m^T Q_1 G_m n(s) + d(-s)G_m^T R_0 G_m d(s)}{d(-s)d(s)} \\ &= \frac{G_m N_1^T(-s)N_1(s)G_m}{d(-s)d(s)} \end{aligned} \quad (4.44)$$

where $N_1^T(-s)N_1(s) \triangleq Q_1 n(-s)n(s) + R_0 d(-s)d(s)$ then

$$F_0(s) = G_m^{-1} N_1(s)^{-1} N_1(o)^{-T} Q_1$$

and the controller:

$$\begin{aligned} C_0(s) &= G_m^{-1} N_1(s)^{-1} N_1(o)^{-T} Q_1 \left(I_m - \frac{n(s)}{d(s)} N_1(s)^{-1} N_1(o)^{-T} Q_1 \right)^{-1} = \\ &= d(s) G_m^{-1} \left[Q_1^{-1} N_1(o)^T N_1(s) - n(s) I_m \right]^{-1} \end{aligned} \quad (4.45)$$

This expression for the closed loop controller is comparable with the one in equation (4.43) as both produce non-interactive loops.

Integral action is a feature usually desirable [88]. This can be achieved with the optimal controller when the dynamic operator in the cost function $L(s) = I_m/s$. With the same assumptions as for the previous Theorem 4.1, the following Theorem 4.2 provides an expression for the controller:

Theorem 4.2

For the system of Theorem 4.1 and $L(s) = I_m / s$ the closed loop optimal controller is given by:

$$C_0(s) = N(s)^{-1} (M_1 + sM_2) \left[I_m - n(s)N(s)^{-1} (M_1 + sM_2) \right]^{-1} G_m^{-1} d(s) \quad (4.46)$$

where

$$N^T(-s)N(s) = G_m^T Q_1 G_m n(-s)n(s) - s^2 R_1 d(-s)d(s) \quad (4.47)$$

$$M_1 = Q_1^{\frac{1}{2}} G_m \quad (4.48)$$

$$M_2 = \lim_{s \rightarrow 0} - \frac{N(s) - n(s)M_1}{s} \quad (4.49)$$

Proof of this theorem is given in Appendix 14.

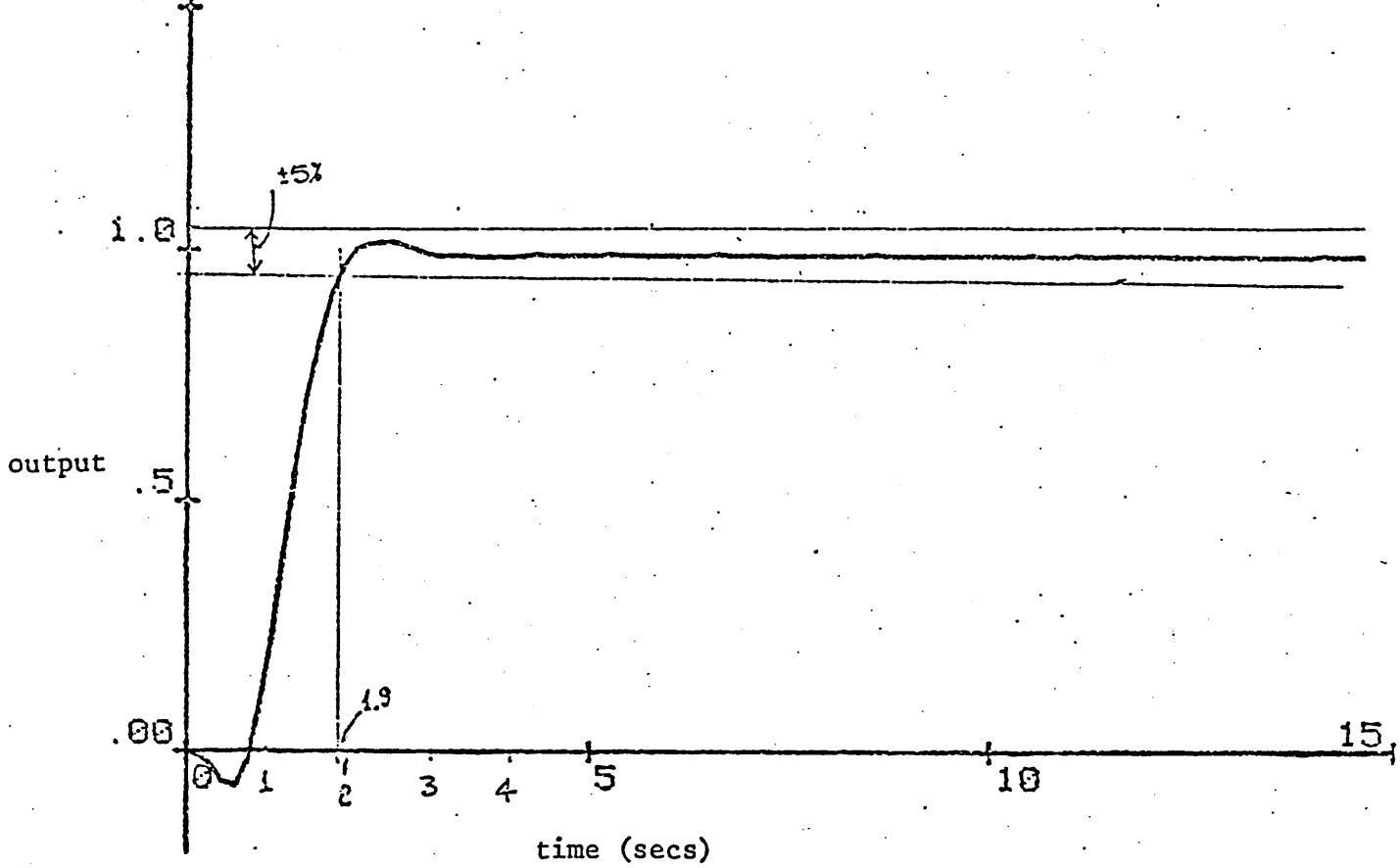
As with the previous discussed case, here the controller exhibits integral action and a suitable choice of the Q_1 , R_1 matrices provide a non-interactive closed loop system. That is if $Q_1 = G_m^{-T} Q_0 G_m^{-1}$ and Q_0 and R_1 are diagonal. The calculation of the above controllers is relatively easy, (Appendix 15), as the matrix to be spectrally factored is diagonal and thus the problem reduces to polynomial factorization. For the selection of Q_0 , R_1 has also to be noticed that there are certain shape defects which are more important than others. For example, loose edge causes difficulties and this situation has to be avoided by proper selection of Q_0 elements weighting the edges shape error.

As the closed loop with the above controller takes the form of m single loop systems, the controller expression for the medium speed (5 m/s) using the plant transfer function (4.23) for each loop is:

$$C_0(s) = \frac{(0.25+1)^2(0.74s+1)(0.01s+1)(0.291s+1)(1.0645+1)}{(0.01+1.33s+0.49s^2+0.127s^3+0.173s^4+0.979 \cdot 10^{-3}s^5+0.302 \cdot 10^{-5}s^6)}$$

This was designed for a steady state error of less than 1% with $q_{ii} = 100$ and $r_{ii} = 1$ the Bode diagram of the loop gain and the time response

for a step input is depicted in figure 16. The controller poles are
 $s_1 = -306$ $s_{2,3} = -1.473 \pm j 4.315$ $s_{4,5} = -7.68 \pm j 3.22$ $s_6 = -0.0075$.
The first pole may be cancelled with the zero $(0.01s + 1)$, as both are
very higher than the rest, to reduce the order of the controller.



TIMAL OUTPUT CONTROLER

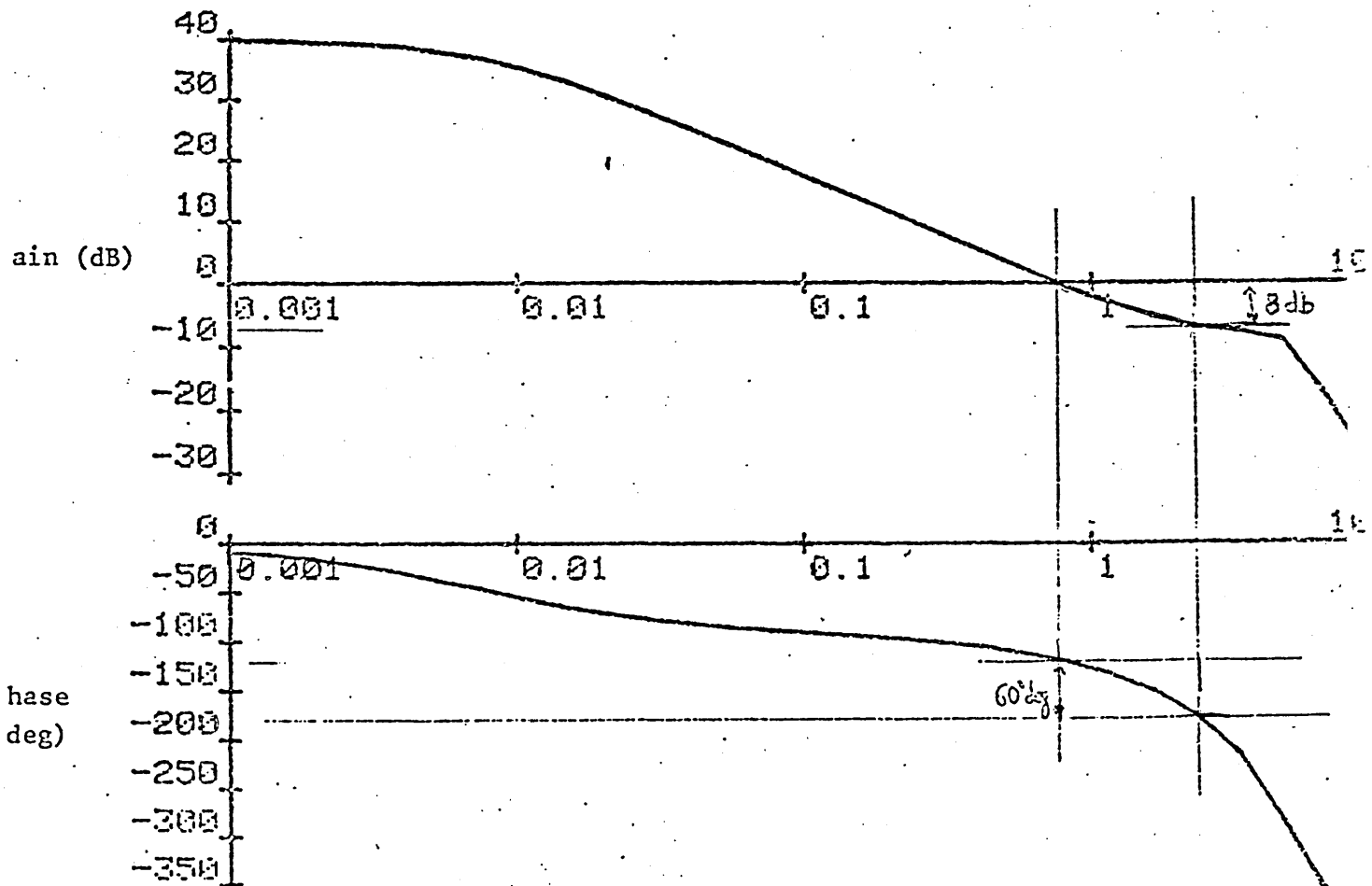


Figure 16 Simulation Results and Bode Diagram

4.10 Discussion of Results - Conclusions

The mechanical construction of a Sendzimir mill is such that there is significant interaction between various actuator inputs and shape changes measured at the roll gap. This interaction is non-dynamic which leads to an interesting special case of the general multivariable problem. The mill gain matrix may be calculated from a static model but the complexity of the model ensures that there is significant uncertainty attached to the value of the gain matrix elements. It is impracticable to reduce this uncertainty by plant tests for more than a few (two or three) rolling schedules. Thus the major objective for the control system design must be to produce a closed loop system which is robust in the presence of modelling errors and uncertainties. This was achieved using an input-output dimension reducing transformation based upon physically desirable control objectives.

The control system design was shown to be relatively insensitive to the changes in line speed for the mill. This allows a minimum number of controller gains and time constants to be used and stored. The approximately upper triangular form of the transformed mill matrix leads to a simple constant precompensator and simple dynamic compensation. The steps in the calculation of the controller were:-

- (a) Calculate the transformed mill matrix G_x ,
- (b) Calculate an approximate diagonalising precompensator P ,
- (c) Calculate a diagonal dynamic compensator $C_0(s)$ using single loop techniques.

The use of the Characteristic Locus CAD package provided more flexibility during the above design steps. The physical reasoning behind the derivation of the controller and the simplicity of the

resulting controller provide confidence in the practicality of the design technique. Further work will be concerned with an extension of the robustness analysis and the development of a control system for the first intermediate rolls (a second shape control mechanism).

Optimal output controllers were considered and it was shown that the system can be reduced to a set of single-input single output loops through a specific choice of the error weighting matrix $Q_1 : Q_1 = G_m^{-T} Q_0 G_m^{-1}$. In this case the diagonal matrix Q_0 penalises errors referred to the mill inputs. This result has some value since adjacent As-U-Roll actuators can only be changed by a limited amount. By choosing Q_0 and R_1 , the relative importance of shape error and control action at any particular As-U-Roll is considered. The optimal control solution produced a high order controller and indicated cancellation of the plant poles would be helpful. The plant has a number of break-points in the same frequency range, and using classical design methods these must also be cancelled to achieve faster, damped responses and relative stability.

CHAPTER 5

A Comparison of Characteristic Locus and Optimal Control Designs in a Dynamic Ship Positioning Application

A Comparison of Characteristic Locus and Optimal Designs in a Dynamic Ship Positioning Application5.1 Introduction

The increasing need to exploit the mineral and oil resources of the seabed has led from exploration in shallow waters close to the shore to deeper less accessible and less hospitable locations. At first platforms and support vessels were held stationary over the required position with the use of anchors and moorings. Deep water exploration and the time needed for setting up an anchoring system for positioning has led to the introduction of Dynamic Ship Positioning systems.

In general, a dynamically positioned vessel must be capable of maintaining a given position and heading by using thrust devices, without the aid of anchors or moorings. The position control system is not expected to hold the vessel absolutely stationary but to maintain its station within acceptable limits, under a range of weather conditions [102]. A maximum allowable radial position error is usually specified eg 4 to 5 percent of water depth

The motions of a vessel stem from wind, current and wave drift forces which are low frequency forces and also from high frequency forces due to the oscillatory components of the sea waves. Only the low frequency forces (less than 0.25 rad/s) are to be counteracted by the use of the thruster. The control system must avoid high frequency variations (eg greater than 0.3 rad/s) in the thrust demand which is referred as thruster modulation. Any attempts to counteract the high frequency motions causes unnecessary wear and energy loss in the thrusters. The

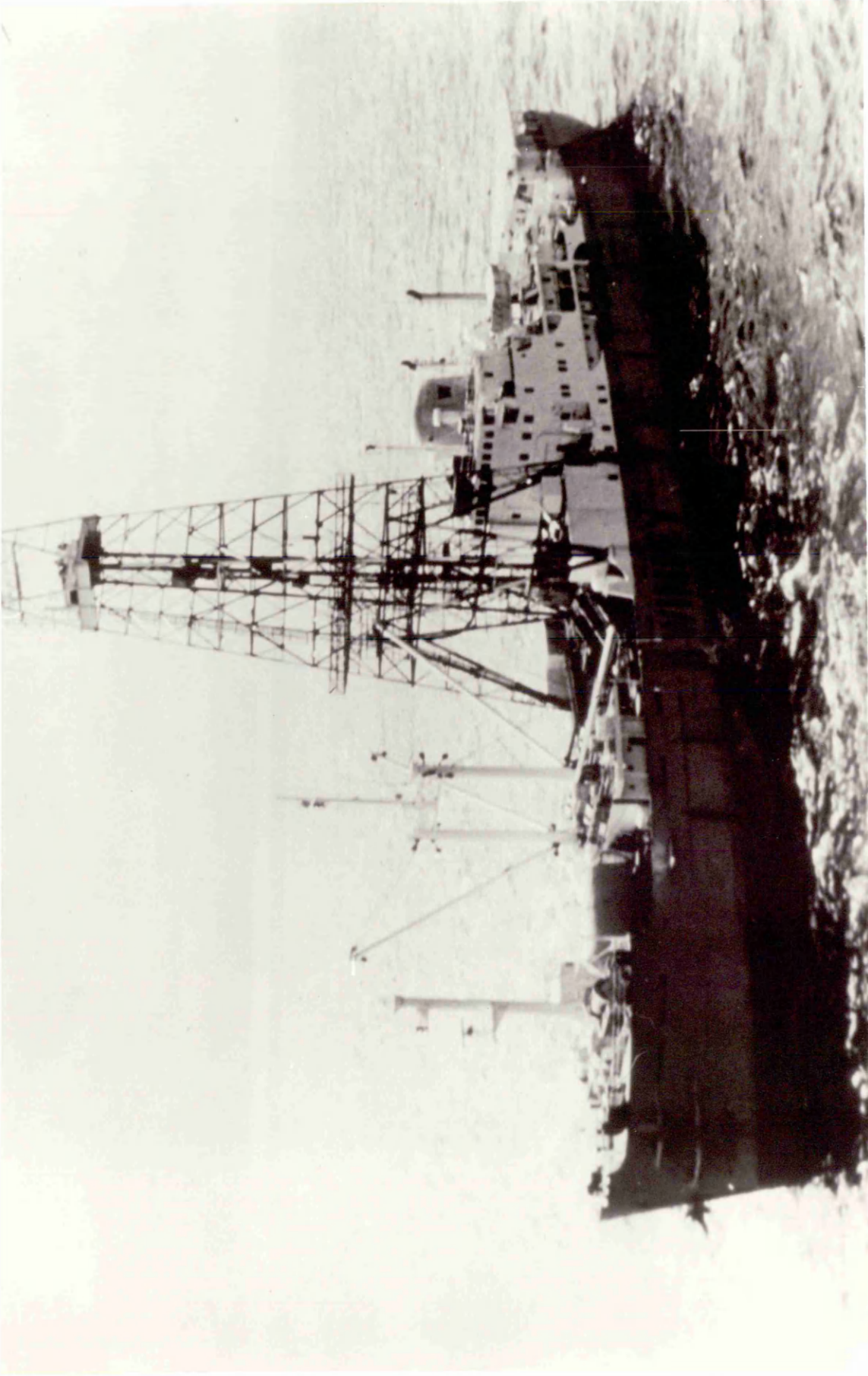
position measurements must be filtered to obtain a 'good' estimate of the low frequency motions of the vessel, control of these low frequency motions may then be applied. The control systems for the first dynamically positioned (DP) vessels [102,103] included notch filters and PID controllers. The notch filters were used to remove the sea wave components on the position measurements. The major difficulty with the conventional PID/Notch filter schemes is that improved filtering action may only be achieved with a deterioration in the control system performance [104].

Difficulties with thruster modulation and with the selection of the "best" notch filters led to the use of optimal control schemes involving Kalman filters [104]. The Kalman filter introduced a smaller phase lag on the position measurements and also offered the possibility of adaptive filtering action via the extended Kalman filter [105,106]. This combination of Kalman filter and optimal control state estimate feedback is now the accepted solution to the DP problem.

Having shown the Kalman filter to be the most appropriate for DP systems there remains the question of the design for the controller. Previous authors have employed optimal control theory via the separation principle. It is now appropriate to consider whether any of the recent multivariable frequency domain design methods might be used for the controller design. Rosenbrock's Inverse Nyquist Array design technique has been used [107] but not in conjunction with a Kalman filter.

The characteristic locus design method [20] has not previously been applied to the design of DP systems. A recent design philosophy integrates this frequency response method with the root locus approach and results in an inner/outer loop structure [108]. This is particularly appropriate for non-square systems formed from a plant and Kalman filter in cascade. Thus, in the following the integrated characteristic locus/

root locus method will be employed for DP system design and the results will be compared with the corresponding optimal control designs.



Wimpey Sealab Dynamic Positioned Vessel

5.2 The Ship Positioning Problem

The major components in a dynamic ship positioning system are the position measurement system, the thrusters and the control computer. Various forms of thruster configuration are employed and the two most common forms are shown in figure 1. The first involves the use of the vessels main propulsion units together with an array of tunnel thrusters. Otherwise steerable thrusters, hung below the vessel and rotated to the desired direction, may be used. The vessel shown in figure 1 is used for offshore drilling operations but DP vessels are also used for survey, fire fighting and oil rig support duties.

Once a desired drilling location has been established (usually by radio navigation) a local position reference is required. A short baseline beacon configuration is often used to provide the position reference. This consists of a single sonar beacon mounted on the sea bed. By measuring the difference in the time of arrival of the acoustic energy at the hydrophones the distance to the beacon, can be accurately measured (figure 1). Other position measurement systems may be used in conjunction with the acoustic system and each has different dynamics and noise characteristics. Problems concerned with the pooling and filtering of signals affect the filter design but do not affect the controller design and are not considered here.

The environmental forces acting on a vessel induce motions in six degrees of freedom (surge, sway, yaw, heave, pitch and roll). In the DP mode of operation, only vessel motions in the horizontal plane (surge, sway and yaw) are controlled. The other motions and their interactions are considered negligible. It is usual to design

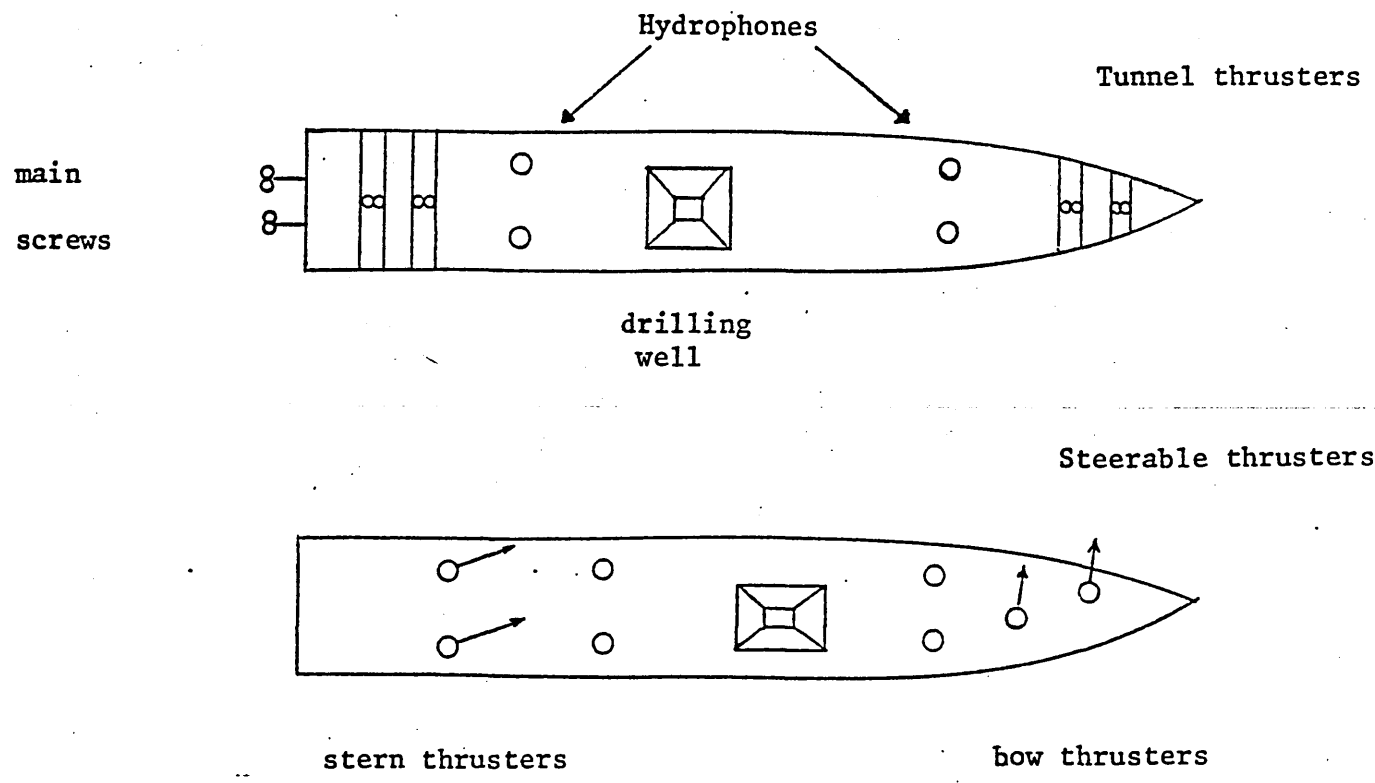
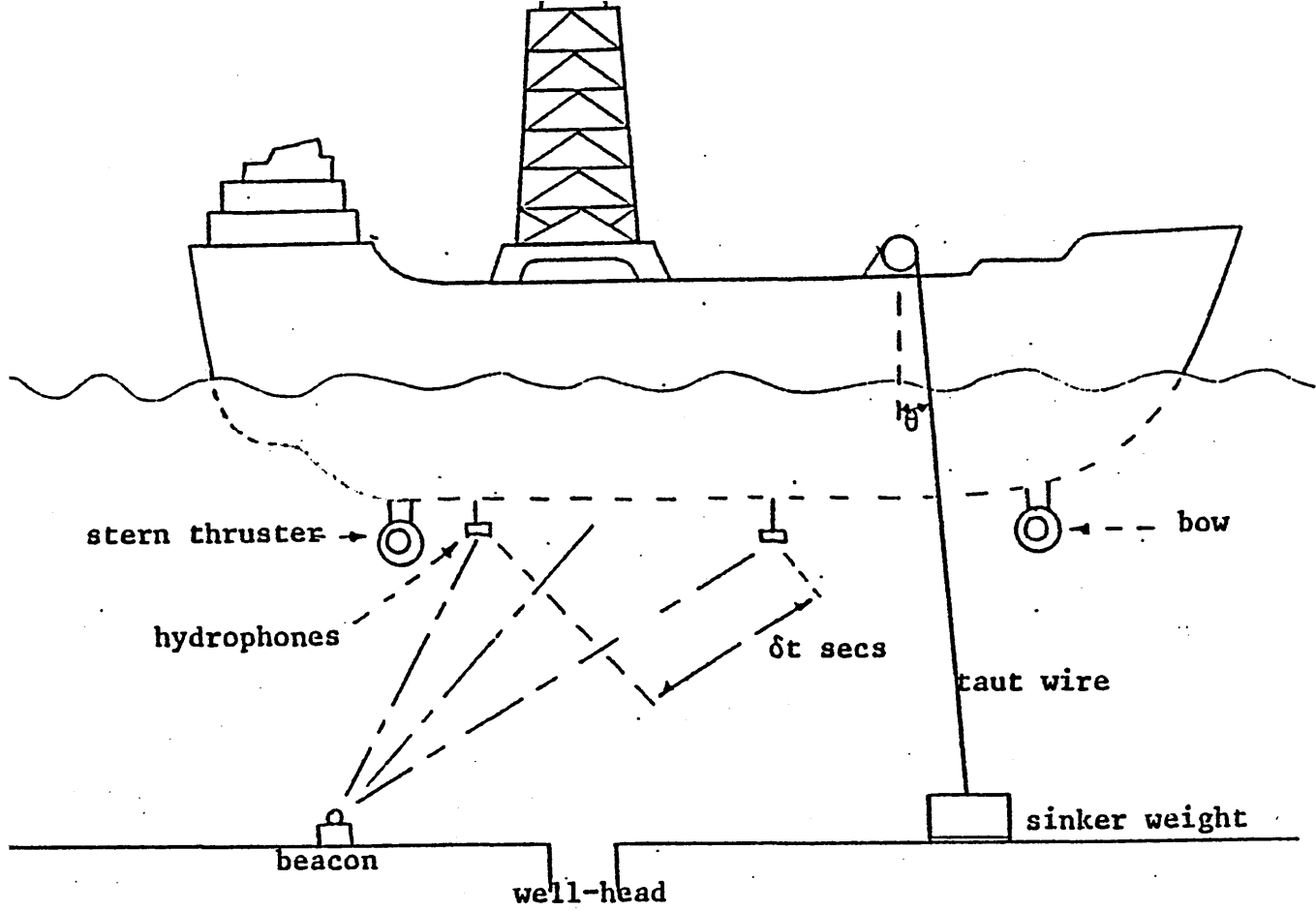


Figure 1: Dynamic Positioning Vessels using Tunnel or Steerable Thrusters

the control for sway and yaw together and then include the surge as a separate design. This is possible because the linearised vessel dynamics for surge are decoupled from those for sway and yaw motions. Thus in the following, the control of sway and yaw motions only will be considered. The major disturbance acting on a vessel is due to wind forces. Wind gusts and drift forces have frequencies in the range 0 - 0.04 c/s whereas the wave induced ship motions are in the range 0.05 - 0.25 c/s. The current speed and direction can be considered constant over long periods of time compared with the wind and wave force changes.

The requirements for a DP system may be summarised as:

- 1 To maintain positional accuracy or heading under specified adverse weather conditions (see Table 5.1)
- 2 Avoidance of high frequency variations in the thrust demand (≥ 0.056)

The positional accuracy can be calculated [119] using:

$$\text{radial error} \approx e_1 d + w/2 + e_2$$

where

e_1 is the per unit error of the position measurement system

d is the water depth

w is the peak to peak wave motion in surge or yaw

e_2 is the error due to the control loop

The wind forces are often the most important disturbance acting on a vessel and they vary much more rapidly than the current or wave drift forces. A wave filter is designed to render the control system insensitive to high frequency first order wave force motions. Wind feed forward control is often used to counteract the effect of steady winds and gusting and it is convenient to assume that the position holding will be affected by a white noise component of wind only. Integral action is normally employed to counter

the wave drift and current forces. The integral action may be introduced in optimal stochastic controllers by modifying the usual performance criterion [109]. However, in practice the integral action is often included as part of a sea current model and not part of the optimal solution. Thus, for simplicity both the feed forward control and the integral action will not be considered here.

Table 5.1

Position Accuracy Requirements				
Duty	Environmental Conditions			Accuracy
	Wind (knots)	Significant Wave Height (m)	Current (knots)	
Drilling	25	3.9	3	3% water depth (minimum of 7 m)
Diving Support	30	4.5	1	± 3 m heading $\pm 2^\circ$
Equipment Supply	20	2.0	1	heading $\pm 1^\circ$ excursion 1.5 m (maximum)
Fire Fighting	Up to severe gale or storm			± 15 metres

The mathematical model for the vessel dynamics is highly non-linear [110, 111] and may be derived from theory and substantiated by model tests. It is usually assumed that the vessel motions are the sum of the outputs from low and high frequency sub-systems. The low frequency sub-system is controllable and has an input from the thruster control signal u . The high frequency sub-system has no connection to the thruster control input. Thus, the total motions of the vessel is the super position of the horizontal manoeuvring motions in a calm sea and the motions induced by the high frequency wave exciting forces. The low frequency equations relating surge, sway and yaw velocities u , v and r may be expressed by the following per unit form, for the oil rig drill vessel Wimpey Sealab [104],

$$1.044 \dot{u} = X_A + 0.092 v^2 - 0.138 uU + 1.84 rv \quad (5.1)$$

$$\dot{x} = u \quad (5.2)$$

$$1.84 \dot{v} = Y_A - 2.58 vU - 1.84 v^3/U + 0.068 r|r| - ru \quad (5.3)$$

$$\dot{y} = v \quad (5.4)$$

$$0.102 \dot{r} = N_A - 0.764 uv + 0.258 vU - 0.162 r|r| \quad (5.5)$$

$$\dot{z} = r \quad (5.6)$$

U is used to denote the vector sum of surge and sway velocities u and v , X_A, Y_A are the applied surge and sway 'direction forces due to the thrusters and the environment. N_A is the applied turning moment on the vessel, and x, y, z are the surge sway and yaw positions. In DP systems it is reasonable to assume that changes in velocity and position are small so that a linearised set of equations may be obtained for sway and yaw motions as the linearisation process removes the interaction with surge: 112:

$$\dot{\underline{x}}_{\ell}(t) = \underline{A}_{\ell} \underline{x}_{\ell}(t) + \underline{B}_{\ell} \underline{u}_{\ell}(t) + \underline{D}_{\ell} \underline{\omega}_{\ell}(t) \quad (5.7)$$

$$\underline{y}_{\ell}(t) = \underline{C}_{\ell} \underline{x}_{\ell}(t) \quad (5.8)$$

where $\underline{x}_\lambda(t) \in \mathbb{R}^6$, $\underline{u}_\lambda(t) \in \mathbb{R}^2$, $\underline{\omega}_\lambda(t) \in \mathbb{R}^2$. The signal $\underline{\omega}(t)$ is assumed to be zero mean, white, noise. The system matrices for Wimpey Sealab are:

$$A_\lambda = \begin{bmatrix} -0.0546 & 0 & 0.0016 & 0 & 0.5435 & 0.272 \\ 1 & 0 & 0 & 0 & 0 & 0 \\ 0.0573 & 0 & -0.0695 & 0 & 3.2680 & -1.6340 \\ 0 & 0 & 1 & 0 & 0 & 0 \\ 0 & 0 & 0 & 0 & -1.55 & 0 \\ 0 & 0 & 0 & 0 & 0 & 1.55 \end{bmatrix}$$

$$B_\lambda^T = \begin{bmatrix} 0 & 0 & 0 & 0 & 1.55 & 0 \\ 0 & 0 & 0 & 0 & 0 & 1.55 \end{bmatrix}$$

$$C_\lambda = \begin{bmatrix} 0 & 1 & 0 & 0 & 0 & 0 \\ 0 & 0 & 0 & 1 & 0 & 0 \end{bmatrix}$$

$$D_\lambda = \begin{bmatrix} 0.5435 & 0 & 0 & 0 & 0 & 0 \\ 0 & 0 & 9.785 & 0 & 0 & 0 \end{bmatrix}$$

The high frequency model is obtained by fitting the spectrum of the output of a dynamical system (driven by white noise) to a standard sea spectrum [113]. This shaping filter output represents the worst case high frequency motions since in practice the vessel dynamics tend to attenuate these motions. The high frequency model has the form:

$$\dot{\underline{x}}_h(t) = A_h \underline{x}_h(t) + D_h \underline{\omega}_h(t) \quad (5.9)$$

$$\underline{y}_h = C_h \underline{x}_h(t) \quad (5.10)$$

where

$$A_h = \begin{bmatrix} A_h^S & 0 \\ 0 & A_h^Y \end{bmatrix} \quad D_h = \begin{bmatrix} D_h^S & 0 \\ 0 & D_h^Y \end{bmatrix}$$

and the sub matrices for the sway, and yaw directions are;

for a typical sea state (Beaufort scale 8):

$$A_h^S = A_h^Y = \begin{bmatrix} 0 & 3.104 & 0 & 0 \\ 0 & 0 & 3.104 & 0 \\ 0 & 0 & 0 & 3.104 \\ 0.15 & -1.884 & -2.44 & -8.555 \end{bmatrix} \quad D_h^S = \begin{bmatrix} 0 \\ 0 \\ 0 \\ 0.088 \end{bmatrix} \quad D_h^Y = \begin{bmatrix} 0 \\ 0 \\ 0 \\ 0.0403 \end{bmatrix}$$

$$C_h = \begin{bmatrix} 0 & 0 & 1 & 0 & 0 & 0 & 0 & 0 \\ 0 & 0 & 0 & 0 & 0 & 0 & 1 & 0 \end{bmatrix}$$

The state equations for the low and high frequency models of the ship can be combined and be written in the form

$$\begin{bmatrix} \dot{x}_\ell \\ \dot{x}_h \end{bmatrix} = \begin{bmatrix} A_\ell & 0 \\ 0 & A_h \end{bmatrix} \begin{bmatrix} x_\ell \\ x_h \end{bmatrix} + \begin{bmatrix} B_\ell \\ 0 \end{bmatrix} \underline{u} + \begin{bmatrix} D_e & 0 \\ 0 & D_h \end{bmatrix} \begin{bmatrix} \omega_\ell \\ \omega_h \end{bmatrix} \quad (5.11)$$

$$\begin{bmatrix} z_1 \\ z_2 \end{bmatrix} = \begin{bmatrix} C_e & C_h \end{bmatrix} \begin{bmatrix} x_\ell \\ x_h \end{bmatrix} + \underline{v} \quad (5.12)$$

Where \underline{v} is a zero mean, white signal representing the measurement noise. The assumption that the above linear models may be employed will be validated by simulation results based on the non-linear model of the vessel.

The linearised equations of the vessel as expressed above are now in the form normally used for specifying the Kalman filtering problem. The Kalman filter provides unbiased state estimates for state feedback control. In the present case the position control system must respond only to the low frequency error signal and the state estimates of the low low frequency sub-system are required for state feedback control. The Kalman filter includes a model of the system, therefore provides separate estimates for the low and high frequency sub-system states. It is shown in figure 2 and defined by the equations:

$$\frac{d\hat{x}(t)}{dt} = A \hat{x}(t) + K^f [z(t) - \hat{y}(t)] + B u(t) \quad (5.13)$$

$$\hat{y}(t) = C\hat{x}(t) \quad (5.14)$$

where the Kalman gain matrix K can be partitioned into low and high frequency gain matrices:

$$K^f = \begin{bmatrix} K_l^f \\ K_h^f \end{bmatrix} \quad (5.15)$$

The matrix K^f is computed using the matrix Riccati equation. Alternatively the steady state value of K may be obtained using s-domain methods [114]. The linearised low frequency equations for the vessel are independent of the sea state and known. The high frequency model depends upon the sea state but may be assumed constant for given weather conditions. The covariance of the white noise signal ω_h feeding the high frequency block is fixed by the assumed sea spectrum. Thus, the only unknown quantities required to compute the Kalman gain K^f are the low frequency process noise covariance $Q_\ell^\delta(t)$ and the measurement noise covariance $R\delta(t)$.

An estimate of the power spectral density of $\underline{\omega}_\ell$ can be based upon the Davenport wind gust spectrum [113]. The measurement noise covariance can often be obtained from the manufacturer of the particular position measurement system.

The steady-state solution for the gain matrix K may be employed since the gains are changing over a relatively short initial period. In the following discussions it will be assumed to be fixed for a given weather condition. Such a solution is easily implemented as a set of gain matrices for different weather conditions and these would be pre-calculated and stored in the vessel's control computer.

The behaviour of the Kalman filter and its suitability for the DP problem has been examined in detail elsewhere [104,105,115,116]. It is noted here and it will be demonstrated in a later section that the transfer function between \underline{u} and \underline{x}_ℓ is the same as that between \underline{u} and $\hat{\underline{x}}_e$, assuming the filter model matches the plant equations. That is the Kalman filter in comparison with a notch filter (the solution used up to now) does not introduce phase lag between the thruster control input and the position error estimates. Thus, even though the filtering performance of the notch and the Kalman filter might be similar there is an essential difference in their transfer characteristics. This difference is due to the fact that the control input is fed to the Kalman filter which is not done in the case of the notch filter..

The optimal control solution to the DP problem may be obtained by the usual method of minimising the performance criterion:

$$J(\underline{u}) = \lim_{T \rightarrow \infty} \frac{1}{2T} E \left\{ \int_{-T}^T (\langle \underline{x}(t), Q_1 \underline{x}(t) \rangle_{E_n} + \langle \underline{u}(t), R_1 \underline{u}(t) \rangle_{E_m}) dt \right. \quad (5.16)$$

The separation principle of stochastic optimal control theory gives that the optimal control signal becomes:

$$\underline{u}_0(t) = - K^C \hat{x}(t) \quad (5.17)$$

where $\hat{x}(t)$ is the estimate of the states $x(t)$ obtained from the Kalman filter. It may be shown [109] that there is no feedback from the uncontrollable high frequency sub-system:

$$\underline{u}_0(t) = - \begin{bmatrix} K_{11}^C & 0 \end{bmatrix} \begin{bmatrix} \hat{x} & (t) \\ \hat{x}_h & (t) \end{bmatrix} \quad (5.18)$$

The gain matrix K_{11}^C may be calculated using the solution of the steady state Riccati equation (Chapter 1)

$$Q_\ell = - P_\ell A_\ell - A_\ell^T P_\ell + P_\ell B_\ell R^{-1} B_\ell^T P_\ell \quad (5.19)$$

$$K_{11}^C = R^{-1} B_\ell^T P_\ell \quad (5.20)$$

It may be noted that the above equation is based upon the fixed low frequency state equation matrices only, so the feedback control gains do not vary with the sea state. This is not the same for the filter whose gains do depend upon the sea spectrum, confirming the view that the ship positioning problem is basically an adaptive filtering rather than an adaptive control problem.

Several authors have described optimal control solutions to the DP problem [103,112] but only recently have methods for selecting the performance criterion weighting matrices [35,36] been developed. These methods are related to the work of Harvey & Stein and the work described in chapter 2.

The optimal control responses which are shown in later sections, were based upon weighting matrices obtained as described in chapter 2.

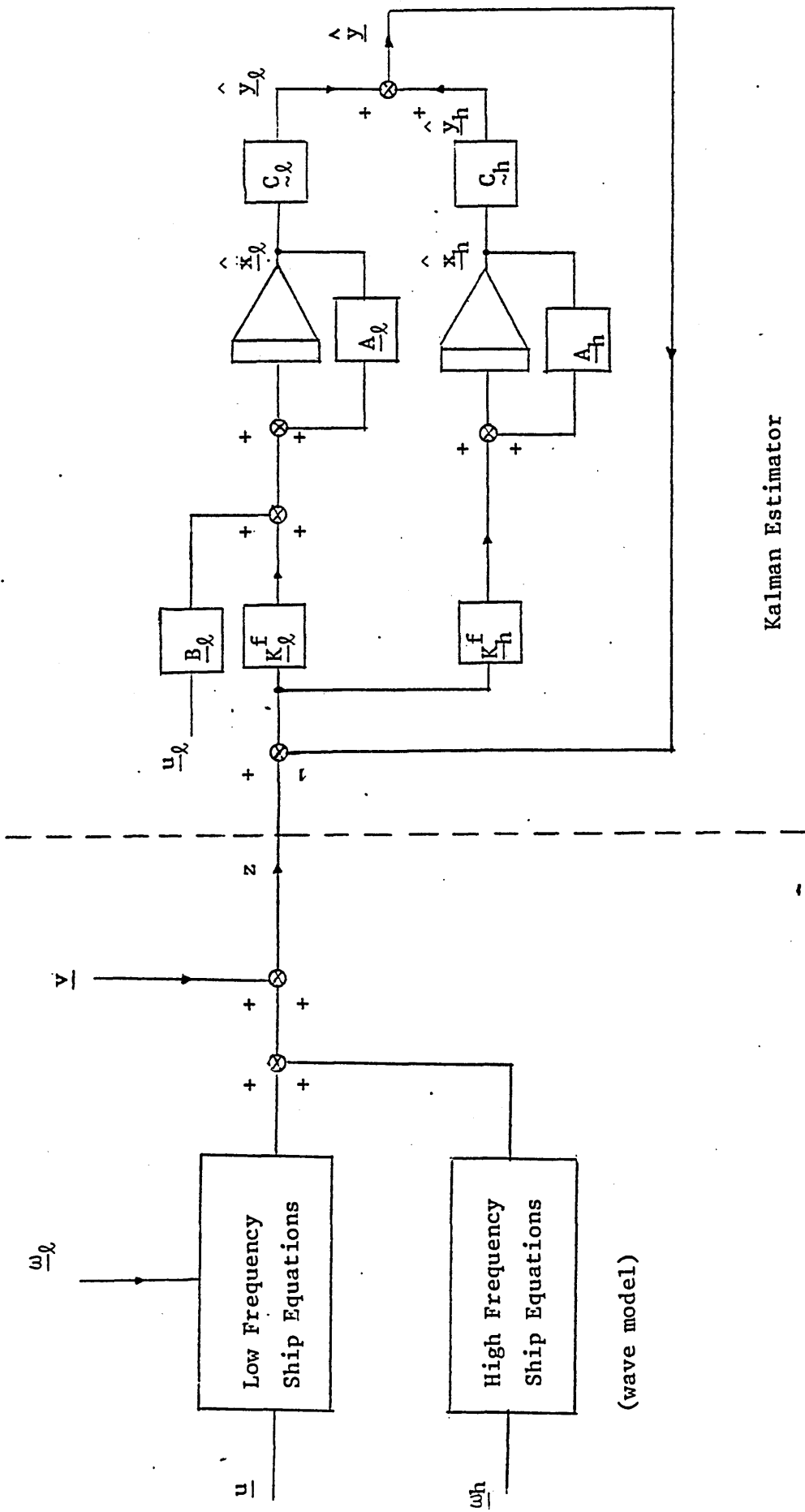


Figure 2 The Ship Equations and the Kalman Estimator

5.5 An Integrated Approach to Multivariable Analysis and Design

The two most important concepts in the classical control theory are Gain and Frequency. The inter-relation between these two concepts forms the basis of the two most powerful approaches to the design of feedback systems, that is the frequency response approach and the root locus approach. The key roles played by gain and frequency may be demonstrated by the following arguments.

It may be stated as a general principle in feedback, that the requirement for an open-loop gain operator of large modulus is a prerequisite for good accuracy of tracking, insensitivity to parameter variations and rejection of disturbances. Unfortunately, the application of gain in a feedback situation alters the system characteristic frequencies and often leads to the violation of the requirement for stability. Thus the inter-relation between gain and frequency causes the conflict between the requirements for accuracy and stability. It is the designer's task to devise feedback configurations that reach the best possible compromise between the two conflicting requirements.

The generalisation of the concepts of gain and frequency to multivariable systems then emerges as the natural way to extend classical control theory. Appropriate use of the theory of algebraic functions of a complex variable leads to the definition of the characteristic gain and characteristic frequency, and gives rise to the characteristic locus (CL) and multivariable root locus (MRL) methods [20,55,117]. These two methods provide the means for the generalisation but also unify the work of Nyquist, Bode and Evans. They

lead to an integrated design philosophy that draws from both the frequency response approach and the root locus approach, combining the two in a complementary manner [108], and is summarized below.

5.5.1 The Characteristic Locus method

Consider the algebraic function $g(s)$ given by

$$|gI - G(s)| = |gI - C(sI - A)^{-1}D| = 0 \quad (5.21)$$

and defined on an appropriate Riemann surface. Then, almost everywhere on this surface, the m branches of $g(s)$ form a set of locally distinct analytic functions, $g_i(s)$, called the 'characteristic transfer functions', to each $g_i(s)$ there corresponds an eigenvector function of s , $\underline{w}_i(s)$, called the 'characteristic direction' of $G(s)$. The paths traced by the eigenvalues of $G(s)$ as s describes the Nyquist contour once in a clockwise direction, are called the 'characteristic loci' (CL). The $g_i(s)$ and the $g_i(j\omega)$ provide the generalisation of the gain and frequency response to multivariable systems.

The importance of $g_i(s)$ and $\underline{w}_i(s)$ stems from the fact that unity feedback leaves the eigenvalues unaltered and leads to eigenfunctions which obey the usual scalar open to closed-loop transfer function relationship. Expressing both the open and closed-loop transfer function matrices, $G(s)$ and $R(s)$ in dyadic form we have:

$$G(s) = \sum_{i=1}^m g_i(s) \underline{w}_i(s) \underline{v}_i^t(s) \quad (5.22a)$$

$$R(s) = \sum_{i=1}^m \frac{g_i(s)}{1 + g_i(s)} \underline{w}_i(s) \underline{v}_i^t(s) \quad (5.22b)$$

The $r_i(s)$ emerge as the scalar transfer functions which coordinate the input signals as seen through the eigenvector frame.

Consideration of equations 5.22 a&b indicates that the CL contains the necessary information about closed-loop stability. Furthermore, the CL together with the misalignment angles (MA), which measure the eigenvector spectral arrangement with respect to the standard basis vectors, characterise most aspects of closed-loop behaviour. A brief summary of the main results of the CL method is given below.

(a) A necessary and sufficient condition for closed-loop stability is that the net sum of counter-clockwise encirclements of the critical point by the CL is equal to the number of open-loop poles.

(b) Low interaction, namely the condition where the system outputs y_i respond primarily to signals applied at the i th input, requires that at any frequency, the moduli of the CL be large and/or the $\underline{w}_i(s)$ be well aligned with the standard basis vectors.

(c) The classical concepts of relative stability margins (gain/phase margins, M-circles etc.), bandwidth, etc. may be applied to the CL in order to assess the closed-loop performance of multivariable systems.

(d) Good accuracy of tracking in the closed-loop requires large CL except in the case of badly skewed eigenvectors when it is necessary to consider the CL of the Hermitian form of $G(s)$ [20].

5.5.2 The Multivariable Root Locus method

To generalise the root locus approach, the MRL considers the dual characteristic equation to 5.21:

$$|sI - S(g)| = |sI - B(gI - D)^{-1}C - A| = 0 \quad (5.23)$$

and thus associating the eigenvalues of the $n \times n$ frequency matrix, $S(g)$, to the algebraic function $s(g)$ called the characteristic frequency function. (Note that as with $g(s)$, $s(g)$ is not defined over

simple copies of the complex plane, but over an n-sheeted Riemann surface).

The systematic study of the variation of $s(g)$ for $g=1/k$ and k varying, reveals that the scalar root locus method is a special case of the multivariable problem. Multivariable root loci do not intersect each other on the Riemann surface, they depart from the open loop pole locations for $k=0$ and as $k \rightarrow \infty$ some loci terminate at finite locations called Finite Zeros (FZ). The remainder, attracted by the set of Infinite Zeros (IZ), go to the point at infinity along asymptotes that arrange themselves into groups of Butterworth patterns. To each group there corresponds an integer number which defines the order of divergence, the number of asymptotes in the group and their special arrangement. The orientation of the patterns and the speed of divergence depend on the non-zero eigenvalues of a set of parameters which are obtained by suitable projections of the Markov parameters [108].

The FZ are the frequencies whose transmission through the system is blocked. They emerge as the characteristic frequencies of the part of the system internal mechanism which is blocked from the inputs and outputs. This blocking action is due to the null spaces N, M of the input and output maps, B and C respectively. The FZ for a proper system with CB full rank are given by the eigenvalues of NAM , where N and M are matrix representations of N and M . When CB is singular the FZ of a proper system are given by the solutions of $\det(sNM - NAM) = 0$ whereas the FZ of a non-proper system with a full rank direct pass operator D , are given by the eigenvalues of the frequency matrix $S(g)$ at $g=0$, ie by $S(0) = A - BD^{-1}C$.

Other aspects of the MRL method concern the angles of departure from the open loop poles, the angles of approach to the FZ, the points of intersection with the imaginary axis, etc. All these quantities may be calculated in terms of the elementary state space matrices A,B,C,D [55].

5.5.3 The Design Procedure

Phase lag is often the source of difficulties in control and it arises out of the non-squareness of the input and output maps B and C. Thus, it would be advantageous to make use of all available inputs and measurements. The classical feedback configuration prescribes the comparison between reference inputs and commanded outputs only. This is restrictive since it does not allow for the utilisation of all available measurements. To emphasise this point we state that the presence of right half plane zeros (finite and infinite) in the classical feedback configurations would prohibit the use of high gain but would not necessarily prohibit the injection of high gain in loops that make use of all the available measured information.

To make efficient use of all available measurements the integrated design philosophy, prescribes two design stages, an inner-loop and an outer-loop stage. In the first, multivariable root locus techniques are employed for the adjustment of the system, closed loop characteristic frequencies. Thus, the measurements are combined by a feedback operator F (figure 3) in such a manner as to produce a set of outputs, equal to the number of inputs. Non-square systems, generically do not have FZ and yet square systems do, so that F may be thought of as generating FZ. Any FZ that are generated in this manner are placed in the left half of the complex plane. Furthermore F may be

chosen judiciously so as to keep the order of asymptotic divergence to a minimum. Subsequently a square full rank compensator K of constant gains may be introduced to manipulate the asymptotic directions and thus secure good stability margins. The inner loop is then closed and a scalar feedback gain k is injected to conduct the characteristic frequencies to preferred sectors of the complex plane.

A transfer function matrix representation $G(s)$ for the system from commanding inputs to commanded outputs with the inner loop closed, is derived and the design enters the second stage, that is the outer loop stage. The purpose of this is to secure good system accuracy by attaining large characteristic gain, a task made possible by the improved stability margins. The overall outer loop controller $K(s)$ is composed in the following manner. The minimisation algorithm ALIGN [20] is first applied to obtain the controller K_h which suppresses interaction at high frequencies. To improve the gain/phase characteristics of CL classical lead/lag controllers $k_i(s)$ are designed and introduced into the feedback configuration through an Approximately Commutative Controller (ACC) $K_m(s)$. Finally, an ACC is used to introduce integral plus proportional action to suppress low frequency interaction, improve steady state accuracy and balance the low frequency gains (see figure 3).

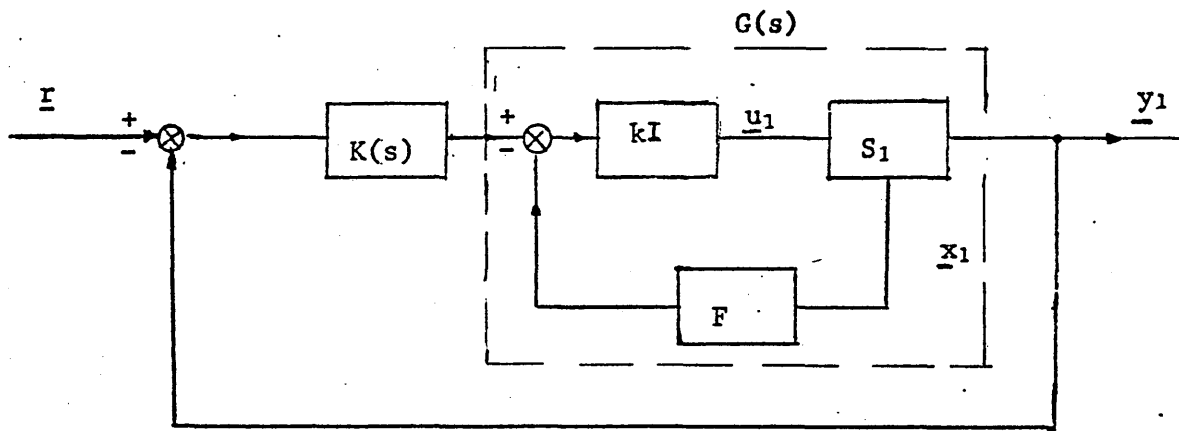


Figure 3 Inner-Outer Loop Configuration

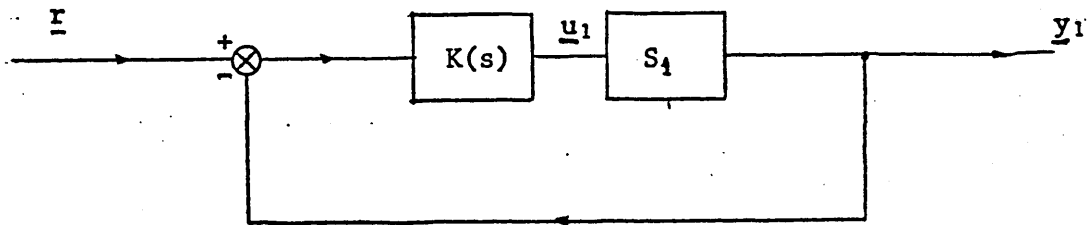


Figure 4 Outer Loop Configuration

5.5.4 The Use of Filters in the Integrated Characteristic Locus Multivariable Root Locus Design Method

The two stage design provides an effective way for reaching a compromise between the requirements for stability and accuracy. It does this by pre-conditioning the system during the inner loop stage, improving its stability margins and subsequently injecting gain into the CL of the outer loop system. Thus, given a system S_1 with state space matrices (A,B,C) , depending on the stability margins it may or may not be necessary to include an inner loop. The corresponding configurations are depicted in figures 3 and 4 where u_1 , y_1 , and x_1 denote the input, output and state vectors of S_1 , respectively.

Note that figure 3 refers to the situation where the entire state vector is available for the purposes of feedback. In general, however, only a limited number of measurements may be available and this will restrict the design freedom available during the inner loop stage. The question then arises as to whether observers may be used to obtain estimates of the required number of states for the purposes of the inner loop design. The answer to this is affirmative and recent work [118] has shown that from the MRL design point of view it is possible to invoke a form of the separation principle to separate the design of the operator F from the design of the observer.

A more challenging situation arises when apart from the unavailability of excess measurements the outputs themselves may not be measured directly due to the presence of various disturbances and noise. A solution to this problem which is often preferred by practising engineers is to use notch filters to remove the effects of

disturbances at known frequencies. An alternative approach would be to introduce into the feedback loop a Kalman filter which would make available estimates of the system states as well as the system outputs and thus would enable the formation of both the inner and outer loops. The feedback configuration resulting from the use of Kalman filter and notch filters are depicted in figures 6 and 7 respectively

In the absence of noise and disturbance the Kalman filter would be designed as a simple observer and by the separation principle one may use exactly the same controllers for the configurations of both figures 3 and 5 [ie: $K'(s)=K(s)$, $k'=k$ and $F'=F$]. It is of interest to know whether the same applies in the presence of noise and disturbances.

Consider the Kalman filtering configuration of figure 2 and assume that the measurement vector z is the sum of the actual output y_1 of the given plant model $S_1=(A_1, B_1, C_1)$, and an output y_2 of a dynamical system $S_2=(A_2, B_2, C_2)$ which describes the effect of disturbances and a vector v of white measurement noise. Assume also that an uncorrelated white noise input vector w , enters the system S_1 . The situation certainly corresponds to the Dynamic Ship Positioning application but is also widely encountered in other industrial applications. Then the state space equation for the Kalman filter may be written as:

$$\dot{\hat{x}}_1 = A_1 \hat{x}_1 + K_1 (z - \hat{y}) + B_1 u_1 \quad (5.24)$$

$$\dot{\hat{x}}_2 = A_2 \hat{x}_2 + K_2 (z - \hat{y}) \quad (5.25)$$

$$\hat{y} = C_1 \hat{x}_1 + C_2 \hat{x}_2 \quad (5.26)$$

where to obtain the matrices K_1 and K_2 one needs to specify the noise covariance matrices. The estimate of the state vector of S_1 is

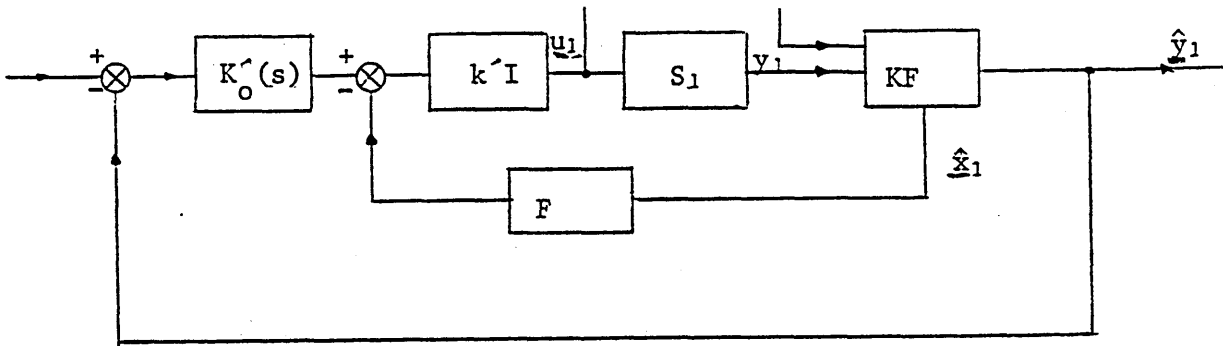


Figure 5 Feedback Configuration with
Kalman Filter

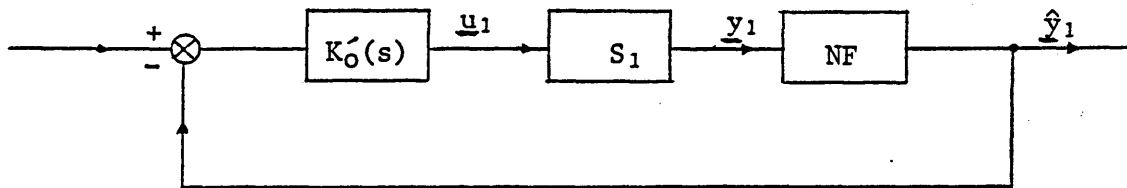


Figure 6 Feedback Configuration with
Notch Filter

provided by the component $\hat{\underline{x}}_1$ of the filter state vector and the estimate for the output vector is given by the vector $C_1 \hat{\underline{x}}_1$.

The description of the transference from the system input \underline{u}_1 to the output of the Kalman filter $\hat{\underline{y}}_1$ is obtained by manipulation of the state space equations of the system S_1 and is given by the augmented state space model:

$$\begin{bmatrix} \dot{\underline{x}}_1 \\ \dot{\underline{\epsilon}}_1 \\ \dot{\underline{x}}_2 \end{bmatrix} = \begin{bmatrix} A_1 & 0 & 0 \\ 0 & A_1 - K_1 C_1 & -K_1 C_2 \\ 0 & -K_2 C_1 & A_2 - K_2 C_2 \end{bmatrix} \begin{bmatrix} \underline{x}_1 \\ \underline{\epsilon}_1 \\ \underline{x}_2 \end{bmatrix} + \begin{bmatrix} B_1 \\ 0 \\ 0 \end{bmatrix} \underline{u}_1 \quad (5.27)$$

$$\hat{\underline{y}}_1 = [C_1 \quad C_1 \quad 0] \begin{bmatrix} \underline{x}_1 \\ \underline{\epsilon}_1 \\ \underline{x}_2 \end{bmatrix} \quad (5.28)$$

where $\underline{\epsilon}_1$ is the estimation error $\underline{x}_1 - \hat{\underline{x}}_1$. Clearly then the filter modes are uncontrollable from \underline{u}_1 and as such do not affect the transference from \underline{u}_1 to $\hat{\underline{y}}_1$ which is given by:

$$\hat{\underline{y}}_1 = C_1 (sI - A_1)^{-1} B_1 \underline{u}_1 \quad (5.29)$$

Thus, the transference from \underline{u}_1 to \underline{y}_1 and \underline{u}_1 to $\hat{\underline{y}}_1$ are identical.

The same result can be obtained for the transference of the inner loop of figure 5 if the matrix C_1 in 5.24 is replaced by F' . We may state therefore that the introduction of the Kalman filter in figure 3 does not affect the MRL properties of the inner loop and the CL properties of the outer loop system. As a consequence, a form of the separation principle may be invoked and we may introduce the same inner and outer loop controllers that we would use, had there been an excess of measurements and no noise and disturbances (see also section 5.5.3).

In contrast to the situation above the same does not apply to the configuration with the notch filter (figure 6). Notch filters do affect the system loop transference and will normally result in a certain deterioration of the system stability margins and speed of response.

5.6 The Characteristic Locus and Multivariable Root Locus design studies

The design specification for the CL/MRL method are formulated with the servo-mechanism problem (rather than the regulator problem) in mind, and include aspects such as closed loop stability, accuracy, dynamic performance and interaction. At first glance the CL/MRL method is best suited to deterministic problems. However, under noisy conditions the introduction of filters provide estimates for the corrupted deterministic signals. The success of the CL/MRL scheme will therefore depend upon the accuracy of estimation. The effects of disturbances and noise will be discussed in a later section.

For the sake of comparison, three different design studies are undertaken. The object of the first two is to investigate the suitability of the Kalman and notch filters in a simple outer loop configuration. The third study examines the effectiveness of Kalman filters in feedback configurations including both inner and outer loops.

5.6.1 The Kalman Filter in an Outer Loop Configuration

We consider the feedback configuration of figure 5 with the inner loop broken ($F'=0$, $k'=1$). Alternatively as a result of the discussion in the previous section the controller $K(s)$ may be designed considering the configuration of figure 3 with $F=0$ and $k=1$. The description of the system S_1 is entered into the computer package using the matrices previously defined to represent the low frequency

ship dynamics (section 5.3).

The analysis begins by assessing the stability properties of the uncompensated plant under unity feedback. For this purpose the frequency response $G_1(s) = C_1(sI - A_1)^{-1}B_1$ is evaluated at a number of points in the range 0.01-10 rad/sec and the eigenvalues of G_1 are computed to give the CL shown in figure 7. Clearly the generalised stability criterion, which requires no net encirclements of the critical point (as the open loop system is stable), is not satisfied for any value of the gain kI and the need for compensation is apparent.

Further evidence of the need for compensation is provided by figure 8 which displays the variation of the MA with frequency w . The MA θ_2 remains small for all values of w and thus predicts low interaction in the second loop. However, for all $w > 0.2$ rad/sec the conditions for suppression of interaction in the first loop are not satisfied.

Following the outlined CL procedure we apply the ALIGN algorithm at $w_h = 0.2$ rad/sec to obtain the controller of constant gains:

$$K_h = \begin{bmatrix} 0.0356 & 0.00651 \\ 0.0729 & -0.0134 \end{bmatrix}$$

Subsequently the dynamic controller $K_m(s) = k(s)I_2$ is introduced where $k(s)$ is a lead network, say

$$k(s) = \frac{10s + 1}{s + 1}$$

Because of the even gain/phase distribution among the CL achieved by K_h it is not necessary to introduce individual compensation to each CL and thus $K_m(s)$ need not be designed to be a commutative controller.

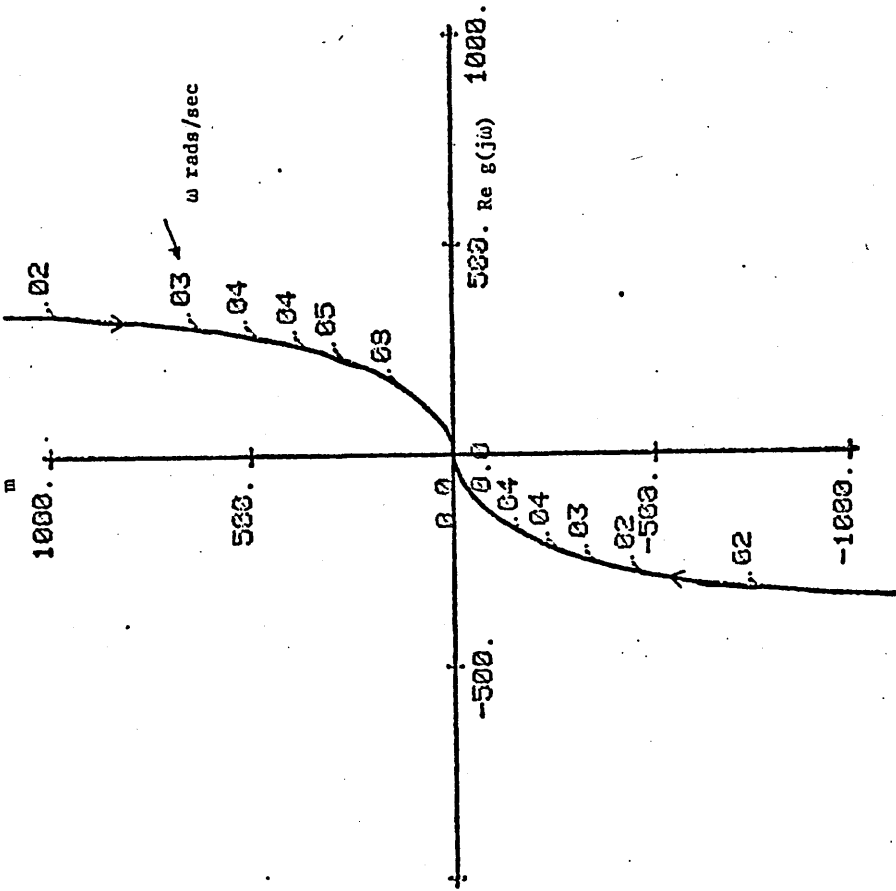


Figure 7 Characteristic Loci for the Uncompensated Plant

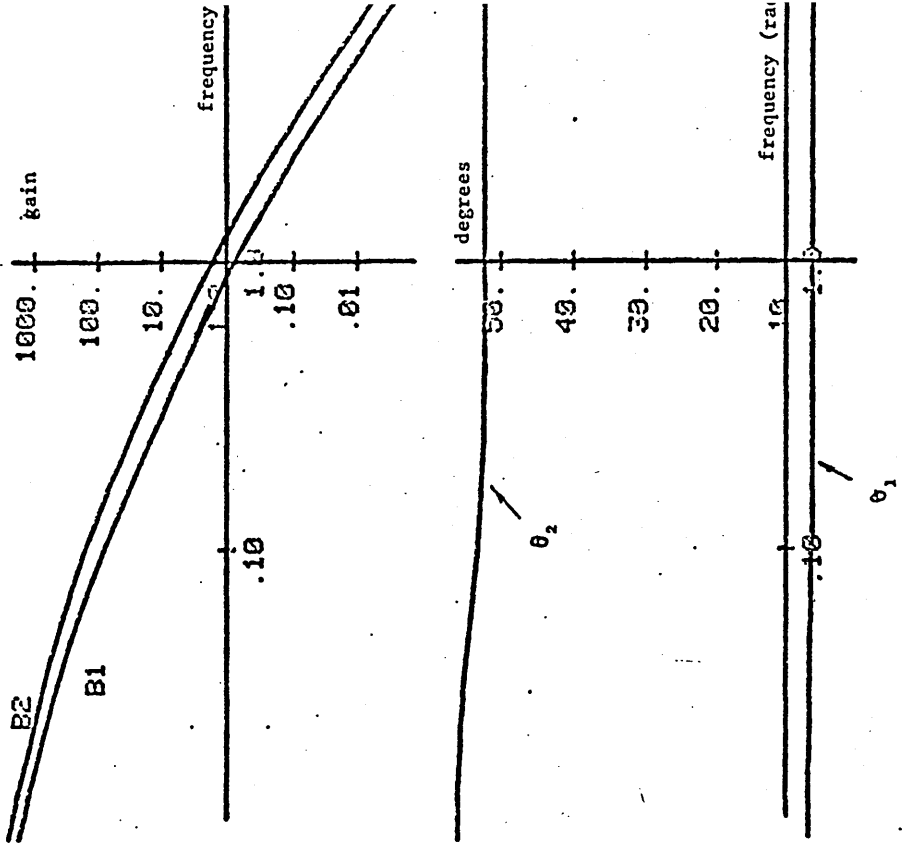


Figure 8 Misalignment angles before compensation

The resulting CL plots together with the constant magnification circle (the M-circle) are shown in figure 9. Thus, the overall compensator $k(s)K_n$, apart from improving the system interactive properties at high frequencies, also yields a set of CL which under unity feedback satisfies the Nyquist criterion. The resulting CL also have large dc gains, ensuring good steady state accuracy and display, ample gain/phase margins, ensuring a non-oscillatory fast response with a predicted maximum overshoot of about 19%. The MA of the compensated plant are shown in figure 10.

The above predictions for the closed loop behaviour is verified by the digital simulation results shown in figures 11a&b. These display the output response when a unit step signal is applied to the first and second reference input, in turn. Because of the flexibility of the method the designer is now in a position to finely tune the parameters of the dynamic controller, in order to reach an acceptable compromise between engineering constants and design specifications.

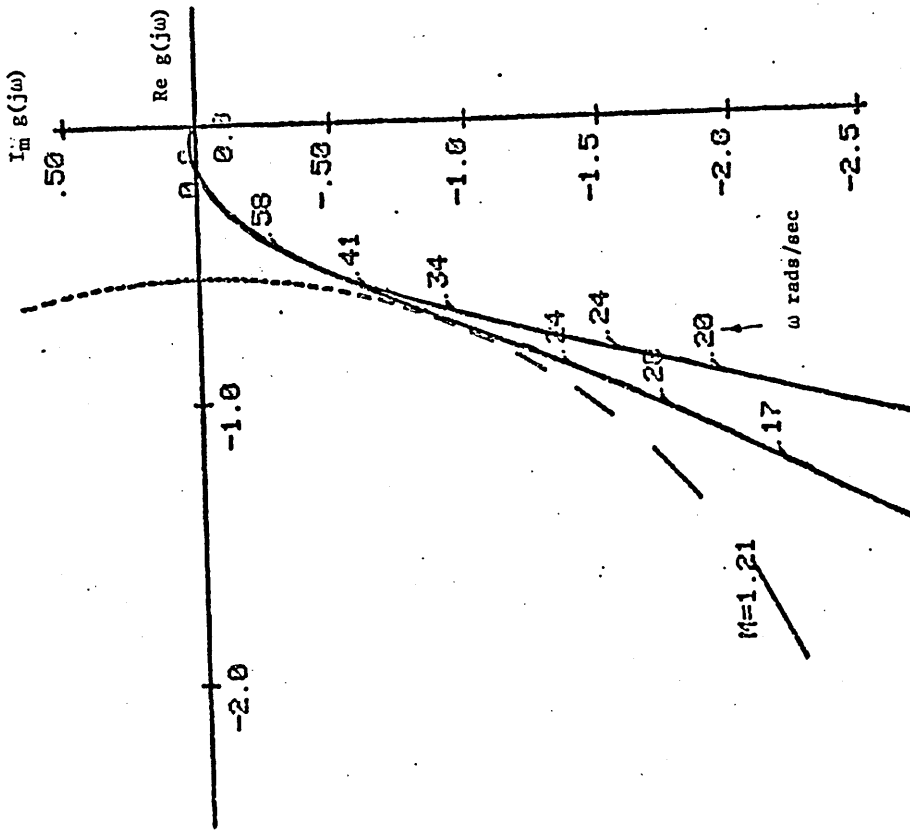


Figure 9 Characteristic Loci with align and lead precompensation

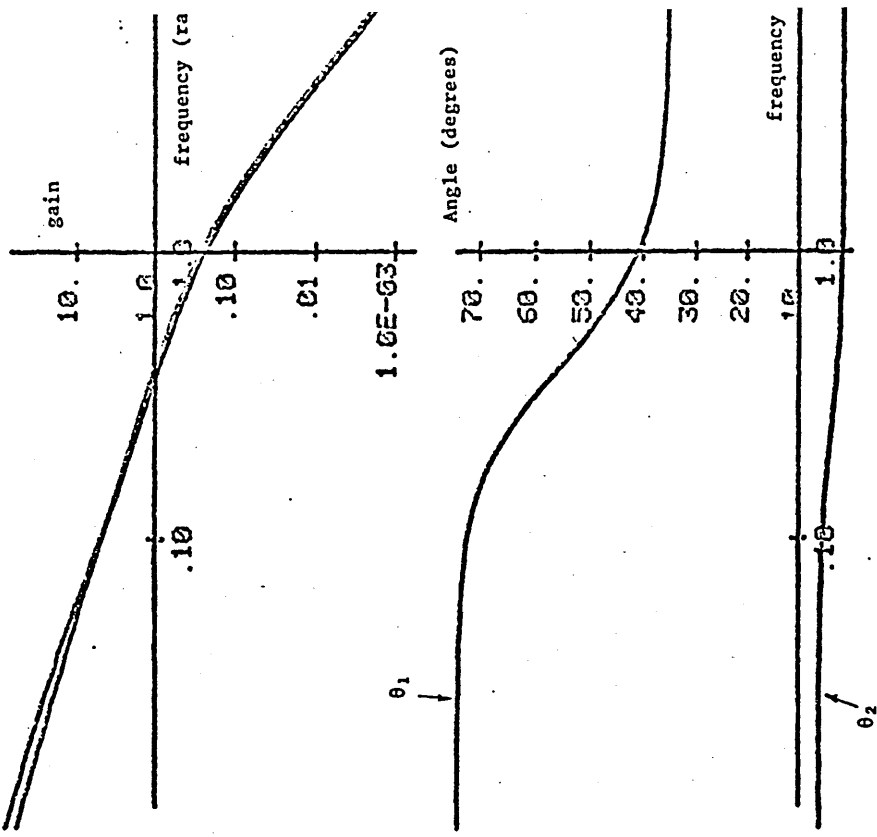
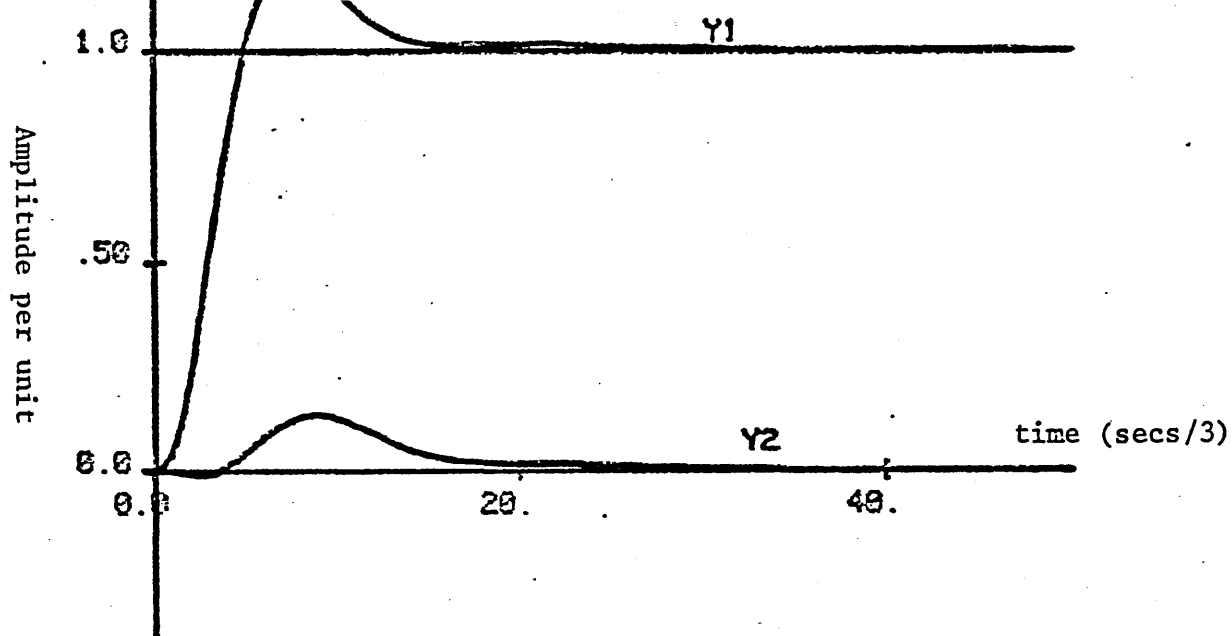
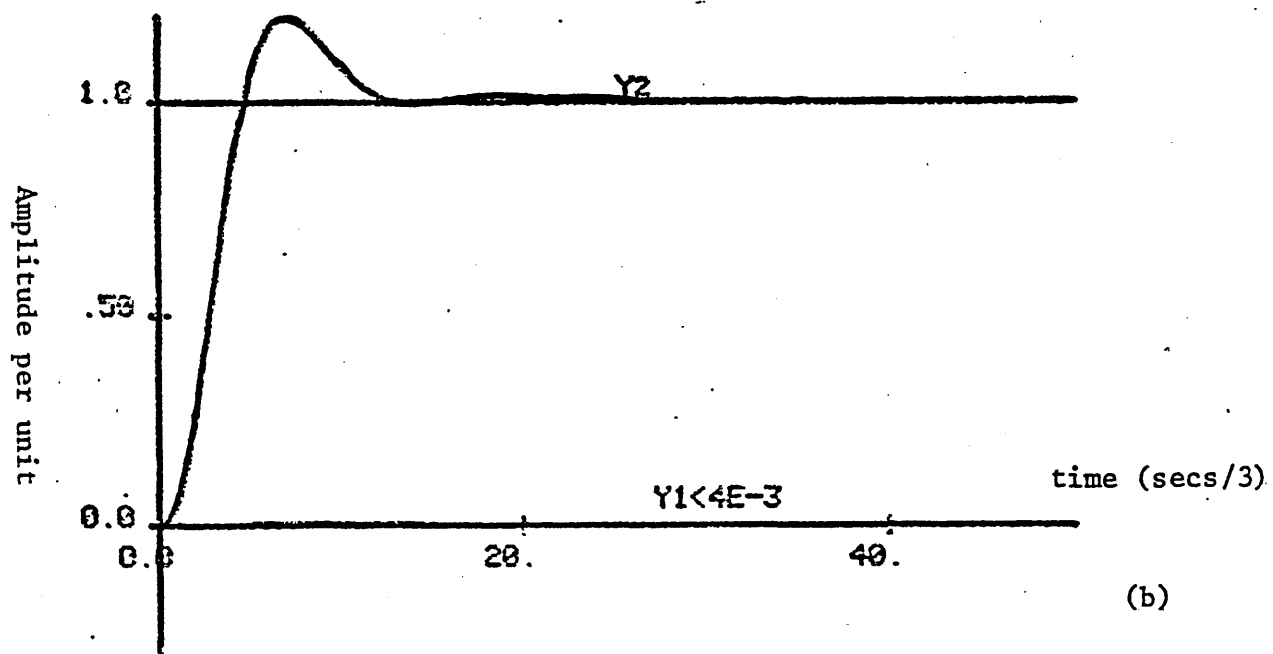


Figure 10 Misalignment angles with align ($\omega = .2$) precompensatio



(a)



(b)

Figure 11 Step response of the closed loop compensated system
with step in (a) input to reference 1
 (b) input to reference 2

5.6.2 Notch Filters in an Outer Loop Configuration

An alternative way to obtain estimates of the output of the low frequency ship dynamics is to use a notch filter which removes the effects of the high frequency wave motion. It is the practise for this application to use a cascade of three notch filters each with a transfer function of the form [102]:

$$h_i(s) = \frac{s^2 + 0.2\omega_i s + \omega_i^2}{s^2 + 2\omega_i s + \omega_i^2} \quad \text{for } i = 1, 2, 3$$

where $\omega_1, \omega_2, \omega_3$ are chosen as: 1.0912, 1.71864 and 2.728. The cascade of the three notch filters $h(s)=h_1(s)h_2(s)h_3(s)$ is introduced into each of the two system loops with the effect of scalling the open loop transference, $G_1(s)$ to give the new loop transference $Q(s)=h(s).G_1(s)$ Thus the introduction of the notch filters will leave the system multivariable structure unaltered and will simply scale the CL by $h(s)$. As a consequence, the design steps of the previous section (5.6.1) may be applied to produce similar results. However, on account of the excessive gain attenuation and phase lagging properties of the notch filters, clearly demonstrated by the Nyquist plot of $h(j\omega)$ shown in figure 12, the resulting CL will display poorer gain/phase margins and will have lower bandwidths. Naturally this will reflect itself on slower and more oscillatory responses. Applying ALIGN at 0.2 rad/sec and using the dynamic controller $k(s)I_2$ with

$$k(s) = \frac{20s+1}{2s+1}$$

yields the CL plotted in figure 13 and the time response results shown in figures 14 a&b. (It is of importance not to apply excessive lead action in higher frequencies as this will counteract the filtering action of the notch filters introduced in order to reject the noise corrupting the outputs [102]).

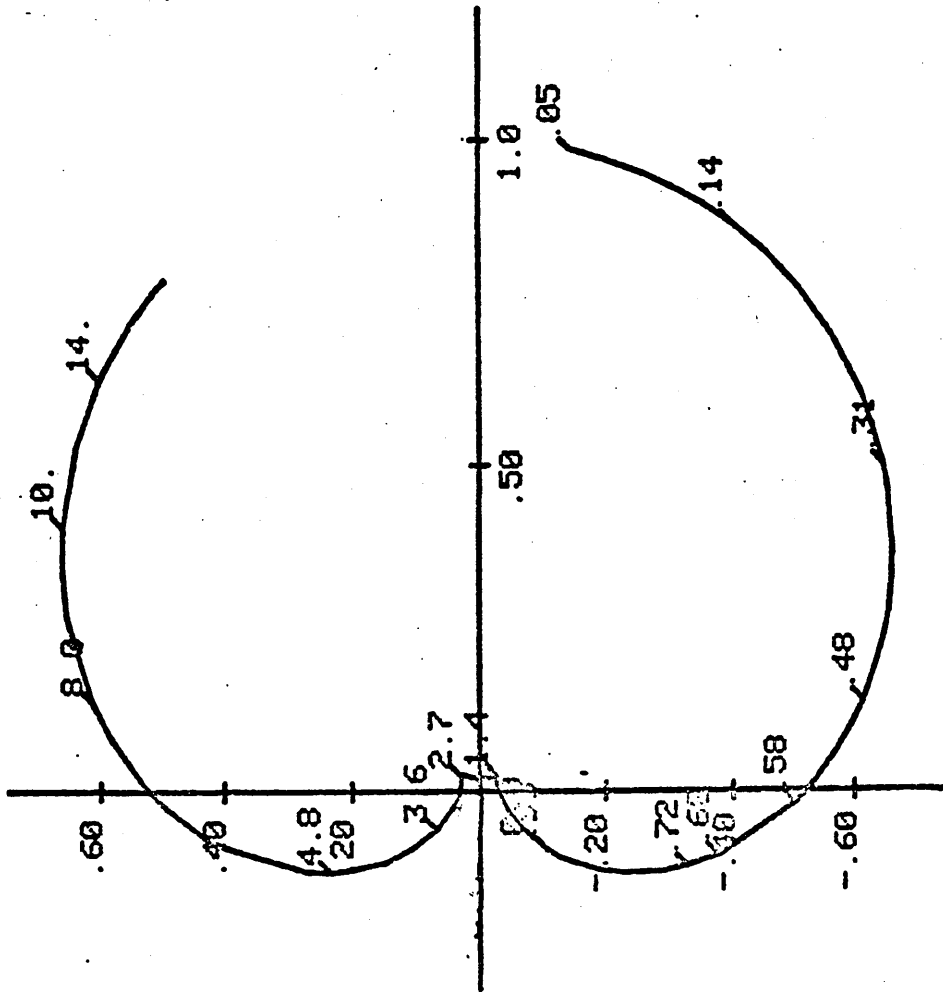


Figure 12 Nyquist plot for the notch filter

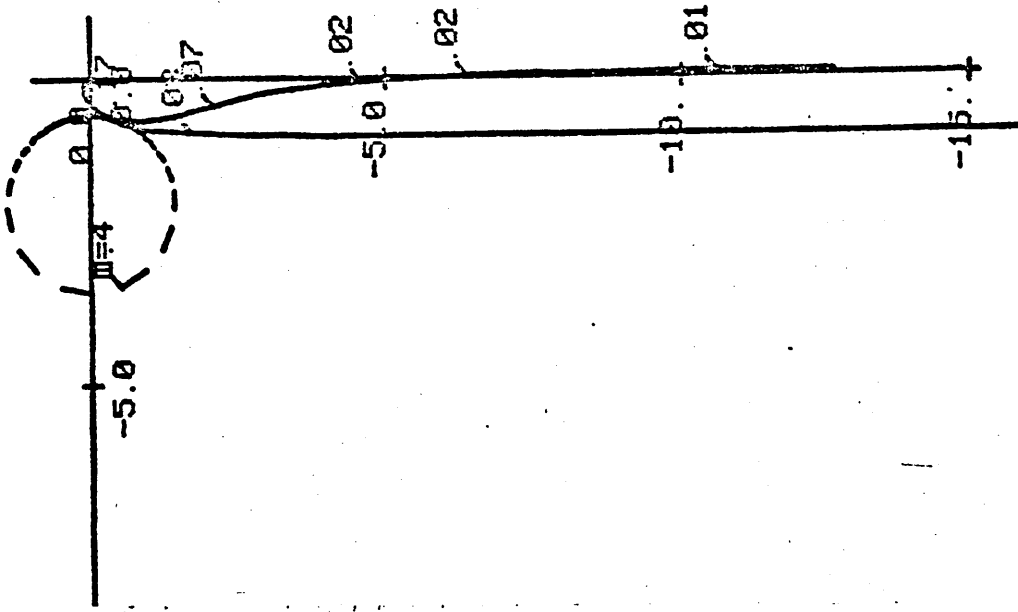
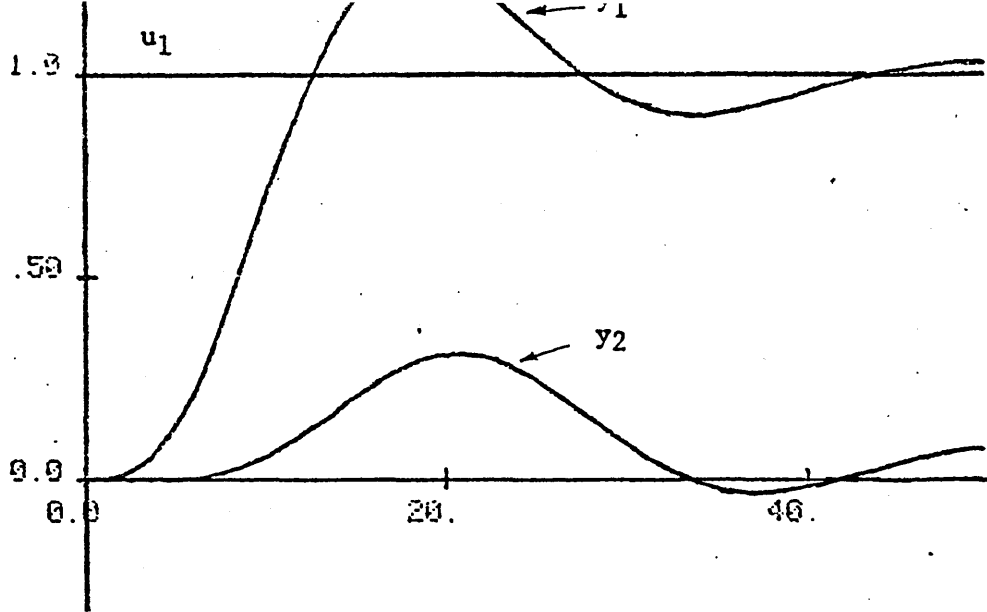
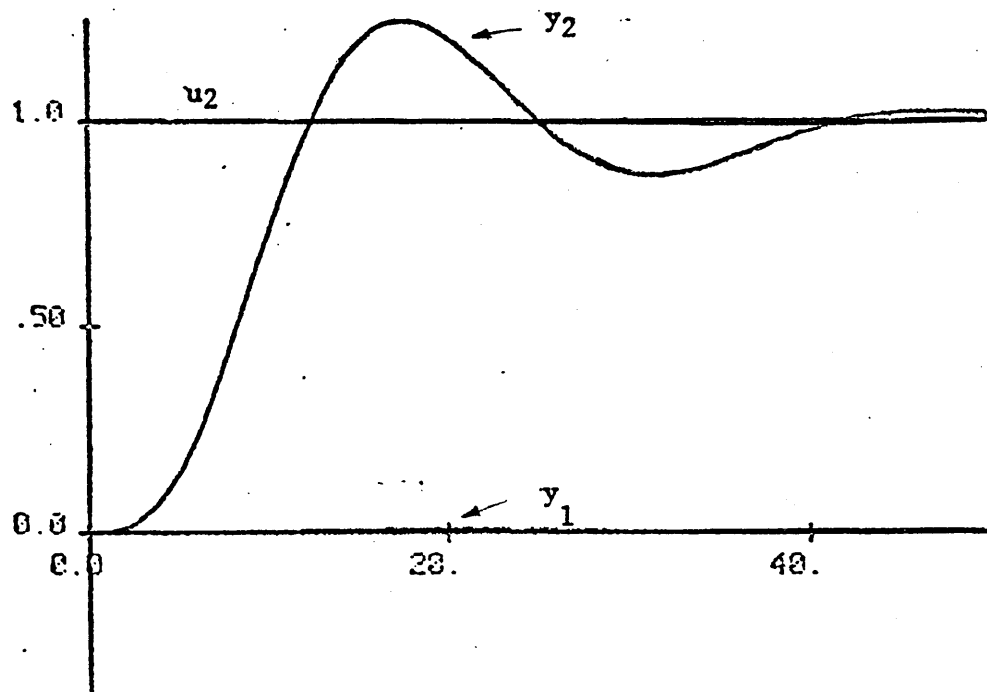


Figure 13 Characteristic Loci with Notch filters and compensation



(a)



(b)

Figure 14 Step response of the closed loop compensated system
with step in (a) input u_1
 (b) input u_2

5.6.3 The Kalman Filter in an Inner and Outer Loop Configuration

The use of an inner as well as an outer loop affords the designer greater flexibility because it enables the utilisation of all the available measurements. The introduction of a Kalman filter into a configuration like this (figure 5) enhances the effectiveness of the integrated design because it provides estimates for all system states and this enables the arbitrary placement of all inner loop zeros (finite and infinite). This facility is of crucial importance for the design of systems which, due to poor stability margins, prohibit the injection of gain in a simple outer loop configuration.

This is the case with the DP problem. An inspection of the products $C_1 B_1$, $C_1 A_1 B_1$ and $C_1 A_1^2 B_1$ shows that the first two Markov parameters are zero whereas the third is non-zero and non-singular with one positive and one negative eigenvalue. Thus the low frequency ship model has third order infinite zeros only and these will be associated with MRL asymptotic directions distributed in space as the cubic roots of +1 and -1. Compensation on the system S_1 may improve the distribution of these asymptotes but cannot alter the order of the IZ. Thus each Butterworth pattern will conduct at least one pole into the unstable half of the complex plane.

In contrast to the outer loop situation where the output map C is fixed, in the inner loop design one is free to choose F. Thus the first Markov parameter of the inner loop system may be made non-singular yielding the maximum number of FZ and IZ of first order. Subsequently, placement of both the FZ and IZ in the stable half of the complex plane would produce an inner loop system with infinite

gain margins.

The inner loop design begins by deriving controllers which affect the placement of the zeros at desirable locations. Unlike the case of pole placement where it is often difficult to choose a desirable pole pattern, in placing zeros one obtains guidance from the shape of the MRL.

To derive suitable solutions for the matrix F we adopt the following procedure. Partition the state vector $x=[x_1, x_2, \dots, x_6]^t$ of S_1 into two vectors $p_1=[x_1, x_2, x_3, x_4]^t$ and $p_2=[x_5, x_6]^t$. Then by conformal partition of the matrices A, B and F and the application of the NAM algorithm [48] it can be shown that the inner loop zeros are given by the eigenvalues of the matrix $A_{11}-A_{12}F_2^{-1}F_1$. Rewriting this matrix in the form:

$$A_{11}-\tilde{k}(A_{12})(F_2^{-1}F_1/\tilde{k})=\tilde{A}-\tilde{k}\tilde{B}\tilde{C} \quad (5.30)$$

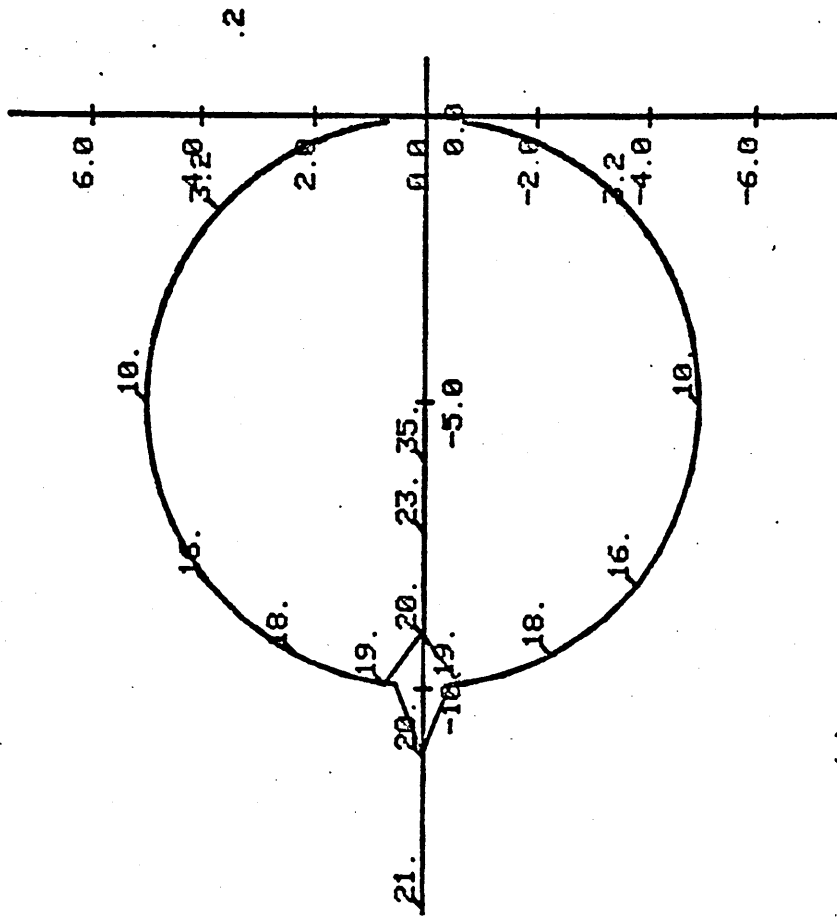
we see that the inner loop zeros are also the closed loop poles of the system $S(\tilde{A}, \tilde{B}, \tilde{C})$ where $\tilde{A}=A_{11}$, $\tilde{B}=A_{12}$ and $\tilde{C}=F_2^{-1}F_1/K$ under the scalar feedback gain K. Hence, to influence the locations of the inner loop zeros we must place the poles of $\tilde{S}(\tilde{A}, \tilde{B}, \tilde{C})$. To calculate these we exploit the structure of the system matrices in the DP problem. Thus, for convenience, interchange the second and third states of \tilde{S} to obtain the equivalent state space description $\hat{S}(\hat{A}, \hat{B}, \hat{C})$. A partition of the vector $\hat{x}=[\hat{x}_1, \hat{x}_2, \hat{x}_3, \hat{x}_4]^t$ into the vectors $p_1=[\hat{x}_1, \hat{x}_2]^t$ and $p_2=[\hat{x}_3, \hat{x}_4]^t$ and application of the NAM algorithm will show that the zeros of \tilde{S} (or S) are given by the eigenvalues of $-\hat{C}_1^{-1}\hat{C}_2$. The matrices \hat{C}_1 and \hat{C}_2 depend entirely upon the parameters of the controller F and so may be chosen freely. One is able to place the zeros of \tilde{S} at z by setting $\hat{C}_2=-z\hat{C}_1$. Furthermore the choice $\hat{C}_1=\hat{B}_1^{-1}$ ensures that all the IZ of \tilde{S} are first order and stable. By a judicious choice of the location

of z of the zeros \tilde{S} and suitable choice of the gain k one is able to attract the closed loop poles of S and hence the zeros of the inner loop system to desired locations. The corresponding solution for the matrix F may be constructed by considering the relation of the components of F , F_1 and F_2 to the matrices \hat{C}_1 and \hat{C}_2 .

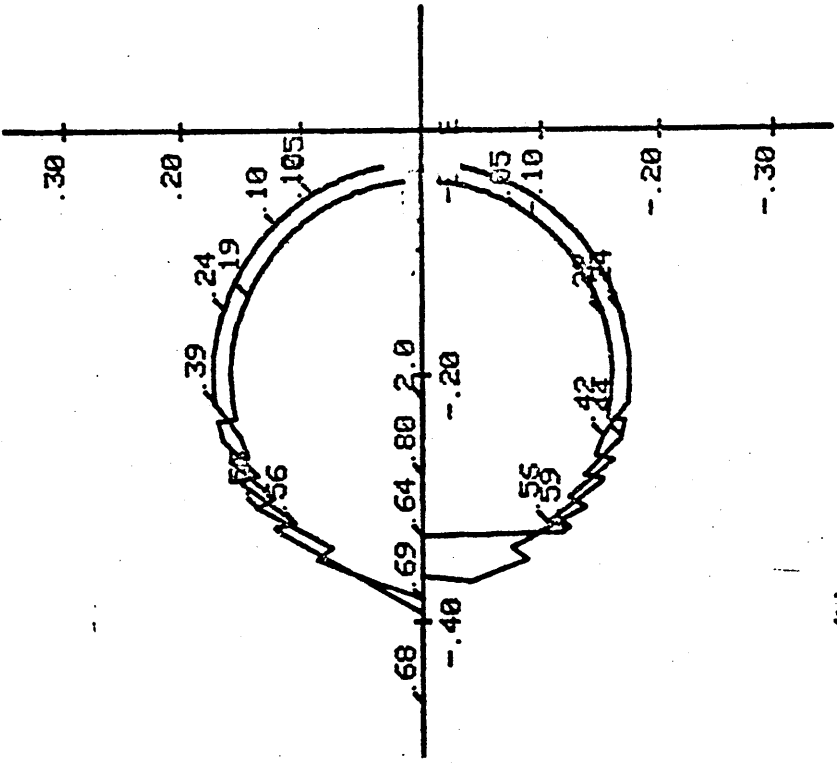
The objective of the inner loop is to conduct the characteristic frequencies further to the left in the complex plane and thus pave the way for the characteristic gain adjustments of the outer loop. At first it seems desirable that the zeros of the inner loop (and hence the zeros of S) should be placed on the real axis and should be made as negative as possible. However, a comparison of the resulting MRL for two different z (figure 15 a&b) shows that the more negative z is chosen the more the root loci are deflected away from the real axis at intermediate gains. For high values of gain of course the root loci will tend to the zeros (finite and infinite) and thus arbitrarily fast and stable responses may be achieved. A limit to this process does exist and is dictated by the amount of gain that is practical to inject into the feedback system. Gain constraints therefore imply constraints on how far to the left the zeros of \tilde{S} and the zeros of the inner loop should be placed.

With the engineering constraints of the DP problem in mind the following two solutions were studied. The first, places the two FZ of \tilde{S} at $z=-0.5$ (figure 15a) and the subsequent choice of $k=2$ places the inner loop FZ at about -1.3 , -1.25 , -0.8 and -0.75 . The resulting controller F is calculated to be

$$F = \begin{bmatrix} 1.839 & 0.919 & 0.306 & 0.153 & 1 & 0 \\ 3.678 & 1.839 & -0.612 & -0.306 & 0 & 1 \end{bmatrix} \quad (5.31)$$



(a)



(b)

Figure 15 Root Loci for (a) $z = -5$ and (b) $z = -0.2$

then a scalar inner loop gain of $k=5$, has the effect of shifting the poles of S_1 from their original locations at $(-1.55, -1.55, -0.0742, -0.0499, 0, 0)$ to $(-7.3, -7.3, -1.02, \pm j0.145, -0.927)$.

In the second case the FZ of S are placed further to the right at $z=-0.2$ (figure 15b) and the gain \tilde{k} is set equal to 1.0 in order to place the inner loop zeros at about $-0.8, -0.85, -0.25$ and -0.28 . The resulting controller has, as expected, reduced gains :

$$F = \begin{bmatrix} 0.919 & 0.1839 & 0.153 & 0.0306 & 1 & 0 \\ 1.839 & 0.3678 & -0.306 & -0.0612 & 0 & 1 \end{bmatrix} \quad (5.32)$$

The effect of this F is to shift the poles of S_1 to $(-3.6, -3.6, -0.53, -0.44, -0.35, -0.3)$. Both schemes therefore result in a marked improvement of the relative stability margins of the low frequency model of the ship.

The outer loop stage may now be entered. This is done by the loops around the estimates of the states of S_1 provided by the Kalman filter and forming the transfer function matrix from the ship inputs to the estimates of the system outputs (namely the estimates of the second and fourth states of S_1). Note that in order to avoid feedback around the estimates of x_2 and x_4 twice (once in the inner loop and once in the outer loop) which would be inefficient, it is necessary to move that part of the feedback compensator F that operates on these two signals around the loop to the forward path. Under unity feedback, in the outer loop, such a rearrangement would not affect the stability improvement achieved by the inner loop design.

The CL of the outer loop system, with the inner loop closed, using the controllers F of equations 5.31 and 5.32 are shown in figures 16 a and b respectively. A comparison of these with the loci

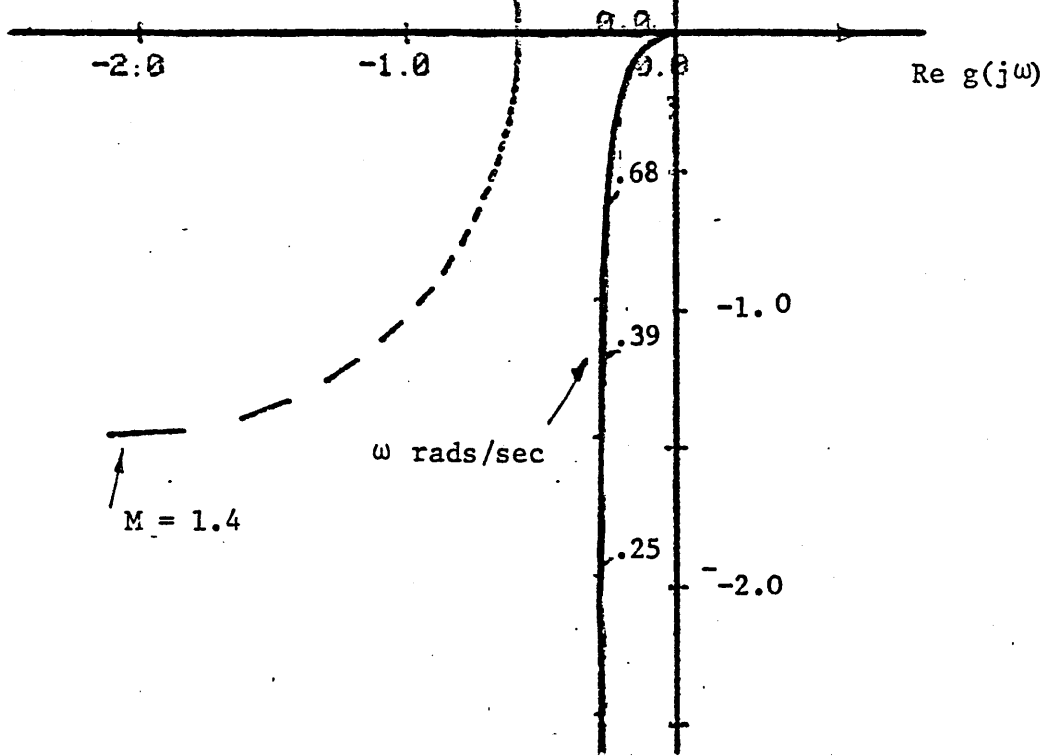


Figure 16(a) Outer loop characteristic loci for inner loop compensator of equation 5.31 and gain 5.

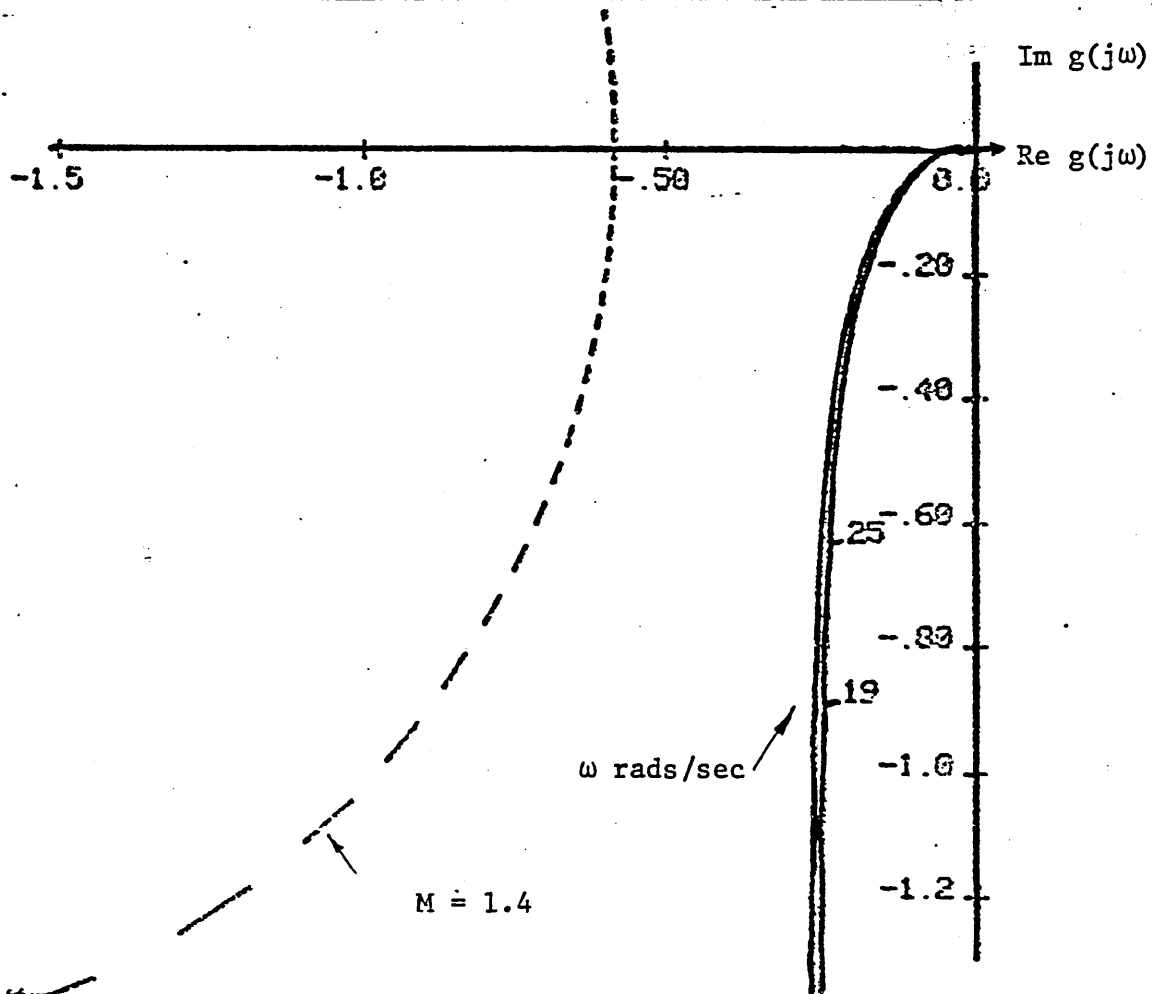


Figure 16(b) Outer loop characteristic loci for inner loop compensator of equation 5.32 and gain 1.8

attained in section 5.6.1 (figure 9) highlights the advantages gained by the use of an inner loop. The inner loop, even though it does not make use of any dynamic compensation, produces compensating action which is comparable to that of a lead network. The gain/phase characteristics of the CL obtained even for the lower gain inner loop compensation of equation 5.32 are substantially better than those obtained by the direct application of phase advance in the design of section 5.6.1 . The new CL have also better bandwidth and M-circle of less dynamic magnification. The resulting time responses therefore are expected to be faster with less overshoot of the CL which will largely suppress interaction in the closed loop.

Figures 17 a&b and 18 a&b show the responses of the inner/outer loop configuration to unit step signals applied at the first and second reference inputs respectively , for the compensators of equations 5.31 and 5.32 . The performance of both schemes satisfies all the design requirements described in section 5.2, namely that of stability, accuracy, speed , damping and low interaction. The assessment above of the scheme designed via the CL method was based on the linearised model of the vessel. Given the non-linear nature of the problem it is important to confirm such an approach by simulations based on the non-linear model of the ship. Figure 19 shows a representative step response for both the linear and non-linear models with feedback through a Kalman filter configuration as developed in this section The good agreement between the two responses justifies our earlier assumption that the design can be based upon a linearised model.

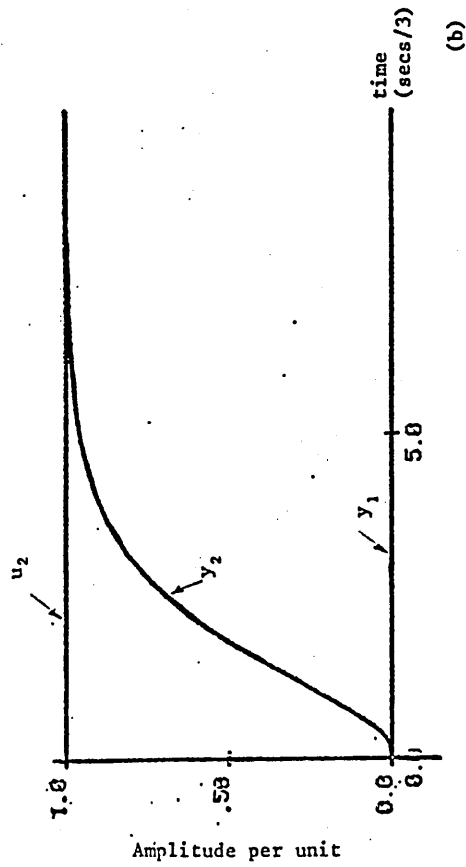
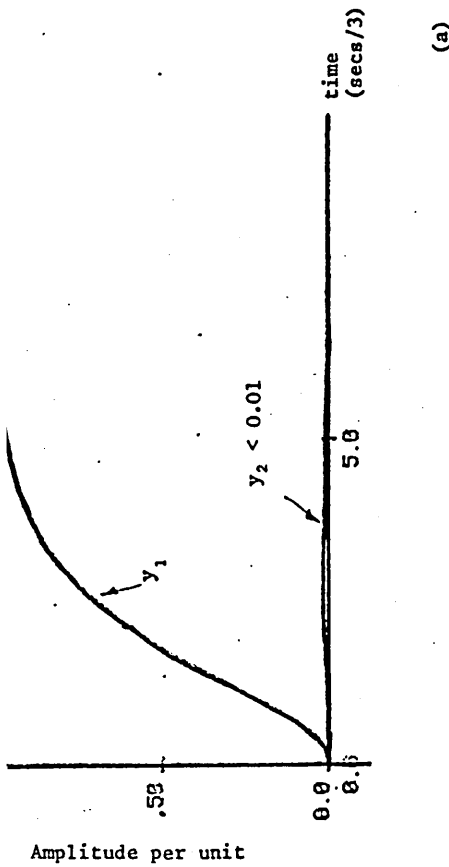


Figure 17 Step response with inner loop compensator of equation 5.31 and gain 5
 Outer loop unity feedback (a) step in reference 1
 (b) step in reference 2

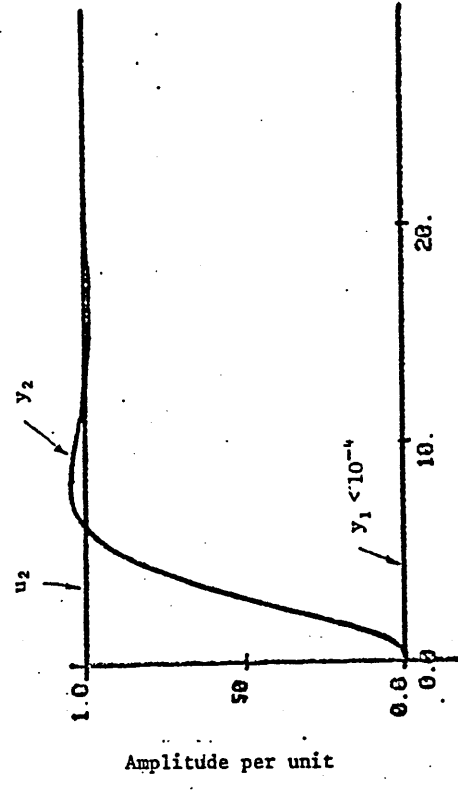
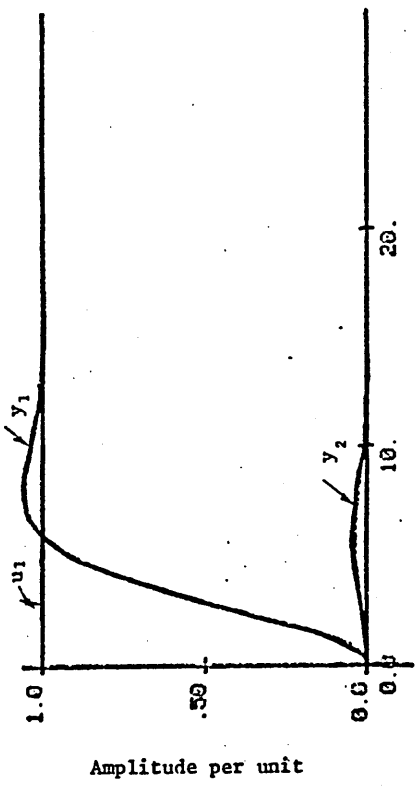


Figure 18 Step response with inner loop compensator of equation 5.31 and gain 1.8
 Outer loop gain = 2 (a) step in reference 1
 (b) step in reference 2

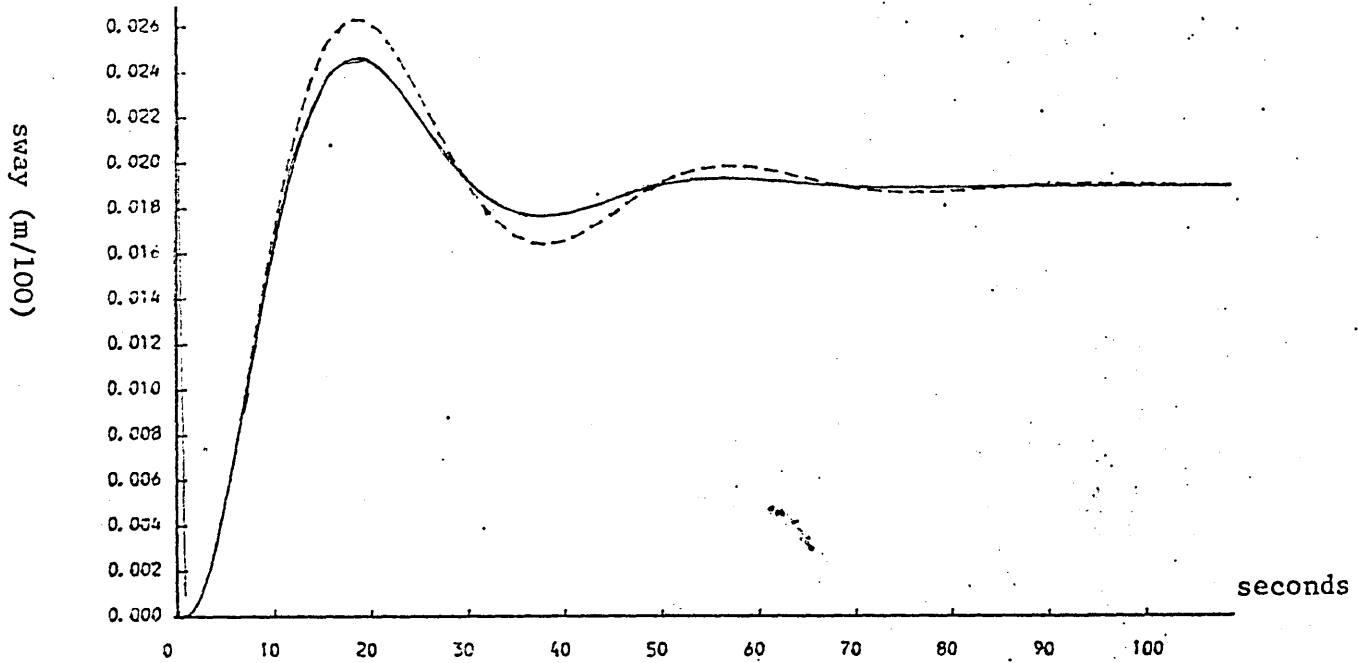


Figure 19: Closed loop step response of linear (continuous line) and non-linear (broken line) plants with state estimate feedback

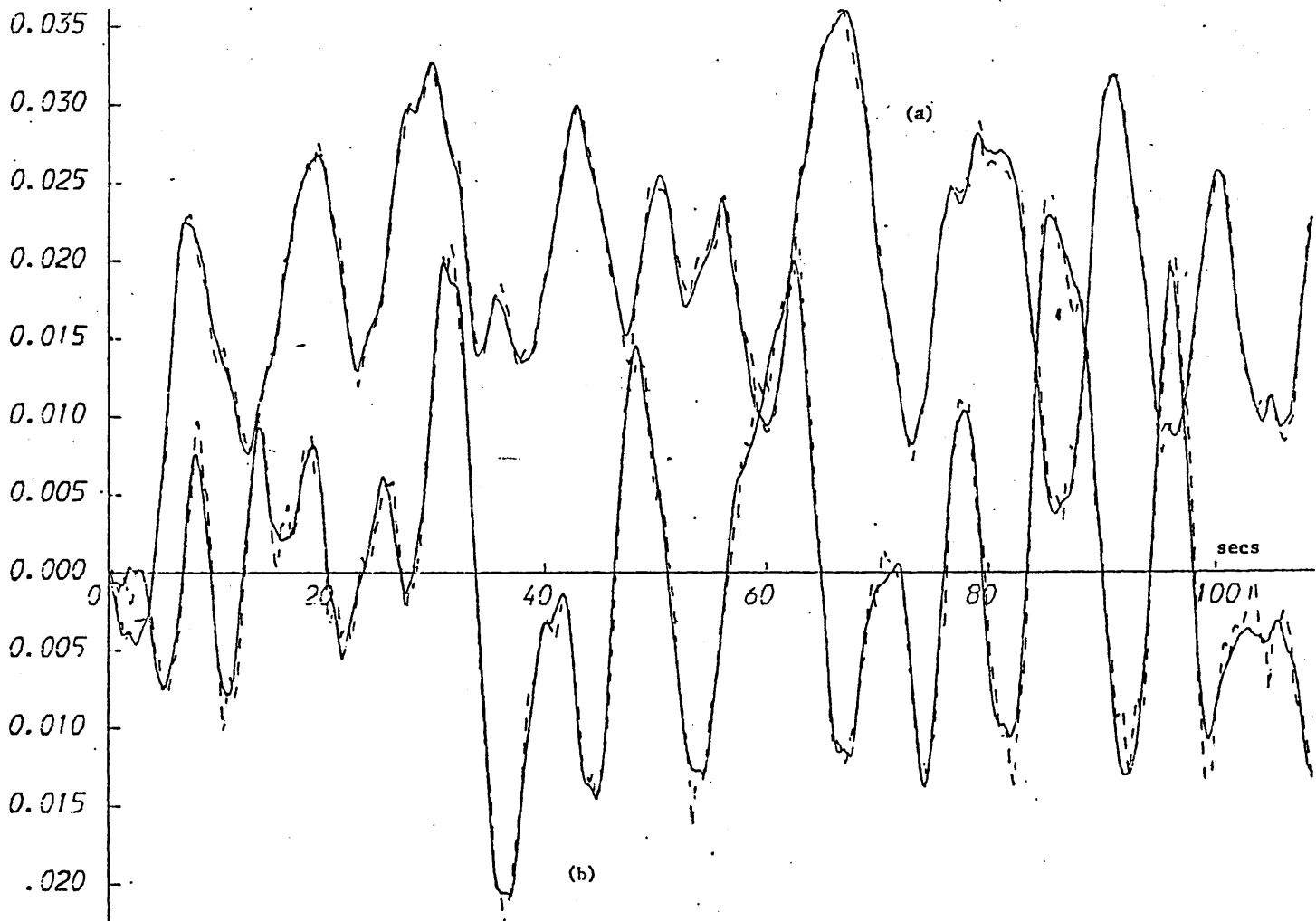


Figure 20 Total sway & yaw position trajectories for sea state Beaufort 8 (a) sway (b) yaw
(dotted curves are estimated trajectories)

Both optimal control and the integrated design technique have been applied to the dynamic ship positioning problem. The integrated CL/MRL leads to a design procedure which requires detailed engineering design effort but also allows the designer to intervene at each stage of the design process. It is also easy to see which changes to make to achieve a given response objective. There is the possibility of producing a formalised design procedure which will reduce the amount of engineering design involved, however, this latter point also applies to the optimal design method. Because of the stochastic nature of the problem and the presence of the Kalman filter, simulation results are probably necessary to confirm design objectives have been achieved. However, the number of design/simulation stages required to reach a given objective are very likely to be less than for the optimal design.

In contrast to the integrated approach, for specified weighting matrices (Q_1, R_1) the optimal control feedback gains are easily obtained. If the optimal control solution is not satisfactory new Q_1, R_1 must be chosen following a trial and error approach and repeated simulations. However, for this application a systematic procedure for the selection of the weighting matrices has been proposed. This involves some delay, due to the time to run simulation programs, but entails little effort on the part of the designer. The structure of the optimal system known beforehand which tends to reduce design engineering time but the useful properties of optimal systems are not guaranteed when ad hoc changes to the structure of the controller are made. For example, integral action can be inserted into the optimal stochastic system by appropriately modifying the performance criterion [109]. However, integral control

is often added with no thought to optimality and this can reduce stability margins and degrade performance. A fixed structure can be specified for the integrated design technique for a particular class of problem and in addition the outer loop controller may be made dynamic.

In its general application optimal control seems more suited to the regulating problem and the integrated approach has advantages regarding the servomechanism problem. In particular certain performance requirements such as low interaction can be met more directly by the latter. In comparing the simulation results note that the plant and noise processes and thence the Kalman filters were the same for both methods.

It is interesting that the structure of the system designed using the integrated CL/MRL approach is the same as that obtained via optimal control theory and this was a natural consequence of the design process. The control gain matrices:

Optimal Control Gain Matrix

$$K^c = \begin{bmatrix} 1.7113 & 0.894 & 1.05 & 1.09 & 1.56 & 0.32 \\ 3.37 & 1.732 & -1.48 & -1.41 & -0.79 & 1.36 \end{bmatrix} \quad (5.33).$$

Integrated Control Design Gain Matrix

$$K^c = \begin{bmatrix} 1.65 & 0.801 & 0.275 & 0.133 & 1.8 & 0 \\ 3.31 & 1.60 & -0.550 & -0.267 & 0 & 1.8 \end{bmatrix} \quad (5.34)$$

are similar although no attempt was made to artificially achieve this condition. The system responses are very similar for the above two cases and thus most of the responses for the integrated design procedures are presented but only selected responses from the optimal design are given.

The total response of the vessel in sway and yaw is shown in

figure 20. However, recall that the low frequency position of the vessel is to be controlled. The low frequency sway and yaw position signals are shown in figure 21. The low frequency sway and yaw velocities are illustrated in figure 22. The high frequency motions of the vessel are due to the sea wave variations and are shown in figure 23. The control signals are illustrated in figure 24. The high frequency variations in the control signal are to be minimised.

The optimal control position and control signals are shown in figures 25 and 26 respectively. The optimal system is faster but the control signal variations are larger. The two designs were not treated competitively since clearly the same responses could be achieved by either method. However, the integrated design approach provided a more direct route to achieving a given requirement.

The integrated characteristic locus/multivariable root locus technique has not previously been applied to the design of essentially stochastic control systems. The use of a Kalman filter together with this design method is also new. In fact, it would be more natural to use a frequency domain based filter, since the integrated design philosophy is itself based in the frequency domain. However the Kalman filter was shown to have several advantages in this system. The filter does not introduce phase lag in the way that the notch filter degrades the control system. The Kalman filter also provides greater flexibility in the number of variables available for feedback which is exploited in the integrated design philosophy.

The study has shown that the integrated CL/MRL design technique may be used for the design of dynamic ship positioning systems. The question arises as to its relative advantages in comparison with optimal control design techniques. This has been discussed at length in the previous section where two facts emerged. Firstly the integrated technique is more versatile and allows a whole range of different performance requirements to meet during the interactive design procedure. For this application the optimal control design can be more straightforward since weighting matrices may be selected according to given rules. However, the actual design process may take longer since simulation results are necessary to ensure desired transient responses are achieved. It is interesting that the structure of the system designed using the integrated CL/MRL approach is the same as that obtained via optimal control theory and this was a natural consequence of the design process; the control gain matrices are also similar although no attempt was made to artificially achieve this condition.

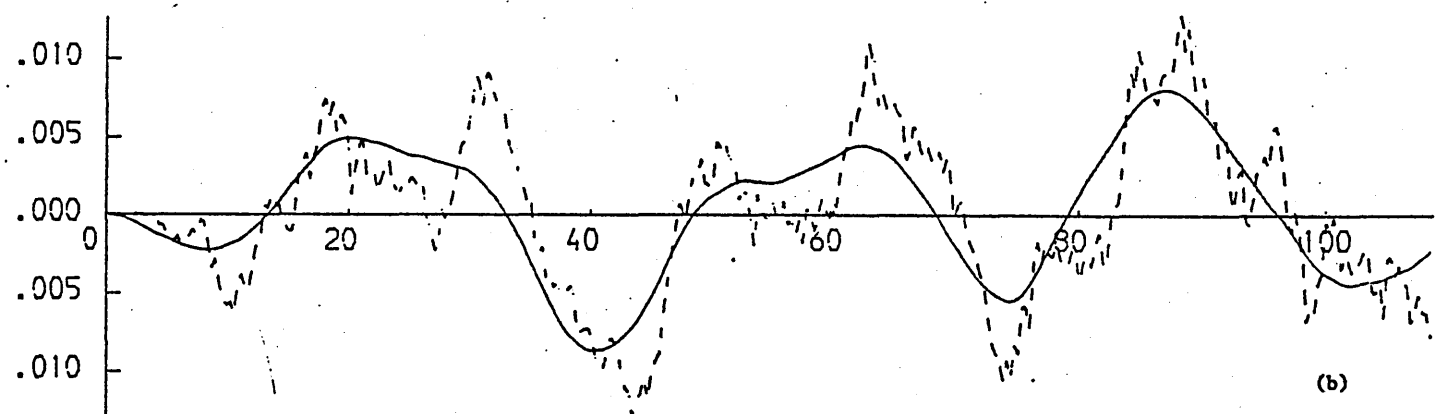
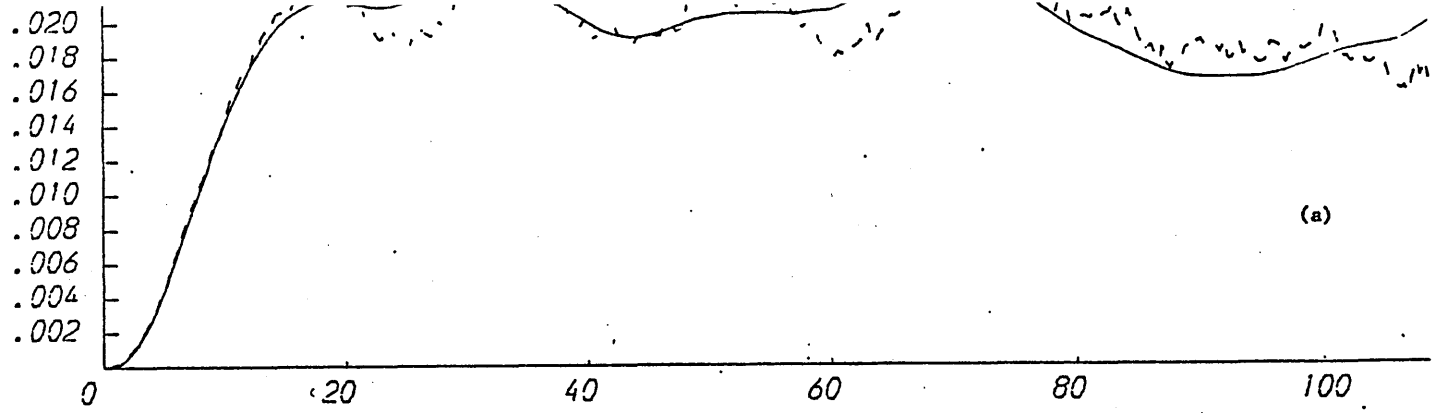


Figure 21 Trajectories for step into sway position, sea state Beaufort 8, closed loop control

(a) state 2, L.F. sway position (b) state 4, L.F. yaw position.

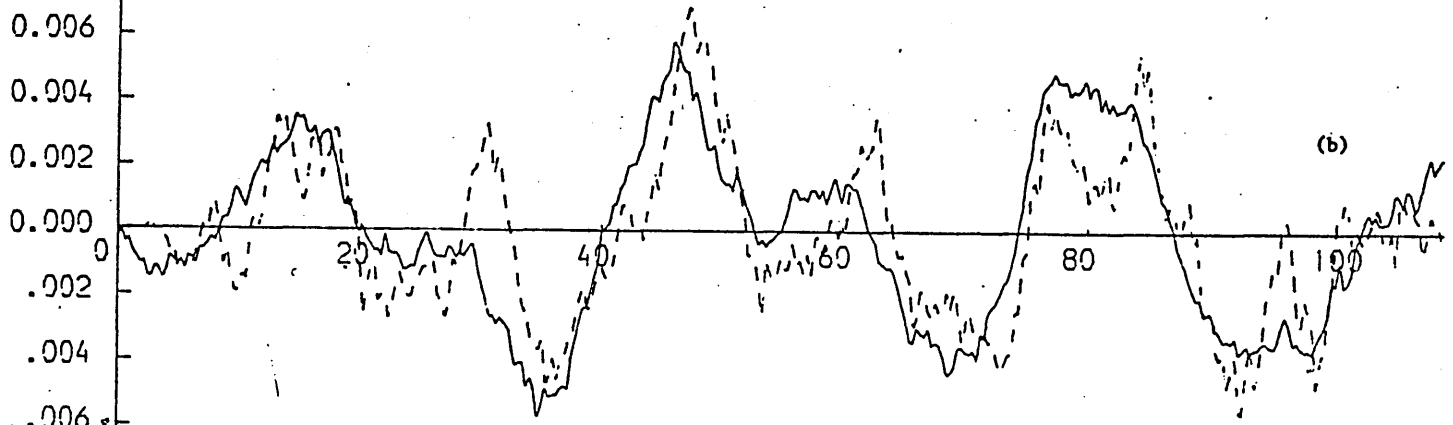
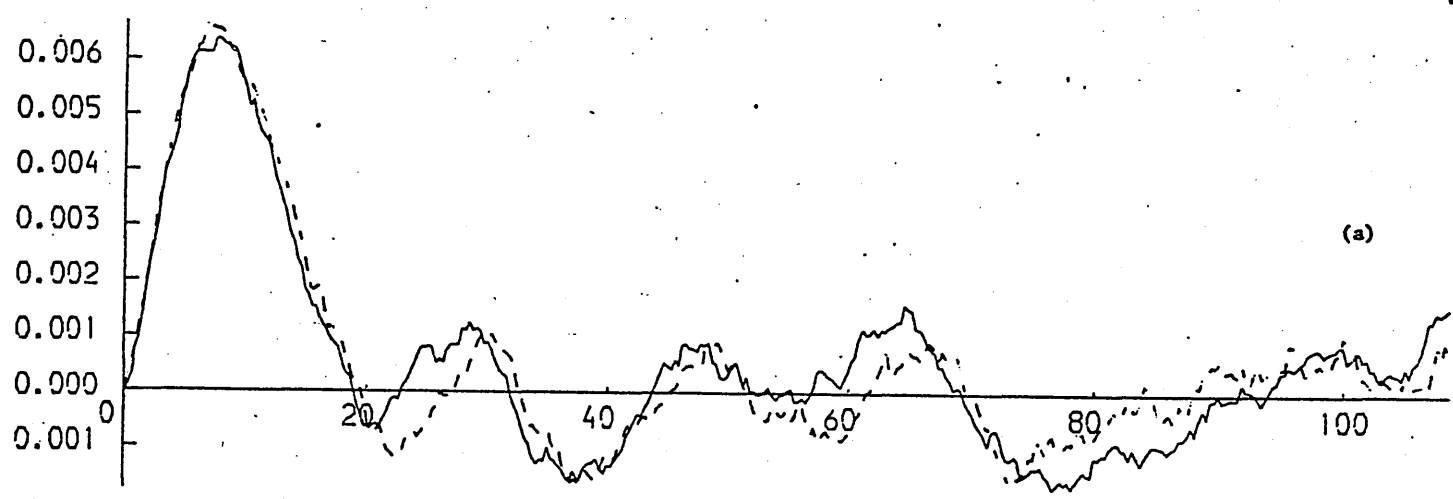


Figure 22 Trajectories for step into sway position, sea state Beaufort 8, closed loop control

(a) State 1, L.F. sway velocity. (b) state 3, L.F. yaw velocity

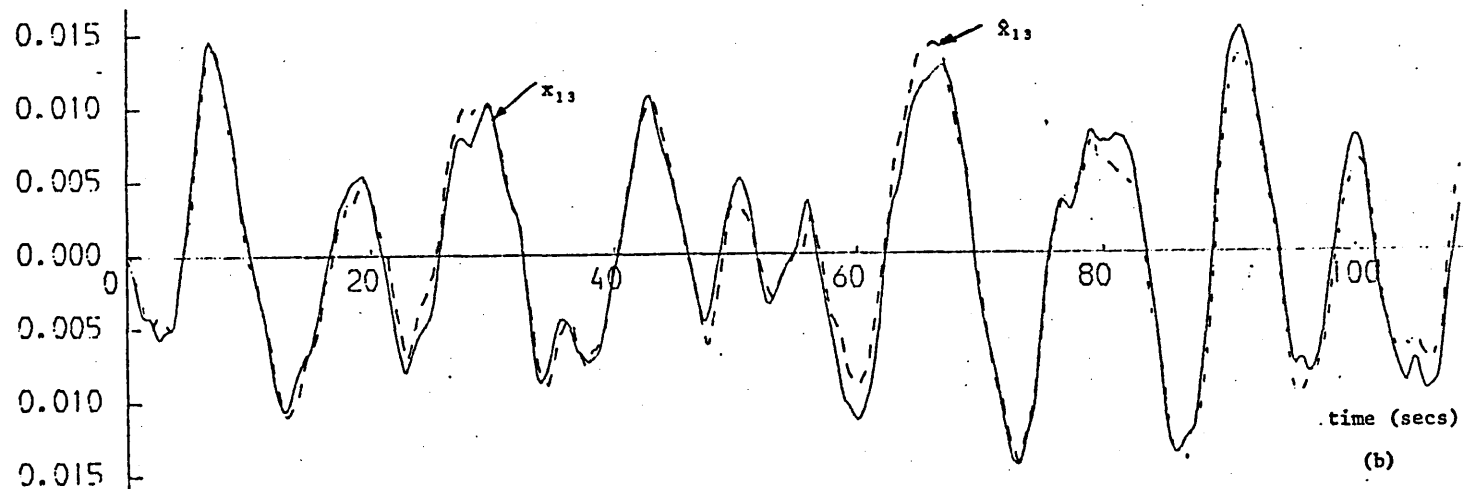
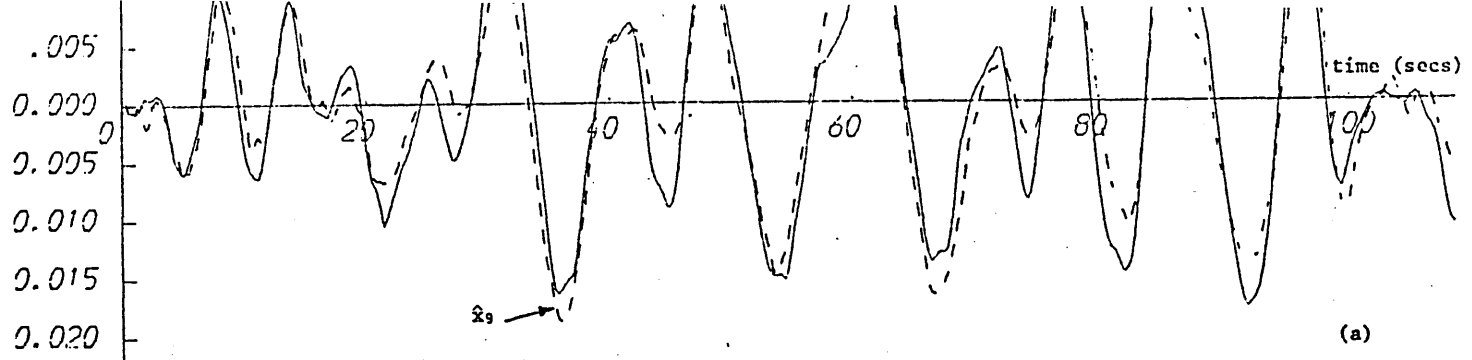


Figure 23 Trajectories for step in sway input sea state Beaufort 8, closed loop control, Eq. 5.34
 (a) state 9, H.F. sway position (b) state 13, H.F. yaw position

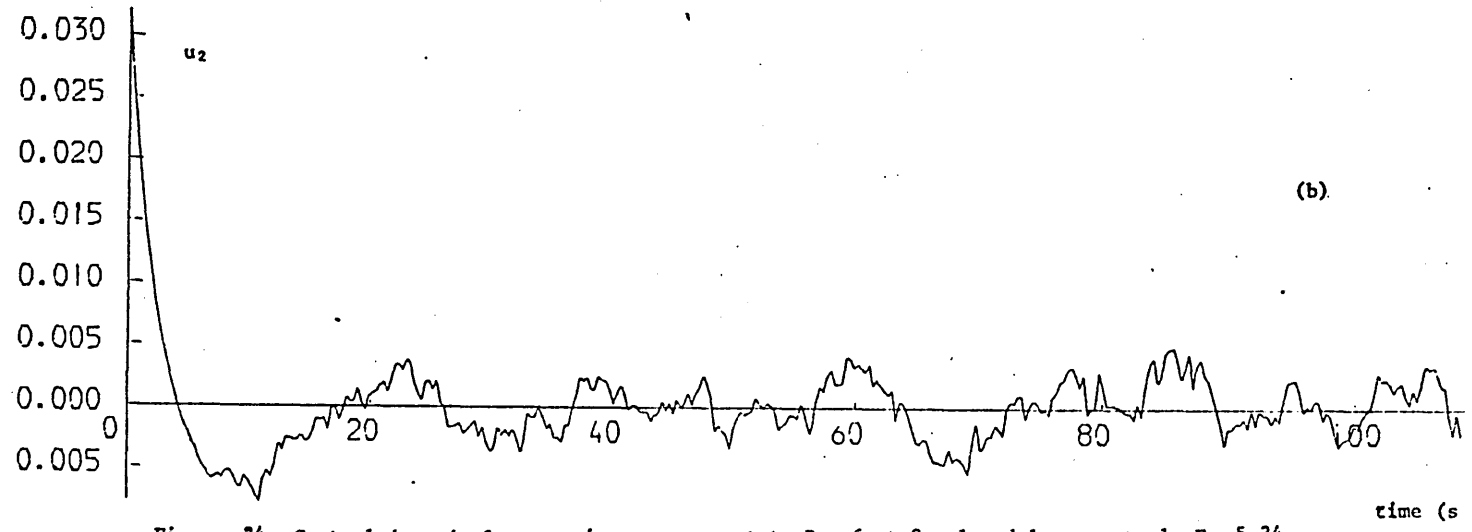
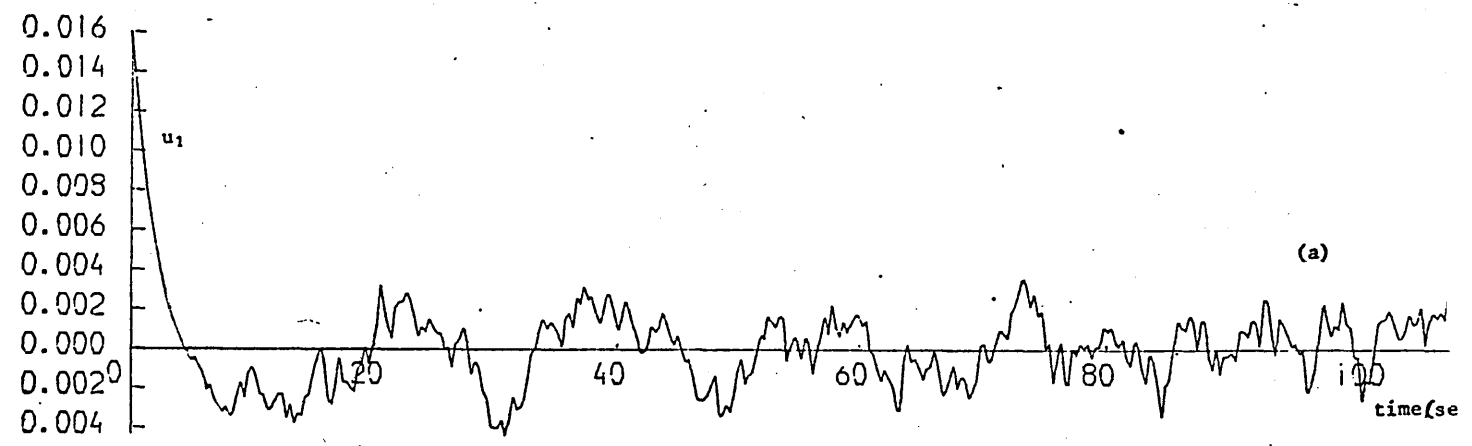


Figure 24 Control demands for step in sway, sea state Beaufort 8, closed loop control, Eq 5.34
 (a) control signal input 1 (u_1) (b) control signal input 2 (u_2)

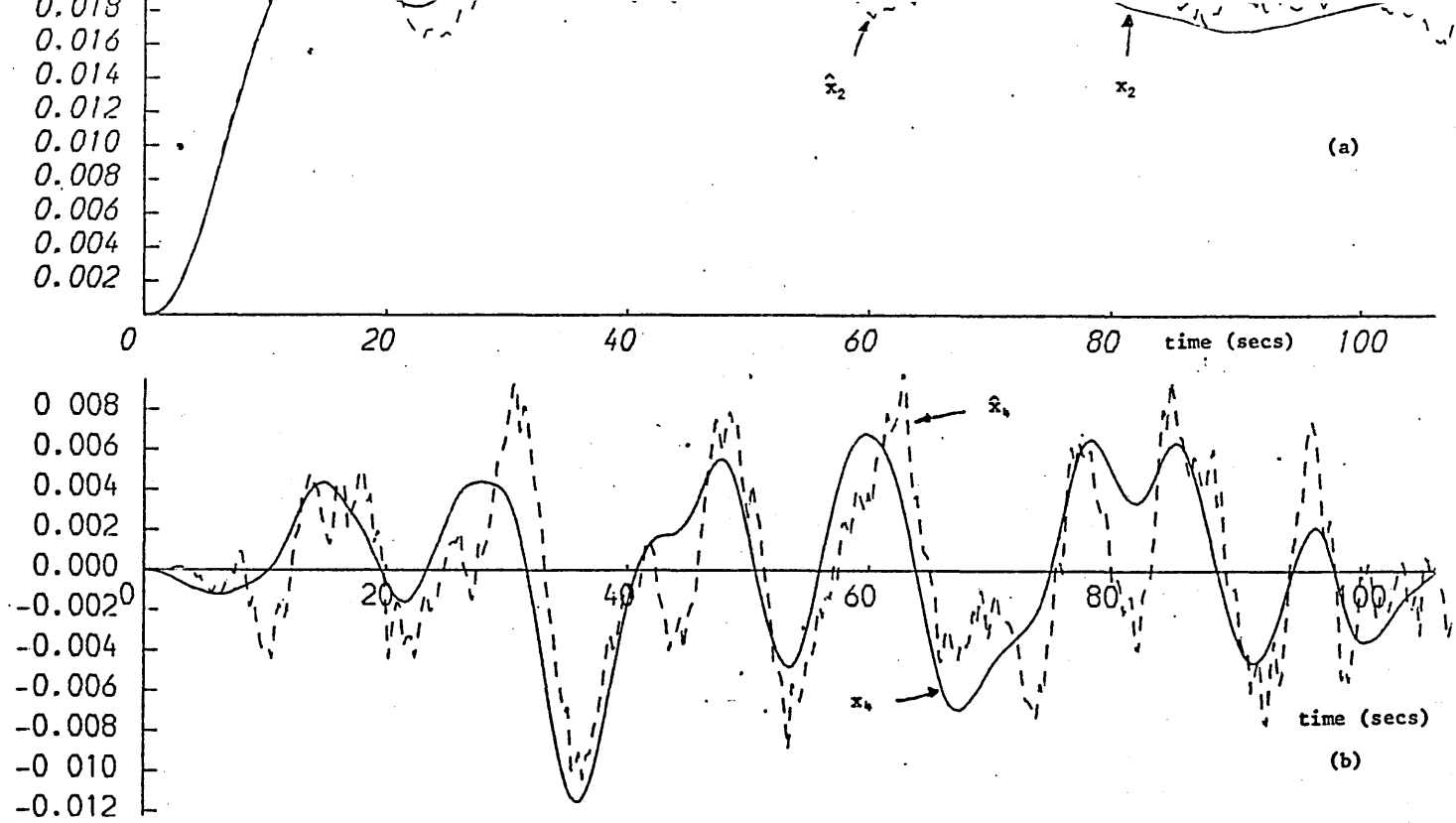


Figure 25 Trajectories for step in sway input, sea state Beaufort 8, closed loop control, Eq. 5.33

(a) state 2, L.F. sway position

(b) state 4, L.F. yaw position

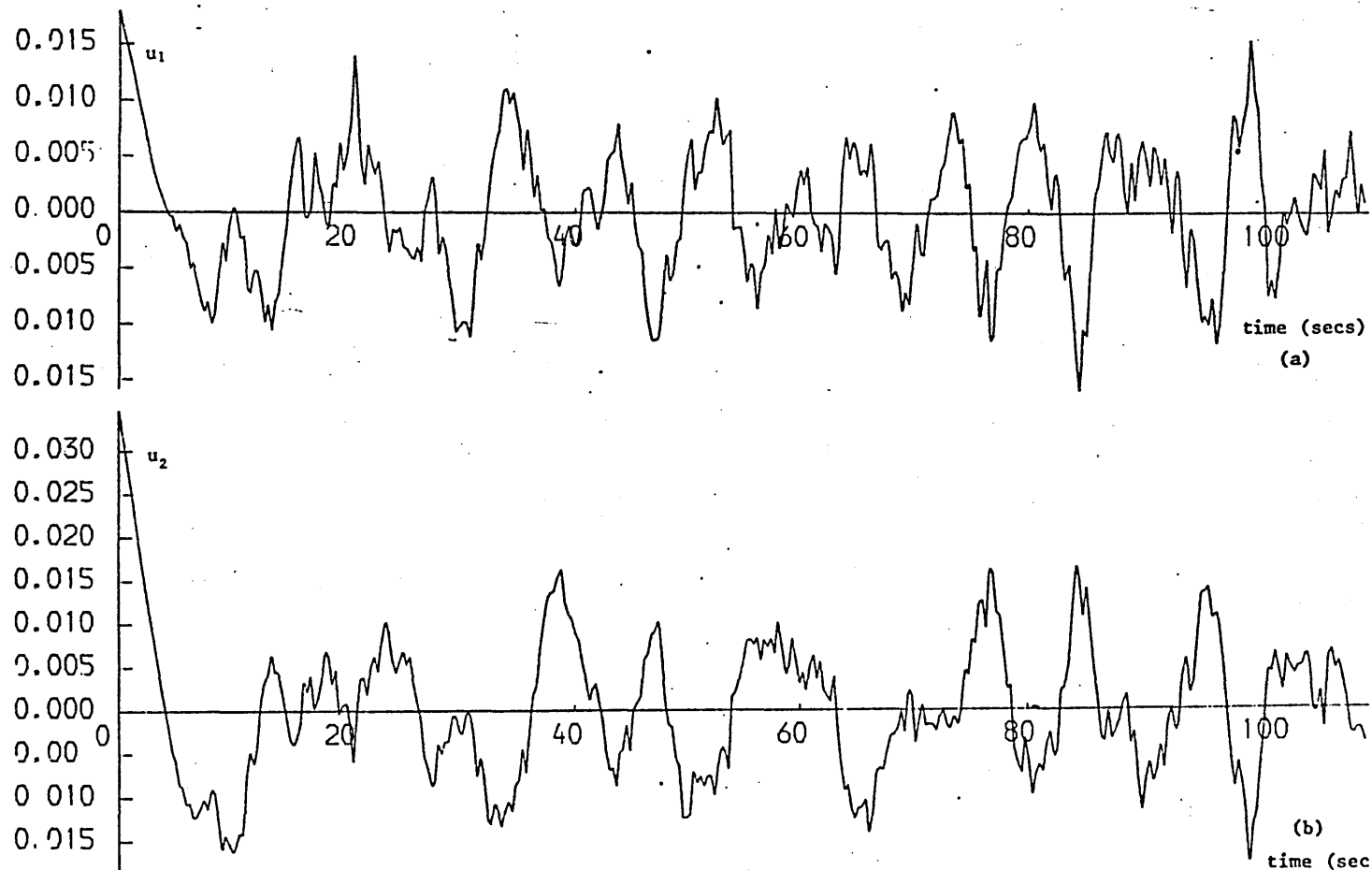


Figure 26 Control demands for step in sway input, sea state Beaufort 8, closed loop control, Eq. 5.33

(a) control signal input 1 (u_1) (b) control signal input 2 (u_2)

Concluding Remarks

In the present thesis two main subjects were treated: new theoretical results in the optimal control field and industrial applications. The theory of optimal control have been extended in both the infinite and finite time situations. New results have been presented on the solution of finite time deterministic optimal control problems and on the selection of the performance criterion matrices. However it may be an indication of the gap between modern control theory and applications that the most successful designs of industrial control systems which have been discussed are based on previous and more 'orthodox' results. The design methods for both the ship positioning problem and the steel mill problem are original and employ results from modern multivariable control theory. Their acceptance by our industrial partners was very dependent upon the intuitive engineering insight that was gained from the methods employed. To convince the engineers in industry that the designs were reasonable required an understanding of the physical situation and a straight forward interpretation of the functions that the rather complicated controllers fulfill.

The multivariable design for the shape control problem is likely to be applied by British Steel Corporation on their Shepcote Lane (Sheffield) Sendzimir mills . An important feature of the design is its implementational simplicity. Optimal controllers were also considered for this application to this problem, as described in

chapter 4, but the simpler non-optimal design was considered more appropriate by the plant engineers (for the present at least). The advantage of the optimal control approach in the above problem, is that constraints on actuator movements, imposed by the mechanical structure of the system, can be more easily incorporated. The disadvantage is the more complicated form of the controller and the fact that the BSC and GEC engineers are more familiar with the frequency domain design methods than with optimal design methods. The steel mills of interest roll materials of different gauges and widths and thus a number of controllers have to be precalculated and stored in the control computer. The non-optimal controllers have the great advantage of simplicity in this situation.

In the design study of the dynamic positioning system both optimal and multivariable frequency domain approaches were compared. For this case it is not so evident that either method is superior or simpler, as both produce controllers of the same complexity. However the actual systems which are being applied, are based mostly upon the optimal design. The Kalman filter had not previously been used in conjunction with the MacFarlane-Kouvaritakis Characteristic Locus-Root Locus design procedures. The design study has shown that not only is possible to use the Kalman filter in this situation but the Kalman filter has obvious advantages, providing the designer with more flexible feedback configurations to achieve the required specifications. Future research could further investigate the various possibilities of using frequency domain controllers together with optimal linear estimators. An interesting feature of this study was the use of multivariable root locus design concepts to square down the system before the application of the characteristic locus procedure.

The finite time optimal control results are not only interesting theoretically but should have interesting applications in self tuning systems. It is usual in self tuning systems to estimate the plant parameters at each sample instant and to apply a control based upon these estimates. During the estimation procedure the parameters vary and so is not appropriate to use infinite time performance criteria. However the existing self tuning strategies involve this type of optimal controller, for example the minimum variance controllers. The finite time optimal controllers presented here seem particularly appropriate in this situation. To improve the estimation or to satisfy identifiability criteria a square wave signal is often inserted into the plant in the same way as that of a reference signal (for example in a chemical plant the square wave may be of small magnitude such as that product quality is not affected); the deterministic optimal controller may easily be derived for such a signal and a calculation procedure for single input single output systems is relatively straight forward. There is therefore the possibility that the finite time optimal controller developed here might be used within an explicit self tuning scheme.

References

- 1 WIENER N. 'The extrapolation, interpolation and smoothing of stationary time series with engineering applications' (Wiley 1949)
- 2 NEWTON G.C., GOULD L.A. and KAISER J.F. 'Analytical design of linear feedback controls' (Wiley 1957)
- 3 KALMAN R.E. 'A new approach to linear filtering and prediction problems' Trans. ASME, 1960, Vol 40, pp 35-45
- 4 KALMAN R.E. and BUCY R.S. 'New results in linear filtering and prediction theory' Trans. ASME, 1961, Vol 41, pp 95-108
- 5 KUCERA V. 'Discrete linear control, the polynomial equation approach' (Wiley 1979)
- 6 PETERKA V. 'On steady state minimum variance control strategy' Kybernetika, 1972, Vol 8, No 3, pp 219-232
- 7 YULA D.C., BONGIORNO J.J., and JABHR J.A. 'Modern Wiener Hopf design of optimal controllers' IEEE Trans. AC21, 1976, pp
- 8 ASTROM K. and WITTENMARK B. 'On self tuning regulators' Automatica, Vol 9, 1973, pp 185-199
- 9 GRIMBLE M.J. 'Solution of the Kalman filtering problem for stationary noise and finite data records' Sheffield City Polytechnic Research Report EEE/7/1976
- 10 FOTAKIS I.E. and GRIMBLE M.J. 'Solution of the finite time optimal control problems for discrete time systems' Intern. Confr. Systems Engineering, Coventry, Sept. 1980
- 11 GRIMBLE M.J. 'Optimal control of linear systems with crossproduct weighting' Proc IEE, Vol 126, No 1, 1979, pp 95-103
- 12 FOTAKIS I.E. 'Some optimal control topics' Research Report EEE/44/ October 1979, Sheffield City Polytechnic

- 13 SHAKED U. 'A general transfer function approach to the steady state linear quadratic Gaussian stochastic control problem' Int J Contr, Vol 24, 1976 pp 771-800
- 14 KALMAN R.E. 'When is a linear control system optimal' Trans ASME, 1964, Vol 86, d, pp 51-60
- 15 ATHANS M. and FALB P.L. 'Optimal control , an introduction to the theory and and its applicati ns' (McGraw Hill 1966)
- 16 MACFARLANE A.G.J. 'Dual-system methods in dynamical analysis' Part 1 and 2 Proc IEE 1969, Vol 116, No 8, pp 1453-1462
- 17 GRIMBLE M.J. 'Design of optimal machine-control systems' Proc IEE 1977, Vol 124, No 9, pp 821-827
- 18 ROSENBROCK H.H. 'Computer aided contol system design' Academic Press, 1974
- 19 MAYNE D.Q. 'Design of linear multivariable systems' Automatica ,Vol 9,1973, No 2, pp 201-208
- 20 MACFARLANE A.G.J. and KOUVARITAKIS B. 'A design technique for linear multivariable feedback systems', Int J Cont, Vol 25, No 6, 1977, pp 837-874
- 21 ROSENBROCK H.H., MCMORRAN P.P. 'Good bad or optimal?' IEEE Trans 1971, AC-16, pp 552-553
- 22 GRIMBLE M.J. 'Optimal control of linear systems with crossproduct weighting' Proc IEE Vol 126, No 1, Jan 1979, pp 96-103
- 23 MACFARLANE A.G.J. 'Return difference and return ratio matrices and their use in analysis and design of multivariable feedback control system' Proc IEE 1970 , 117, pp 2037-2049
- 24 MACFARLANE A.G.J. 'Two necessary conditions in the frequency domain for the optimality of a multiple-input linear control system' Proc IEE 1970, 117, pp 464-466

- 25 ANDERSON B.D.O. and MOORE J.B. 'Linear optimal control'. Prentice Hall 1971
- 26 PORTER B. 'Necessary conditions for the optimality of a class of multiinput closed-loop linear control systems' Electron Lett. 1970, 6, pp 324
- 27 HSU C.H. and CHEN C.T. 'A proof of the stability of multivariable feedback systems' Proc IEE 1963, Vol 56, pp 2061-2062
- 28 PERKINS W. R. 'Feedback properties of linear regulators' IEEE Trans 1971, AC-16, pp 659-663
- 29 FALLSIDE F. and SERAJI H. 'Design optimal systems by a frequency domain technique' Proc IEE 1970, 117, pp 2017-2024
- 30 CHANG S.S.L. 'Synthesis of optimum control systems' McGraw-Hill, 1961
- 31 TYREL J.S. and TUTEUR F.B. 'The use of a quadratic performance index to design multivariable control systems' IEEE Trans, AC-11, No 1, Jan 1966, pp 84-92
- 32 HOUPIS C.H. and CONSTADINIDIS C.T. 'Correlation between conventional control figures of merit and the Q matrix of the quadratic cost function' Proc of 14th Mid West Symposium on Circuit Theory, May 1971, pp 11.3.1-11.3.10
- 33 CHEN R.T.N. and SHEN D.W.C. 'Sensitivity analysis and design of multivariable regulators using a quadratic performance criterion' Proc JACC, 1969, pp 229- 238
- 34 SOLHEIM O.A. 'Design of optimal control systems with prescribed eigenvalues ', Int J Control, 1972, Vol 15, No 1, pp 143-160
- 35 HARVEY C.A. and STEIN G. 'Quadratic weights for asymptotic regulator properties' IEEE Trans, AC-23, No 3, JUNE 1978, pp 378-387

- 36 GRIMBLE M.J. 'Design of optimal output regulators using multivariable root loci' Proc IEE 1981, 128, pp 41-49
- 37 KWAKERNAAK H. and SIVAN R. 'Linear optimal control systems' (Wiley-Interscience, 1972) pp 497
- 38 KOUVARITAKIS B. 'The optimal root loci of linear multivariable systems', Univ Cambridge, Dept Eng Research Report, CUED/F-CAMS/TR148, Mar 1977
- 39 ROSENBROCK H.H. 'State space and multivariable theory', (Nelson, 1970) pp 13
- 40 MOORE B.C. 'On the flexibility offered by state feedback in multivariable systems beyond closed loop eigenvalue assignment' IEEE Trans, AC-21, Oct 1976, pp 689-692
- 41 KWAKERNAAK H. 'The maximally achievable accuracy of linear optimal regulators and linear optimal filters' IEEE Trans, AC-17, No 1, Feb 1972, pp 79-86
- 42 FALLSIDE F. 'Control system design by pole-zero assignment' (Academic Press, 1977), p 6
- 43 OWENS D.H. 'First and second-order-like structures in linear multivariable control systems design' Proc IEE, Vol 122, No 9, Sept 1975, pp 935-941
- 44 SHAKED U. 'The asymptotic behaviour of the root-loci of multivariable optimal regulators' Trans IEEE, AC-23, No 3, June 1978, pp 425-430
- 45 SHAKED U. and KARCANIAS N. 'The use of zero-directions in model reduction' Int J Cont, Vol 23, No 1, 1976, pp 113-135
- 46 MACFARLANE A.G.J. and KARCANIAS N. 'Poles and zeros of linear multivariable systems: a survey of the algebraic, geometric and complex-variable theory', Univ Cambridge Report, CUED/F-Control/TR105

- 47 KARCANIAS N. and KOUVARITAKIS B. 'The output zeroing problem and its relationship to the invariant zero structure: a matrix pencil approach', Univ Cambridge, Dept Engineering CUED/F-CAMS/TR168(1978)
- 48 KOUVARITAKIS B. and MACFARLANE A.G.J. 'Geometric approach to analysis and synthesis of system zeros, Part 1 Square Systems', Int J Control, Vol 23, No 2, 1976, pp 149-166
- 49 PORTER B. and D'AZZO J.J. 'Comment on the flexibility offered by state feedback in multivariable systems beyond closed-loop eigenvalue assignment'
- 50 SHAKED U. 'The zeros of linear optimal control systems and their role in high feedback gain stability design', Cambridge Univ, CUED/F-CAMS/TR117, 1976
- 51 KOUVARITAKIS B. and SHAKED U. 'Asymptotic behaviour of root-loci of linear multivariable systems', Int J Control, Vol 23, No 3, 1976, pp 297-340
- 52 BULLOCK T.E. and ELDER J.M. 'Quadratic performance index generation for optimal regulator design', IEEE Conf on Decision and Control, Dec 1971, W8-3, pp 123-124
- 53 POSTLETHWAITE I. 'A note on the characteristic frequency loci of multivariable linear optimal regulators' IEEE Trans, AC-23, No 4, Aug 1978, pp 757-760
- 54 OWENS D.H. 'On the computation of optimal system asymptotic root-loci' Univ Sheffield Research Report, No 77, Nov 1978
- 55 KOUVARITAKIS B. and EDMUNDS J.M. 'Multivariable root-loci: a unified approach to infinite zeros' Int J Cont, Vol 29, No 3, 1979, pp 393-428

- 56 JAMSHIDI M. 'A parameter adjustable regulator for a winding process' Int J Cont, Vol 15, No 4, 1972, pp 725-736
- 57 JAMSHIDI M. 'A new-optimum controller for cold-rolling mills' Int J Cont, Vol 16, No 6, 1972, pp 725-736 1137-1154
- 58 JAMSHIDI M., D'ANS G.C. and KOKOTOVIC P. 'Application of a parameter-imbedded Riccati equation' IEEE Trans, AC-15, Dec 1970, pp 682-683
- 59 KWAKERNAAK H. 'Assymptotic root loci of multivariable linear optimal regulators' IEEE Trans, AC-21, June 1976, pp 378-382
- 60 WOODHEAD M.A. and PORTER B. 'Optimal modal control' Measurement and Control, Vol 6, July 1973, pp 301-303
- 61 GRIMBLE M.J. 'S-domain solution for the fixed end-point optimal control problem', Proc IEE, Vol 124, No 9, Sept 1977, pp 802-808
- 62 GRIMBLE M.J. 'The design of finite-time optimal multivariable systems', Int J Systems, 1978, Vol 9, No 3, pp 311-334
- 63 GRIMBLE M.J. 'Solution of finite-time optimal control problem with mixed end constraints in the s-domain', IEEE Trans on AC-24, No 1, Feb 1979, pp 100-108
- 64 GRIMBLE M.J. 'Solution of Kalman filtering problem for stationary noise and finite data records', Int J Systems Science, 1979, Vol 10, No 2, pp 177-196
- 65 GRIMBLE M.J. 'Solution of the linear estimation problem in the s-domain', Proc IEE, Vol 125, No6, June 1978, pp 541-549
- 66 GRIMBLE M.J. 'A new finite-time linear smoothing filter', research Report No EEE/26/December 1978
- 67 CLARK D.W., COPE S.N. and CAWTHOROP P.J. 'Feasibility study of the application of microprocessors to self tuning controllers', Univ Oxford, Engineering Dept Science Report, No 1137/75

- 68 ASTROM K.J. and WITTENMARK B. 'Analysis of a self-tuning regulator for non-minimum phase systems', IFAC Symposium on Stochastic Control, Budapest 1974
- 69 GRIMBLE M.J. 'Solution of the discrete-time stochastic optimal control problem in the z-domain', Int J Systems Science, Vol 10, No 12, pp 1369-1390
- 70 ANDERSON B.D.O. and MOORE J.B. 'Linear optimal control' (Perntice Hall 1971), pp 239
- 71 SAGE A.P and WHITE C.C. 'Optimum systems control', (Prentice Hall 1977)
- 72 TUEL W.G. 'Computer algorithm for the spectral factorisation of rational matrices' IBM Journal, Vol 12, March 1968, pp 163-170
- 73 STRINTZIS M.G. 'A solution to the matrix factorisation problem', IEEE Trans IT-18, No 2, March 1972, pp 225-232
- 74 DAVIS M.C. 'Factoring the spectral matrix', IEEE Trans , ACS, 296
- 75 SHAKED U. 'A general transfer function approach to linear stationary filtering and steady state optimal control problems', Research Report, Dept of Engineering, Univ Cambridge, TR126, 1976
- 76 PIMENTEL J.R. 'A simple solution for the optimum discrete regulator problem', Proc of Southeastern IEEE, April 1979, Roanoke, VA, USA, pp 254-256
- 77 KUCERA V. 'State space approach to discrete linear control', Kybernetika, Vol 8, No 3, 1972, pp 231-149
- 78 GRIMBLE M.J. 'Frequency domain solution to the multivariable tracking problem', Trans Int MC, Vol 1, No 2, June 1979, pp 74-78
- 79 WELLSTEAD P.E. PRAGER P and ZANKER P. 'Pole assignment self-tuning regulator' Proc IEE, Vol 126, No 8, August 1979

- 80 BERTSEKAS D.P. and SHREVE S.E. 'Stochastic optimal control, the discrete time case', (Academic Press, 1978)
- 81 GRIMBLE M.J. 'New finite time linear filters and smoothers', Third IMA Conference on Control Theory, University of sheffield, September 1980
- 82 MACFARLANE A.G.J. 'A linear vector space approach to z-transform and s-transform theory' Cambridge Univ Dept Eng, CUED/F-Control/TR90, 1974
- 83 GRIMBLE M.J. 'Shape control for rolled strip', Cme, November 1975, pp 91-93
- 84 SHEPPARD T. and ROBERTS J.M. 'Shaper control correction in strip and sheet' The Inst of metals, Vol 18, pp 1-18, 1973
- 85 SPOONER P.D. and BRYANT G.F. 'Analysis of shape and discussion of problems of scheduling set-up and shape control' Proc Shape Control Conf, Metals Soc, Chester, 1976
- 86 PEARSON W.K.J. 'Shape measurement and control', J of Inst of Metals , Vol 93, No 65, 1964, pp 169-178
- 87 SABATINI B., WOODCOCK J.W. and YEOMANS K.A. 'Shape regulation in flat rolling' Journal of Iron and Steel Inst, Vol 206, pp 1214-1217, 1968
- 88 SABATINI B. and YEOMANS K.A. 'An algebra of strip shape and its application to mill scheduling', Iron and Steel inst, Vol 206, pp 1207-1213, Dec 1968
- 89 KNOX T.K. 'Operating experience with the Loewy Robertson vidimon shapemeter at Shotton Works' Proc of Conf by Metals soc, Chester, Shape Control, March 1976, pp 55
- 90 WISTREICH J.G. 'Measurement and control of strip shape in cold rolling' Proc ICSTIS Suppl, Trns ISIJ, Vol 11, 1971, pp 674-679

- 91 BRYANT G. F. 'Automatation of tandem mills' The Iron & Steel Inst
- 92 BRAVINGTON C.A., BARRY D.C. and McCLURE C.H. 'Design and development of a shape control system' Shape Control, Proc of conf, Metals Soc, Chester, March 1976, pp 82-88
- 93 SIVILOTTE O.G., DAVIES W.E. HENZE M. and DAHLE O. 'ASEA-Alcan AFC System for cold rolling flat strip' Iron and Steel Eng, June 1973, pp 83-90
- 94 GRIMBLE M.J. 'Tension controls in strip processing lines' Metals Technology, October 1976, pp 445-453
- 95 GUNAWARDENE G.W.D.M., GRIMBLE M.J. and THOMSON A. 'A static model for a Sendzimir cold rolling mill' Metal Technology, 1980
- 96 GRIMBLE M.J. 'Catenary controls in metal-strip processing lines' GEC Journal of Science and Technology, Vol 41, No 1, pp 21-26, 1974
- 97 GRIMBLE M.J. 'An optimal output feedback solution to the strip shape multivariable control problem' Sheffield City Polytechnic Report EEE/55/1980
- 98 CARTER C.E. and GRIMBLE M.J. 'Dynamic simulation and control of a Sendzimir cluster mill', Internatinal Conf on Systems Engineering, Lanchester Polytechnic, September 1980
- 99 POSTLETHWAITE I., EDMUNDS J.M. and MACFARLANE A.G.J. 'Principal gains phases in the analysis of linear multivariable feedback systems', IEEE Trans AC26, No 1, 1981, pp 32-46
- 100 SAFONOV M.G., LAUB A.J., HARTMANN G.L. 'Feedback properties of multivariable systems: The role and use of the return difference matrix' IEEE Trans AC26, No 1, 1981, pp 47-65
- 101 ATHANS M. 'The role and use of the stochastic linear quadratic Gaussian problem in control system design' IEEE Trans AC16, 1971, pp 529-552

- 102 BALL A.E. and BLUMBERG J.M. 'Development of a dynamic ship positioning sytem' GEC J of Science&Technology, 1975, Vol 42, pp 29-36
- 103 MORGAN M.J. 'Dynamic positioning of offshore vessels' Petroleum publishing Company, 1978)
- 104 GRIMBLE M.J., PATTON R.J. and WISE D.A. 'The use of Kalman filtering techniques in dynamic ship positioning systems', Oceanology Int. Conf, Brighton March 1978
- 105 BALCHEN J.G., JENSSEN N.A. and SAELID S. 'Dynamic positioning using Kalman filtering and optimal control theory' Automation in Offshor Oil Field Operation, 1976, pp 183-188
- 106 GRIMBLE M.J., PATTON R.J. and WISE D.A. 'The design of dynamic ship potioning control systems using extended Kalman filtering techniques', Oceans 1979 Coference (IEEE), San Diego, California, Sept 1979
- 107 TRIANTAFILLOU M.S. 'The design of a dynamic potioning system' Presented at Oceans 1979 Conf (IEEE), San Diego, California, Sept 1979
- 108 MACFARLANE A.G.J., KOUVARITAKIS B. and EDMUNDS J. 'Alternatives for multivariable control' Proc National Engineering Consortium, Inter forum, 1977, Chicago
- 109 GRIMBLE M.J. 'Design of optimal stochastic regulating systems including integral action' Proc IEE, Vol 126, No 9, Sept 1978 , pp 841-848
- 110 WISE D.A. and ENGLISH J.W. 'Tank and wind tunnel tests for a drill ship with dynamic position control' Offshore Technology Conf, Dallas, Paper No OTC 2345, 1975

- 111 ENGLISH J.H. and WISE D.A. 'Hydrodynamic aspects of dynamic positioning' Trans, Vol 92, No 3, North East Coast Inst of Engineers And Shipbuilders, pp 53-72
- 112 GRIMBLE M.J., PATTON R.J. and WISE D.A. 'The design of dynamic ship potioning control system using stochastic otpimal control theory' Optimal Control Applications and Methods, 1980, Vol 1, pp 167-202
- 113 DAVENPORT A.G. 'The spectrum of horizontal gustiness near the ground in high winds' Quarterly Royal Meteorological Society, Vol 87, London 1961, pp 194-211
- 114 GRIMBLE M.J.' Solution of the linear estimation problem in the s-domain' Proc IEE, Vol 125, No 6, June 1978, pp 541-549
- 115 GRIMBLE M.J. 'Realtionship between Kalmen and Ntch filters used in dynamic ship positioning systems' Elect Letters, June 1978, Vol 14, No 13, pp 399
- 116 TAMEHIRO M. and KASAI H. 'On dynamic positioning system desing in particularreference to the positional signal filtering technique' J.S.N.A. Japan, Vol 142, Dec 1977, pp 173-
- 117 MACFARLANE A.G.J. and POSTLETHWAITE I. 'Characteristic frequency functions and characteristic gain functions' Int J Control, Vol 26, No 2, 1977, pp 265
- 118 KOUVARITAKIS B. 'The role of observers in multivariable root locus design' (to be published) I.J.S.S.
- 119 BARTON P.H. 'Dynamic positioning systems' G.E.C. Journal for Industry, Vol 2, No 3, October 1978, pp 119-125
- 120 WONHAM W.M. 'Lecture notes in economics and mathematical systems ' (Springer-Verlag, 1970), p 317

A brief review is given below of optimal root-locus theory based upon the work of Kwakernaak [37], Wonham [120], Kouvaritakis [38] and Shaked [44] but for $G \neq 0$ and CB full rank. From (2.40):

$$F^T(-s)RF(s) = W^T(-s)QW(s)/\mu^2 + (W^T(-s)G + G^TW(s))/\mu + R$$

For small μ (as in deriving equation (19)) and as $|s| \rightarrow \infty$

$$F^T(-s)RF(s) \rightarrow (R^{\frac{1}{2}})^T (I_m - (R^{-\frac{1}{2}})^T (CB)^T QCB R^{-\frac{1}{2}} / (s^2 \mu^2)) R^{\frac{1}{2}}$$

The faraway regulator poles are the left-half plane roots of

$$s^2 - \gamma_i / \mu^2 = 0 \quad \text{for } i = \{1, 2, \dots, m\}$$

where γ_i are the positive eigenvalues of the positive-definite (rank $Q^{\frac{1}{2}}CB = m$) symmetric matrix:

$$(R^{-\frac{1}{2}})^T (CB)^T QCB R^{-\frac{1}{2}}$$

For each i a first-order stable Butterworth pattern is obtained, consisting of a single pole $-\gamma_i^{\frac{1}{2}}/\mu$ on the negative real axis. There are exactly m faraway closed-loop poles.

Notice that the closed-loop system poles are the left half-plane zeros of:

$$I_m + (R^{-\frac{1}{2}})^T (W^T(-s)QW(s) + \mu(W^T(-s)G + G^TW(s))) R^{-\frac{1}{2}} k$$

where $k = 1/\mu^2$. Thus, the root-loci of the optimal regulator can be obtained by considering the root-loci of a system $S(A^*, B^*, C^*)$ with output feedback control law:

$$\underline{u} = -k\underline{y}$$

The transfer-function matrix of the open-loop system $S(A^*, B^*, C^*)$ is

$$W^*(s) = (R^{-\frac{1}{2}})^T (W^T(-s)QW(s) + \mu(W^T(-s)G + G^TW(s))) R^{-\frac{1}{2}}$$

It may easily be verified that the following theorem holds:

One realization of the triplet (A^*, B^*, C^*) is given by:

$$A^* = \begin{bmatrix} A & 0 \\ -C^T Q C & -A^T \end{bmatrix}$$

$$B^* = \begin{bmatrix} B \\ -\mu C^T G \end{bmatrix} R^{-\frac{1}{2}}$$

$$C^* = (R^{-\frac{1}{2}})^T \begin{bmatrix} \mu G^T C & B^T \end{bmatrix}$$

The proof follows by calculating $C^*(sI - A^*)^{-1}B^*$. Notice that B^* and C^* depend upon μ unless $G = 0$.

The $(n-m)$ asymptotically finite closed-loop poles, or optimal finite zeros³⁸, will now be determined. Recall that the zeros of $S(A^*, B^*, C^*)$ are defined to be the values of s for which the system matrix:

$$P^*(s) = \begin{bmatrix} sI - A^* & B^* \\ C^* & 0 \end{bmatrix}$$

loses rank. After multiplying by non-singular transformations:

$$\hat{P}(s) = \begin{bmatrix} sI - A & 0 & B \\ C^T Q C & sI + A^T & -\mu C^T G \\ \mu G^T C & B^T & 0 \end{bmatrix}$$

The $(n-m)$ asymptotically finite closed-loop poles $\{\lambda_i^0\}$ are given by the left half-plane zeros of the system $S(A^*, B^*, C^*)$ as $\mu \rightarrow 0$. These are equal to the left-half plane zeros of the polynomial $z(s) \triangleq \det \hat{P}(s)$ for $\mu = 0$. Note that the cross-product matrix term goes to zero as $\mu \rightarrow 0$ and thus does not influence the asymptotically finite closed-loop poles.

Moore [40] has shown that in state-feedback systems the freedom one has, beyond specifying the closed-loop eigenvalues, is to choose one set from the class of allowable closed-loop eigenvectors. The gain K is uniquely defined, if it exists, by the selection of a set of distinct eigenvalues together with a corresponding set of eigenvectors. While the overall speed of response of the closed-loop system is determined by its eigenvalues, the shape of the transient response depends to a large extent on the closed-loop eigenvectors. The following theorem was established by Moore [40] ::

Theorem A2.1 (Moore)

Let $\{\lambda_i\}$ be a self-conjugate set of distinct complex numbers. There exists a matrix K of real numbers, such that $(A + BK)\underline{x}_i = \lambda_i \underline{x}_i$ if and only if the following three conditions are satisfied for $i \in \{1, 2, \dots, n\}$.

- (a) Vectors $\{\underline{x}_i\}$ are linearly independent in C^n .
- (b) Vector $\underline{x}_i = \underline{x}_j^*$ whenever $\lambda_i = \lambda_j^*$.
- (c) The vectors $\underline{x}_i \in \text{span}(N_{\lambda_i})$, where $S_{\lambda} \triangleq \begin{bmatrix} \lambda I - A & B \end{bmatrix}$ and

$T_{\lambda} = \begin{bmatrix} N_{\lambda}^T & M_{\lambda}^T \end{bmatrix}^T$ has columns which constitute a basis for $\text{Ker}(S_{\lambda})$, (m -dimensional). The matrix $N_{\lambda} = n \times m$ and $M_{\lambda} = m \times m$.

Corollary A2.1 Eigenvector and Input Directions

The vectors $\{\underline{x}_i\}$ and associated distinct complex numbers $\{\lambda_i\}$ are closed loop eigenvalues and eigenvectors of the square system $\dot{\underline{x}} = A\underline{x} + B\underline{u}$, $\underline{u} = -K\underline{x}$, if and only if, there exist $\underline{w}_i \in R^m$, such that

$$(\lambda_i I - A)\underline{x}_i - B\underline{w}_i = 0$$

$$\underline{w}_i = -K\underline{x}_i, \quad \text{for } i = \{1, 2, \dots, n\}$$

Proof: Sufficiency follows from direct substitution. Necessity follows from theorem A2.1.

The following theorem is concerned with the closed-loop eigenvalues which do not belong to the spectrum of A. These eigenvalues are necessarily controllable. First note the following definitions.

Definition A2.1 Algebraic Multiplicity

The zero polynomial for the square system S(A,B,C) is defined as $z(s) = \det P(s)$ where P(s) is the Rosenbrock system matrix. Let p denote the number of the distinct zeros of the system S, then writing

$$z(s) = \sum_{i=1}^p (s - z_i)^{q_i}$$

the constant q_i is defined as the algebraic multiplicity of the zero z_i , for all $i \in \{1, 2, \dots, p\}$.

Definition A2.2 Geometric Multiplicity (MacFarlane and Karcanias [46])

The geometric multiplicity of a zero z_i , for the system S(A,B,C), is defined as the rank-deficiency of $P(z_i)$.

Theorem A2.2 Input Direction Vectors

Let λ_i represent a controllable distinct closed-loop eigenvalue $\lambda_i \notin \sigma(A)$. The vectors $\{\underline{w}_i\}$ are identical (except possibly for magnitude) to the vectors \underline{v}_i , determined by the return-difference equation:

$$F(\lambda_i)\underline{v}_i = 0$$

Proof: From the previous equations

$$\begin{aligned} F(\lambda_i)\underline{w}_i &= \underline{w}_i + K\Phi(\lambda_i)B\underline{w}_i \\ &= \underline{w}_i + K\underline{x}_i = 0 \end{aligned}$$

The set of λ_i values may be interpreted as transmission zeros of F(s).

The solution of $F(\lambda_i)\underline{v}_i = 0$ are then unique (except possibly for magnitude)

providing these zeros have unit algebraic and geometric multiplicity [42].

The above results do not apply to the closed-loop eigenvalues belonging to the spectrum of A. Assuming that these eigenvalues are distinct $\det F(\lambda_i) = \rho_c(\lambda_i)/\rho_o(\lambda_i) \neq 0$. Thus $F(\lambda_i)$ is non-singular and $F(\lambda_i)\underline{v}_i = 0 \Rightarrow \underline{v}_i = 0$.

The asymptotically-infinite eigenvectors $\{\underline{x}_i^\infty\}$ are determined by the following theorem:

Theorem A2.3 Asymptotically Infinite Eigenvectors

The eigenvectors $\{\underline{x}_i^\infty\}$ corresponding to the asymptotically infinite eigenvalues are given by:

$$\underline{x}_i^\infty = B\underline{v}_i^\infty$$

Proof: The asymptotically infinite eigenvalues $\{\lambda_i^\infty/\mu\}$ are controllable and do not belong to the spectrum of A. Thus, from corollary A2.1 and theorem A2.2, as $\mu \rightarrow 0$

$$\underline{x}_i = ((\lambda_i^\infty/\mu)I - A)^{-1}B\underline{v}_i \rightarrow B(\lambda_i^\infty/\mu)\underline{v}_i \text{ or } \underline{x}_i^\infty = B\underline{v}_i^\infty$$

The following theorems and results are used in section [27] to calculate the asymptotically finite modes and directions.

Definition A3.1 (MacFarlane and Karcanias [46])

The vector $[(\underline{\omega}_0)^T \quad (\underline{\sigma}_0)^T]^T$ is a zero-direction $S(A,B,C)$, corresponding to the zero λ_0 , if and only if,

$$P(\lambda_0) \underline{m}_0 = \begin{bmatrix} \lambda_0 I - A & B \\ C & 0 \end{bmatrix} \begin{bmatrix} \underline{\omega}_0 \\ \underline{\sigma}_0 \end{bmatrix} = 0$$

$\underline{\omega}_0 \in R^n$ and $\underline{\sigma}_0 \in R^m$ are called the state and input zero directions, respectively. For square systems the zero polynomial is simply $z(s) = \det P(s)$. In the case of a multiple zero, the zero directions that correspond to this zero are by definition to be independent.

Definition A3.2 Unobservable System Modes

A mode of the system $S(A,B,C)$ will be unobservable if there exists a vector \underline{w} and a complex number λ such that

$$(\lambda I - A) \underline{w} = 0 \quad \text{and} \quad C \underline{w} = 0$$

Theorem A3.1 (Shaked and Karcanias [45])

The state zero directions of a non-degenerate system are linearly independent.

Theorem A3.2 (Shaked and Karcanias [45])

Given a pair $(\lambda^0, \underline{\omega}^0)$ a necessary and sufficient condition for a matrix K to exist such that $(\lambda^0 I - A + BK) \underline{\omega}^0 = 0$ and $C \underline{x}^0 = 0$, is that λ^0 is a zero of the system and $\underline{\omega}^0$ is its corresponding state zero direction.

This theorem implies that the only candidate pairs for the closed-loop unobservable modes and vectors (definition A3.2) are the pairs of zeros and their corresponding zero directions.

The following results are used in the selection of the scalar μ as described previously.

Theorem A4.1 Zeros of $W(s)$

If $W(s)$ is square and M_0 is full rank the zero polynomial $\psi_0(s)$ has degree $(n-m)$. If M_k is full rank and all lower order Markov parameters are zero then $\psi_0(s)$ has degree p where $p = n - (k+1)m$.

Proof: Note that $\lim_{|s| \rightarrow \infty} s\phi(s) = I_n$ and the zero polynomial $\psi_0(s)$ is defined as:

$$\psi_0(s) = \rho_0(s) \det W(s)$$

but

$$\lim_{|s| \rightarrow \infty} s^{(k+1)m} \psi_0(s) / \rho_0(s) = \lim_{|s| \rightarrow \infty} \det (Cs^{k+1}\phi(s)B) = \det CA^k B$$

and thus $\psi_0(s)$ has degree $p = n - (k+1)m$. Also note that

$$\psi_0(s) = \alpha \prod_{i=1}^p (s - \beta_i)$$

where $\alpha = \det CA^k B$.

Theorem A4.2 Faraway Closed Loop Poles

The distance of the faraway closed-loop^[37] poles from the origin is approximately:

$$(\alpha^2 \det Q / (\mu^{2m} \det R))^{1/(2(n-p))}$$

where p is defined in theorem A4.2.

Proof: From equation 2.40:

$$\rho_c(-s)\rho_c(s) = \rho_0(-s)\rho_0(s) \det (R^{-1}W^T(-s)\frac{Q}{\mu^2}W(s) + I_m + \frac{R^{-1}}{\mu}(W^T(-s)G + G^TW(s)))$$

for all small μ and G ,

$$\rho_c(-s)\rho_c(s) = \psi_0(-s)\psi_0(s) \det Q / (\mu^{2m} \det R)$$

The closed-loop polynomial therefore has the form:

$$\rho_c(-s)\rho_c(s) = ((-s^2)^n + \dots + \frac{\alpha^2 \det Q}{\mu^{2m} \det R} (-s^2)^p + \dots)$$

An approximation of the faraway roots, for small μ , follows from:

$$(-1)^n s^{2n} + \alpha^2 \det Q (-s^2)^p / (\mu^{2m} \det R) = 0$$

and the stable solutions satisfy:

$$s = ((-1)^{n-p-1} \alpha^2 \det Q / (\mu^{2m} \det R))^{1/(2(n-p))}$$

The above approximation shows that these poles are distributed in a Butterworth configuration [37] of the order $(n-p)$.

An improved estimate of the distance of each of the faraway poles from the origin is obtained from equation (2.47)

$$\det (s^{2(k+1)} \mu^2 I_m - (-1)^k R^{-\frac{1}{2}} (CA^k B)^T QCA^k BR^{-\frac{1}{2}}) = 0$$

Let the non-zero (positive) eigenvalues of the positive definite symmetric matrix $R^{-\frac{1}{2}} (CA^k B)^T QCA^k BR^{-\frac{1}{2}}$ be given by γ_i for $i = \{1, 2, \dots, m\}$. The faraway regulator poles are the left half-plane roots of,

$$s^{2(k+1)} = \gamma_i / \mu^2 \quad \text{for } i = \{1, 2, \dots, m\}$$

For each i a $(k+1)$ th order Butterworth pattern is obtained including a single pole $s = -(\gamma_i / \mu^2)^{1/(2(k+1))}$ on the negative real axis. Note that the geometric mean of these distances becomes:

$$\left(\prod_{i=1}^m (\gamma_i / \mu^2)^{1/(2(k+1))} \right)^{1/m} = \det (R^{-\frac{1}{2}} M_k^T Q M_k R^{-\frac{1}{2}} / \mu^{2m})^{1/(2m(k+1))}$$

or

$$r_f = \frac{(\alpha^2 \det Q)^{1/(2m(k+1))}}{\mu^{2m} \det R}$$

This latter result agrees with the expression given in theorem A4.2 above.

The limiting values of the n closed-loop pole positions, as $\mu \rightarrow \infty$, are determined below [37] From the return-difference relationship [27]

$$\det (F(s)) = \rho_c(s)/\rho_o(s)$$

and from equation 2.40:

$$\rho_c(-s)\rho_c(s) \det R = \rho_o(-s)\rho_o(s) \det (R + W^T(-s)\frac{Q}{\mu^2}W(s) + W^T(-s)\frac{G}{\mu} + \frac{G^T}{\mu}W(s))$$

In the limit as $\mu \rightarrow \infty$

$$\rho_c(-s)\rho_c(s) \rightarrow \rho_o(-s)\rho_o(s)$$

Thus, if the set of zeros of $\rho_o(s)$ are denoted by $\{s_i^o\}$ then the closed-loop eigenvalues approach the numbers s_i^c , for $i = \{1, 2, \dots, n\}$, where

$$s_i^c = \begin{cases} s_i^o & \text{if } \operatorname{Re}(s_i^o) \leq 0 \\ -s_i^o & \text{if } \operatorname{Re}(s_i^o) > 0 \end{cases}$$

The cheapest stabilizing control-law is therefore one that relocates the unstable plant poles to their mirror images in the left-half plane.

An approximate expression for the state feedback gain matrix, K for small μ , and of the limiting value K^∞ , may be obtained as follows.

Assume that $G = 0$ and let $P = P_1\mu$ then from equation (2.39):

$$P_1BR^{-1}B^TP_1 = C^TQ_1C + \mu(P_1A + A^TP_1)$$

where P_1 is symmetric and $P_1 \geq 0$. For small μ

$$P_1BR^{-1}B^TP_1 \approx C^TQ_1C$$

Substituting from equations (2.55,2.56) and defining $\Lambda = (\Lambda^\infty)^{-\frac{1}{2}}$ gives:

$$P_1BNA\Lambda N^TB^TP_1 = C^TE^TE C$$

or

$$\Lambda N^TB^TP_1 = (CBN)^{-1}C$$

The optimal control gain matrix is given by

$$K = R^{-1}B^TP/\mu^2 = R^{-1}B^TP_1/\mu$$

thence

$$K = NA^2N^TB^TP_1/\mu = NA(CBN)^{-1}C/\mu$$

and the closed-loop system matrix A_c becomes:

$$A_c = A - BNA(CBN)^{-1}C/\mu$$

Example A6.1

The above expressions for the gain matrix and the system matrix are evaluated below for the system discussed in sections 2.6 and 2.7

$$K = NA(CBN)^{-1}C/\mu = \begin{bmatrix} 5.78 & 0 & 2.195 \\ 0.078 & 0 & 5.219 \end{bmatrix} /\mu$$

and for $\mu^2 = 0.001$

$$K = \begin{bmatrix} 182.8 & 0 & 69.4 \\ 2.5 & 0 & 165 \end{bmatrix}$$

The closed-loop system matrix A_c becomes:

$$A_c = \begin{bmatrix} -1.25 - 5.78/\mu & 0.75 & -0.75 - 2.195/\mu \\ 1 - 0.078/\mu & -1.5 & -0.75 - 5.22/\mu \\ 1 - 0.078/\mu & -1.0 & -1.25 - 5.22/\mu \end{bmatrix}$$

$$(sI_n - A_c) = \begin{bmatrix} s + 5.78/\mu & -0.75 & 2.195/\mu \\ 0.078/\mu & s + 1.5 & 5.22/\mu \\ 0.078/\mu & 1.0 & s + 5.22/\mu \end{bmatrix}$$

The characteristic frequencies are obtained using $\det (sI_n - A_c) = 0$ for small μ . The finite frequency is obtained as $s_1 = -0.5$ and the asymptotically infinite frequencies are given by $s_2 = -5/\mu$ and $s_3 = -6/\mu$.

The eigenvector corresponding to the finite mode is given by

$$\underline{x}_1 = \begin{bmatrix} 0 & 1 & 0 \end{bmatrix}^T \text{ which belongs to the kernel of } C.$$

The above results may be compared with the following computed values of gain matrix, eigenvalues and eigenvectors, for the case $\mu^2 = 0.001$.

$$K = \begin{bmatrix} 182 & 0.62 & 79 \\ 2.9 & -0.97 & 163 \end{bmatrix}$$

$$\{\lambda_1, \lambda_2, \lambda_3\} = \{-0.5, -158, -189\}$$

$$\{\underline{x}_1, \underline{x}_2, \underline{x}_3\} = \begin{bmatrix} 0.00079 & 0.9125 & 0.995 \\ 0.991 & -0.289 & 0.072 \\ -0.00017 & -0.289 & 0.072 \end{bmatrix}$$

The input direction \underline{v}_1 , corresponding to the mode λ_1 , is given by

$$\underline{v}_1 = -K\underline{x}_1 = \begin{bmatrix} -0.75 \\ 1.0 \end{bmatrix}$$

This agrees with σ_1 in example 3. Notice, however, that the above approximate values for the gain K and \underline{x}_1 fail to give this result, due to small errors in the gain matrix.

Results are derived below which enable the state-feedback gain matrix to be calculated for all values of μ within a chosen finite interval.

From the Riccati equation (2.39):

$$\mu^2(C^T Q_1 C + PA + A^T P) = (PBR^{-1}B^T P + \mu PBR^{-1}G^T C + \mu C^T GR^{-1}B^T P)$$

where the solution P is a function of μ . Differentiating with respect to μ gives:

$$\begin{aligned} \frac{dP}{d\mu} (\mu^2 A - \mu BR^{-1}G^T C - BR^{-1}B^T P) \\ + (\mu^2 A^T - \mu C^T GR^{-1}B^T - PBR^{-1}B^T) \frac{dP}{d\mu} \\ + 2\mu C^T Q_1 C + P(2\mu A - BR^{-1}G^T C) \\ + (2\mu A^T - C^T GR^{-1}B^T)P = 0 \end{aligned}$$

If $G = 0$ this equation simplifies to

$$\begin{aligned} \frac{dP}{d\mu} (\mu^2 A - BR^{-1}B^T P) + (\mu^2 A^T - PBR^{-1}B^T) \frac{dP}{d\mu} \\ + 2PBR^{-1}B^T P/\mu = 0 \end{aligned}$$

for $\mu \in [\mu_0, \mu_T]$. This equation may be solved numerically [58] using a combination of standard linear algebraic and integration routines. The initial condition $P(\mu_0)$ may be calculated from the above steady-state Riccati equation. The gain matrix may be calculated for all values of μ within the interval using equation 2.38.

The physical significance of the input direction vectors is important and is investigated below.

Theorem A8.1

The optimal control signal may be expressed as a linear combination of the exponentially weighted input vectors \underline{v}_i .

Proof: Using the notation in equation 2.59 the state trajectory is given by:

$$\underline{x}(t) = \sum_{j=1}^n \alpha_j \underline{x}_j e^{\lambda_j t}$$

where $\alpha_j \triangleq \underline{p}_j^T \underline{x}_0$. By definition $\underline{v}_i = -K\underline{x}_i$ and thus

$$\underline{u}(t) = -K\underline{x}(t) = \sum_{j=1}^n \alpha_j \underline{v}_j e^{\lambda_j t}$$

Clearly the m fast modes may be decoupled by choosing \underline{v}_i^∞ appropriately.

If for example $\underline{v}_j^\infty = \underline{e}_j$ (a standard basis vector), for $i = \{1, 2, \dots, m\}$, then $N = I_m$ and the speed of each input may be controlled independently.

In the special case when $\alpha_j = 0$ for $m < j \leq n$ then $\underline{u}(t) = NE = E$ where $E \triangleq \text{diag} \{ \alpha_1 e^{\lambda_1 t}, \dots, \alpha_m e^{\lambda_m t} \}$.

The response of a linear system with zero initial conditions may be obtained from the convolution relationship:

$$\underline{y}(k) = \sum_{m=1}^k w(m) \underline{u}(k - m) \quad (\text{for, } 0 < k < \infty; k \in \mathbb{Z})$$

or

$$\underline{y}(k) = \sum_{j=0}^{k-1} w(k - j) \underline{u}(j) \quad (\text{for, } 0 < k < \infty; k \in \mathbb{Z})$$

where the weighting sequence is denoted by $w(k)$. For a causal system

$w(k) \underline{\Delta} 0$ for $k \leq 0$. The inner product between the vectors

$\underline{y} \underline{\Delta} \{y_0, y_1, y_2, \dots\}$ and $\underline{e} \underline{\Delta} \{e_0, e_1, e_2, \dots\}$ may be defined as:

$$\langle \underline{y}, \underline{e} \rangle_{H_r} = \sum_{k=0}^{\infty} y(k) \underline{e}(k), \quad \text{for } \underline{y}, \underline{e} \in \ell_2^r[0, \infty]$$

Thus, the adjoint operator W^* can be found from the defining relationship:

$$\begin{aligned} \langle W\underline{u}, \underline{e} \rangle_{H_r} &= \langle \underline{u}, W^*\underline{e} \rangle_{H_m} \\ &= \sum_{k=0}^{\infty} \left(\sum_{j=0}^{\infty} w(k - j) \underline{u}(j) \right) \underline{e}(k) \quad (\text{let } m = j + 1) \\ &= \sum_{j=0}^{\infty} \underline{u}(j) \underline{e}(k) \left(\sum_{k=0}^{\infty} w^T(k - j) \underline{e}(k) \right) \\ &= \langle \underline{u}, W^*\underline{e} \rangle_{H_m} \end{aligned}$$

where

$$(W^*\underline{e})(i) \underline{\Delta} \sum_{k=0}^{\infty} w^T(k - i) \underline{e}(k) = \sum_{k=i+1}^{\infty} w^T(k - i) \underline{e}(k)$$

The output from the adjoint system is only dependent upon the system inputs for $k > i$ and the adjoint system is therefore non-causal. For example, for an input $\underline{e}(k) = \delta(k)$, then the adjoint system output becomes:

$$\begin{aligned} (W^*\delta)(i) &= w^T(-i) \quad (\text{for } i < 0) \\ &= 0 \quad (\text{for } i \geq 0) \end{aligned}$$

The z-transform of the adjoint operator relationship may be obtained as follows. Let

$$\underline{c}(i) \underline{\Delta} (W^*\underline{e})(i), \quad \text{for all } i \in (-\infty, \infty)$$

then

$$\begin{aligned} Z_2(\underline{c}(i)) &= \underline{c}(z) \triangleq \sum_{i=-\infty}^{\infty} \underline{c}(i)z^{-i} \\ &= \sum_{i=-\infty}^{\infty} \sum_{k=-\infty}^{\infty} w^T(k-i)\underline{e}(k)z^{-i} = \sum_{k=-\infty}^{\infty} \left(\sum_{i=-\infty}^{\infty} w^T(k-i)z^{-i} \right) \underline{e}(k) \\ &= \sum_{k=-\infty}^{\infty} \left(\sum_{n=-\infty}^{\infty} w^T(n)z^{-(k-n)} \right) \underline{e}(k) \quad (\text{where } n = k - i) \\ &= \sum_{k=-\infty}^{\infty} \left(\sum_{n=1}^{\infty} w^T(n)z^n \right) \underline{e}(k)z^{-k} \\ &= w^T(z^{-1})\underline{e}(z) \end{aligned}$$

Appendix 10 Adjoint of the Delay Operator

The adjoint of the delay operator may be found as follows:

$$(D_0 \underline{u})(i) \triangleq \underline{u}(i - k_0)$$

$$\begin{aligned} \langle \underline{y}, D_0 \underline{u} \rangle_{H_r} &= \sum_{k=0}^{\infty} \underline{y}(k) \underline{u}(k - k_0) \quad (\text{let } m = k - k_0) \\ &= \sum_{m=0}^{\infty} \underline{y}(m + k_0) \underline{u}(m) = \langle D_0^* \underline{y}, \underline{u} \rangle_{H_r} \end{aligned}$$

and

$$(D_0^* \underline{y})(i) = \underline{y}(i + k_0), \quad \text{for all } i \geq 0$$

The z-transform of the delay operator is well known to be $Z_2((D_0 \underline{u})(i)) = \underline{u}(z)z^{-k_0}$. The z-transform of the adjoint operator becomes:

$$\begin{aligned} Z_2((D_0^* \underline{y})(i)) &= \sum_{i=-\infty}^{\infty} \underline{y}(i + k_0) z^{-i}, \quad (\text{let } m = i + k_0) \\ &= \sum_{m=-\infty}^{\infty} \underline{y}(m) z^{-m+k_0} \\ &= \underline{y}(z) z^{k_0} \end{aligned}$$

Appendix 11 Z Transformation for $w^T(N - i - k_0)$

The above two-sided z-transform is required in the transformation of the gradient function:

$$Z_2(w^T(N - i - k_0)) = \sum_{i=-\infty}^{\infty} w^T(N - i - k_0) z^{-i}$$

Let $m = N - i - k_0$, then

$$\begin{aligned} Z_2(w^T(N - i - k_0)) &= \sum_{m=1}^{\infty} w^T(m) z^{m-N+k_0} \\ &= w^T(z^{-1}) z^{-N+k_0} \end{aligned}$$

As has been defined in equations (3.37) and (3.42):

$$N(z)_+ = \underline{n}_{11}(z) + \underline{n}_{12}(z) + \underline{n}_2(z)$$

The first term $\underline{n}_{11}(z)$ can be evaluated easily because \underline{r}_0 does not contain any z^{-N} terms and $M^T(z^{-1})$ is the transform of a non-causal system. Thus, the transform of the positive time terms in the partial fraction expansion of $\underline{n}_{11}(z)$ result only from the poles of $\underline{r}_0(z)$. The time function $\underline{n}_{11}(i)$ follows directly from a table of single sided z transforms.

The reference terms in the $\underline{n}_{12}(z)$ represent an input $\underline{r}_N(i - n)H(i - N)$ into an adjoint system of transfer function matrix $M^T(z^{-1})Q$. This input is zero for $i < N$ and since only the transform of terms within the interval $[0, N - 1]$ is required, these will be determined by the adjoint system. To calculate $\underline{n}_{12}(z)$ from the partial fraction expansion of $M^T(z^{-1})Q\underline{r}_N(z)z^{k_0-N}$ the terms due to the poles of the adjoint system $M^T(z^{-1})$ are selected. In transforming $\underline{n}_{12}(i)$ any terms which include z^{-N} can be neglected since they only affect the control for $i \geq N$.

The final term $\underline{n}_2(z)$ includes the transform of an impulse occurring at time N with magnitude \underline{c} . Using the observation that $M^T(z^{-1})$ represents an adjoint system:

$$\underline{n}_2(z) = \{M^T(z^{-1})z^{k_0-N}\}_+ \underline{c}$$

Now if $m(i)$ is the impulse response of the adjoint system, then

$$\begin{aligned} \underline{n}_2(i) &= \sum_{k=i+1}^{\infty} m^T(k - i)\underline{c}\delta(k - N + k_0), & \text{for } i \in [0, N] \\ &= m^T(N - k_0 - i)\underline{c} & \text{for } 0 \leq i \leq N - k_0 - 1 \\ &= 0 & \text{for } N - k_0 \leq i < 0 \end{aligned}$$

where $m(i) = Z^{-1}(M(z))$.

The transformation X may be based on the Chebyshev orthogonal polynomials (similar results are obtained using discrete orthogonal polynomials):

$$X = \begin{bmatrix} 1.0 & 1.0 & 1.0 & 1.0 \\ 0.714 & 0.02 & -0.685 & -0.999 \\ 0.428 & -0.632 & -0.97 & -0.199 \\ 0.143 & -0.959 & -0.417 & 0.84 \\ -0.143 & -0.959 & 0.417 & 0.84 \\ -0.428 & -0.632 & 0.97 & -0.199 \\ -0.714 & 0.02 & 0.685 & -0.999 \\ -1.0 & 1.0 & -1.0 & 1.0 \end{bmatrix}$$

Using G_m defined in 4.1 the transformed matrix $G_x = (X^T X)^{-1} X^T G_m X$ becomes:

$$G_x = \begin{bmatrix} 8.37 & 0.0 & -1.97 & 0.0 \\ 0.0 & 6.03 & 0.0 & -1.5 \\ 0.2 & 0.0 & 3.04 & 0.0 \\ 0.0 & -0.32 & 0.0 & 0.9 \end{bmatrix}$$

The eigenvalues of G_x are $\{0.807, 3.117, 6.119, 8.295\}$ and the corresponding eigenvectors are respectively:

$$\underline{x}_1 = \begin{bmatrix} 0 \\ 0.276 \\ 0 \\ 0.96 \end{bmatrix}, \quad \underline{x}_2 = \begin{bmatrix} 0.35 \\ 0 \\ 0.93 \\ 0 \end{bmatrix}, \quad \underline{x}_3 = \begin{bmatrix} 0 \\ 0.99 \\ 0 \\ -0.06 \end{bmatrix}, \quad \underline{x}_4 = \begin{bmatrix} 0.99 \\ 0 \\ 0.04 \\ 0 \end{bmatrix}$$

Using \tilde{G}_m defined in 4.4 the transformed matrix \tilde{G}_x becomes:

$$\tilde{G}_x = \begin{bmatrix} 6.61 & 0.38 & -1.54 & 0.3 \\ 0.36 & 5.0 & 0.27 & -1.34 \\ -0.79 & 0.42 & 3.44 & 0.02 \\ -0.09 & -0.21 & 0.07 & 2.15 \end{bmatrix}$$

The eigenvalues of \tilde{G}_x are {2.038, 3.02, 5.16, 6.98} and the eigenvectors are respectively:

$$\underline{x}_1 = \begin{bmatrix} -0.17 \\ 0.43 \\ -0.24 \\ 0.85 \end{bmatrix}, \underline{x}_2 = \begin{bmatrix} 0.40 \\ -0.15 \\ 0.90 \\ 0.06 \end{bmatrix}, \underline{x}_3 = \begin{bmatrix} 0 \\ 1 \\ 0.24 \\ 0.06 \end{bmatrix}, \underline{x}_4 = \begin{bmatrix} 0.97 \\ 0.17 \\ -0.2 \\ -0.03 \end{bmatrix}$$

The eigenvalue spectra may be compared with the spectra for the full 8 x 8 system. The eigenvalues corresponding to G_m (equation 4.1) and \tilde{G}_m (equation 4.4) become:

$$\{-0.039, -0.028 \pm j0.102, 0.205, 0.943, 3.31, 6.46, 8.34\}$$

and

$$\{0.00125, 0.119, 0.6, 1.7, 2.2, 3.19, 5.78, 7.18\}$$

The singular values of G_x and \tilde{G}_x are respectively:

$$\{0.792, 3.00, 6.23, 8.61\}$$

and

$$\{1.963, 3.03, 5.30, 7.04\}$$

The singular values of G_m and \tilde{G}_m lie within the ranges $[0.01, 9]$ and $[0.001, 8]$.

Multivariable Deterministic Systems/Integral Controller Calculation

The expression for the closed-loop controller with integral action, given in Theorem 4.2, is derived below. From 4.4 4

$$Y^T(-s)Y(s) = \frac{G_m^T Q_1 G_m \gamma(-s)\gamma(s) - s^2 R \sigma(-s)\sigma(s)}{-s^2 \sigma(-s)\sigma(s)} = \frac{N^T(-s)N(s)}{-s^2 \sigma(-s)\sigma(s)}$$

where $Y(s) = N(s)/(s\sigma(s))$ and $N(0) = Q_1^{\frac{1}{2}} G_m$. Assuming G_m^{-1} exists

$$\{N(-s)^{-T} \gamma(-s) G_m^T Q_1 \frac{1}{s^2}\}_+ = (M_1/s^2 + M_2/s) G_m^{-1}$$

Now

$$N(-s)^{-T} \gamma(-s) G_m^T Q_1 \frac{1}{s^2} = N(0)^{-T} G_m^T Q_1 \frac{1}{s^2} + M_2 G_m^{-1} \frac{1}{s} + V(s)$$

$$M_1 = Q_1^{\frac{1}{2}} G_m \tag{A.2.1}$$

$$M_2 = \lim_{s \rightarrow 0} (N(-s)^{-T} \gamma(-s) G_m^T Q_1 G_m - Q_1^{\frac{1}{2}} G_m) / s$$

but

$$N^T(-s)N(s) = G_m^T Q_1 G_m \gamma(-s)\gamma(s) - s^2 R \sigma(-s)\sigma(s)$$

thence

$$N(-s)^{-T} \gamma(-s) G_m^T Q_1 G_m = (N(s) + s^2 N(-s)^{-T} R \sigma(-s)\sigma(s)) / \gamma(s)$$

and

$$M_2 = \lim_{s \rightarrow 0} (N(s) - Q_1^{\frac{1}{2}} G_m \gamma(s)) / s$$

$$= \lim_{s \rightarrow 0} (N'(s) - Q_1^{\frac{1}{2}} G_m \gamma'(s))$$

where the dash denotes differentiation with respect to s . Thence

from (A.2.1)

$$F_0(s) \underline{k} / s = Y(s)^{-1} \left(\frac{M_1}{s} + M_2 \right) G_m^{-1} \underline{k} / s$$

or

$$F_0(s) = Y(s)^{-1} \left(\frac{M_1}{s} + M_2 \right) G_m^{-1} = N(s)^{-1} (M_1 + s M_2) G_m^{-1} \sigma(s)$$

The closed loop optimal controller follows from 5.36.

$$C_0(s) = N(s)^{-1} (M_1 + s M_2) (I_m - \gamma(s) N(s)^{-1} (M_1 + s M_2))^{-1} G_m^{-1} \sigma(s)$$

In the limit as $s \rightarrow 0$ $C_0(s) \rightarrow G_m^{-1} \eta$ where $\eta \rightarrow \infty$, signifying the presence of integral action.

Non-Interactive Deterministic Systems/Controller Calculation

Let the plant transfer function $w(s) = g\gamma(s)/\sigma(s)$, $\gamma(0) = \sigma(0) = 1$, and $r(s) = 1/s$ then for the non-integral control case ($L(s) = 1$):

$$Y^T(-s)Y(s) = (g^2q\bar{\gamma}\gamma + r\bar{\sigma}\sigma)/(\bar{\sigma}\sigma) = \bar{n}n/(\bar{\sigma}\sigma)$$

thence

$$Y(s) = n(s)/\sigma(s)$$

$$F_0(s) = \sigma g q / (n(s)n(0))$$

thus

$$C_0(s) = \frac{q\sigma(s)g^{-1}}{(g^{-2}n(s)n(0) - q\gamma(s))}$$

If $g = 1$ then $n(s)n(-s) = q\gamma(s)\gamma(-s) + r\sigma(s)\sigma(-s)$ and

$$C_0(s) = \frac{q\sigma(s)}{(n(s)(q+r)^{\frac{1}{2}} - q\gamma(s))}$$

where $n(0) = (q+r)^{\frac{1}{2}}$ and $C_0(0) = q/r$.

If the cost function includes the term $L(s) = 1/s$ then integral control results and the closed-loop controller is obtained as follows:

$$Y^T(-s)Y(s) = (g^2q\bar{\gamma}\gamma - s^2r\bar{\sigma}\sigma)/(-s^2\bar{\sigma}\sigma) = \bar{n}n/(-s^2\bar{\sigma}\sigma)$$

thence

$$Y(s) = n(s)/(s\sigma(s))$$

$$F_0(s) = \frac{\sigma(s)}{n(s)} (m_1 + sm_2)$$

where $n(0) = q^{\frac{1}{2}}$, $m_1 = gq^{\frac{1}{2}}$ and $m_2 = \lim_{s \rightarrow 0} (n(s) - q^{\frac{1}{2}}\gamma(s))g/s$. Thence,

$$C_0(s) = \frac{\sigma(s)(m_1 + sm_2)g^{-1}}{(g^{-1}n(s) - \gamma(s)m_1 + sm_2)}$$

If $g = 1$ then $n(s)n(-s) = q\gamma(s)\gamma(-s) - rs^2\sigma(s)\sigma(-s)$ and

$$C_0(s) = \frac{\sigma(s)(m_1 + sm_2)}{(n(s) - \gamma(s)(m_1 + sm_2))}$$

where $C_0(0) \rightarrow \infty$.